Epithelial cell death induced by Candidalysin, a cytolytic peptide toxin of Candida albicans

Blagojevic, Mariana

Awarding institution:
King's College London

Epithelial cell death induced by Candidalysin, a cytolytic peptide toxin of *Candida albicans*

Mariana Blagojevic

Thesis submitted for the degree of
Doctor of Philosophy

Mucosal and Salivary Biology Division
King's College London
2018

Abstract

Microbial infections contribute significantly to morbidity and mortality in humans. Fungi are often an under-represented component of the microbial communities that colonise mucosal surfaces. The most common human fungal pathogens are the *Candida* species, of which *Candida albicans* is the most prevalent. *C. albicans* has an asymptomatic carriage rate of approximately 60% in the human population, where it resides as a member of the microflora that colonises the mucosal surfaces of the body.

C. albicans is a polymorphic fungus capable of growing in a number of distinct morphological forms. At mucosal surfaces, growth of *C. albicans* in the unicellular yeast form is typically associated with commensalism, whereas the production of filamentous hyphae is associated with fungal overgrowth and pathogenesis. In healthy individuals, the immune system functions to restrict the growth of *C. albicans* hyphae, preventing infection. However, in the absence of effective immune surveillance, *C. albicans* hyphae can invade the mucosal surfaces of the body, causing infection and tissue damage. Translocation of *C. albicans* across mucosal barriers and invasion of underlying tissues is a major risk-factor for the development of life-threatening systemic infection in immune-compromised individuals.

The hyphae of *C. albicans* secrete Candidalysin, a toxin essential for epithelial damage and activation of mucosal immune responses. Cellular damage sustained during infection can often result in cell death by apoptosis, necrosis, necroptosis or pyroptosis. While cell death is often regarded as being beneficial for microbial pathogenesis, it is becoming increasingly clear that cell death can also influence host defence by initiating specific immune responses that contribute to microbial clearance.

Collectively, these data demonstrate that oral epithelial cells respond to the secreted fungal toxin Candidalysin by triggering numerous cellular stress responses that are intimately linked with the induction of cellular death. Candidalysin was observed to induce necrosis, but not apoptosis, necroptosis or pyroptosis, and promoted inflammatory responses through a mechanism involving necrosis-dependent release of pro-IL-1β and pro-IL-18.

Acknowledgements

I would like to express my deep gratitude to Prof Julian Naglik for his excellent guidance, caring, enthusiasm and continuous support throughout this project. My PhD has been an amazing experience and I could not have imagined having a better supervisor for my studies. Your advice on both research as well as on my career have been invaluable.

I wish to thank my friend and mentor Dr Jonathan Richardson, he has taught me more than I could ever give him credit for here. He has shown me what a good scientist and person should be. Thank you for always believing in me. I owe it all to you.

My sincere thanks also goes to Prof Steven Challacombe and Dr David Moyes for their advice and insightful comments.

I am grateful to all of those with whom I have had the pleasure to work with during my PhD. I would like to extend my thanks to Mahvash, Charles, Juraj, Durdana, Andrew and Kathy for their advice, help and kindness.

A special thanks goes to my lab mates Shirley, Simona, Nessim, Carlo, Marta, Hersi, Ahmed, MJ, Nina, Jessica, Giulia and Luis for the sleepless nights we worked together before deadlines, and for all of the fun we have had in the last four years.

I also thank my fellow ESRs/ERs and PIs of the ImResFun ITN for the stimulating discussions and constructive suggestions during the development of this research. A special thanks to Claudia for her constant encouragement and friendship.

My grateful thanks are also extended to my friends who provided a much needed form of escape from my studies. Thank you Anna, Alice, Lutz, Kate, Sean, Momo, Tiz, Lucia, Frenkie, Cele, Tino, Bruno, Ingvild, Luciana, Balla, Fra, Sam, Fede, Alessa', Richi, Ambros, Kev and Camille for sharing many moments together.

I especially want to thank my favourite Londoners Emma and Yutetsu for their emotional support and the best times in London. I am grateful for our special friendship. I miss you.

Most importantly, none of this could have happened without my fantastic family. Thank you Mama, Ana, Baba and Bruno for your unconditional love and for always spurring me to strive towards my goal.

Last but not least, to my love Mario. Thank you for always being there for me.

Table of contents

Abstract 2

Acknowledgements 3

Table of contents 4

List of Figures 9

List of Tables 13

List of Abbreviations 14

Chapter 1: Introduction 19

1.1 Host-Pathogen interaction 19

1.2 *Candida* species 20

1.3 *Candida* infections 21

1.3.1 Treatment of *Candida* infections 22

1.4 *Candida albicans* virulence factors 23

1.4.1 Hyphae 24

1.4.2 *C. albicans* virulence factors 26

1.4.3 Adhesion 26

1.4.4 Invasion 27

1.4.5 Damage 30

1.5 Physical barrier against *C. albicans* infection 30

1.6 Host immune responses against *C. albicans* infection 31

1.6.1 Host recognition of microbes 31

1.6.2 Innate responses to *C. albicans* 33

1.6.3 Adaptive responses to *C. albicans* 37

1.7 Host cell death as a defence against infection 38

1.7.1 The interplay between apoptosis and necrosis 40

1.7.2 Apoptosis 42

1.7.3 Necrosis 48

1.7.4 Programmed necrosis 48
1.7.5 Summary of the characteristic features of different cell death pathways 57
1.8 Project Aims 59
Chapter 2: Materials and Methods 60
2.1 General materials and equipment 60
2.1.1 General chemicals 60
2.1.2 General equipment 61
2.2 Fungal culture 61
2.2.1 *C. albicans* growth medium 61
2.2.2 Creation of *C. albicans* mutants, growth and maintenance 61
2.2.3 Candidalysin peptides 63
2.3 Cell culture 63
2.3.1 Cell line growth and maintenance 63
2.3.2 Cell counting 64
2.3.3 Cell freezing and thawing 64
2.3.4 Cell seeding 65
2.4 Cell response assays 66
2.4.1 LDH (Epithelial cell damage) assay 66
2.4.2 Detection of epithelial cell death by fluorescence microscopy 66
2.4.3 Measurement of epithelial mitochondrial fitness by MTT assay 67
2.4.4 Intracellular ROS quantification by DCFH-DA staining 67
2.4.5 Intracellular ATP quantification by Luminescence assay 68
2.4.6 Intracellular calcium quantification by fura-2 staining 68
2.4.7 Caspase activity measurement by Luminescence assay 68
2.4.8 Cytochrome c and Cytokine quantification by ELISA assay 69
2.5 Protein assays 69
2.5.1 Protein extraction 69
2.5.2 Bicinchoninic Acid (BCA) assay 69
2.5.3 Sodium Dodecyl Sulphate Polyacrylamide Gel Electrophoresis (SDS-PAGE). 70
2.5.4 Western blot analysis 70

2.6 Statistical analysis of data 71

Chapter 3: Role of *C. albicans* Candidalysin peptides in driving cell death processes in human oral epithelial cells. 72

3.1 Introduction 72

3.2 Methods 73

3.2.1 Epithelial cell damage assay 73

3.2.2 Fluorescent microscopy 73

3.2.3 MTT assay 73

3.2.3 Detection of intracellular ROS 74

3.2.4 Detection of intracellular ATP 74

3.2.5 Detection of intracellular calcium 74

3.3 Results 74

3.3.1 Damage of oral epithelial cells is Candidalysin dependent 74

3.3.2 Induction of cell death processes by Candidalysin peptides 76

3.3.3 Candidalysin peptides induce loss of mitochondrial fitness in TR146 cells 81

3.3.4 Candidalysin peptides induce production of intracellular ROS in TR146 cells 85

3.3.5 Candidalysin peptides cause depletion of intracellular ATP in TR146 cells 87

3.3.6 Candidalysin induces calcium influx in TR146 cells 91

3.4 Discussion 94

Chapter 4: Role of Candidalysin in driving apoptotic death in human oral epithelial cells 100

4.1 Introduction 100

4.2 Methods 101

4.2.1 Western blot 101

4.2.2 Quantification of Caspase activity 101

4.2.3 Quantification of cytochrome c 101

4.2 Results 102

4.2.1 Ripoptosome assembly is Candidalysin-independent 102

4.2.2 Caspase-8 activity is not induced by Candidalysin 103

4.2.3 Candidalysin contributes to Cytochrome c release only in the context of a fungal infection 105
4.2.5 Caspase-3 activity is not induced by Candidalysin 107
4.2.6 PARP is not activated by Candidalysin 109
4.3 Discussion 110
Chapter 5: Role of Candidalysin in driving regulated necrotic cell death in human oral epithelial cells 115
5.1 Introduction 115
5.2 Methods 116
5.2.1 Western blot 116
5.2.2 Quantification of Caspase activity 116
5.2.3 Quantification of IL-1β and IL-18 117
5.3 Results 117
5.3.1 Expression and phosphorylation of RIPK1 in epithelial cells treated with Candidalysin and *C. albicans ECE1* mutants 117
5.3.2 Expression and phosphorylation of RIPK3 in TR146 epithelial cells treated with Candidalysin and *C. albicans ECE1* mutants 118
5.3.3 Expression and phosphorylation of MLKL in TR146 epithelial cells treated with Candidalysin and *C. albicans ECE1* mutants 120
5.3.4 Secretion of IL-1β and IL-18 from TR146 oral epithelial cells in response to Candidalysin and *C. albicans ECE1* mutant strains 122
5.3.5 Expression of intracellular IL-1β and IL-18 in oral epithelial cells in response to Candidalysin and *C. albicans ECE1* mutant strains 126
5.3.6 Expression of NLRP3 in oral epithelial cells in response to Candidalysin and *C. albicans ECE1* mutants 129
5.3.7 Expression of ASC in oral epithelial cells in response to Candidalysin and *C. albicans ECE1* mutants 130
5.3.8 Expression and activity of Caspase-1 in TR146 epithelial cells treated with Candidalysin and *C. albicans ECE1* mutants 131
5.3.9 Detection of IL-1β and IL-18 secreted from TR146 epithelial cells in response to Candidalysin and *C. albicans ECE1* mutants 134

5.3.10 Expression of gasdermin D in epithelial cells in response to Candidalysin and *C. albicans ECE1* mutants 136

5.4 Discussion 138

5.4.1 The epithelial necroptotic response to Candidalysin 138

5.4.2 The epithelial pyroptotic response to Candidalysin 140

Chapter 6: General discussion 147

6.1 Epithelial cell death responses to Candidalysin 147

6.2 Epithelial apoptotic responses to Candidalysin 150

6.3 Epithelial necrotic responses to Candidalysin 150

6.3.1 Epithelial necroptotic responses to Candidalysin 151

6.3.2 Epithelial pyroptotic responses to Candidalysin 151

6.4 Conclusions 153

References 155

Appendix A: Published papers 181

List of Figures

Figure 1-1	Morphological plasticity of *C. albicans*
Figure 1-2	Summary of hyphal induction in *C. albicans*
Figure 1-3	Stages of *C. albicans* mucosal infection
Figure 1-4	Epithelial responses to *C. albicans* yeast and hyphae
Figure 1-5	Epithelial induction of innate immunity during *C. albicans* infection
Figure 1-6	Apoptotic caspases
Figure 1-7	Initiation of the TNF-induced extrinsic apoptotic pathway
Figure 1-8	Initiation of the intrinsic apoptotic pathway
Figure 1-9	Extrinsic and intrinsic apoptotic signalling pathways
Figure 1-10	Necroptotic pathway induced by TNFα
Figure 1-11	Phagocytosed *C. albicans* can escape from macrophages by hypha-mediated lysis and pyroptosis
Figure 1-12	Organisation of the NLRP3 (A) and the NLRC4 (B) inflammasome cascades
Figure 1-13	Pyroptosis is induced by canonical and non-canonical inflammasome activation
Figure 3-1	Damage of oral epithelial cells by *C. albicans ECE1* mutants
Figure 3-2	Damage of oral epithelial cells by *C. albicans* Candidalysin peptides
Figure 3-3	Cell death markers induced in epithelial cells by Candidalysin peptides after 3 h
Figure 3-4	Cell death markers induced in epithelial cells by Candidalysin peptides after 6 h

Figure 3-5	Cell death markers induced in epithelial cells by Candidalysin peptides after 24 h
Figure 3-6	Reduction in mitochondrial fitness in response to Candidalysin peptides
Figure 3-7	Time-course of mitochondrial fitness following treatment with Candidalysin peptides
Figure 3-8	Quantification of intracellular ROS in oral epithelial cells treated with *C. albicans* Candidalysin peptides
Figure 3-9	Intracellular ATP levels following treatment with *C. albicans* Candidalysin peptides
Figure 3-10	Time-course of intracellular ATP levels following treatment with Candidalysin peptides
Figure 3-11	Intracellular calcium levels of oral epithelial cells in response to treatment with *C. albicans* Candidalysin peptides
Figure 3-12	Intracellular calcium levels of oral epithelial cells in response to treatment with Candidalysin
Figure 4-1	Expression of cIAP2 in oral epithelial cells in response to Candidalysin and *Candida ECE1* mutant strains
Figure 4-2	Expression of caspase-8 in oral epithelial cells in response to Candidalysin
Figure 4-3	Caspase-8 activity in oral epithelial cells infected with Candidalysin and *C. albicans ECE1* mutants
Figure 4-4	Quantification of cytochrome c release from oral epithelial cells in response to Candidalysin and *C. albicans ECE1* mutant strains
Figure 4-5	Expression of caspase-3 in oral epithelial cells in response to Candidalysin and *C. albicans ECE1* mutant strains

Figure 4-6	Caspase-3 activity in oral epithelial cells treated with Candidalysin and *C. albicans ECE1* mutant strains
Figure 4-7	Expression of PARP in oral epithelial cells treated with Candidalysin and *C. albicans ECE1* mutant strains
Figure 5-1	Expression and phosphorylation of RIPK1 in oral epithelial cells in response to Candidalysin and *C. albicans ECE1* mutant strains
Figure 5-2	Expression and phosphorylation of RIPK3 in oral epithelial cells in response to Candidalysin and *C. albicans ECE1* mutant strains
Figure 5-3	Expression and phosphorylation of MLKL in oral epithelial cells treated with Candidalysin and *C. albicans ECE1* mutants
Figure 5-4	Secretion of IL-1β from TR146 oral epithelial cells treated with Candidalysin and *C. albicans ECE1* mutant strains
Figure 5-5	Secretion of IL-18 from oral epithelial cells treated with Candidalysin and *C. albicans ECE1* mutants
Figure 5-6	Epithelial expression of intracellular pro-IL-1β in response to Candidalysin and *C. albicans ECE1* mutant strains
Figure 5-7	Epithelial expression of intracellular pro-IL-18 in response to Candidalysin and *C. albicans ECE1* mutants
Figure 5-8	Expression of NLRP3 in epithelial cells treated with Candidalysin and *C. albicans ECE1* mutants
Figure 5-9	Expression of ASC in epithelial cells treated with Candidalysin and *C. albicans ECE1* mutants
Figure 5-10	Expression of Caspase-1 in epithelial cells treated with Candidalysin and *C. albicans ECE1* mutants
Figure 5-11	Caspase-1 activity in oral epithelial cells treated with Candidalysin and *C. albicans ECE1* mutants

Figure 5-12	Secretion of IL-1β from epithelial cells in response to Candidalysin and *C. albicans ECE1* mutant strains
Figure 5-13	Secretion of IL-18 from epithelial cells in response to Candidalysin and *C. albicans ECE1* mutants
Figure 5-14	Epithelial expression of Gasdermin D in response to Candidalysin and *C. albicans ECE1* mutants

List of Tables

Table 1.1	Host PRRs that recognise *C. albicans* PAMPs
Table 1.2	Summary of the characteristic features of different cell death pathways
Table 2.1	Description of *C. albicans* strains used in this study
Table 2.2	Cell seeding conditions
Table 2.3	Cell death stainings
Table 2.4	Detection antibodies for epithelial signalling proteins

List of Abbreviations

%	Percent
°C	Degree Celsius
µg	Microgram
µL	Microliter
µM	Micromolar
mM	Millimolar
w/v	Weight/volume
v/v	Volume/volume
V	Volts
mL	Millilitre
mU	Milliunit
s	Seconds
min	Minutes
h	Hours
AhR	Aryl hydrocarbon receptor
Akt	Protein kinase B
Als	Agglutinin-like sequence
ASC	Apoptosis-associated speck-like protein containing a CARD
BCA	Bicinchoninic acid
BIR	Baculovirus inhibitor of apoptosis repeat
CARD	Caspase recruitment domain-containing protein

CCL20	C-C motif chemokine ligand 20
CFU	Colony forming units
cIAPs	Cellular inhibitors of apoptosis
CLRs	C-type lectin receptors
DAMPs	Danger associated molecular patterns
DCFH-DA	2,7'-Dichlorodihydrofluorescin diacetate
DCs	Dendritic cells
DED	Death effector domain
DD	Death domain
DMEM	Dulbecco's modified eagle medium
DMSO	Dimethyl sulfoxide
D-PBS	Dulbecco's phosphate-buffered saline
DRs	Death receptors
DTT	Dithiothreitol
Eap1p	Enhanced adherence to polystyrene
Ece1p	Extent of cell elongation protein 1
EDTA	Ethylenediaminetetraacetic acid
ELISA	Enzyme-linked immunosorbent assay
ERK	Extracellular signal-regulated kinase
Eth Homo III	Ethidium Homodimer III
FADD	Fas-associated protein with death domain
FBS	Foetal bovine serum

G-CSF	Granulocyte colony-stimulating factor
GlcNac	*N*-acetyl-D-glucosamine
GM-CSF	Granulocyte-macrophage colony-stimulating factor
GPI	Glycosylphosphatidylinositol
HCl	Hydrochloric acid
Hgc1p	Hyphal G1 cyclin protein 1
Hwp1p	Hyphal wall protein 1
iATP	Intracellular Adenosine Triphospate
ICAD	Inhibitor of Caspase-activated DNase
IL	Interleukin
IMM	Inner mitochondrial membrane
JNK	c-Jun N-terminal kinase
LDH	Lactate dehydrogenase
LIUBAC	Linear ubiquitin chain assembly complex
LPS	Lipopolysaccharide
LRR	Leucine rich repeat sequence
MAPK	Mitogen-activated protein kinase
MHC II	Major histocompatibility complex II
MLKL	Mixed lineage kinase domain-like protein
MMP	Mitochondrial membrane permeability
MOI	Multiplicity of infection
MPT	Mitochondrial permeability transition

mTOR	Mammalian target of rapamycin
MTT	3-(4,5-dimethylthiazol-2-yl)-2,5-diphenyltetrazolium bromide
Nec-1	Necrostatin-1
NEDD	Neural precursor-cell-expressed developmentally downregulated protein
NETs	Neutrophil extracellular traps
NF-κB	Nuclear factor kappa-light-chain-enhancer of activated B cells
NLRs	Nucleotide-binding domain leucine-rich receptors
NOD	Nucleotide-binding oligomerization domain
OMM	Outer mitochondrial membrane
PAMPs	Pathogen associated molecular patterns
PARP	Poly (ADP-ribose) polymerase
PC	Phosphatidylcholine
PDGF BB	Platelet-derived growth factor BB
PE	Phosphatidylethanolamine
PI3K	Phosphatidylinositide 3-kinase
PRRs	Pattern recognition receptors
PS	Phosphatidylserine
PYD	Pyrin domain
RHIM	RIP homotypic interaction motifs
RIPA	Radio Immuno-Precipitation Assay
RIPK	Receptor interacting protein kinase
ROS	Reactive Oxygen Species

S100A8/9	S100 calcium-binding protein A8/A9
Sap	Secreted aspartyl protease
SDS	Sodium dodecyl sulphate
SM	Sphingomyelin
SODs	Superoxide dismutases
TBS	Tris-buffered saline
TLRs	Toll-like receptors
TNFα	Tumour Necrosis Factor alpha
TRADD	TNFR1-associated death domain protein
TRAF2	TNF-receptor-associated factor 2
TRIF	TIR-domain-containing adaptor-inducing interferon-β
YPD	Yeast peptone dextrose

Chapter 1: Introduction

1.1 Host-Pathogen interaction

Infectious diseases are a leading cause of morbidity and mortality worldwide and are a major challenge for the biomedical sciences. Recent research has improved our understanding of the complex and dynamic interplay that occurs between pathogens and the human host, and how these interactions influence disease outcome. However, despite these advances, the molecular mechanisms that drive microbial pathogenicity and host responses to infection remain to be characterised in full.

Historically, all microbes were considered to be detrimental organisms responsible for the propagation of disease in humans. However, this traditional view of microbial pathogenesis changed substantially with the observation that the acquisition of certain microbes was not always correlated with symptomatic infection and disease outcome. Our view of microbial pathogenicity and host-pathogen interactions has expanded to accommodate an awareness of commensal and opportunistic microbes and their role(s) in health and disease.

The human body provides a challenging but nevertheless common niche for microbes. Several body surfaces including the skin and the mucosal surfaces of the mouth, gastrointestinal, respiratory and urogenital tracts are colonised by a diverse range of bacteria, fungi and viruses (Dethlefsen et al., 2007). Collectively, the microbial communities that colonise the skin and mucosal surfaces are referred to as the microbiota. The microbes that comprise the microbiota may persist in a state of co-existence with the host (commensalism) or may cause disease (pathogenicity) (Magalhaes et al., 2007). However, the classification of microbes as either "commensals" or "pathogens" is not mutually exclusive. Indeed, opportunistic pathogens can colonise a mucosal surface without causing harm to a host, but may cause disease under suitably predisposing conditions.

Fungi are common members of the microbiota found on all mucosal surfaces, and attention to these organisms is increasing in order to better understand how fungi may contribute to health and disease. Fungal infections contribute significantly to morbidity and mortality in humans (Brown et al., 2012). Like the bacterial microbiota, the *myco*biota is often altered in disease, and understanding how these alterations

contribute to fungal pathogenesis is a growing area of research. Patients with a wide spectrum of immune abnormalities, ranging from impaired host defence to alterations in the microbial flora often develop fungal infections (Fidel, 2006; Hasan et al., 2009).

Fungi are a frequently-encountered, but under-represented component of the microbial communities that colonise mucosal surfaces. Nevertheless, their contribution to morbidity and mortality is significant. The interaction(s) between the fungus *Candida albicans* and the epithelial cells that form the mucosal surfaces of the soft palate within the oral cavity are the focus of this study.

1.2 *Candida* species

At least 60% of humans harbour *Candida* species in various parts of the body, making *Candida* one of the most common fungal genuses that colonises humans (Odds, 1988). *Candida* species normally colonise the skin and mucosal surfaces of healthy individuals, where they coexist with the host (commensalism). However, during periods of microbial dysbiosis or impaired host immunity, *Candida* can cause infection. Infections caused by *Candida* species are predominantly superficial and occur as a consequence of fungal overgrowth at the mucosal surface (Odds, 1988). However, superficial infections caused by *Candida* can also become systemic where *Candida* species access the bloodstream. Systemic candidiasis can occur following medical procedures (Leibovitz et al., 1992), from immunosuppressive therapy following transplantation (Sganga et al., 2014), surgery (Tortorano et al., 2004) and exposure to broad spectrum antibiotics (Chahoud et al., 2013). Systemic candidiasis (often called candidaemia), is reported to be the seventh most common bloodstream infection and the fourth most recurrent infection in intensive care units with mortality rates of 40-50%, despite the use of appropriate antifungal therapies (Ostrosky-Zeichner et al., 2010). Therefore, *Candida* infections are a major clinical problem for global healthcare (Odds, 1988; Pfaller et al., 2007).

Candida infections are caused by at least 17 different *Candida* species (Sardi et al., 2013). The most common *Candida* species that cause infection are *Candida albicans*, *C. glabrata*, *C. tropicalis*, *C. parapsilosis* and *C. krusei* (Pfaller et al., 2007). More recently, *C. auris* has emerged as an important cause of *Candida* infections worldwide (Ruiz Gaitan et al., 2017). The predominant species of *Candida* responsible for invasive candidiasis in

Europe is *C. albicans* (50% of all reported cases), followed by *C. glabrata* and *C. parapsilosis* (14%), *C. tropicalis* (7%) and *C. krusei* (2%) (Tortorano et al., 2006).

1.3 *Candida* infections

There are three predominant forms of candidiasis. Candidiasis of the mouth or throat (oral thrush or oropharyngeal candidiasis); vaginal candidiasis (vaginal thrush); and candidaemia that develops when *Candida* species enter the bloodstream and disseminate throughout the body.

C. albicans accounts for approximately 50% of all reported cases of oropharyngeal candidiasis (Williams and Lewis, 2011). *Candida* infections of the oral cavity manifest with three primary forms, which are described based on clinical presentation. Pseudomembranous candidiasis (sometimes referred to as oral thrush) presents as white patches on the tongue or other areas of the mouth and throat (Reichart et al., 2000). Erythematous candidiasis frequently occurs after receipt of a broad-spectrum antibiotic, which alters the oral microbial population facilitating overgrowth of *Candida*. Erythematous candidiasis presents as reddened lesions on the dorsum of the tongue and palate (Reichart et al., 2000). Chronic hyperplastic candidiasis is usually found in middle-aged men who smoke (Arendorf et al., 1983). This form appears either as smooth or nodular white patches and is characterised by invading *C. albicans* hyphae.

Secondary forms of oral candidiasis are described as *Candida*-associated lesions. Angular cheilitis is an infection that occurs at the corners of the mouth and is often caused by co-infection of *Candida* and *Staphylococcus aureus* (Dias and Samaranayake, 1995). Another secondary form of oral candidiasis is *Candida*-associated denture stomatitis, which is a chronic inflammatory condition affecting more than 65% of individuals who wear dental prosthesis and is characterised by erythema of the palate and alveolar ridges (chronic atrophic candidiasis). *Candida* is commonly found on the acrylic surfaces of dentures where it forms biofilms, which can serve as reservoirs for recurrent infection of the palatal mucosa.

Vulvovaginal candidiasis is characterised by genital itching, burning, and sometimes white discharge from the vagina. Approximately 75% of the female population are likely to experience at least one episode of vulvovaginal candidiasis over the course of their

lifetime (Ferrer, 2000), and approximately 5% of women develop recurrent vulvovaginal candidiasis, resulting in chronic episodes of vaginal irritation that require antifungal maintenance therapy (Sobel, 2007).

In severely immunocompromised patients, *Candida* infections of the mucosa can progressively develop into severe invasive infections that culminate in the acquisition of life-threatening candidaemia (Eggimann and Pittet, 2014). In healthy individuals, translocation of *Candida* across the gut often occurs during abdominal surgery or following major trauma, and is a major risk-factor for systemic infection.

Chronic mucocutaneous candidiasis is associated with inherited disorders that result in defective $CD4^+$ T helper 17 (Th17) lymphocyte function. Chronic mucocutaneous candidiasis presents as chronic and recurrent superficial candidiasis of the skin, nails, and mucosal membranes of infected individuals (Eyerich et al., 2010).

1.3.1 Treatment of *Candida* infections

Treatment of *Candida* infections relies on an extremely limited repertoire of antifungals that are classified into three main groups: polyenes, azoles and echinocandins. Polyenes such as nystatin and amphotericin were introduced into the clinic in the 1950s as the first class of antifungals. Amphotericin kills *Candida* by specifically targeting ergosterol present in the fungal cell membrane causing pores and lysis of the cell (Sokol-Anderson et al., 1986). The azole class of antifungals were introduced during the 1980s and 1990s and are the most commonly used antifungals in the clinical setting. Three generations of azole formulations are used for the treatment of *Candida* infections and include clotrimazole, ketoconazole and fluconazole, respectively. Azoles inhibit the fungal enzyme lanosterol-14α demethylase required for the biosynthesis of ergosterol. Depletion of ergosterol from the fungal cell plasma membrane causes destabilisation of plasma membrane integrity (Odds et al., 2003). The echinocandin class of antifungals were introduced in the 2000s and are the newest class of antifungals available. Anidulafungin, micafungin and caspofungin inhibit the enzyme β-1,3 glucan synthase required for the synthesis of β-1,3 glucans found in the fungal cell wall. Depletion of β-1,3 glucans causes loss of cell wall integrity resulting in lysis of the fungal cell (Ostrosky-Zeichner et al., 2010).

The emergence of resistance to antifungals poses a significant threat to the effective treatment of *Candida* infections and indeed, to the treatment of fungal infections in general. Mechanisms of antifungal resistance in *Candida* are varied and species specific, and include mutation of the *ERG11* gene that encodes lanosterol-14αdemethylase and overexpression of drug efflux pumps (Sanglard, 2016).

In recent years, cell-wall polysaccharides (Bromuro et al., 2010; Xin et al., 2008), fungal proteins (De Bernardis et al., 2012; Ibrahim et al., 2006; Lin et al., 2009; Luo et al., 2010; Raska et al., 2005; Schmidt et al., 2012) and live attenuated fungi (Saville et al., 2008, 2009) have been studied as therapeutic targets for the development of vaccines against *Candida* infection. Despite this progress however, there are no anti-*Candida* vaccines available for clinical use at this time.

1.4 *Candida albicans* virulence factors

Among all pathogenic *Candida* species, *C. albicans* remains the most common species causing superficial and life-threatening invasive candidiasis (Hasan et al., 2009). *C. albicans* is a polymorphic fungus that is part of the resident microflora of mucosal surfaces in at least 50% of humans (Odds, 1988). Importantly, the morphological plasticity of *C. albicans* (Figure 1-1) is widely regarded to facilitate mucosal pathogenicity. Yeast growth (defined as spherical/ovoid unicellular budding cells), is typically associated with commensal carriage, whereas hyphae (defined as elongated filaments with parallel cell walls that display no constriction at the site of septation) are more closely associated with mucosal infection and pathogenesis. *C. albicans* can also adopt a pseudohyphal morphology defined as elongated filaments that are wider than hyphae and which display constrictions at the site of separation to form chains of cells (Fig 1-1).

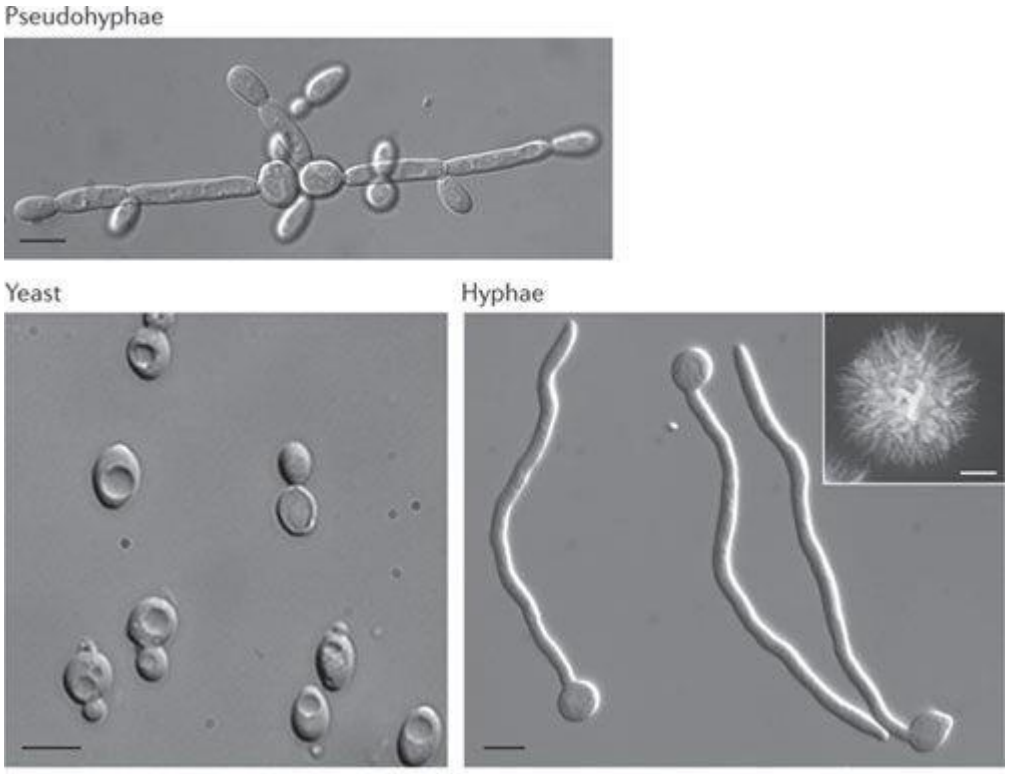

Figure 1-1. Morphological plasticity of *C. albicans*. Three panels illustrating *C. albicans* pseudohyphal, yeast and hyphal morphology. Scale bars represent 5 µm. The inset in the hyphae panel shows a hyphal colony cultured for 5 days on Spider medium. Scale bar in the inset of the hyphae panel represents 1 µm (Sudbery, 2011).

1.4.1 Hyphae

In the presence of a healthy immune system and low fungal burdens, *C. albicans* successfully colonise human mucosal surfaces without host challenge. However, changes in the effectiveness of host immune surveillance and increased fungal burdens with associated hypha formation allow *C. albicans* to initiate pathogenic growth, causing infection. Mutant strains of *C. albicans* that are unable to produce filaments are non-invasive and avirulent *in vitro* and *in vivo* (Kamai et al., 2001; Lo et al., 1997). Accordingly, the formation of hyphae is considered to be a key virulence trait.

C. albicans forms hyphae under a range of environmental conditions, such as in the presence of serum (Taschdjian et al., 1960), neutral pH (Buffo et al., 1984), 5% CO_2 (Mardon et al., 1969) and *N*-acetyl-D-glucosamine (GlcNac) (Simonetti et al., 1974). The hypha-stimulating capacity of these conditions is further enhanced by temperature (37^{o}C). Environmental cues activate signal transduction pathways and transcription factors within the fungus such as Efg1p (Stoldt et al., 1997) and Cph1p (Liu et al., 1994)

(Figure 1-2). Efg1p and Chp1p are activated through different signalling pathways. While activation of Efg1p depends on cyclic AMP (Stoldt et al., 1997), Cph1p is activated through a mitogen-activated protein kinase (MAPK) pathway (Csank et al., 1998). The activation of these transcription factors drive the expression of *EED1, UME6* and *HGC1* that are key hypha-associated genes that encode proteins involved in hypha development and maintenance (Figure 1-2). Activation of Ume6p (via Eed1p) is required for hyphal maintenance, whereas Hgc1p is a hypha-specific cyclin required for the initiation of germ tube development and long-term hyphal maintenance (Sudbery, 2011).

When *C. albicans* yeast cells initiate the switch to hyphal growth, a single germ tube emerges from the yeast cell and elongates. Elongation of hyphal cells is characterised by polarized growth (Soll et al., 1985; Sudbery, 2001) and inhibition of cell separation, which is Hgc1p-dependent in association with Cdc28p (Wang et al., 2009) (Figure 1-2). During germ tube extension the nucleus migrates out of the mother cell in the tube where it undergoes mitosis. As the hypha continues to grow, septa are created which divide new daughter cells, generating a mature hyphae consisting of a linear chain of elongated cells.

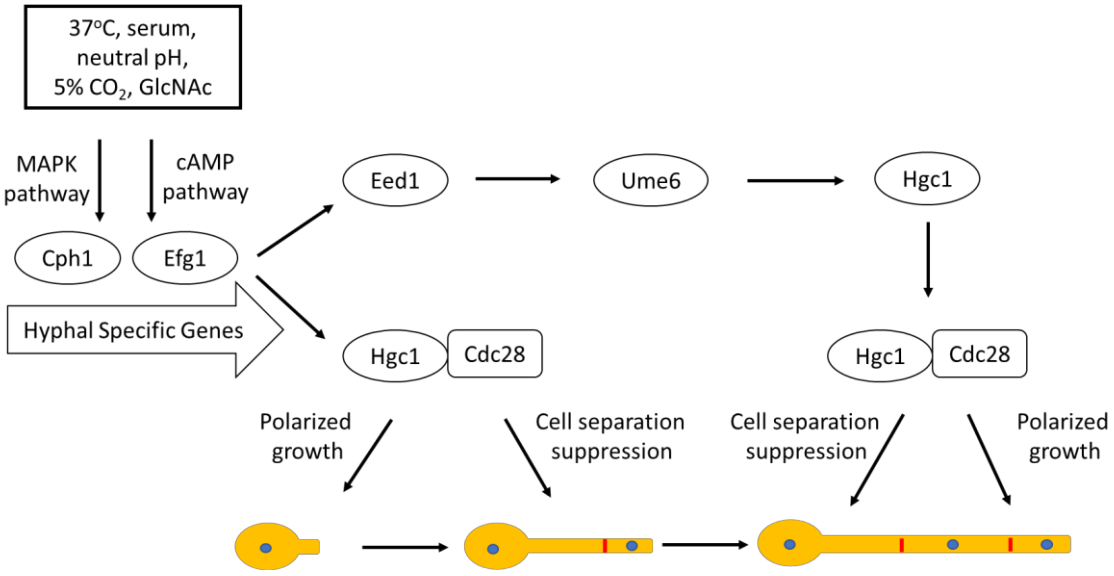

Figure 1-2. Summary of hyphal induction in *C. albicans*. Environmental stimuli induce signal transduction, activation of transcription factors (Efg1p and Cph1p) and the expression of hyphal associated genes. Emergence of a polarized germ tube occurs through Hgc1p-Cdc28p. Long-term maintenance is dependent on Eed1p and Ume6p expression. Adapted from (Sudbery, 2011).

1.4.2 *C. albicans* virulence factors

The activation of *C. albicans* signal transduction pathways results in the expression of hypha-associated virulence factors that promote pathogenicity but are not required for hyphal growth *per se*. These genes encode for hyphal wall protein 1 (Hwp1p), secreted aspartyl protease (Sap) family proteins, agglutinin-like sequence 3 protein (Als3p), extent of cell elongation 1 protein (Ece1p) and hyphal regulated 1 protein (Hyr1p). These hyphal proteins play crucial roles during specific stages of *C. albicans* infection. These stages can be divided into adhesion, invasion and damage to host cells (Figure 1-3).

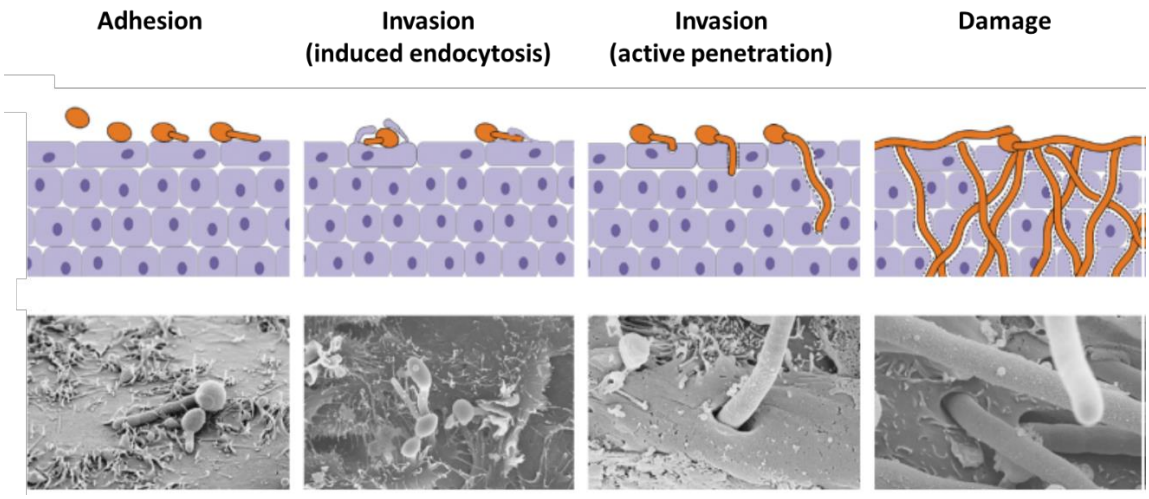

Figure 1-3. Stages of *C. albicans* mucosal infection. Representative schematic panels and scanning electron micrographs showing the initiation and progression of a *C. albicans* infection in human oral epithelial cells. The three main stages of infection include adhesion, invasion (induced endocytosis and/or active penetration) and tissue damage (Wilson et al., 2009).

1.4.3 Adhesion

Adhesion of *C. albicans* to host epithelial cells is an important step required for mucosal colonisation and infection. Initial adhesion between *C. albicans* yeast and epithelial cells promotes hyphal growth (Moyes et al., 2015). Hyphal growth is accompanied by the expression of specific adhesins that facilitate strong attachment to the epithelial surface. Indeed, the hyphal morphology of *C. albicans* is considered to be more adherent when compared with the corresponding yeast morphology (Sandin et al., 1982).

The most studied *C. albicans* adhesins comprise the Als protein family consisting of eight members (Als1-7p and Als9p). Als are glycosylphosphatidylinositol (GPI) proteins that

are linked to the β-1,6-glucans present in the fungal cell wall (Hoyer, 2001). Als are thus located on the surface of *C. albicans* and are able to interact with host proteins. Als family members share three distinct domains; an N-terminal domain which contains the substrate binding region, a central serine/threonine-rich domain with variable tandem repeat sequences, and a C-terminal domain containing the GPI-anchor sequence (Hoyer, 2001). Studies conducted with *C. albicans* deletion mutants demonstrated the importance of Als1p, Als2p, Als3p and Als4p in the ability of *C. albicans* to adhere to epithelial cells (Kamai et al., 2002; Zhao et al., 2004; Zhao et al., 2005). In contrast, deletion of *ALS5*, *ALS6* or *ALS7* increases the adhesion of *C. albicans* to epithelial cells (Zhao et al., 2007).

Hwp1p is another important adhesin that mediates interaction with host epithelial cells. Host transglutaminase enzymes cross-link *C. albicans* hyphae (via the N-terminus of Hwp1p) to the epithelial surface (Staab et al., 2004; Staab et al., 1999). Hwp1p plays an essential role in *C. albicans* adhesion, as a *hwp1*Δ/Δ null mutant strain was unable to cause oropharyngeal candidiasis in mice (Sundstrom et al., 2002).

Other *C. albicans* adhesins include the enhanced adherence to polystyrene 1 protein (Eap1p), responsible for adherence to polystyrene beads, epithelial cells and *Streptococcus gordonii* (Li and Palecek, 2003, 2008). *C. albicans* Iff4p is another protein involved in *C. albicans* adhesion*;* since overexpression of *IFF4* results in increased adherence to oral epithelial cells and increased virulence in a mouse model of vulvovaginal candidiasis (Fu et al., 2008). Other proteins reported to be important during *C. albicans* adhesion to the host but which have not been characterised in terms of their structure and/or capacity to mediate attachment to epithelial cells include, fimbriae (Yu et al., 1994), Csh1p (Singleton et al., 2005), Ywp1p (Granger et al., 2005) and Pra1p (Soloviev et al., 2007).

1.4.4 Invasion

Adhesion of *C. albicans* to the host epithelium is a critical event that precedes invasion of the fungus into the mucosa and underlying tissues. The invasion stage is essential for the pathogenesis of candidiasis and can occur through two distinct mechanisms: induced endocytosis and active penetration (Wachtler et al., 2012).

1.4.4.1 Induced endocytosis

Induced endocytosis is triggered by *C. albicans* in numerous epithelial cell lines, including HeLa cervical cells (Drago et al., 2000), HET1-A oesophageal cells (Enache et al., 1996), TR146 buccal cells (Dalle et al., 2010), FaDu pharyngeal cells (Park et al., 2005), OKF6/TERT-2 oral epithelial cells (Zhu et al., 2012) and reconstituted human epithelium (Zakikhany et al., 2007). Induced endocytosis is a host-driven process since dead hyphae are engulfed similarly to live hyphae (Park et al., 2005). *C. albicans* Als3p and Ssa1p are two key proteins that stimulate the uptake of fungus into the epithelial cell.

Both Als3p and Ssa1p are thought to bind to epithelial E-cadherin, epithelial growth factor receptor (EGFR) and human EGF receptor 2 (HER2), activating the clathrin-dependent endocytosis machinery (Moreno-Ruiz et al., 2009; Phan et al., 2007; Sun et al., 2010; Zhu et al., 2012). The endocytosis pathway involves the recruitment of clathrin, dynamin and cortactin to the site of hyphal engulfment and results in cytoskeleton reorganization (Moreno-Ruiz et al., 2009). siRNA knockdown of proteins involved in this pathway reduced endocytosis by 60% (Moreno-Ruiz et al., 2009). The incomplete inhibition of endocytosis suggests that other pathways may be involved in this process. Indeed, pathways such as PDGF BB (platelet-derived growth factor BB) and NEDD9 (neural precursor-cell-expressed developmentally downregulated protein 9) have been implicated in *C. albicans* endocytosis (Liu et al., 2015). Furthermore, recent work has demonstrated a role for the aryl hydrocarbon receptor (AhR) in the endocytosis of *C. albicans* through Src family kinase phosphorylation of EGFR (Solis et al., 2017). However, the fungal ligand(s) responsible for AhR activation has yet to be identified.

1.4.4.2 Active penetration

Active penetration is a fungal-driven process that requires live hyphae to penetrate through epithelial cells or pass between intercellular junctions between epithelial cells (Dalle et al., 2010). Active penetration of oral mucosal surfaces is particularly important, since the upper most layer of oral epithelium is comprised of differentiated, non-proliferative cells that are incapable of mediating endocytosis. Thus, in order to breach the mucosal barrier to cause infection, *C. albicans* must invade these cells through the alternative route of active penetration (Naglik and Moyes, 2011). The specific mechanism by which active penetration occurs has yet to be elucidated. However, factors that contribute to this process include hyphal extension, physical force exerted

by elongating hyphae and the secretion of hydrolytic enzymes (Villar et al., 2007; Wachtler et al., 2012). Different mechanisms of invasion can be observed depending on the type of epithelial cell. For instance, oral epithelial cells are invaded through endocytosis and active penetration (Wachtler et al., 2012), whereas gastrointestinal epithelial cells are invaded via active penetration only (Dalle et al., 2010).

Many studies have reported an important contribution of Saps in active penetration by *C. albicans* (Dalle et al., 2010; Naglik et al., 2008; Wachtler et al., 2012). Pre-treatment of epithelial cells with the inhibitor pepstatin A (inhibits Sap activity) caused a partial reduction (but not complete elimination) of invasion and epithelial damage (Naglik et al., 2008; Ruchel et al., 1990; Schaller et al., 1999). Saps have been demonstrated to contribute to invasion through various mechanisms, including the degradation of host glycoproteins such as mucins and E-cadherins (Colina et al., 1996; Villar et al., 2007). However, the role of Saps in the process of active penetration remains controversial, since work has also demonstrated that Sap1–6p play a limited role during invasion *in vitro* (Lermann and Morschhauser, 2008) and *in vivo* (Correia et al., 2010).

The phospholipases are a family of secreted hydrolytic enzymes that degrade a variety of phospholipids (Ghannoum, 2000). Phospholipase *PLB1* has been proposed to contribute to *C. albicans* active penetration by degrading host lipids found in epithelial cell plasma membranes (Ghannoum, 2000). However, a *C. albicans PLB1*-deficient mutant was observed to invade epithelial cells with no loss of efficiency (Dalle et al., 2010), thus the contribution of *PLB1* to *C. albicans* active penetration remains controversial.

Lipases are hydrolytic enzymes encoded by *LIP1-10* gene family. The lipases of *C. albicans* have been implicated in fungal invasion (Hube et al., 2000), however the role of lipases in invasion remains controversial. A *C. albicans lip8*Δ/Δ mutant was observed to have reduced virulence in a mouse model of systemic infection (Gacser et al., 2007). However, ibogaine-mediated inhibition of lipase activity did not reduce invasion in oral epithelial cells and enterocytes, suggesting that lipases contribute little to the process of active penetration (Dalle et al., 2010).

1.4.5 Damage

Following invasion of the mucosal surface, a characteristic manifestation of oropharyngeal candidiasis is loss of superficial epithelium through epithelial damage caused by invading *C. albicans* (Villar et al., 2007). Epithelial damage requires *C. albicans* filamentation (hyphae), adhesion and invasion. Importantly, epithelial cells can internalise dead *C. albicans* hyphae but are not damaged (Park et al., 2005), suggesting that epithelial damage is fungus-driven and requires the production of damage-inducing factors.

The *C. albicans ECE1* gene encodes the damage-inducing factor required for infection of mucosal surfaces (Moyes et al., 2016). A *C. albicans ece1*Δ/Δ mutant can grow as hyphae, adhere to and invade epithelial cells, but is incapable of causing damage *in vitro* and *in vivo* (Moyes et al., 2016). *ECE1* encodes a 271 amino acid protein (Ece1p) which is enzymatically cleaved by the endoproteinase Kex2p (Bader et al., 2008). Ecep1 is cleaved into eight distinct peptides, one of which (SIIGIIMGILGNIPQVIQIIMSIVKAFKGNKR (Ece1p$_{62-93}$)) is further processed by the carboxyproteinase Kex1p, which removes the terminal arginine (R) to produce mature Candidalysin (SIIGIIMGILGNIPQVIQIIMSIVKAFKGNK (Ece1p$_{62-92}$)) (Moyes et al., 2016). Candidalysin is an amphipathic 31 amino acid cytolytic toxin that is secreted from *C. albicans* hyphae during mucosal infection. Oral epithelial cells respond to Candidalysin in a dose dependent manner, with sub-lytic Candidalysin concentrations (< 15 μM) activating pro-inflammatory responses, and lytic Candidalysin concentrations (> 15 μM) causing epithelial damage and robust pro-inflammatory responses (Moyes et al., 2016). Like *ece1*Δ/Δ, a *C. albicans* mutant in which only the region of *ECE1* encoding Candidalysin was deleted (*ece1*Δ/Δ+*ECE1*$_{\Delta 184-279}$) was also unable to cause epithelial damage, pro-inflammatory responses or mucosal infection *in vivo* (Moyes et al., 2016). These data identify Candidalysin as a critical factor required for *C. albicans* pathogenesis and immune activation at mucosal surfaces.

1.5 Physical barriers against *C. albicans* infection

Pathogens persist within a specific niche by virtue of virulence factors, which permit microbial survival and dissemination in the host. Pathogenic dissemination is associated

with cell and tissue damage. Damage at the cellular level includes apoptosis and different forms of necrosis, whereas damage at the tissue level includes granulomatous inflammation, fibrosis and tumour growth (Casadevall and Pirofski, 2014).

The *C. albicans*-host interaction is characterised by a complex interplay between fungal virulence factors and host protective mechanisms. The host adopts different protective strategies to prevent fungal invasion and restrict the fungus to the commensal state. Epithelial cells can function as a passive physical barrier against microorganisms, protecting the underlying tissue from invasion. This physical protection is provided by a network of strong inter-epithelial cell connections called tight junctions, which maintain the structural integrity of the mucosal barrier. Furthermore, goblet cells present within the epithelia secrete mucins that reduce direct contact of *C. albicans* with the mucosal surface (Linden et al., 2008). In the oral cavity, saliva can prevent adhesion of *C. albicans* to mucosal and dental surfaces through constant flushing (Bokor-Bratic et al., 2013) and through antimicrobial agents contained in saliva such as lysozyme, lactoferrin, histatins, cathelicidins, calprotectins and defensins (Hibino et al., 2009).

1.6 Host immune responses against *C. albicans* infection

In addition to the physical barrier provided by the mucosal surface, the epithelial cells that comprise mucosal barriers are capable of recognising *C. albicans* and directing appropriate immune responses during mucosal infection.

1.6.1 Host recognition of microbes

Host cells use pattern recognition receptors (PRRs) to recognise microbes. PRRs modulate host immunity via inflammation and cell death (Broz and Monack, 2013; Mogensen, 2009) and are required to interact with specific molecular structures present on microbes called pathogen associated molecular patterns (PAMPs). PRRs are also capable of interacting with danger associated molecular patterns (DAMPs), which are released from infected tissues or tissues undergoing destruction. There are three main families of PRRs; toll-like receptors (TLRs), C-type lectin receptors (CLRs) and nucleotide-binding domain leucine-rich receptors (NLRs). These receptors can be expressed at the cell surface, in endosomes or in the cytoplasm of cells. The ligation of extracellular or intracellular PRRs with PAMPs or DAMPs induces the expression of chemokines,

antimicrobial peptides and pro-inflammatory cytokines required for clearance of the infecting microbe. Expression of PRRs varies in a tissue- and cell-specific manner, and since PRRs recognise different classes of PAMP, different responses to microbes may occur. The interactions known to occur between host PRRs and *C. albicans* PAMPs are summarised in Table 1.

Table 1. Host PRRs that recognise *C. albicans* PAMPs.

Family	Host PRR	Fungal PAMP	Reference
TLR	TLR2	Phospholipomannan	(Jouault et al., 2003)
	TLR3	Double-stranded RNA	(Muller et al., 2007)
	TLR4	Mannan O-linked Mannan residues	(Tada et al., 2002) (Netea et al., 2006)
	TLR9	CpG DNA	(Miyazato et al., 2009)
CLR	Dectin-1	β-1,3-glucan	(Brown and Gordon, 2001)
	Dectin-2	High-mannose structures α-mannans	(McGreal et al., 2006) (Sato et al., 2006)
	Mannose receptor	Mannan	(Ezekowitz et al., 1990)
	MINCLE	High-mannose structures	(Wells et al., 2008)
	Galectin-3	β-1,2-Mannosides	(Jouault et al., 2006)
	DC-SIGN	High-mannose structures	(Cambi et al., 2003)
NLR	NLRP3	DAMPs?	(Gross et al., 2009)
	NLRC4	DAMPs?	(Tomalka et al., 2011)
Others	Cdw17	?	(Jimenez-Lucho et al., 1990)
	EphA2	β-glucans	(Swidergall et al., 2017)

PRR-PAMP interaction studies between host and *C. albicans* have focused on fungal recognition by myeloid cells rather than epithelial cells. However, epithelial cells express a range of PRRs including dectin-1, galectins and several TLRs that are expressed constitutively in the oral epithelium.

TLR2 and TLR5 are strongly expressed in oral epithelial cells (Shaykhiev et al., 2008) while TLR4 is expressed at low levels (Backhed and Hornef, 2003), suggesting that epithelial cells may not respond effectively to stimulation by TLR4 ligands such as lipopolysaccharide (LPS) and thus Gram-negative bacteria. Indeed, it has been reported that TLR2, TLR4, and Dectin-1 are not involved in activating epithelial immune responses to *C. albicans* as blockade or inhibition of these receptors did not affect cytokine responses (Moyes et al., 2010). However, an indirect mechanism of epithelial immunity to *C. albicans* exists that is mediated through epithelial TLR4. Following challenge with *C. albicans*, epithelial cells respond by secreting immune modulators that stimulate neutrophils to produce TNFα, which in turn induces upregulation of TLR4 at the epithelial surface, enhancing protection against *C. albicans* infection (Weindl et al., 2007). More recently, the epithelial receptor tyrosine kinase Ephrin A2 (EphA2) has been identified an epithelial receptor for β-glucans on *C. albicans* yeast cells that stimulates a pro-inflammatory anti-fungal response (Swidergall et al., 2017).

Together, these observations suggest that epithelial cells may use different receptors and mechanisms for the recognition of *C. albicans* compared with myeloid cells.

1.6.2 Innate responses to *C. albicans*

Epithelial cells respond to *C. albicans* via the NF-κB and MAPK signalling pathways (Moyes et al., 2010; Moyes et al., 2014; Moyes et al., 2016). Activation of the MAPK pathway appears crucial for the ability of epithelial cells to discriminate between the yeast and hyphal morphologies of *C. albicans*, and to induce appropriate innate immune responses to infecting fungus (Moyes et al., 2010). Epithelial cells respond to the presence of *C. albicans* in a "biphasic" fashion. Initially, responses to colonising yeast include activation of the NF-κB and PI3K signalling pathways, together with a weak and transient activation of all three MAPK pathways (p38, JNK and ERK1/2) (Figure 1-4). JNK and ERK1/2 activate the transcription factor c-Jun, whereas the role played by p38 during the colonisation stage is presently unknown. Nevertheless, the transient activation of signalling pathways appears to result in a non-inflammatory response since no inflammatory mediators are secreted from epithelial cells following challenge with the yeast morphology (Figure 1-4).

In contrast, as hyphal burdens increase at the mucosal surface and fungal invasion occurs (a process that is accompanied by Candidalysin secretion), epithelial cells

respond with a robust and sustained activation of NF-κB, MAPK and PI3K signalling (Figure 1-4). The activation of these pathways (and in particular the p38 pathway), lead to the activation of the c-Fos transcription factor and a strong induction of inflammatory responses mediated by the secretion of immune modulators. Immune modulators include cytokines, chemokines and antimicrobial peptides including interleukin (IL)-1α, IL-8, granulocyte colony-stimulating factor (G-CSF), granulocyte-macrophage colony-stimulating factor (GM-CSF), β-defensin 3, C-C motif chemokine ligand 20 (CCL20) and S100 calcium-binding protein A8/A9 (S100A8/9). In addition, ERK1/2 activation induces the phosphorylation of MAPK phosphatase 1 (MKP1), which regulates MAPK-induced immune responses by inhibiting the activation of p38 and JNK (Figure 1-4). The PI3K signalling pathway (activated via mTOR) appears to participate in protecting the epithelial tissue from hypha-induced damage (Moyes et al., 2014) (Figure 1-4).

The MAPK pathway is thus clearly implicated in multiple physiological processes (Zhang and Liu, 2002). Despite its importance however, the study of MAPK signalling using *in vivo* models is hampered due to the embryonic lethality of p38, JNK, ERK1/2 and MKP1 gene knockouts in mice (Mudgett et al., 2000; Satoh et al., 2011; Yamasaki et al., 2012; Zhao et al., 2006). Consequently, studies describing candidiasis in these models is lacking.

Recently, it was shown that *C. albicans* strains lacking *ECE1* or the Candidalysin encoding region of *ECE1*, were unable to trigger p38/p-MKP1/c-Fos activation or inflammatory mediators in oral epithelial cells (Moyes et al., 2016). *C. albicans ECE1* or Candidalysin null strains were also attenuated in a murine model of oropharyngeal candidiasis and a zebrafish swimbladder model, concomitant with a lack of epithelial damage and neutrophil recruitment (Moyes et al., 2016). Therefore, epithelial activation and immune induction by *C. albicans* hyphae seems to be largely due to the damage-inducing activity of Candidalysin.

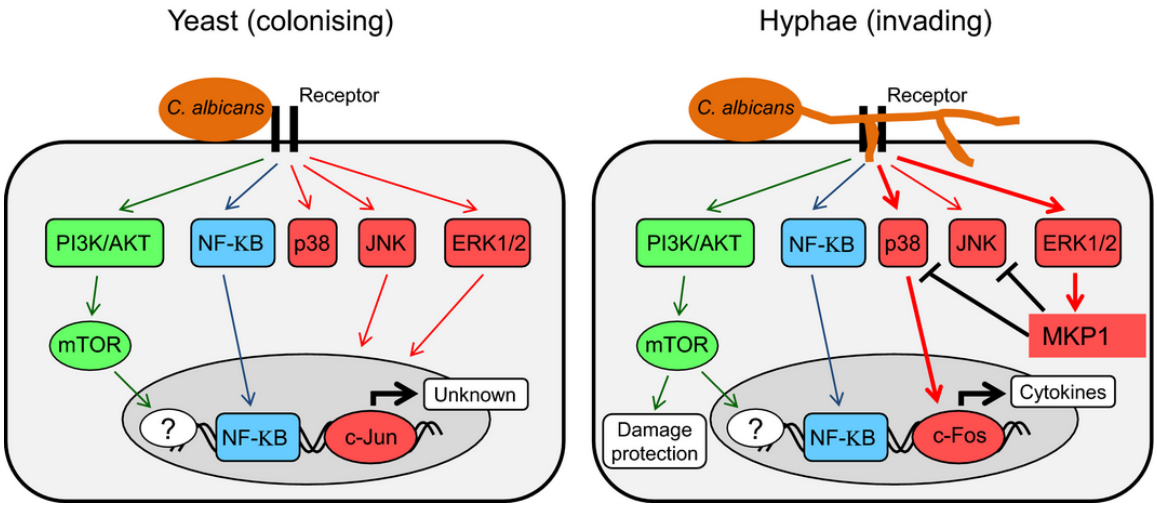

Figure 1-4. Epithelial responses to *C. albicans* yeast and hyphae. Epithelial responses to *C. albicans* yeast and hyphae involve activation of MAPK pathways. Epithelial colonisation by yeast triggers a weak and transient activation of PI3K/NF-κB/p38/JNK/ERK1/2/c-Jun signalling, resulting in a non-inflammatory response. In contrast, the presence of Candidalysin-producing hyphae stimulates robust activation of PI3K/NF-κB/p38/JNK/ERK1/2/MKP1/c-Fos signalling and subsequent secretion of immune modulators (Tang et al., 2016).

Fungal invasion of the mucosal surface, concomitant with Candidalysin activity, results in the secretion of immune modulatory cytokines from epithelial cells, which stimulate the recruitment of host immune cells to the site of infection, thus invoking both innate and adaptive defences against *C. albicans* infection (Figure 1-5).

Epithelial cells respond to Candidalysin-producing *C. albicans* hyphae by releasing IL-1α, IL-8, G-CSF, GM-CSF, β-defensin 3, CCL20 and S100A8/9 (Moyes et al., 2010; Moyes et al., 2016). Production of these molecules promotes the recruitment of neutrophils, monocytes, macrophages, innate type 17 cells (T cell receptor αβ (TCR αβ) positive) and dendritic cells (DCs) to the site of infection, which help combat the infecting fungus (Naglik and Moyes, 2011; Verma et al., 2017). Once these immune cells are recruited, recognition of the fungus occurs through interaction of host TLR2, TLR3 TLR4 and TLR9 with *C. albicans* cell wall mannans and nucleic acids, and through interaction of host CLRs such as Dectin-1 and Dectin-2, DC-SIGN or Mincle with *C. albicans* cell wall β-glucan and mannose structures (Netea et al., 2006) (Table 1). These interactions drive the induction of NF-κB/MAPK/Syk signalling pathways and secretion of immune modulators.

Neutrophils are key players in the antifungal response and phagocytose *C. albicans* yeast and short hyphae through TLR- and CLR-mediated interactions, which results in fungal engulfment and killing via oxidative mechanisms. Long hyphae can be killed by

neutrophil extracellular traps (NETs) (Urban et al., 2006). Innate Type 17 cells (T cell receptor αβ (TCR αβ) positive) are also recruited and activated via the IL-1 receptor (IL-1R) in response to IL-1α and IL-1β secreted from epithelial cells due to Candidalysin activity (Verma et al., 2017). These innate TCR αβ T cells secrete IL-17, which further recruits neutrophils and promotes mucosal barrier function (Verma et al., 2017).

In addition to TLRs and CLRs, NLRs are activated by DAMPs leading to inflammasome activation, induction of pyroptosis and IL-1β and IL-18 release to help combat infection (Cheng et al., 2012). This mechanism is explored in further detail in Section 1.7.4.2.

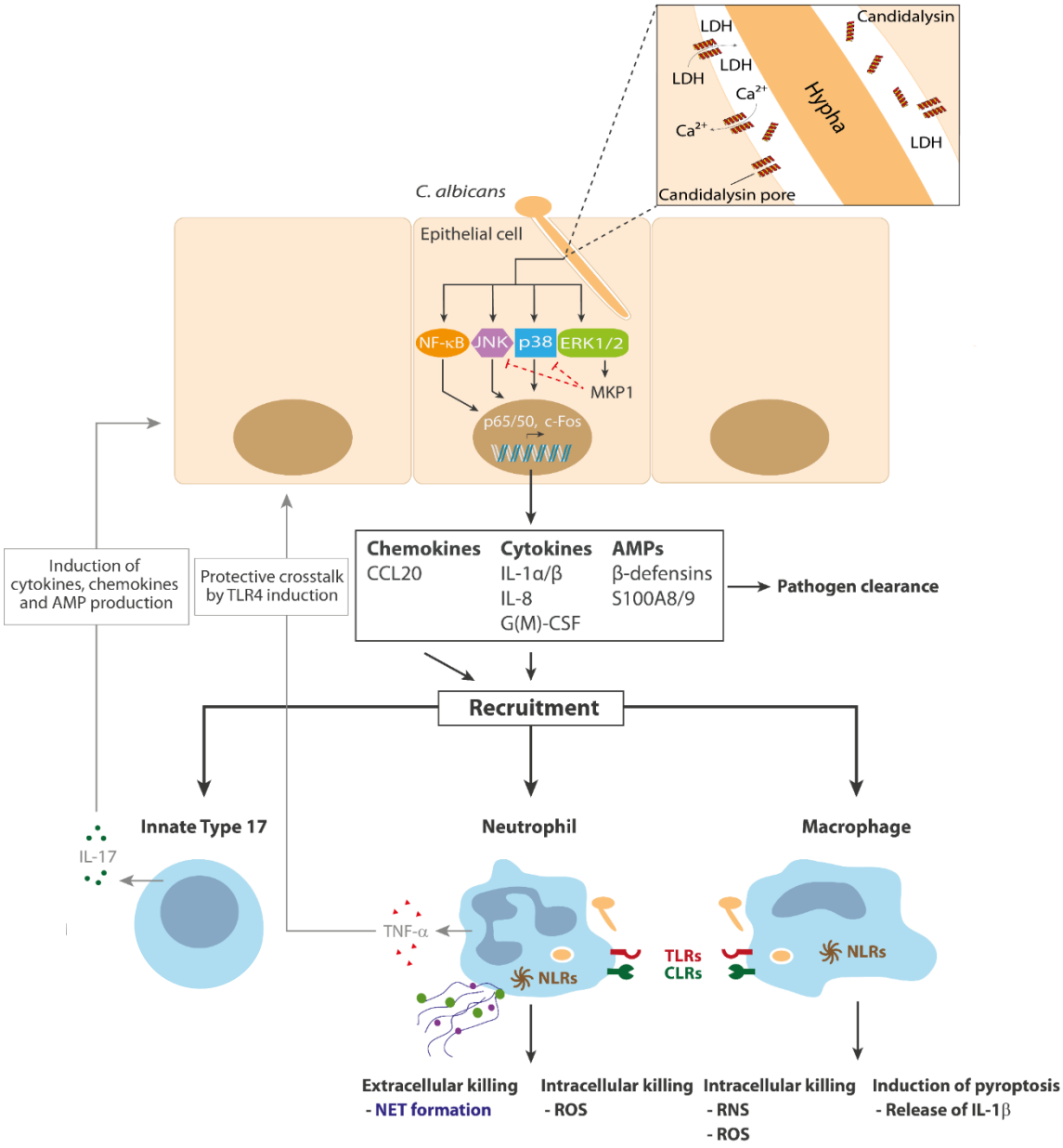

Figure 1-5. Epithelial induction of innate immunity during *C. albicans* infection. Invasion and damage of epithelial cells due to Candidalysin activity results in the production of immune modulators through the NF-κB/p38/MAPK pathways. Immune modulators in turn recruit immune cells to the site of infection. Neutrophils and macrophages are involved in fungal phagocytosis and removal through NET formation, intracellular oxidative stress and pyroptosis. Innate type 17 cells facilitate inflammatory protective responses. Adapted from (Naglik et al., 2017).

1.6.3 Adaptive responses to *C. albicans*

DCs are a key link between innate and adaptive antifungal host immune responses. DCs are recruited to the site of infection in response to chemokines and antimicrobial peptides including CCL20 and β-defensins that are secreted from infected epithelial cells (Netea et al., 2008). Recognition of the *C. albicans* PAMP β-glucan by the DC PRR Dectin-

1 leads to activation of Syk/Caspase recruitment domain-containing protein 9 (CARD9) signal transduction within DCs (Rogers et al., 2005; Taylor et al., 2007). Upon fungal recognition, DCs phagocytose and degrade the fungus into antigens that are assembled onto class II molecules of the major histocompatibility complex (MHC II) and transported to the surface of the activated DC. This process of antigen presentation occurs as the DC migrates to the local lymph node where the MHC:antigen complexes are presented to naïve $CD4^+$ T-helper (Th) cells. Following antigen recognition by a naïve Th cell, cytokines produced by the DC stimulate T-cell subset differentiation into one of four classes (Th1, Th2, Th17 or Treg (regulatory)).

In recent years, it has been determined that Th17 cells are the predominant cell type that confer protection against *C. albicans* infections at different mucosal sites in the body (Hernandez-Santos et al., 2013). Th17 cells secrete IL-17A, IL-17F and IL-22 cytokines, which play a key role in the recruitment and activation of neutrophils and enhancement of epithelial barrier function (De Luca et al., 2010; Huang et al., 2004). Mice deficient in the IL-17 receptor exhibit an increased susceptibility to oropharyngeal (Conti et al., 2009) and systemic candidiasis (Huang et al., 2004). Individuals with inherent disorders in Th17 antifungal responses often manifest chronic mucocutaneous candidiasis (Puel et al., 2011), highlighting the importance of the Th17 response against *C. albicans* infections.

1.7 Host cell death as a defence against infection

Host cell death is a fundamental defence mechanism that occurs in response to microbial infection. Cell death sacrifices infected cells for the benefit of remaining tissues. Historically, apoptosis was thought to be the only programmed cell death pathway involved in cell development, homeostasis, infection and pathogenesis (Elmore, 2007), whereas necrosis was considered to occur incidentally following physiochemical insult. Recently however, significant advances in our understanding of cell death processes and identification of pathways that describe regulated necrotic events have changed this historical viewpoint (Vanden Berghe et al., 2014). The signalling pathways that promote cell death are present in all somatic cells in the body and play a crucial role in eliminating infected cells and triggering inflammatory

responses (Moriwaki and Chan, 2013). Biological processes including apoptotic, necrotic, necroptotic and pyroptotic cell death are critical defence mechanisms against microbial infection (Jorgensen et al., 2017). Indeed, cell death in response to specific microbial stimuli can be induced as a host innate immune response.

Cells undergoing apoptosis may indirectly contribute to host immunity through the release of chemoattractant molecules that recruit DCs that subsequently phagocytose dying cells and infecting microbes, and thus may contribute to a protective immune response (Elliott and Ravichandran, 2010). Necrotic death modalities play a critical role in host defence by releasing a plethora of immune modulators that recruit a variety of immune cells to combat the infecting pathogen (Jorgensen et al., 2017).

However, pathogens can also benefit from host cell death, as destruction of the cellular niche can facilitate infection of neighbouring cells, evasion of immune cells and acquisition of nutrients. Thus, to maintain their replicative niche within the host, pathogenic microbes have developed multiple mechanisms to manipulate host cell death and survival pathways (Labbe and Saleh, 2008; Lamkanfi and Dixit, 2010). For instance, some pathogens trigger death of immune cells to destabilise host defence mechanisms and avoid elimination from the host. In this regard, microbes have evolved mechanisms to cause host cell death and kill phagocytes in order to prevent pathogen clearance and promote pathogenicity. A major contributor to host cell death involves the production of microbial pore-forming toxins (Bischofberger et al., 2012). Bacteria such as *Staphylococcus aureus* (Kitur et al., 2015), *Bacillus anthracis* (Fink et al., 2008), *Pseudomonas aeruginosa* (Morimoto and Bonavida, 1992) and *Bordetella pertussis* (Khelef et al., 1993) can produce pore-forming toxins that kill macrophages before phagocytosis occurs. In contrast, *Chlamydiae* spp. require a viable host cell in order to replicate and spread. Indeed, *Chlamydiae* spp. prevent infected cells from undergoing cell death by blocking apoptosis via inhibition of cytochrome c release from the mitochondria (Fan et al., 1998).

Pathogenic bacteria such as *Streptococcus pneumoniae* (Gonzalez-Juarbe et al., 2017; Hirst et al., 2002), *Clostridium difficile* (Chumbler et al., 2012) and *Staphylococcus aureus* (Gonzalez-Juarbe et al., 2017) use pore-forming toxins to facilitate epithelial cell death, invasion, and the development of systemic infection. However, pathogens are also able to inhibit epithelial cell death to facilitate successful infection. For example, *Neisseria*

gonorrhoae has evolved mechanisms to inhibit epithelial cell death in order to maintain its replicative niche and successfully colonise the epithelium (Nudel et al., 2015).

Host–pathogen interactions and their role in cell death are thus highly complex, involving a fine balance between pro- and anti-death strategies for both host and pathogen. Different mechanisms of host cell death are triggered in response to different microbes. However, apoptosis, necrosis, necroptosis and pyroptosis are the most common cell death pathways observed to be activated during microbial infection (Bergsbaken et al., 2009; Lamkanfi and Dixit, 2010; Zitvogel et al., 2010). The main features of these cell death modalities will be described in the following sections.

1.7.1 The interplay between apoptosis and necrosis

Apoptosis and necrosis are the two major modes of cell death. Initially these processes were viewed as mutually exclusive cellular states; however, recent findings reveal that there is interplay between apoptosis and necrosis. Many death initiators, effector molecules and organelles have been identified as key mediators of both processes, either by playing a role in both death modalities or by functioning as regulators that determine which fate the cell will undertake.

Both apoptosis and necrosis are initiated in cells that receive stress signals classified as extracellular (such as damage, PAMPs and/or DAMPs), or intracellular (including mitochondrial damage, oxidative stress and alterations in the level of intracellular ATP and calcium) (Fulda et al., 2010). Both extracellular and intracellular stress signals are able to initiate destabilisation of the host cell plasma membrane; either directly by causing damage, or indirectly by inducing changes in the composition of the lipid bilayer. The cell plasma membrane exhibits considerable asymmetry in its bilayer. The outer leaflet of the plasma membrane contains large quantities of sphingomyelin (SM) and phosphatidylcholine (PC), while the inner leaflet has an abundance of phosphatidylserine (PS) and phosphatidylethanolamine (PE) (van Meer, 1989). This asymmetry plays an important role in the process of apoptosis (Fadeel and Xue, 2009). Indeed, during apoptosis PS is redistributed to the outer leaflet of the plasma membrane, an essential step for the recognition of apoptotic cells by macrophages (Fadok et al., 1992). While apoptotic cells maintain an intact plasma membrane and exhibit changes in lipid bilayer stoichiometry, necrosis is characterized by plasma

membrane rupture that causes release of intracellular contents, which attract immune cells and initiate inflammation (Elmore, 2007; Hirsiger et al., 2012).

During cell death, extracellular and intracellular stress signals affect cell organelles, in particular the mitochondria that play a critical role during both apoptotic and necrotic processes (Orrenius et al., 2007). The importance of mitochondria in cell death is linked to their role as a major source of reactive oxygen species (ROS), the majority of which are generated on the inner mitochondrial membrane (IMM), via complex I and III of the respiratory chain (Brand et al., 2004). Reactive products of oxygen are extremely damaging to cells. Extracellular or intracellular sources of ROS can cause auto-oxidation of mitochondrial electron transport chain components generating toxic free radicals that can be neutralised by antioxidant enzymes such as superoxide dismutases (SODs) (Genestra, 2007). Cells maintain equilibrium between pro-oxidant species and antioxidant defence mechanisms, but when this balance is disturbed, oxidative stress occurs (Brune, 2005). Sustained production of ROS can cause oxidation of macromolecules including nucleic acids, proteins, carbohydrates and lipids that can lead to apoptotic or necrotic cell death (Orrenius et al., 2007).

Increases in ROS are associated with cytochrome c release from mitochondria and activation of the apoptotic caspase cascade (Orrenius et al., 2007). Cytochrome c is normally bound to the IMM in association with the phospholipid cardiolipin (Ott et al., 2002). Dissociation of cytochrome c from the IMM is promoted by ROS-dependent oxidation of cardiolipin. Oxidation of cardiolipin, together with permeabilization of the outer mitochondrial membrane (OMM) by pro-apoptotic proteins enables release of cytochrome c into the cytosol and propagation of the apoptotic signal (Ott et al., 2002).

However, ROS can also circumvent apoptosis to induce necrotic death by two distinct mechanisms; inactivation of caspases or by reducing levels of intracellular ATP. Inactivation of caspases by ROS is driven through the oxidation of the active site cysteine nucleophile contained in all caspase enzymes (Hampton and Orrenius, 1997; Samali et al., 1999). Depletion of intracellular ATP can occur following ROS-induced damage to the IMM via lipid peroxidation, resulting in loss of mitochondrial membrane potential and consequently, loss of ATP production (Chen et al., 1995). The level of intracellular ATP can influence whether cell death occurs by apoptosis or necrosis; successful execution of the apoptotic program is energy-dependent, while depletion of ATP prevents

apoptosis and instead promotes death by necrosis (Eguchi et al., 1997). In addition to the production of ROS and ATP, mitochondria play a crucial role in the regulation of intracellular calcium homeostasis. Calcium signals orchestrate a variety of critical cell functions and are necessary for cell survival (Contreras et al., 2010). However, it is also well established that calcium influx or perturbation of intracellular calcium compartmentalisation, can cause cytotoxicity, resulting in apoptotic or necrotic cell death (Zhivotovsky and Orrenius, 2011).

Mitochondria can take up and retain calcium, thereby participating actively in the process of intracellular calcium compartmentalisation (Carafoli, 2002). Under pathological conditions, levels of cytosolic calcium often rise. In response, excess cytosolic calcium is stored by the mitochondria in the matrix of the organelle (Kim et al., 2003). However, accumulation of excessive calcium in the mitochondrial matrix activates the mitochondrial permeability transition (MPT). The MPT is a process that results in the IMM becoming permeable to molecules responsible for maintaining the osmotic balance between the mitochondrial matrix and the mitochondrial intermembrane space. Following IMM permeabilisation, aqueous solutions move from the intermembrane space into the matrix, causing mitochondrial swelling that culminates in disruption of the OMM and release of mitochondrial proteins accompanied by oxidative stress and ATP depletion (Kim et al., 2003).

In summary, numerous cellular stresses including oxidation and impaired calcium homeostasis contribute to mitochondria-mediated cellular damage (Fulda et al., 2010). Cellular stresses can cause mitochondrial failure that can lead to apoptosis if the cell is able to maintain mitochondrial membrane potential and ATP production, or necrosis in response to severe ATP depletion (Kim et al., 2003). Thus, cell stresses can initiate, propagate and/or mediate apoptosis and necrosis. These processes will be described in the following sections.

1.7.2 Apoptosis

Apoptosis describes a specific, tightly-regulated form of cellular death. Previous work has demonstrated that *C. albicans* can induce apoptosis in epithelial cells (Villar et al., 2012; Wagener et al., 2012), macrophages (Gasparoto et al., 2004; Ibata-Ombetta et al., 2003) and neutrophils (Rotstein et al., 2000). While transcript profiling data showed no changes in pro- and anti-apoptotic genes in oral epithelial cells 4 h after *C. albicans*

infection (Villar et al., 2012), differences were observed at later time points (8 h and 24 h) with upregulation of anti-apoptotic genes (Moyes et al., 2014; Villar et al., 2012). Increased expression of anti-apoptotic proteins was also observed in macrophages infected with *C. albicans* (Reales-Calderon et al., 2013). Importantly, while *C. albicans* was observed to induce early apoptotic signalling events in oral epithelial cells and macrophages, these events were transient, and cell death was observed to occur by necrosis rather than apoptosis (Gasparoto et al., 2004; Villar and Zhao, 2010).

Little is known about the fungal moieties that induce apoptotic events. Currently, only three components have been proposed to play a role in the induction of apoptosis by *C. albicans*. First, glycan moieties were shown to induce apoptosis in mucosal epithelial cells, where apoptosis was defined as an increase in the number of epithelial cells that exhibited caspase-3 activity and PS exposure following 24 h glycan treatment (Wagener et al., 2012). Second, proteins secreted from *C. albicans* have also been proposed to play a role in driving apoptosis in epithelial cells. Apoptosis was triggered in lung and oral epithelial cells exposed to Sap4p, Sap5p and Sap6p for 23 h (Wu et al., 2013). PS was observed to be redistributed to the outer leaflet of the epithelial plasma membrane in response to Sap4p, Sap5p and Sap6p but not in response to *sap4*Δ/Δ, *sap5*Δ/Δ or *sap6*Δ/Δ mutant strains (Wu et al., 2013). Third, treatment of epithelial cells with farnesol, a secreted quorum sensing molecule, was observed to promote caspase activation and PS redistribution leading to apoptosis after 48 h (Scheper et al., 2008).

The mechanisms of apoptosis are highly complex, involving an energy-dependent cascade of molecular events. Apoptosis can be initiated through extrinsic and intrinsic pathways. The extrinsic pathway is triggered by extracellular stimuli such as damage, PAMPs or DAMPs that are sensed by host death receptors, whereas the intrinsic pathway occurs in response to a wide range of intracellular damage or stress signals including oxidative stress, cytosolic calcium overload and mitochondrial dysfunction through the loss of mitochondrial membrane potential (Elmore, 2007). Extrinsic and intrinsic pathways result in activation of the caspase family of proteins that play a central role in the initiation and execution of apoptosis (Zamaraev et al., 2017).

Apoptotic caspases can be divided into two main groups: initiator caspases (caspase-2, -8, -9, -10) and effector caspases (caspase-3, caspase-6 and caspase-7) (Zamaraev et al., 2017) (Figure 1-6). Caspases are composed of a single amino acid chain that contains

three domains: a pro-domain containing a CARD or death effector domain (DED), a large fragment (p20) and a small fragment (p10) (Zamaraev et al., 2017) (Figure 1-6).

Figure 1-6. Apoptotic caspases. Initiator and effector caspases are the two main groups of caspases involved during apoptosis. Initiator caspases include caspase-2, -9, -8 and -10. Effector caspases include caspase-3, -7 and -6. Adapted from (Zamaraev et al., 2017).

All caspases are expressed within cells as inactive zymogens, also known as pro-caspases. Activation of initiator caspase zymogens occurs through proximity-induced dimerisation and subsequent autocatalytic cleavage (Dickens et al., 2012). Effector caspases are cleaved by initiator caspases. The effector caspases play an essential role in the execution of apoptosis by cleaving multiple cellular substrates resulting in destruction of the cell (Stennicke and Salvesen, 2000).

1.7.2.1 Extrinsic apoptotic pathway

Extrinsic apoptosis is activated by transmembrane receptor-mediated interactions. These interactions require death receptors that contain a death domain on the cytoplasmic face of the receptor (Ashkenazi and Dixit, 1998; Locksley et al., 2001). The death domain is critical for transmission of the death signal from the cell surface to the intracellular environment.

The best characterised death receptor and its cognate ligand are TNFR1 and TNFα, respectively (Rath and Aggarwal, 1999). Upon ligand binding, adaptor proteins are recruited to the cytoplasmic domain of the death receptor. Binding of TNFα to TNFR1 results in recruitment of the adaptor TNFR1-associated death domain protein (TRADD), receptor interacting protein kinase 1 (RIPK1), TNF-receptor-associated factor 2 (TRAF2), cellular inhibitors of apoptosis (cIAPs) and the linear ubiquitin chain assembly complex (LIUBAC), forming Complex 1 (Haas et al., 2009) (Figure 1-7). cIAPs mediate ubiquitination of RIPK1 which stimulates activation of NF-κB signalling, thus Complex 1

favours pro-inflammatory signalling via NF-κB activation (Bianchi and Meier, 2009). In the absence of cIAPs, Complex 1 dissociates and a ripoptosome complex composed of RIPK1, Fas-associated protein with death domain (FADD) and pro-caspase-8 forms in the cytosol (Tenev et al., 2011; Wang et al., 2008) (Figure 1-7). The binding between FADD and pro-caspase-8 promotes the autocatalytic activation of pro-caspase-8, potentiating extrinsic apoptosis (Kischkel et al., 1995).

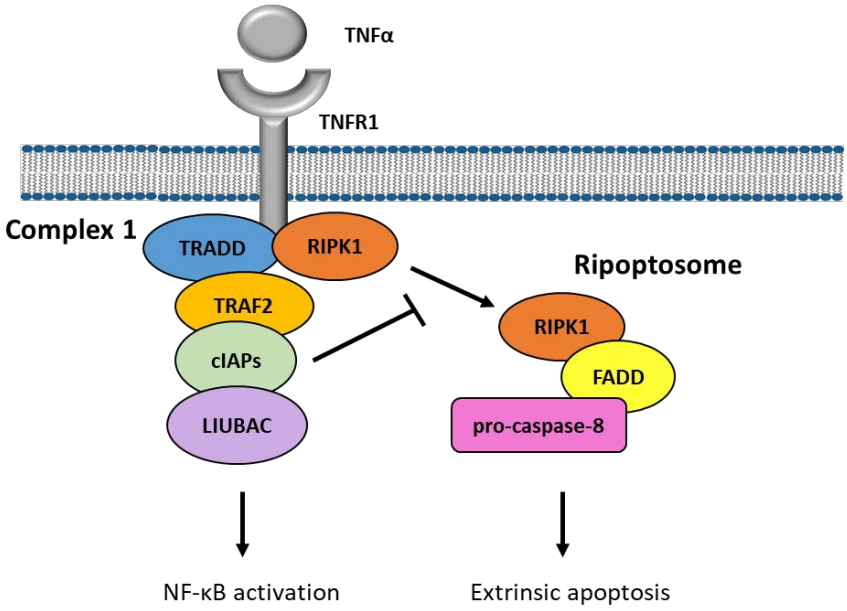

Figure 1-7. Initiation of the TNF-induced extrinsic apoptotic pathway. Binding of TNFα to TNFR1 induces the formation of Complex 1 that activates NF-κB. In the absence of cIAPs, ripoptosome formation occurs, leading to activation of pro-caspase-8 and extrinsic apoptosis.

1.7.2.2 Intrinsic apoptotic pathway

Intrinsic apoptosis is induced by numerous non-receptor mediated stimuli that generate intracellular signals through the mitochondria. Stimuli that trigger intrinsic apoptosis include radiation, hypoxia, free radicals and toxins (Elmore, 2007). All intrinsic apoptotic inducers can trigger the mitochondrial permeability transition (MPT) and release of pro-apoptotic proteins from the mitochondrial intermembrane space into the cytosol of the cell (Saelens et al., 2004). Cytochrome c is a major pro-apoptotic protein that binds Apaf-1 and pro-caspase-9 to form the apoptosome complex. Once formed, the apoptosome activates pro-caspase-9 (Chinnaiyan, 1999) (Figure 1-8).

The intrinsic apoptotic pathway is regulated by members of the Bcl-2 family (Cory and Adams, 2002). The Bcl-2 family of proteins contain pro- and anti-apoptotic factors that

control mitochondrial membrane permeability (MMP) and hence release of cytochrome c (Luo et al., 1998). The ratio of pro- and anti-apoptotic Bcl proteins expressed within a cell determines whether the pro-apoptotic proteins Bax and Bak are activated (Cory and Adams, 2002). Once active, Bax and Bak oligomerise into homodimers and permeabilise the mitochondrial membrane causing release of cytochrome c and activation of pro-caspase-9 through apoptosome formation (Wei et al., 2001) (Figure 1-8).

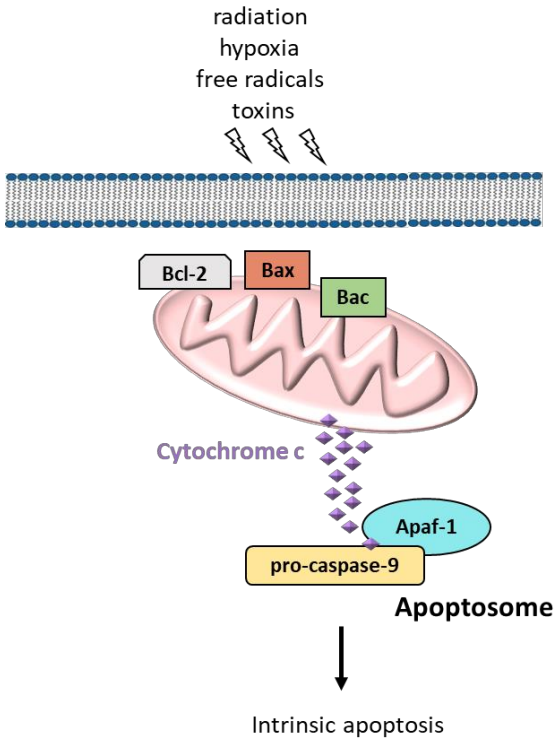

Figure 1-8. Initiation of the intrinsic apoptotic pathway. Radiation, hypoxia, free radicals and toxins are some of the stimuli that activate the intrinsic apoptotic pathway. These stimuli induce the expression of the pro-apoptotic protein Bcl-2 which induces Bax and Bak to act on the mitochondria, causing release of cytochrome c. Cytochrome c binds to Apaf-1 with pro-caspase-9, forming the apoptosome complex, which in turn activates pro-caspase-9, propagating intrinsic apoptosis.

1.7.2.3 Execution apoptotic pathway

Both extrinsic and intrinsic apoptotic pathways converge and activate the execution phase of cell death. The execution phase initiates with the activation of effector caspases including caspase-3, -6 and -7. Caspase-3 is considered the most important of the effector caspases and can be cleaved by initiator caspases (caspase-8, -9 or -10) (Slee et al., 2001). Once activated, caspase-3 cleaves numerous substrates including the Inhibitor of Caspase-activated DNase (ICAD) and Poly (ADP-ribose) polymerase (PARP) (Kaufmann et al., 1993; Sakahira et al., 1998).

During apoptosis, ICAD cleavage generates CAD, which is a major nuclease involved in DNA fragmentation (Enari et al., 1998). PARP is a protein involved in DNA repair. Cleavage of PARP prevents the repair of double stranded breaks in genomic DNA, potentiating DNA fragmentation (Boulares et al., 2001).

In addition to ICAD and PARP, caspase-3 also degrades the cytoskeleton of the host cell, leading to cell shrinkage and display of PS on the outer leaflet of the plasma membrane (Elmore, 2007). Exposure of PS has been associated with loss of amino-phospholipid translocase activity and nonspecific flip-flop of phospholipids (Bratton et al., 1997). PS externalisation facilitates non-inflammatory phagocytic recognition that allows clearance of apoptotic cells by macrophages without eliciting an inflammatory response (Fadok et al., 2001).

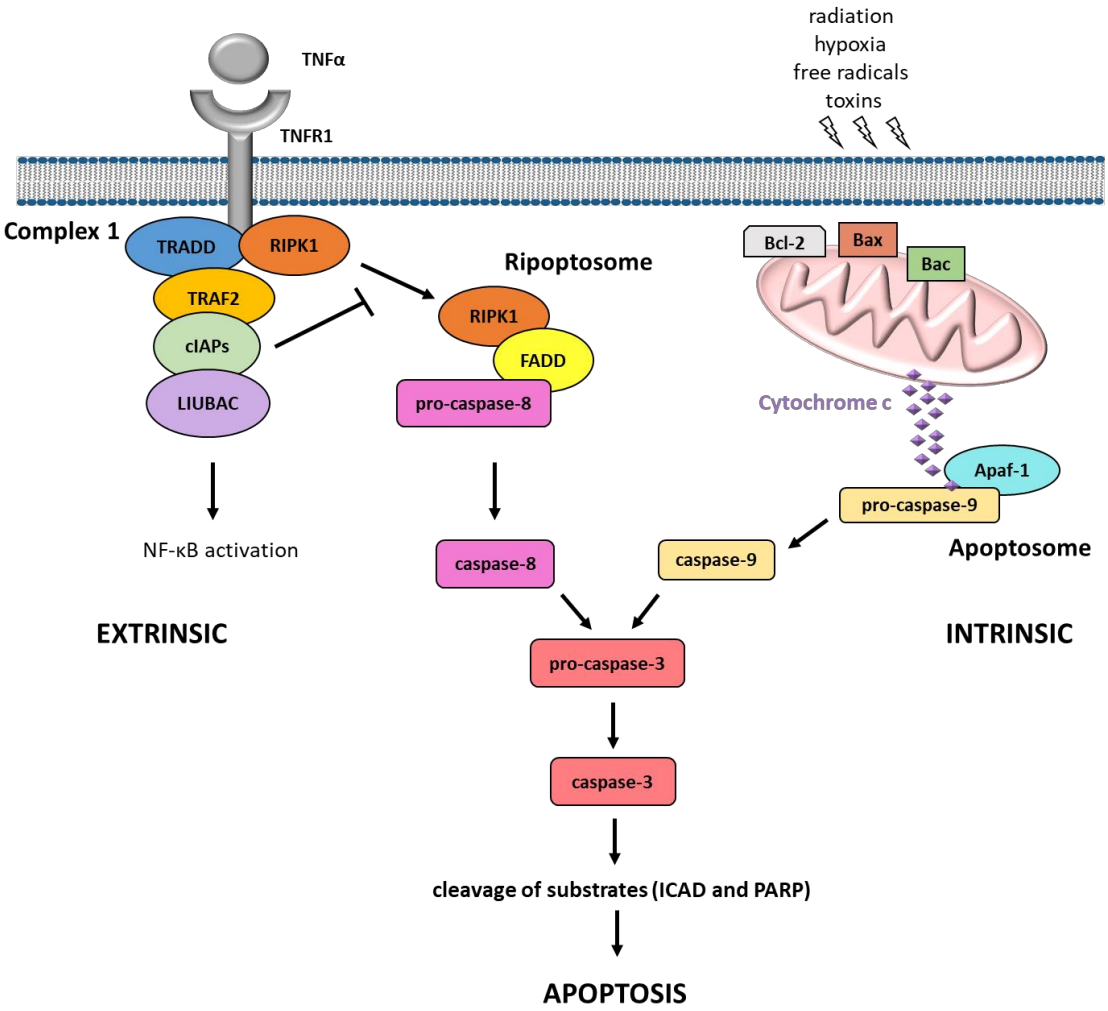

Figure 1-9. Extrinsic and intrinsic apoptotic signalling pathways. Extrinsic and intrinsic apoptotic pathways feed into the execution phase of the apoptotic pathway which is characterised by activation of caspase-3. Active caspase-3 cleaves numerous intracellular substrates including ICAD and PARP, causing apoptotic cell death.

1.7.3 Necrosis

Unlike apoptosis, necrosis is a caspase-independent cell death modality. Necrosis manifests with gross changes in cellular morphology via distinct biochemical processes leading to cellular rounding followed by swelling (oncosis) and plasma membrane rupture (Festjens et al., 2006). Loss of membrane integrity provokes an inflammatory response by exposing cellular contents to the immune system. Such contents include DAMPs and immune modulators including IL-1α, IL-33, S100, S100A8, S100A9 and S100A12 and ATP (Kaczmarek et al., 2013). These molecules behave in a similar manner to PAMPs that, through interaction with their cognate PRRs, activate inflammatory responses (Wallach et al., 2014).

Although *C. albicans* induces apoptotic events in epithelial cells (Villar et al., 2012) and phagocytes (Gasparoto et al., 2004; Ibata-Ombetta et al., 2003), the apoptotic response does not progress to completion, and the predominant cell death modality observed was necrosis (Gasparoto et al., 2004; Villar and Zhao, 2010). Importantly, while the presence or absence of necrosis reflects the viability status of the associated cell/tissue, the presence of necrosis alone does not indicate precisely how cell death has occurred. In order to elucidate the specific mechanism(s) of cell death that are induced during the process of necrosis, examination of specific signalling pathways is required. Necroptosis and pyroptosis are programmed necrosis pathways that are triggered by microbes to promote pathogenicity, and by host cells to induce defence mechanisms against pathogens (reviewed in (Ashida et al., 2011).

1.7.4 Programmed necrosis

Investigation of programmed cellular necrosis has been undertaken predominantly in the context of bacterial infections. Among cell death triggers, secreted bacterial toxins have been reported to activate necroptosis and pyroptosis in macrophages and epithelial cells. Some examples include toxins of *Bacillus anthracis* (Fink et al., 2008), *Staphylococcus aureus* (Kitur et al., 2015) and *Streptococcus pneumoniae* (Gonzalez-Juarbe et al., 2017). Recent studies have shown that *C. albicans* triggers pyroptosis in macrophages that phagocytose yeast cells (Wellington et al., 2014). Furthermore, given the role of bacterial toxins in inducing programmed cell necrosis (Fink et al., 2008; Gonzalez-Juarbe et al., 2017; Kitur et al., 2015), it may be possible that Candidalysin plays a role in triggering pyroptosis, and possibly the unexplored mechanisms of

necroptosis. The mechanisms driving necroptosis and pyroptosis will be described in the following sections.

1.7.4.1 Necroptosis

Necroptosis is a caspase-independent pro-inflammatory cell death pathway that is critical for immune activation following injury. Necroptotic death can be triggered by ligation of specific cell surface receptors, toxins, excessive ROS and numerous cellular stresses (Weinlich et al., 2017).

Responses to TNF may induce a necroptotic response (Holler et al., 2000). Initially, necroptosis proceeds in the same fashion as extrinsic apoptosis (Figure 1-7) with the formation of Complex 1 in response to TNF (Haas et al., 2009) (see section 1.7.2.1). In the absence of cIAPs, Complex 1 dissociates forming a ripoptosome complex in the cytosol comprised of RIPK1, FADD and pro-caspase-8 (Figure 1-10) (Tenev et al., 2011; Wang et al., 2008). The ripoptosome complex promotes autocatalytc activation of pro-caspase-8, which propagates the apoptotic signal (Feoktistova et al., 2012). However, in the absence of active caspase-8, RIPK1 dissociates from the ripoptosome to form the necrosome complex in the cytosol with RIPK3 (Cho et al., 2009) (Figure 1-10). Caspase-8 cleaves and inactivates RIPK1 (Lin et al., 1999) and RIPK3 (Feng et al., 2007), thus acting as a negative regulator of necrosome assembly.

RIPK1 and RIPK3 interact through RIP homotypic interaction motifs (RHIM) (Li et al., 2012), which triggers a series of auto- and trans-phosphorylations between RIPK1 and RIPK3 that results in the activation of the necrosome (Cho et al., 2009). Phosphorylation of RIPK3 is particularly important for recruitment and phosphorylation of the mixed lineage kinase domain-like protein (MLKL) (Figure 1-10), which is a key pseudokinase mediator of necroptosis signalling downstream of RIPK3 (Murphy et al., 2013; Sun et al., 2002).

The cell death signals that occur downstream of MLKL have yet to be characterised in full. However, it is known that phosphorylation of MLKL stimulates its oligomerisation and translocation to intracellular and plasma membranes causing membrane rupture. Little is known about the precise mechanism by which MLKL induces membrane destabilisation. Phosphorylated MLKL induces necroptosis via the influx of calcium or sodium through ion channels (Cai et al., 2014; Chen et al., 2014) and can also bind to

membrane phosphatidylinositol phosphates, causing loss of membrane integrity (Dondelinger et al., 2014).

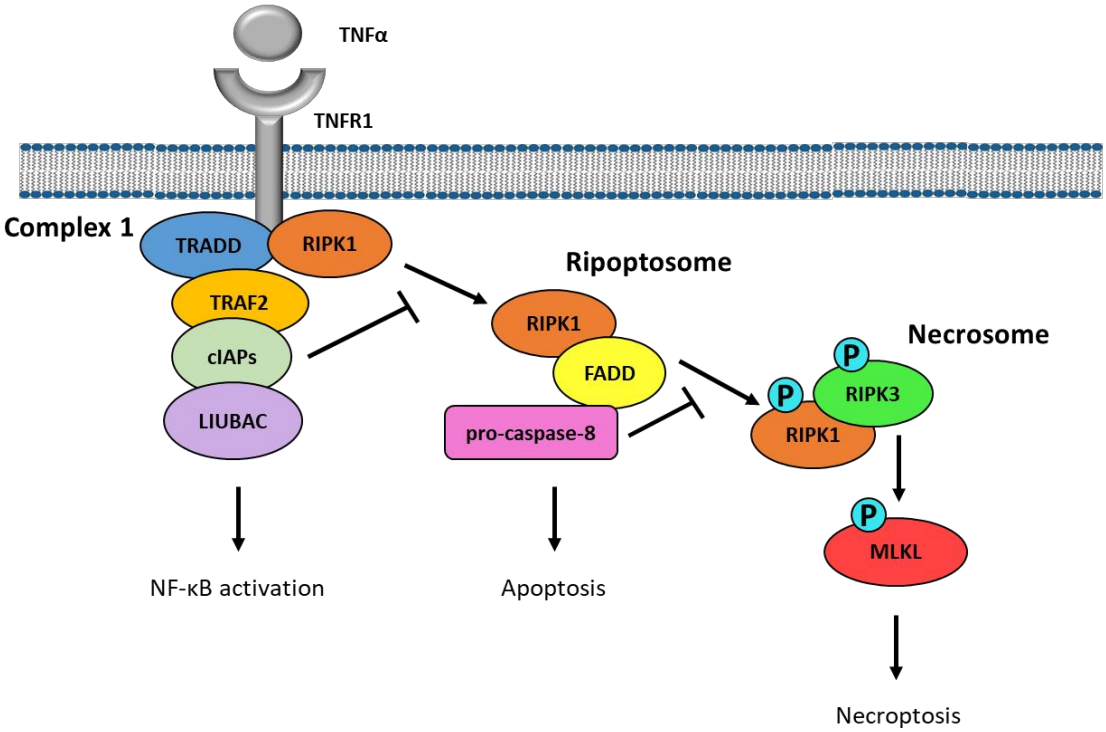

Figure 1-10. Necroptotic pathway induction by TNFα. Binding of TNFα to TNFR1 induces the formation of Complex 1 that activates NF-κB signalling. In the absence of cIAPs, the ripoptosome platform assembles, causing activation of pro-caspase-8 and extrinsic apoptosis. In the absence of active caspase-8, RIPK1 dissociates from the ripoptosome and forms a necrosome complex with RIPK3. Association of RIPK1 with RIPK3 stimulates auto- and trans-phosphorylation events that cause recruitment and activation of MLKL which executes necroptotic cell death.

RIPK1 is an important component of inflammation, apoptosis and necrosis (Pasparakis and Vandenabeele, 2015). The study of cell necrosis has been greatly facilitated by the discovery of the RIPK1 inhibitor necrostatin-1 (Nec-1) (Degterev et al., 2005), which facilitated the identification of RIPK3 as a crucial regulator of necroptosis (Cho et al., 2009). Indeed, there are instances where the necroptotic pathway can be RIPK3-dependent but RIPK1-independent (Kaiser et al., 2013; Upton et al., 2010). It has been demonstrated that necroptosis can occur following stimulation of TLR4 or TLR3, leading to an interaction between TIR-domain-containing adaptor-inducing interferon-β (TRIF), RIPK3 and MLKL (Kaiser et al., 2013). More recently, non-receptor mediated RIPK3-MLKL-necroptosis was observed to be stimulated by ion dysregulation caused by pore-forming toxins (Gonzalez-Juarbe et al., 2017). Therefore, given the recurrent role of

RIPK3, necroptosis is defined as a RIPK3-dependent molecular cascade that promotes regulated necrosis (Moriwaki and Chan, 2014).

1.7.4.2 Pyroptosis

Similar to necroptosis, pyroptosis is an inflammatory form of cell death with important functions in host defence and inflammation. However, unlike necroptosis, pyroptosis is induced by inflammasome activation (Bergsbaken et al., 2009).

Pyroptosis is triggered in macrophages following *C. albicans* infection (O'Meara et al., 2015; Uwamahoro et al., 2014; Wellington et al., 2014). In response to *C. albicans* hyphae, epithelial cells release immune modulators and immune cells are recruited to the site of fungal infection (Moyes et al., 2010; Steele and Fidel, 2002) (see Section 1.6.1). Macrophages play a key role in protecting the host by recognising and phagocytosing *C. albicans* yeast cells (Lewis et al., 2012) (Figure 1-11). During engulfment, the phagosome containing the yeast fuses with a lysosome generating a phagolysosome essential for fungal killing (Figure 1-11). During this process, hydrolytic enzymes, antimicrobial peptides, and ROS destroy the engulfed *C. albicans* within the phagolysosome (da Silva Dantas et al., 2016). However, *C. albicans* has evolved strategies to survive and escape from macrophages. One of these strategies involves morphological switching of *C. albicans* from a yeast to a hypha that pierces through the phagolysosome membrane and macrophage plasma membrane to escape (Wellington et al., 2014). Interestingly, prior to hyphal escape, *C. albicans* induces macrophage programmed cell death via pyroptosis (Uwamahoro et al., 2014).

Although *C. albicans* is able to physically escape from the macrophage phagolysosome, the induction of pyroptotic cell death plays an important role in host defence against pathogens (Jorgensen et al., 2017). Indeed, pyroptosis leads to the release of immune modulators that facilitate the recruitment of additional immune cells including DCs and neutrophils. The expression and release of immune modulators during pyroptosis is specifically attributed to the activation of a protein platform named the inflammasome, which is essential for initiation of the pyroptotic death pathway (Jorgensen et al., 2017).

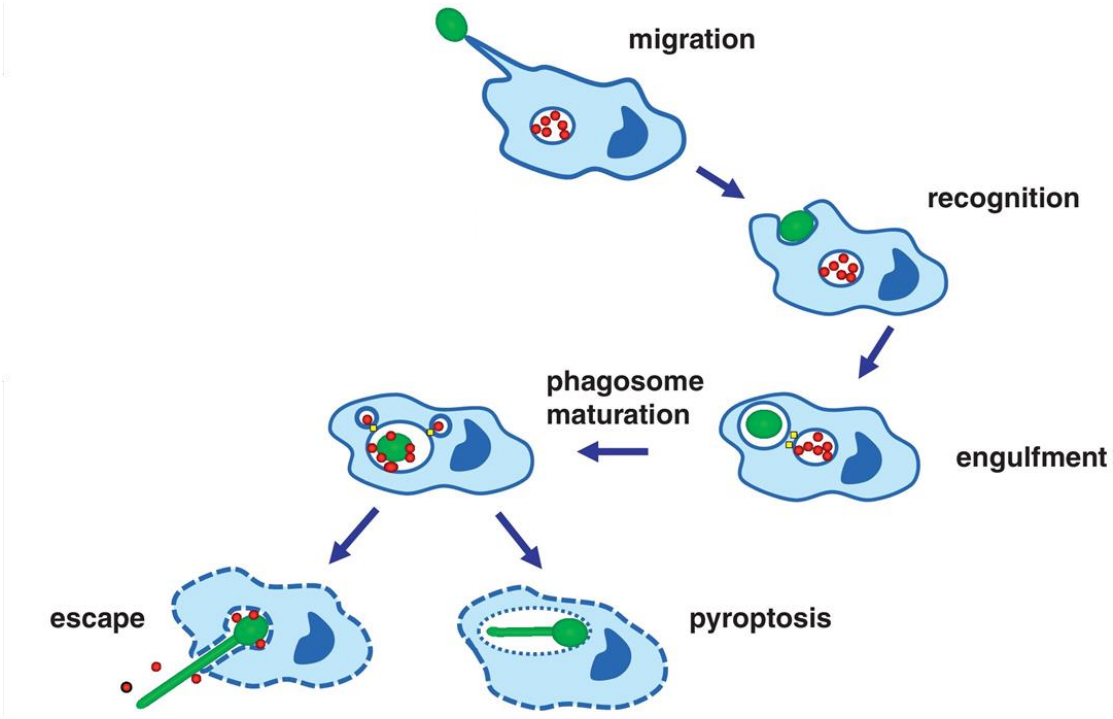

Figure 1-11. Phagocytosed *C. albicans* can escape from macrophages by hypha-mediated lysis and pyroptosis. Following recognition of *C. albicans* yeast cells (green), macrophages engulf the fungus into a phagosome. The phagosome fuses with a lysosome, creating a phagolysosome that can kill the internalised fungus. However, *C. albicans* can circumvent this process by producing a hypha that induces pyroptosis and cell lysis, enabling the fungus to escape from the macrophage. Adapted from (da Silva Dantas et al., 2016).

1.7.4.2.1 The canonical inflammasome

The inflammasome is a pro-inflammatory, multi-protein complex comprised of an NLR. Inflammasomes can be activated in response to exogenous or endogenous PAMPs and DAMPs. NLRs consist of three domains: a CARD, a pyrin domain (PYD) or baculovirus inhibitor of apoptosis repeat (BIR) domain; a central nucleotide-binding oligomerization domain (NOD); and a C-terminal leucine-rich repeat sequence (LRR) (Martinon et al., 2002).

There are different types of inflammasome, but those most closely associated with *C. albicans* infections are the NLRP3 and the NLRC4 inflammasomes (Hise et al., 2009; Tomalka et al., 2011; van de Veerdonk et al., 2011; Wellington et al., 2014). NLRP3 is the crucial NLR involved in *C. albicans* infections and is present in both immune cells and stromal compartments (Hise et al., 2009; Wellington et al., 2014). In addition to NLRP3, *C. albicans* can also trigger the inflammasome via NLRC4 (Tomalka et al., 2011). NLRC4 is involved in mucosal defences against *C. albicans* (Tomalka et al., 2011).

In myeloid cells, two independent signals are required to activate the inflammasome. The first signal (mediated by the recognition of *C. albicans* PAMPs by myeloid cell PRRs) stimulates the expression of pro-caspase-1, pro-IL-1β and pro-IL-18, and is followed by assembly of the inflammasome complex and activation of caspase-1 (Afonina et al., 2015; Joly and Sutterwala, 2010). The *C. albicans* factor(s) that comprise the second activator signal remain elusive (Joly and Sutterwala, 2010; Wellington et al., 2014). Nonetheless, when myeloid cells interact with *C. albicans*, NLRP3 recruits an adaptor protein (apoptosis-associated speck-like protein containing a CARD (ASC)) which provides a molecular bridge between NLRP3 and pro-caspase-1 (Figure 1-12).

In contrast to NLRP3, NLRC4 binds directly to pro-caspase-1 through a CARD-CARD interaction (Figure 1-12 B). The interaction between NLRC4 and pro-caspase-1 culminates in the assembly of the canonical inflammasome, which results in the autocatalytic activation of caspase-1. Active caspase-1 then processes pro-IL-1β and pro-IL-18 from their immature, biologically inactive forms into the biologically functional cytokines IL-1β and IL-18 (Fantuzzi and Dinarello, 1999) (Figure 1-12).

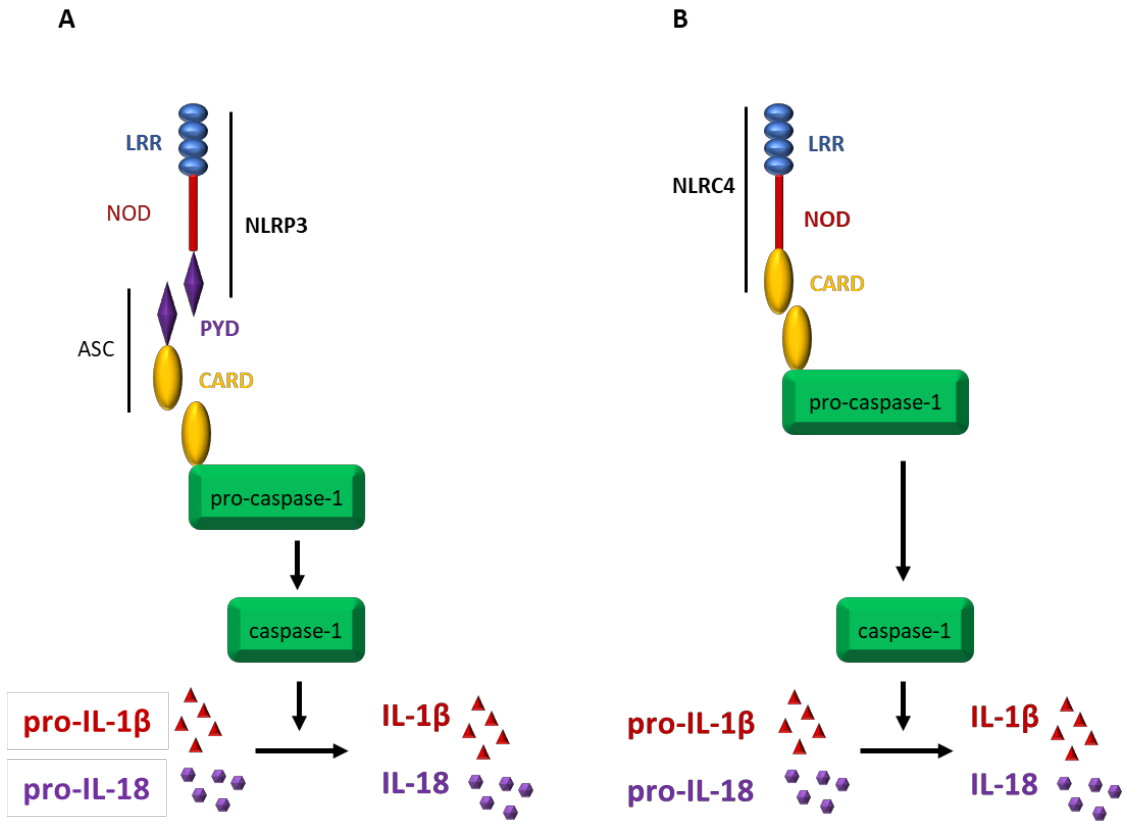

Figure 1-12. Organisation of the NLRP3 and the NLRC4 inflammasome cascades. (A) The NLRP3 inflammasome contains an NLRP3 receptor, the adaptor protein ASC and caspase-1. The NLRP3 receptor contains an LRR, NOD and PYD. (B) The NLRC4 inflammasome contains the NLRC4 receptor and caspase-1. The NLRC4 receptor is comprised of an LRR, NOD and CARD. Both NLRP3 and NLRC4 inflammasome complexes culminate with pro-caspase-1 activation which cleaves pro-IL-1β and pro-IL-18.

In addition to PAMPs, Saps have been associated with the activation of the NLRP3 inflammasome in macrophages (Pietrella et al., 2013). Saps contribute to *C. albicans*-mediated host damage and evasion of the immune response (Naglik et al., 2003). Sap2p and Sap6p in particular have been shown to be endocytosed by macrophages where they trigger ROS production, release of cathepsin B and efflux of potassium ions prior to inflammasome assembly (Pietrella et al., 2013). Once assembled, activation of caspase-1 occurs, which is required for processing and secretion of active IL-1β and IL-18 (Pietrella et al., 2013).

Inflammasome activation has been studied extensively in myeloid cells. Interestingly, the two-step process of inflammasome activation may not be required in epithelial cells, since NLRC4 and pro-IL-18 are constitutively expressed (Lei-Leston et al., 2017), suggesting that assembly of the epithelial inflammasome may not require priming.

1.7.4.2.2 The non-canonical inflammasome

The non-canonical inflammasome is an alternative platform that promotes processing of pro-IL-1β and pro-IL-18 in macrophages and epithelial cells (Kayagaki et al., 2011; Knodler et al., 2014). The inflammatory caspase-11 can interact directly with LPS and intracellular bacteria leading to pro-IL-1β and pro-IL-18 processing and pyroptotic death (Hagar et al., 2013; Kayagaki et al., 2013) (Figure 1-13). Caspase-11 induces cytokine processing by promoting assembly and activation of the NLRP3 inflammasome (Kayagaki et al., 2011) (Figure 1-1). *C. albicans* Sap2p and Sap6p were observed to stimulate activation of the non-canonical inflammasome in macrophages, resulting in caspase-11 activation and NLRP3 inflammasome-mediated processing and secretion of IL-1β (Gabrielli et al., 2015).

1.7.4.2.3 IL-1β and IL-18 secretion by active inflammasomes elicit immune responses

Activation of canonical and non-canonical inflammasomes promotes the cleavage and secretion of IL-1β and IL-18 from immune and epithelial cells (Dinarello et al., 2013; Schaller et al., 2004; Tardif et al., 2004a; Tardif et al., 2004b; Wellington et al., 2014). IL-1β is a strong chemoattractant for leukocytes and a potent pro-inflammatory cytokine that promotes recruitment of immune cells to the site of infection. When the immune cells are recruited, IL-1β activates dendritic cells, macrophages and neutrophils, which remove invading microbes from the body (Dinarello, 1996). Furthermore, IL-1β participates with other cytokines in the process of T-cell activation to induce Th17 cell differentiation and adaptive immunity (Ben-Sasson et al., 2009). Similar to IL-1β, IL-18 is also expressed as inactive precursor (pro-IL-18) that is secreted from cells following inflammasome activation. IL-18 in combination with IL-12 has been shown to promote IFN-γ secretion by T cells to induce Th1 differentiation crucial for controlling disseminated fungal infection (Mencacci et al., 2000).

The NLRP3 and the NLRC4 inflammasomes have important roles in host defence against *C. albicans* infection. Indeed, NLRP3-deficient mice and mice deficient in the inflammasome components ASC and caspase-1 are more susceptible to disseminated *C. albicans* infection, due to a lack of neutrophil influx to the site of infection (Gross et al., 2009; Hise et al., 2009; Joly et al., 2009; van de Veerdonk et al., 2011). However, during the early stages of invasive infection, the absence of caspase-1 did not have a clear effect on IL-1β production or neutrophil influx *in vivo*, suggesting that early

neutrophil influx was not dependent on the NLRP3 inflammasome (Mencacci et al., 2000; van de Veerdonk et al., 2011).

Neutrophils release proteinase 3, neutrophil elastase and cathepsin G that process pro-IL-1β into mature biologically active IL-1β (Afonina et al., 2015; Joosten et al., 2009). During the later stages of *C. albicans* infection, the inflammatory response becomes increasingly dependent upon the inflammasomes of macrophages and T-cells, which produce IL-1β that contributes to Th17 responses, and IL-18 that contributes to robust Th1 responses (van de Veerdonk et al., 2011).

1.7.4.2.4 Gasdermin D cleavage by inflammasomes causes pyroptotic cell death

Besides pro-IL-1β and pro-IL-18, another recently discovered target of canonical and non-canonical inflammasomes is gasdermin D, which is also required for the execution of pyroptotic cell death (Kayagaki et al., 2015; Shi et al., 2015). Caspase-1 and caspase-11 cleave gasdermin D, resulting in release of the gasdermin D N-terminus that induces pores in plasma membranes, thereby dissipating cellular ionic gradients and resulting in lytic cell death (Kayagaki et al., 2015; Shi et al., 2015) (Figure 1-13). Gasdermin D is highly expressed in epithelial cells, suggesting a potential role of this protein in driving pyroptosis at mucosal surfaces (Liu and Lieberman, 2017).

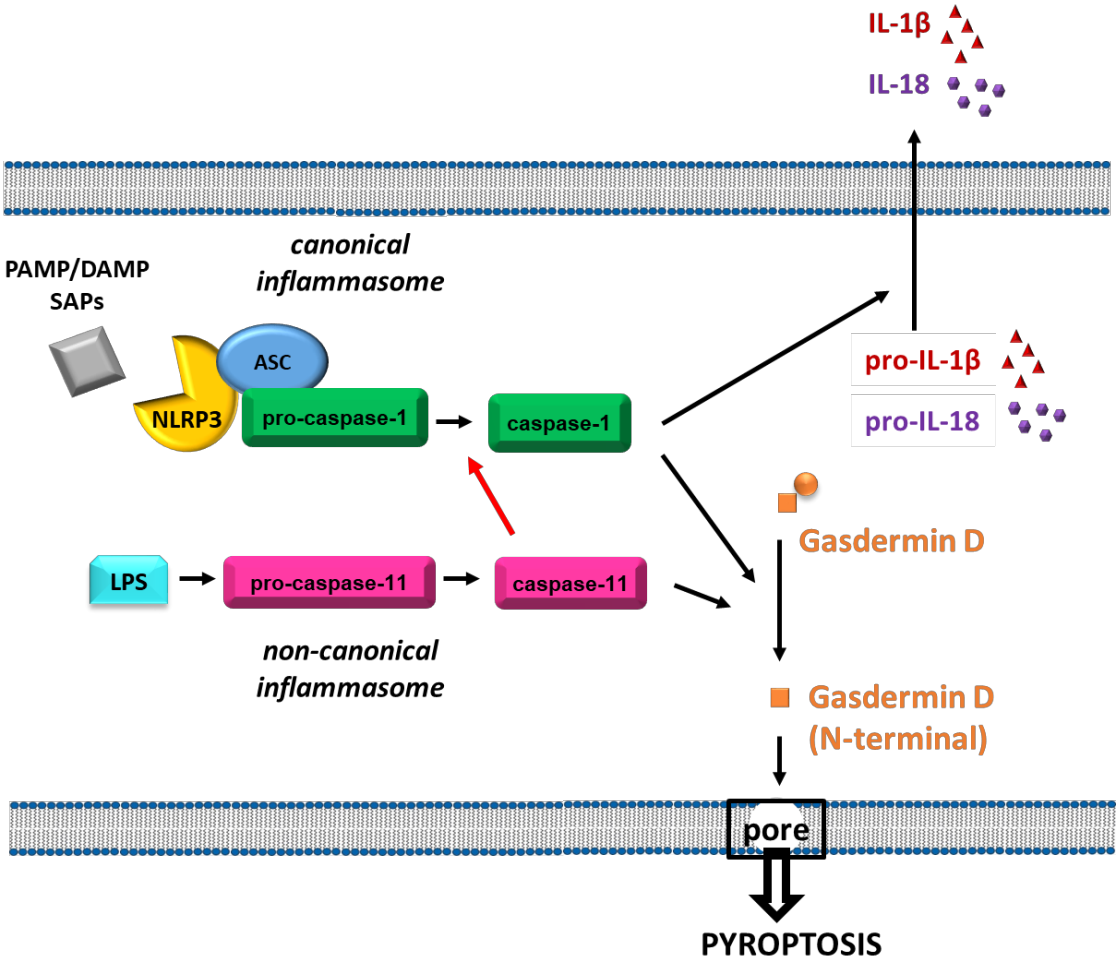

Figure 1-13. Pyroptosis is induced by canonical and non-canonical inflammasome activation. Canonical inflammasomes act as sensors for a variety of pathogens and cellular insults. Assembly of the NLRP3 inflammasome involves recruitment of the adaptor protein ASC and pro-caspase-1, resulting in caspase-1 activation. In the non-canonical pathway, LPS is bound by pro-caspase-11 resulting in activation. Caspase-1 processes the interleukins IL-1β and IL-18. Caspase-11 participates in pro-IL-1β and pro-IL-18 cleavage by potentiating the canonical inflammasome. Both caspase-1 and caspase-11 process gasdermin D, resulting in the release of the gasdermin D N-terminus, which forms a pore in the host cell plasma membrane. Pore formation results in rapid loss of membrane integrity, dissipation of the electrochemical gradient, and cell death.

1.7.5 Summary of the characteristic features of different cell death pathways

The study of pathogen-induced host cell death has gained attention with the recognition that this phenomenon may not be an incidental occurrence during infection, but a controlled process with significant implications for disease pathogenesis. As described above, pathogen-induced cell death may occur by a variety of complex mechanisms including apoptosis, necrosis, necroptosis and pyroptosis. Table 2 summarises the features characterising these different modes of cellular death.

Table 2. Summary of the characteristic features of different cell death pathways.

Characteristics of the dying cell	**Apoptosis**	**Necrosis**	**Regulated necrosis - Necroptosis**	**Regulated necrosis - Pyroptosis**
Cell lysis/membrane permeability	-	+	+	+
Cell swelling	-	+	+	+
Mitochondrial fitness	-	-	-	?
ROS	+	+	+	+
ATP	+	-	-	-
Calcium	+	+	?	?
cIAP	-	?	-	?
Caspases involved	-8, -9, -7, -3	-	-	-1, -11, -4, -5
Cytochrome c release	+	+	?	?
PARP cleavage	+	+	?	?
RIPK1/RIPK3	+/-	-/-	+/+	-/-
Membrane pore formation (intracellular source)	-	-	+ (p-MLKL)	+ (Gasdermin D)
DAMPs release	-	+	+	+
IL-1β and IL-18 release	-	?	?	+

1.8 Project Aims

Essential information is still missing from our understanding of how epithelial cells respond to *C. albicans* infection. Epithelial cells that comprise mucosal surfaces are typically the first-line barrier against *C. albicans* and are targeted by *C. albicans* virulence factors to cause cell death at the mucosal surface, which may facilitate infection. To date, it has been demonstrated that *C. albicans* induces apoptotic events and necrosis in oral epithelial cells (Villar et al., 2012; Villar and Zhao, 2010; Wagener et al., 2012) and pyroptosis in macrophages (Uwamahoro et al., 2014; Wellington et al., 2014).

C. albicans pathogenicity is multifactorial, thus there may be numerous factors that contribute to the induction of epithelial cell death. The discovery that Candidalysin is required for epithelial damage during mucosal infection (Moyes et al., 2016) establishes an intriguing link between host cell stress and death.

Cell death is an important defence mechanism in response to microbial infection. Thus, given the essential role of Candidalysin in causing epithelial damage and triggering epithelial signalling pathways during mucosal infection, the central aim of this study is to determine whether epithelial cell death responses and signalling pathways are activated in response to Candidalysin.

The specific aims of this project are to:

1. Determine the role of Candidalysin in activating oral epithelial cell death responses by investigating classical hallmarks of cellular stress.
2. Investigate oral epithelial apoptotic responses to Candidalysin.
3. Examine the role of Candidalysin in driving programmed necrosis in oral epithelial cells focusing on the study of necroptosis and pyroptosis pathways.

Since the activity of Candidalysin was originally characterised on TR146 oral epithelial cells (Moyes et al., 2016), the same cell line was used to investigate cell death responses. This project will expand upon our understanding of the role played by Candidalysin during infection at mucosal surfaces and will provide insight into the ability of Candidalysin to trigger cell death in epithelial cells.

Chapter 2: Materials and Methods

2.1 General materials and equipment

2.1.1 General chemicals

Dulbecco's phosphate-buffered saline (D-PBS; Sigma) consisted of 1.4 M NaCl, 27 mM KCl, 80 mM Na_2HPO_4 x H_2O, 15 mM KH_2PO. For MTT assays, 3-(4,5-dimethylthiazol-2-yl)-2,5-diphenyltetrazolium bromide (MTT) was supplied by Merck and solubilisation solution consisted of 50% dimethylformamide (Prolabo), 0.2% glacial acetic acid (BDH Chemicals), 20 mM hydrochloric acid (HCl; BDH Chemicals), 10% (w/v) sodium dodecyl sulphate (SDS; Severn Biochem Ltd).

For protein extraction, Radio Immuno-Precipitation Assay (RIPA) buffer was made of (50 mM Tris-HCl pH 7.5 (Sigma), 150 mM NaCl (Sigma), 1% (v/v) Triton X-100 (Sigma), 1% (w/v) sodium deoxycholate (Sigma), 0.1% (w/v), SDS (Severn Biochem Ltd) and 20 mM ethylenediaminetetraacetic acid (EDTA; Sigma). Protease inhibitor was supplied by Fisher Scientific and phosphatase inhibitor was supplied by Sigma.

For western blotting, 4X Laemmli sample buffer was supplied by Alfa Aesar and dithiothreitol (DTT) from Sigma. Running buffer 10X (Sigma) consisted of 250 mM Tris base, 2.5 M glycine, and 1% SDS. Transfer buffer 10X consisted of 3% (w/v) Tris (VWR chemicals) and 14.5% (w/v) glycine (Sigma). 10% methanol (VWR chemicals) was added to 1X transfer buffer. Tris-buffered saline 10X (TBS) buffer (Severn Biotech) consisted of 2.5 M Tris and 15 M NaCl, supplied at pH 7.4. 0.1% TWEEN20 (Sigma) was added to 1X TBS to make TBS and TWEEN20 (TBS-T). In all cases, ddH_2O was used for dilutions to 1X. Antibodies were diluted in 1X TBS-T, using either 5% (w/v) bovine serum albumin (BSA; Sigma) or 5% (w/v) milk powder (Sainsbury's, UK).

General Caspase Inhibitor Z-VAD-FMK was purchased from R&D. TNF was a kind gift provided by Prof Sarah Gaffen (University of Pittsburgh, USA). Recombinant Human IL-1β was purchased from R&D Systems and Recombinant Human IL-18 was purchased from MBL. Peptides were purchased from Proteogenix (France) and Peptide Protein Research Ltd (UK).

2.1.2 General equipment

Tissue culture flasks (T182) and 15 mL Falcon tubes were purchased from Jet Biofil. Tissue culture plates (96 well, 24 well, 12 well and 6 well) were supplied by Cellstar. Black 96-well plates were purchased from Costar. Falcon tubes (50 mL) were purchased from Corning. Pipettes (25 mL, 10 mL and 5 mL) and white 96 well plates were purchased from Fisher Scientific. Pipette tips (1000 µL, 200 µL and 10 µL), 1.5 mL Eppendorf tubes and 10 µL sterile disposable loops were purchased from StarLab. Immulon 96 well plates were purchased from Thermo Scientific. Petri dishes (90 mm) were purchased from Sterilin. Dual chamber counting slides were purchased from BIORAD. Sterile Nalgene Cryogenic vials were purchased from Nalge Nunc International. Microbank Cryovial beads were purchased from Pro-Lab Diagnostics.

Sterile tissue culture was performed in a Scanlaf MARS Class II safety cabinet. Infections were carried out in a NUAIRE Class II biological safety cabinet. Epithelial cell cultures were incubated in a Binder humidified incubator at 37°C, 5% CO_2. Centrifugation at 25°C was performed in an Eppendorf Centrifuge 5415C (up to 1.5 mL sample volume) and a MSE Mistral 3000 Centrifuge (up to 25 mL sample volume). Centrifugation at 4°C was performed in a Howe Sigma 3K10 Centrifuge (up to 50 mL sample volume). Centrifugation at 20°C was performed in a MSE Mistral 1000 Centrifuge (MSE Scientific Instruments). A Tecan Infinite F50 plate reader was used to read microplates for lactate dehydrogenase (LDH) and enzyme-linked immunosorbent assay (ELISA). A Jenway 6300 spectrophotometer was used to obtain the absorbance of microbial cultures. Fluorescence and luminescence were measured using a FlexStation 3 Multi-Mode microplate reader (Molecular Devices).

2.2 Fungal culture

2.2.1 *C. albicans* growth medium

C. albicans cells were cultured in liquid yeast peptone dextrose (YPD) or on solid YPD agar, consisting of 1% (w/v) yeast extract (Oxoid), 2% (w/v) Peptone (Melford), 2% (w/v) dextrose (BDH Chemicals) and 1.5% (w/v) agar (Melford).

2.2.2 Creation of *C. albicans* mutants, growth and maintenance

C. albicans ECE1 mutants used in this study (Table 2.1) were generated by our collaborator Professor Bernhard Hube (Moyes et al., 2016).

Table 2.1 Description of *C. albicans* strains used in this study.

***C. albicans* strain**	**Description**	**Genotype**
BWP17+Clp30	Derived from SC5314 (Gillum et al., 1984). Parent strain of *ece1*Δ/Δ and *ece1*Δ/Δ+*ECE1* (Moyes et al., 2016).	*ura3::λimm434/ura3::λimm434 iro1::λimm434/iro1::λimm434 his1::hisG/his1::hisG arg4::hisG/arg4::hisG RPS1/rps1::(URA3-HIS1-ARG4*)
*ece1*Δ/Δ	Homozygous null mutant (Moyes et al., 2016).	*ura3::λimm434/ura3::λimm434 iro1::λimm434/iro1::λimm434 his1::hisG/his1::hisG arg4::hisG/arg4::hisG ece1::HIS1/ece1::ARG4 RPS1/rps1::URA3*
*ece1*Δ/Δ+*ECE1*	Homozygous null mutant complemented with a single wild type copy of *ECE1*. Parent strain of *ece1*Δ/Δ+*ECE1*$_{\Delta 184\text{-}279}$ (Moyes et al., 2016).	*ura3::λimm434/ura3::λimm434 iro1::λimm434/iro1::λimm434 his1::hisG/his1::hisG arg4::hisG/arg4::hisG ece1::HIS1/ece1::ARG4 RPS1/rps1::*(*URA3-ECE1*)
*ece1*Δ/Δ+*ECE1*$_{\Delta 184\text{-}279}$	Homozygous null mutant complemented with a single copy of *ECE1* with Candidalysin excised (Moyes et al., 2016).	*ura3::λimm434/ura3::λimm434 iro1::λimm434/iro1::λimm434 his1::hisG/his1::hisG arg4::hisG/arg4::hisG ece1::HIS1/ece1::ARG4 RPS1/rps1::*(*URA3-ECE1*$_{\Delta 184\text{-}279}$)

Stocks of *C. albicans* yeast strains were stored in cryogenic beads (Pro-lab Diagnostics) at -80°C. YPD agar was autoclaved and poured into sterile Petri dishes. Once set, *C. albicans* strains were streaked for single colonies and incubated at 37°C for 2 days in a static incubator. For liquid culture, a single colony of *C. albicans* was inoculated into YPD liquid medium and cultured at 30°C in an orbital shaker at 200 rpm overnight. Saturated culture (1 mL) was centrifuged and the pellet washed twice with filter-

sterilised PBS. The absorbance of the culture at a 1:100 dilution was measured at 600 nm using a spectrophotometer (Jenway 6300). This was used to determine the colony forming units (CFU)/mL using previously established growth curves. The fungal cells were then diluted to the appropriate number of CFU/mL required for the infection.

In order to freeze down a stock of *C. albicans*, 1 mL of an overnight culture of *C. albicans* was added to cryogenic beads according to the manufacturer's instructions and stored at -80°C.

2.2.3 Candidalysin peptides

In this study, two Candidalysin peptides (Ece1-III$_{62\text{-}93KR}$ (KR) and Ece1-III$_{62\text{-}92K}$ (Candidalysin or K)) were used. Both Candidalysin peptides are derived from the processing of a larger 271 amino acid *C. albicans* protein, Ece1p (Moyes et al., 2016; Richardson et al., 2018). In order for *C. albicans* to produce mature Candidalysin from Ece1p, two sequential processing events are required. First, Ece1p is processed by the endoproteinase Kex2p, generating the immature Candidalysin peptide Ece1-III$_{62\text{-}93KR}$. Once produced, the immature Ece1-III$_{62\text{-}93KR}$ peptide is subsequently processed by the carboxypeptidase Kex1p, resulting in the removal of a carboxyl arginine residue to generate mature Candidalysin.

Both Ece1-III$_{62\text{-}93KR}$ (KR) and Ece1-III$_{62\text{-}92K}$ (Candidalysin or K) were synthesised and purified by Proteogenex and Peptide Protein Research; and reconstituted to a stock concentration of 10 mg/mL in water. Peptide stocks were stored at -20°C. Amino acid sequences are shown below.

Ece1-III$_{62\text{-}93KR}$ (KR)	SIIGIIMGILGNIPQVIQIIMSIVKAFKGNKR
Ece1-III$_{62\text{-}92K}$ (Candidalysin or K)	SIIGIIMGILGNIPQVIQIIMSIVKAFKGNK

2.3 Cell culture

2.3.1 Cell line growth and maintenance

In this study the oral epithelial cell line TR146 was used. TR146 cells were established from a biopsy specimen of a squamous cell carcinoma of the buccal mucosa that had infiltrated a lymph node (Rupniak et al., 1985). TR146 cells form a non-differentiated and non-keratinised stratified epithelium that share morphological and functional

characteristics of normal buccal mucosa. The TR146 cell line is well characterised and is routinely used for infection studies *in vitro* and represents a robust model of the human mucosa (Yadev et al., 2011).

TR146 cells were grown in Dulbecco's Modified Eagle Medium Nutrient Mixture F-12 HAM (DMEM F-12; Thermo Fisher Scientific) supplemented with 15% (v/v) foetal bovine serum (FBS; PAA) and 1% (v/v) penicillin/streptomycin (Sigma).

Cell cultures were passaged when confluent. To passage, cells were washed once with 10 mL D-PBS and incubated for 20 min in 4 mL 0.05% trypsin-EDTA solution (PAA) at 37°C and 5% CO_2. After detachment, cells were re-suspended in fresh DMEM F-12 medium and either counted and seeded at specific cell densities according to experimental requirements or maintained until confluent as described above.

2.3.2 Cell counting

A TC20 Automated Cell Counter (BIORAD) was used to determine the number of trypsinised (detached) cells per mL of culture medium. Adherent cells were detached with Trypsin-EDTA as described and approximately 10 µL of cell suspension was pipetted into the cell counter slide. Upon insertion of a counting slide, the TC20 cell counter provides a total cell count.

2.3.3 Cell freezing and thawing

After trypsin treatment, cells were collected and centrifuged at 4°C at 300 x g for 5 min. The culture medium was discarded and the cell pellet (containing at least 2 x 10^6 cells) was re-suspended in 1 mL of freezing medium (90% (v/v) FBS and 10% (v/v) DMSO) and transferred to a cryovial. In order to slowly freeze the cells, cryovials were stored at -80°C in an isopropanol bath and after 7 days transferred to a liquid nitrogen tank (-200°C) for long-term storage.

To re-culture frozen cell stocks, cells were rapidly thawed in a 37°C water bath, then re-suspended in 10 mL of DMEM F-12 medium and centrifuged at 4°C at 300 x g for 5 min. The cell pellet was re-suspended in 10 mL of fresh DMEM F-12 and cells transferred to a T182 tissue culture flask. Fresh media was added in order to reach a final volume of 24 mL and incubated at 37°C, 5% CO_2.

2.3.4 Cell seeding

Cells were seeded at different densities depending on the assay performed. The number of cells per mL of medium was determined using an automated cell counter as described and diluted into fresh DMEM F-12 medium to achieve the desired seeding density. Cells were then seeded accordingly in cell culture plates (Table 2.2) and incubated for 24 h at 37°C, 5% CO2.

Table 2.2 Cell seeding conditions.

Assay	Plate	Volume	Density
LDH, ELISA and western blot	12 well	1 mL	5×10^5
Fluorescent microscopy	96 well	100 µL	5×10^4
MTT	96 well	100 µL	1×10^5
ROS, Calcium, iATP and Caspase activity	96 well	100 µL	5×10^5

LDH assay, ELISA and western blot: Seeded plates were serum-starved and further incubated 24 h prior to infection with *C. albicans ECE1* mutants and Candidalysin peptides. Time points of 6 h (MOI = 5; 5 fungal cells to 1 epithelial cell) and 24 h (MOI = 0.01; 1 fungal cell to 100 epithelial cells) were assessed. Candidalysin peptides were used at 70, 30, 15 and 3 µM concentration. Following infection, exhausted culture medium was collected and either stored at 4°C for quantification of LDH activity or stored at -20°C for quantification of proteins by ELISA assay. Protein lysates were also extracted (see Section 2.5.1) and stored at -20°C for ELISA assay and western blot.

Fluorescent microscopy: Time points of 3 h, 6 h and 24 h were assessed. Candidalysin peptides were used at 70, 30, 15 and 3 µM concentration. Following treatment, cells were washed and treated with different fluorescent dyes (see section 2.4.2).

MTT, iATP and caspase activity assays: Time points of 5 min, 15 min, 30 min, 1 h, 1.5 h, 2 h, 2.5 h, 3 h, 6 h and 24 h were assessed. Candidalysin peptides were used at 70, 60, 45, 30, 15, 3 and 1.5 µM concentration. Infected cells were then assayed for mitochondrial fitness (MTT assay), intracellular ATP content, and caspase activity.

ROS and Calcium assays: These assays were performed in real time. Candidalysin peptides were used at 70, 15, 3 and 1.5 µM concentration. Prior to treatment, cells were stained with different fluorescent dyes (see section 2.4.4 and 2.4.6).

2.4 Cell response assays

2.4.1 LDH (Epithelial cell damage) assay

Epithelial cell damage was determined by a colorimetric assay that quantitatively measures the activity of lactate dehydrogenase (LDH). LDH is a stable enzyme present in the cell cytosol that is released into the culture medium only when cell membrane integrity is compromised. LDH was measured using a Cytox 96 Non-Radioactive Cytotoxicity Assay Kit (Promega) according to the manufacturer's protocol. Briefly, exhausted cell culture medium was diluted 1:10 (v/v) in PBS. Recombinant porcine LDH (Sigma) was used to create a standard curve ranging from 15 to 960 milliunits (mU) of enzymatic activity/mL. Samples and standards were analysed in technical duplicates. Substrate solution (50 µL) was added to each sample and standard and incubated for 20 min at room temperature protected from light. LDH activity was detected using a coupled enzymatic assay, in which a tetrazolium salt (INT) is converted into a red formazan product. The intensity of colour is proportional to the amount of LDH enzymatic activity. Following incubation, the absorbance at 492 nm was quantified using a Tecan Infinite F50 plate reader.

2.4.2 Detection of epithelial cell death by fluorescence microscopy

Epithelial cell death was investigated using three different fluorescent stainings (Table 2.3) contained in the Apoptotic/Necrotic/Healthy Cell Detection Kit (Promokine). Following cell treatment with Candidalysin peptides, wells were washed twice with 5X binding buffer. Staining solution (5 µL FITC-Annexin V, 5 µL Ethidium Homodimer III (Eth Homo III) and 5 µL of Hoechst 33342 in 100 µL 5x Binding Buffer) was added to cells and incubated for 15 min at room temperature protected from light. Cells were then washed once with 5x Binding buffer and images were acquired using an Olympus CKX41 inverted microscope using FITC, Texas Red and DAPI filter sets with 10x magnification. Staurosporine 0.1 µM (Sigma) was used to induce apoptosis and 1% (v/v) Triton X-100 (Sigma) was used to induce cell necrosis as positive controls.

Table 2.3 Characteristics of stains used to detect cell death.

Cell death	Stain	Filter	Fluorescence colour
Apoptosis	FITC-Annexin V	FITC	Green
Necrosis	Eth Homo III	Texas Red	Red
Healthy	Hoechst 33342	DAPI	Blue

2.4.3 Measurement of epithelial mitochondrial fitness by MTT assay

The MTT assay relies on the activity of a mitochondrial enzyme, the NAD(P)H oxidoreductase which acts as a reporter of active mitochondria. The MTT assay was performed by incubating control and treated cells with 20 µL of yellow MTT solution containing a tetrazole compound (5 mg of 3-(4,5-dimethylthiazol-2-yl)-2,5-diphenyltetrazolium bromide prepared in 1 mL of PBS) at 37°C for 3 h. Following the addition of MTT solution, active mitochondria reduced the yellow tetrazole compound to a purple insoluble formazan. After incubation, 150 µL of MTT solubilisation solution (50% (v/v) dimethylformamide, 0.2% (v/v) acetic acid, 20 µM HCl and 20% (w/v) SDS) was added to each well to dissolve the formazan, and the plate was incubated at 37°C overnight. A solution of 1% (v/v) Triton X-100 was used as a positive control for inactive mitochondria. The intensity of colour is proportional to the number of active mitochondria. Following overnight incubation, the absorbance at 580 nm was quantified using a Tecan Infinite F50 plate reader.

2.4.4 Intracellular ROS quantification by DCFH-DA staining

Intracellular ROS was measured using an OxiSelect™ Intracellular ROS Assay Kit (Cell Biolabs) according to the manufacturer's protocol. Briefly, culture medium was removed from cells and 50 µL of 2',7'-Dichlorodihydrofluorescin diacetate (DCFH-DA) solution (20x DCFH-DA stock diluted in 1x DMEM F-12 media) added and the plate incubated for 1 h at 37°C, 5% CO_2. The DCFH-DA solution was replaced with 50 µL D-PBS and baseline fluorescence readings (excitation 480 nm/emission 530 nm) were taken for 10 min using a FlexStation 3 (Molecular Devices). Ece1 peptides were added and readings were taken immediately for up to 30 min. When added to cells, DCFH-DA diffuses into cells and is deacetylated by cellular esterases to non-fluorescent 2,7'-Dichlorodihydrofluorescin (DCFH), which is rapidly oxidized to highly fluorescent 2',7'-Dichlorodihydrofluorescein

(DCF) by ROS. The fluorescence intensity is proportional to the ROS levels within the cell cytosol. The data was analysed using Softmax Pro software.

2.4.5 Intracellular ATP quantification by luminescence assay

Intracellular ATP was measured using a CellTiter-Glo® Luminescent Cell Viability Assay (Promega) according to the manufacturer's protocol. Briefly, a substrate solution containing luciferin and inactive luciferase (CellTiter-Glo® Reagent) was added to control and treated cells (1:1 ratio of CellTiter-Glo® Reagent volume to sample volume). Catalytic oxidation of luciferin by luciferase in the presence of cellular ATP, Mg^{2+} and molecular oxygen generates a luminescent signal which is proportional to the amount of ATP present within the cells. Luminescence was measured using a FlexStation 3 (Molecular Devices) and data was analysed using Softmax Pro software.

2.4.6 Intracellular calcium quantification by fura-2 staining

Intracellular calcium was quantified by pre-incubating epithelial cells with 50 µL/well of a fura-2-AM solution. Fura-2 solution consisted of 5 µL fura-2-AM (Life Technologies) (prepared at a concentration of 2.5 mM in 50% Pluronic F-127 (Life Technologies):50% DMSO), 5 µL probenecid (Sigma) in 5 mL saline solution (140 mM NaCl, 5 mM KCl, 1 mM $MgCl_2$, 2 mM $CaCl_2$, 10 mM glucose and 10 mM HEPES, adjusted to pH 7.4). Plates were then incubated for 1 h at 37°C, 5% CO_2. For experiments performed with Calcium free saline solution, 2 mM $CaCl_2$ was replaced with 1 mM EGTA. During the 1 h incubation step, the fura-2-AM enters the cell where cellular esterases catalyse the hydrolysis of the AM-ester, releasing fura-2 that generates fluorescence in the presence of free Ca^{2+} ions. Following incubation, excess fura-2 solution was removed and replaced with 50 µL of saline solution and baseline fluorescence readings (excitation 340 nm/emission 520 nm) were taken for 10 min using a FlexStation 3 (Molecular Devices). After baseline acquisition, Candidalysin peptides were added and readings immediately taken for up to 3 h. Data were analysed using Softmax Pro software and expressed as the ratio between excitation and emission spectra.

2.4.7 Caspase activity measurement by luminescence assay

Caspase-3, caspase-8 and caspase-1 activity was measured using a Caspase-Glo® 3/7, Caspase-Glo® 8 or Caspase-Glo® 1 Assay (Promega), according to the manufacturer's protocol. Briefly, a solution containing a cell lysis reagent and a quenched (non-luminescent) caspase-specific substrate was added to control and treated cells (1:1 ratio

of assay reagent volume to sample volume). The addition of the reagent to cells results in cell lysis followed by cleavage of the quenched substrate by active caspase-3, -8 or -1, and the generation of a luminescent signal. The luminescent signal is proportional to the amount of active caspase present within the cells. Luminescence was measured 30 min incubation with the substrate for caspase-3, 1 h for caspase-8 and caspase-1 using a FlexStation 3 (Molecular Devices). Data was analysed using Softmax Pro software.

2.4.8 Cytochrome c and cytokine quantification by ELISA assay

ELISA kits were used to determine concentration of cytochrome c, IL-1β and IL-18. Cell lysates and/or exhausted cell culture medium were quantified for cytochrome c, IL-1β and IL-18.

Determination of cytochrome c, or cytokine concentration was performed by measuring absorbance at 450 nm using a Tecan Infinite F50 plate reader. Analyte concentration was obtained from a dose response curve based on the reference standards.

2.5 Protein assays

2.5.1 Protein extraction

Whole cell lysates were collected by washing cells with ice cold D-PBS and lysing cells in RIPA buffer containing 1X protease inhibitors and 1X phosphatase inhibitors. Plates were kept on ice and cells were scraped using a sterile cell scraper. After incubation on ice for 30 min, the crude lysate was clarified by centrifugation at 20,000 x g, 4^{o}C for 10 min. The supernatant containing soluble proteins was collected and stored at -20^{o}C until required or used immediately in a bicinchoninic acid (BCA) assay to determine protein concentration.

2.5.2 Bicinchoninic Acid (BCA) assay

Total protein concentrations were determined using a BCA Protein Assay kit (Thermo Scientific) according to the manufacturer's protocol. This biochemical assay is based on a reduction of Cu^{2+} ions to Cu^{1+} in the BCA reagent. The amount of Cu^{2+} reduced is proportional to the amount of protein present. This is illustrated by a colour change of the sample solution. The amount of protein present is quantified with a BSA (Sigma) standard curve. BSA was used at a concentration range of 2000 to 31.25 µg/mL. Absorbance was measured at 562 nm using a Tecan Infinite F50 plate reader.

2.5.3 Sodium Dodecyl Sulphate Polyacrylamide Gel Electrophoresis (SDS-PAGE)

Protein samples (10 µg) were mixed with 1X Laemmli (Sample buffer) containing 100 µM DTT and appropriate volumes of filtered-sterilised PBS. Samples were heated at 80^{o}C for 5-10 min (ThermoQ BIOER) and used directly for gel electrophoresis. SDS-PAGE gels (12% acrylamide) were fitted into a glass chamber filled with 1X running buffer. Pre-stained protein ladder (3 µL) (New England BioLabs) and 15 µL of sample were applied to the gel and electrophoresis was performed at 90 V for approximately 2 h using a Tetracell System (Biorad). After separation, proteins were analysed by western blot analysis.

2.5.4 Western blot analysis

Following electrophoresis, western blot analysis was used to visualise target proteins. Briefly, separated proteins were transferred onto nitrocellulose membranes (BIORAD) using a blotting tank. Gel and membrane were placed between a double layer of chromatography paper (Whatman), and were then placed between the sponges of a transfer cassette. The sandwiched cassette was inserted into a tank between two electrodes, with the gel facing the cathode. The tank was filled with transfer buffer and the proteins transferred to membrane at 100 V for 1 h (BIORAD).

Following transfer, the membrane was removed from the cassette and incubated on a shaker for 1 h in a blocking solution (5% dry milk prepared in 1X TBS-T). This step is required to prevent non-specific binding of the primary antibody to the membrane.

Membranes were subsequently incubated overnight with primary antibodies (Table 2.4) diluted in either 5% dry milk or 5% BSA prepared in TBS-T at 4^{o}C and washed 3X for 10 min with 1X TBS-T. Secondary IgG horseradish peroxidase (HRP)-conjugated antibodies (Jackson ImmunoResearch) were diluted in 5% dry milk in TBS-T (1:10000), and were added to the membranes and incubated at room temperature for 1 h. After washing the membranes 3X for 10 min, target proteins were detected by incubating membranes in a chemiluminescent solution (Immobilon western, Chemiluminescent Substrate; Millipore) for 5 min and exposing the membrane to film (GE Healthcare Life Sciences).

The primary antibody for the loading control Actin (diluted 1:10000) and secondary antibody (diluted 1:20000) were incubated with membrane for 30 min at room

temperature. Before exposure to film, membranes were incubated with the chemiluminescent solution for 30 sec.

Table 2.4. Detection antibodies for epithelial signalling proteins.

Primary antibody	Secondary antibody	Band size (kDa)	Dilution	Company
Caspase-8	Anti-Rabbit	10, 57	1:1000	Cell signalling
Caspase-3	Anti-Rabbit	17, 19, 35	1:1000	Cell Signalling
PARP	Anti-Rabbit	96, 116	1:1000	Cell Signalling
cIAP2	Anti-Rabbit	70	1:1000	Cell Signalling
RIPK1	Anti-Rabbit	78	1:1000	Cell Signalling
P-RIPK1	Anti-Rabbit	78-82	1:1000	Cell Signalling
RIPK3	Anti-Rabbit	57	1:1000	Abcam
P-RIPK3	Anti-Rabbit	57-70	1:2000	Abcam
MLKL	Anti-Rat	52	1:1000	Millipore
P-MLKL	Anti-Rabbit	54	1:1000	Abcam
NLRP3	Anti-Rabbit	85, 110	1:1000	Cell Signalling
ASC	Anti-Rabbit	22	1:1000	Cell Signalling
Caspase-1	Anti-Rabbit	20, 30-45, 50	1:1000	Cell Signalling
IL-1β	Anti-Rabbit	17, 31	1:1000	Cell Signalling
IL-18	Anti-Rabbit	22	1:2000	Millipore
Gasdermin D	Anti-Mouse	54, 31, 22	1:1000	Santa Cruz
actin	Anti-Mouse	43	1:10000	Millipore

2.6 Statistical analysis of data

Assay data was analysed by one-way analysis of variance (ANOVA) using Sigma Plot 12.5 software and the Holm-Sidak method was applied to establish statistically significant differences. In all cases, $p < 0.05$ was taken to be significant.

Chapter 3: Role of *C. albicans* Candidalysin peptides in driving cell death processes in human oral epithelial cells.

3.1 Introduction

The balance between cell death and cell survival is a critical factor that determines the correct growth and development of tissues and organs within the body, and is a vital process that enables health to be maintained, particularly during periods of microbial infection. Epithelial cells form the mucosal surfaces of the body and are usually the first point of contact between host and pathogen and are the first line of defence against microbes. Since epithelial cells are in continuous contact with commensal and pathogenic microbes, their ability to discriminate between the two is essential to health (Naglik et al., 2011).

During oropharyngeal candidiasis, the interaction between *C. albicans* and the oral mucosa results in cell death pathways being induced in oral epithelial cells (Chiang et al., 2007; Park et al., 2005; Villar et al., 2012; Villar and Zhao, 2010). Activation of specific death pathways in response to microbial stimuli plays an essential role in modulating the pathogenesis of a variety of infectious diseases.

The ability of *C. albicans* to switch from commensal to pathogenic growth at mucosal surfaces is accompanied by a change in the physical morphology of the fungus from spherical yeast to elongated hyphae that cause damage, inflammation and consequent release of inflammatory mediators including cytokines and damage-associated molecular patterns (DAMPs) (Villar et al., 2005). Research in our group has demonstrated that the hypha-associated protein Ece1p, is a key virulence factor of *C. albicans*. Subsequent analysis of Ece1p has identified that this protein is processed within the fungus into eight smaller peptides; first into a 32 amino acid (aa) peptide (termed Ece1-III$_{62\text{-}93KR}$) and then into a 31 aa peptide (termed Candidalysin). Both Candidalysin peptides act by inserting into epithelial cell membranes, which results in the induction of pro-inflammatory responses and damage (Moyes et al., 2016).

The signalling pathways that promote cell death are present in all somatic cells in the body and play a crucial role in eliminating infected cells and triggering inflammatory

responses (Moriwaki and Chan, 2013). Thus, the aim of this chapter is to determine the role of *C. albicans* Ece1p and Candidalysin peptides in activating oral epithelial cell death responses by investigating classical hallmarks of cellular stress including membrane permeability, mitochondrial fitness, intracellular levels of reactive oxygen species (ROS), adenosine triphosphate (ATP) and calcium. To study these responses, an oral epithelial cell line (TR146) was used. TR146 were isolated from a biopsy specimen of a squamous cell carcinoma of the buccal mucosa (Rupniak et al., 1985) representing closely the site where *C. albicans* colonizes, infiltrates and causes infection. This cell line has been extensively used in epithelial - *C. albicans* and epithelial – Candidalysin interaction studies, with TR146 seeding densities, *C. albicans* multiplicity of infection (MOI) and Candidalysin peptide concentrations optimised in previous publications (Moyes et al., 2010; Moyes et al., 2014; Moyes et al., 2016).

3.2 Methods

3.2.1 Epithelial cell damage assay

TR146 monolayers were treated with *C. albicans* strains (Table 3-1) at an MOI of 0.01 and with Ece1-III$_{62\text{-}93KR}$ or Candidalysin (described in section 2.2.3) at 70, 30, 15 and 3 µM for 24 h. Epithelial cell damage was determined by measuring LDH activity in exhausted cell culture medium using a Cytox 96 Non-Radioactive Cytotoxicity Assay (Promega). Recombinant porcine LDH (Sigma) was used to produce a standard curve (see section 2.4.1).

3.2.2 Fluorescent microscopy

TR146 oral epithelial cells were treated with Ece1-III$_{62\text{-}93KR}$ or Candidalysin at 70, 30, 15 and 3 µM, 0.1 µM staurosporine, and 1% (v/v) Triton X-100 for 3, 6 and 24 h. After staining with FITC-Annexin V, Ethidium Homodimer III (Eth Homo III) and Hoechst 33342, cells were imaged with an Olympus CKX41 inverted microscope (for full details see section 2.4.2).

3.2.3 MTT assay

TR146 oral epithelial cells were treated with Ece1-III$_{62\text{-}93KR}$ or Candidalysin at 70, 60, 45, 30, 15, 3 and 1.5 µM for 5 min, 15 min, 30 min, 1 h, 1.5 h, 2 h, 2.5 h, 3 h, 6 h and 24 h. Mitochondrial fitness was assessed by quantifying the activity of the NAD(P)H-

oxidoreductase by adding MTT solution for 3 h followed by solubilisation solution overnight (for full details see section 2.4.3).

3.2.4 Detection of intracellular ROS

TR146 oral epithelial cells were pre-incubated for 1 h with DCFH-DA and treated with Ece1-III$_{62\text{-}93KR}$ or Candidalysin at 70, 15 and 3 µM. Fluorescence readings were immediately taken for up to 30 min (for full details see section 2.4.4).

3.2.5 Detection of intracellular ATP

TR146 oral epithelial cells were treated with Ece1-III$_{62\text{-}93KR}$ or Candidalysin at 70, 60, 45, 30, 15, 3 and 1.5 µM for 5 min, 15 min, 30 min, 1 h, 1.5 h, 2 h, 2.5 h, 3 h and 6 h. Intracellular ATP levels were quantified by adding a substrate solution and immediately measuring luminescence (see section 2.4.5).

3.2.6 Detection of intracellular calcium

TR146 oral epithelial cells were pre-incubated for 1 h with Fura-2 solution and treated with Ece1-III$_{62\text{-}93KR}$ or Candidalysin at 70, 15, 3 and 1.5 µM in assay buffers that contained and lacked calcium. Fluorescence readings were immediately taken for up to 3 h (see section 2.4.6).

3.3 Results

3.3.1 Damage of oral epithelial cells is Candidalysin dependent

The role of Candidalysin in causing epithelial cell damage was first examined using *Candida* strains (Section 3.2.1, Table 3-1). The TR146 cell line was cultured to confluency and infected with *Candida* strains at a MOI of 0.01 for 24 h. After incubation, exhausted medium was collected and quantified for LDH activity (Figure 3-1).

Infection of epithelial cells with BWP17 and *ECE1* revertant (*ece1*Δ/Δ+*ECE1*) caused significant LDH activity when compared with the vehicle control. In contrast, *C. albicans* mutant strains unable to express and secrete Candidalysin (*ece1*Δ/Δ and *ece1*Δ/Δ+*ECE1*$_{\Delta 184\text{-}279}$) were reduced of damaging the epithelium. These data demonstrate that the region encoding Candidalysin is essential for inducing epithelial damage.

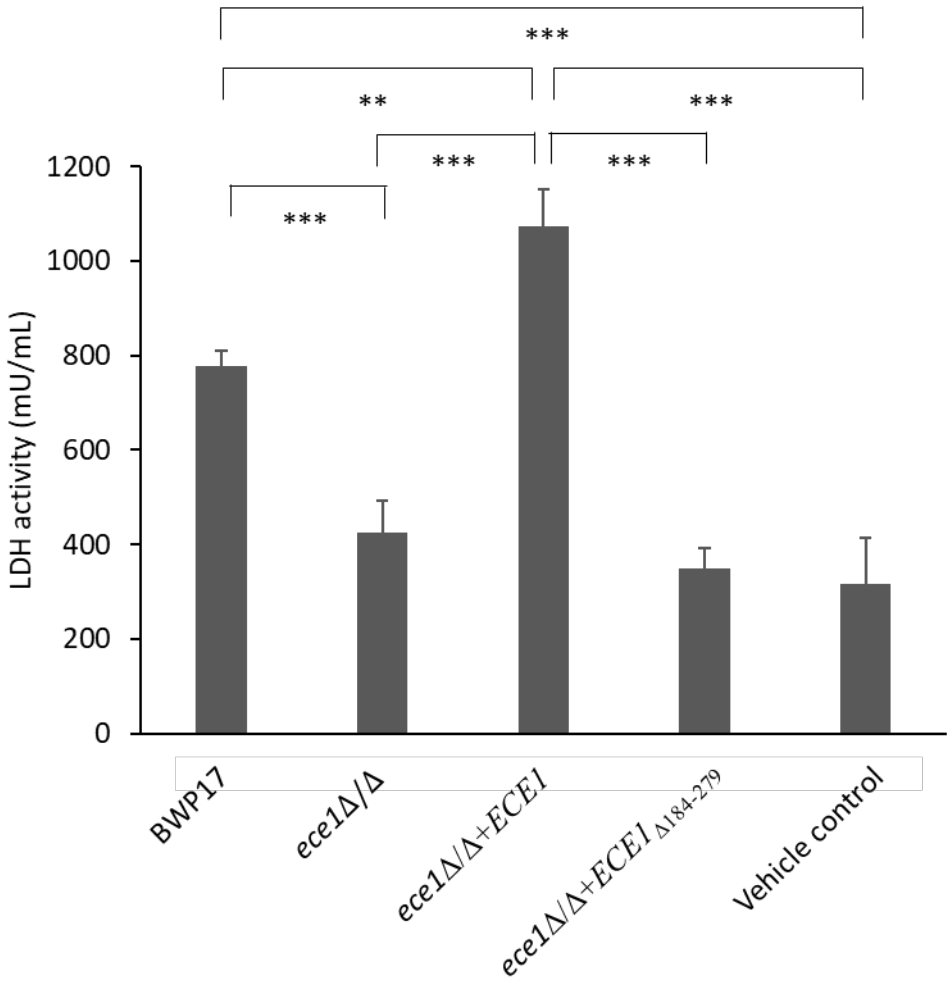

Figure 3-1. Damage of oral epithelial cells by *C. albicans ECE1* mutants. TR146 oral epithelial cells were infected with a panel of *C. albicans ECE1* mutant strains (MOI of 0.01) for 24 h and exhausted cell medium was quantified for LDH activity as a marker of cellular damage. Data are the mean of three biological replicates (+SEM). Statistical significance was calculated by one way ANOVA, *** P<0.001.

Next, I determined if direct application of Candidalysin peptides could also induce epithelial damage in a manner similar to *C. albicans* infection. TR146 monolayers were incubated with Ece1-III$_{62\text{-}93KR}$ or Candidalysin (see section 2.2.3) at 70, 30, 15 and 3 µM for 24 h. Following treatment, exhausted medium was assayed for LDH activity (Figure 3-2).

This data demonstrates that TR146 cells released LDH in response to Candidalysin peptides in a dose-dependent manner. Treatment with Ece1-III$_{62\text{-}93KR}$ or Candidalysin at a concentration of 70 and 30 µM caused significant epithelial damage when compared with the vehicle control. Damage was not observed at peptide concentrations below 15

µM. These results confirm the importance of this toxin for *C. albicans*-induced epithelial damage.

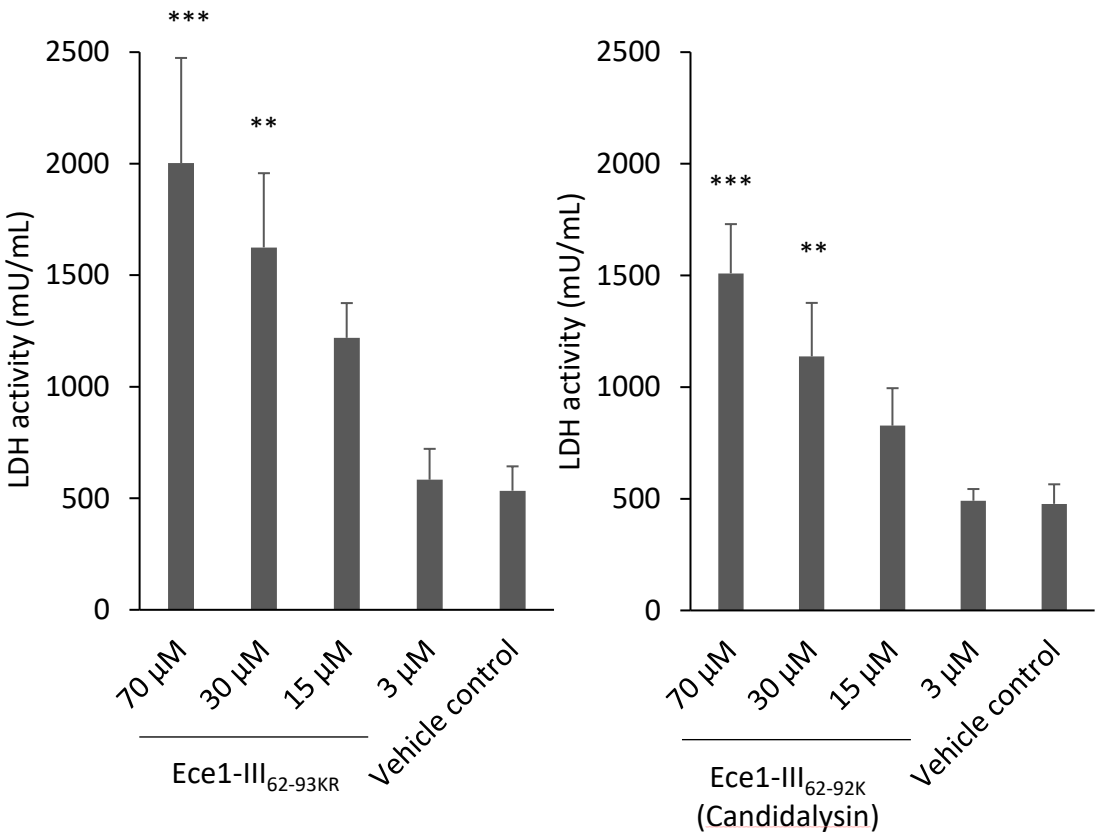

Figure 3-2. **Damage of oral epithelial cells by *C. albicans* Candidalysin peptides.** TR146 oral epithelial cells were incubated with *C. albicans* Candidalysin peptides at different concentrations (70, 30, 15 and 3 µM) for 24 h and cell exhausted culture medium was assayed for LDH activity as a marker of cellular damage. Data are the mean of three biological replicates (+SEM). Statistical significance was calculated by one way ANOVA, ** P<0.01, *** P<0.001.

3.3.2 Induction of cell death processes by Candidalysin peptides

Cell damage can occur in response to different stress stimuli including chemical, physical, infectious, biological, nutritional or immunological factors. Depending on the extent of injury, the cell is able to repair itself or can undergo cell death. Cell death involves physical changes to the cell membrane and disruption of cellular homeostasis. Thus, a qualitative approach was initially used to investigate epithelial membrane permeability in oral epithelial cells exposed to Candidalysin peptides.

TR146 oral epithelial cells were treated with Candidalysin peptides and fluorescence microscopy was performed to visualise markers associated with cell damage and death. Cells were pre-incubated with FITC-Annexin V, Eth Homo III and Hoechst 33342 prior to

treatment with Candidalysin peptides. FITC-Annexin V produces green fluorescence when bound to phosphatidylserine residues exposed on the outer surface of the lipid bilayer of apoptotic cells. Eth Homo III is unable to cross intact epithelial plasma membranes, but is able to enter cells with damaged membranes where it intercalates with DNA to produce red/yellow fluorescence. Hoechst 33342 (blue fluorescence) was used to visualise epithelial nuclei. As positive controls, 0.1 µM staurosporine was used to induce apoptosis (Kabir et al., 2002) and 1% (v/v) Triton X-100 was used to induce cell necrosis (Kwon et al., 2011).

Treatment with Ece1-III$_{62\text{-}93KR}$ or Candidalysin resulted in TR146 epithelial cells that were weakly positive for Annexin V but strongly positive for Eth Homo III staining (Figures 3-3, 3-4 and 3-5), particularly at higher concentrations of peptides (30 and 70 µM) at all time points tested (3, 6 and 24 h). Epithelial cells appeared more fluorescent for both Annexin V and Eth Homo III when treated with Ece1-III$_{62\text{-}93KR}$ compared with Candidalysin and, in general, the quantity of cells that exhibited positive staining increased over time.

In summary, epithelial cells treated with Candidalysin peptides display a change in membrane permeability with Annexin V binding to phosphatidylserine and Eth Homo III penetrating into cells. Thus, treatment of epithelial cells with Candidalysin peptides results in characteristic features associated with both apoptotic and necrotic death, but predominantly necrotic cell death.

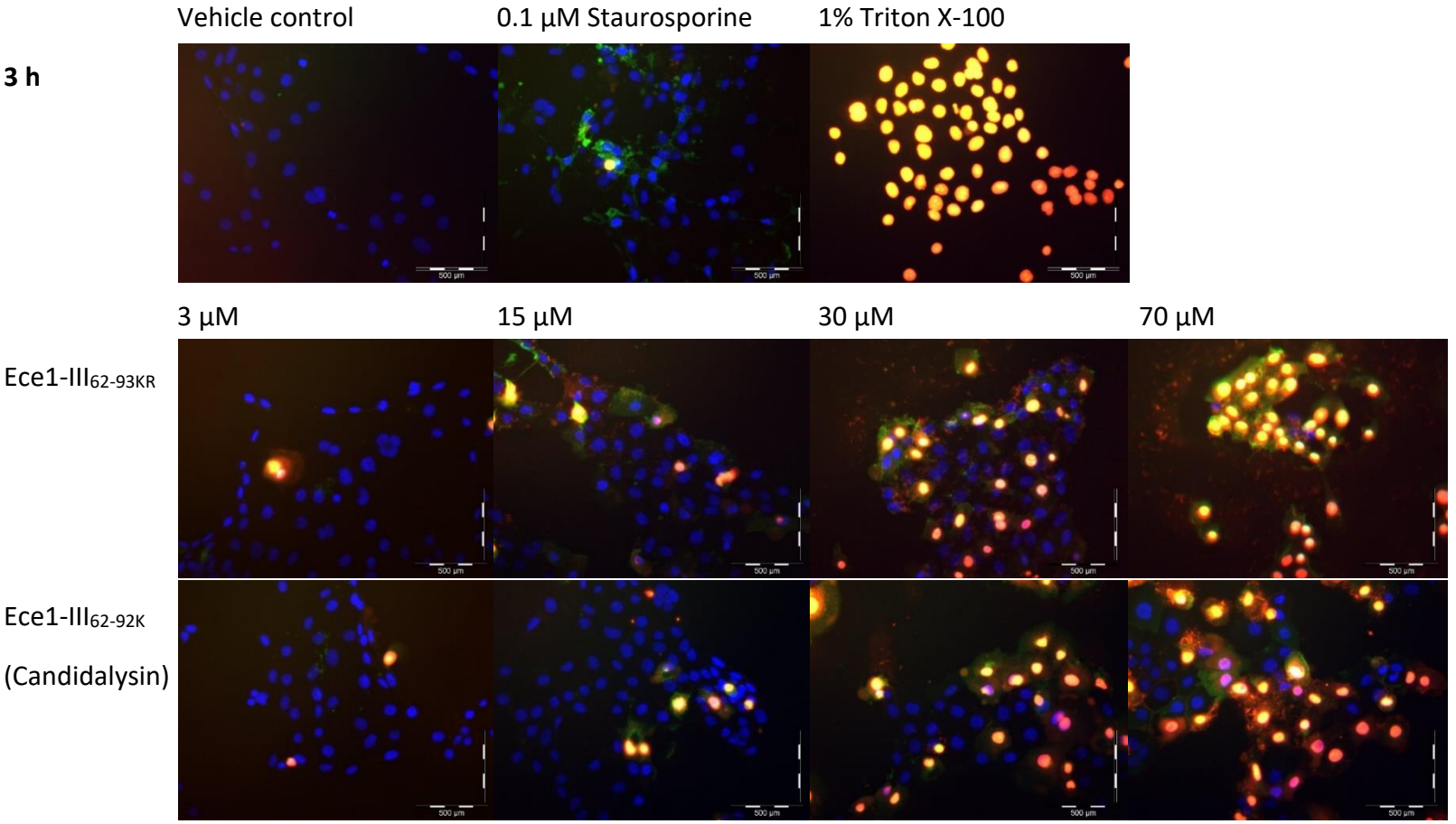

Figure 3-3. **Cell death markers induced in epithelial cells by Candidalysin peptides after 3 h.** TR146 oral epithelial cells were pre-incubated with Hoechst 33342 (blue-fluorescent staining of the entire cell population), FITC Annexin V fluorochromes (apoptotic stain: Green), Eth Homo III (necrotic stain: Red/Yellow) and incubated with Candidalysin peptides (70, 30, 15 and 3 µM) for 3 h. 0.1 µM staurosporine was used as control to induce Annexin V postive cells and 1% (v/v) Triton X-100 for Ethidium Homodimer III positive cells. Data are representative of three biological replicates. Images were taken with a fluorescence microscope at 100x magnification. Scale bars are 500 µm.

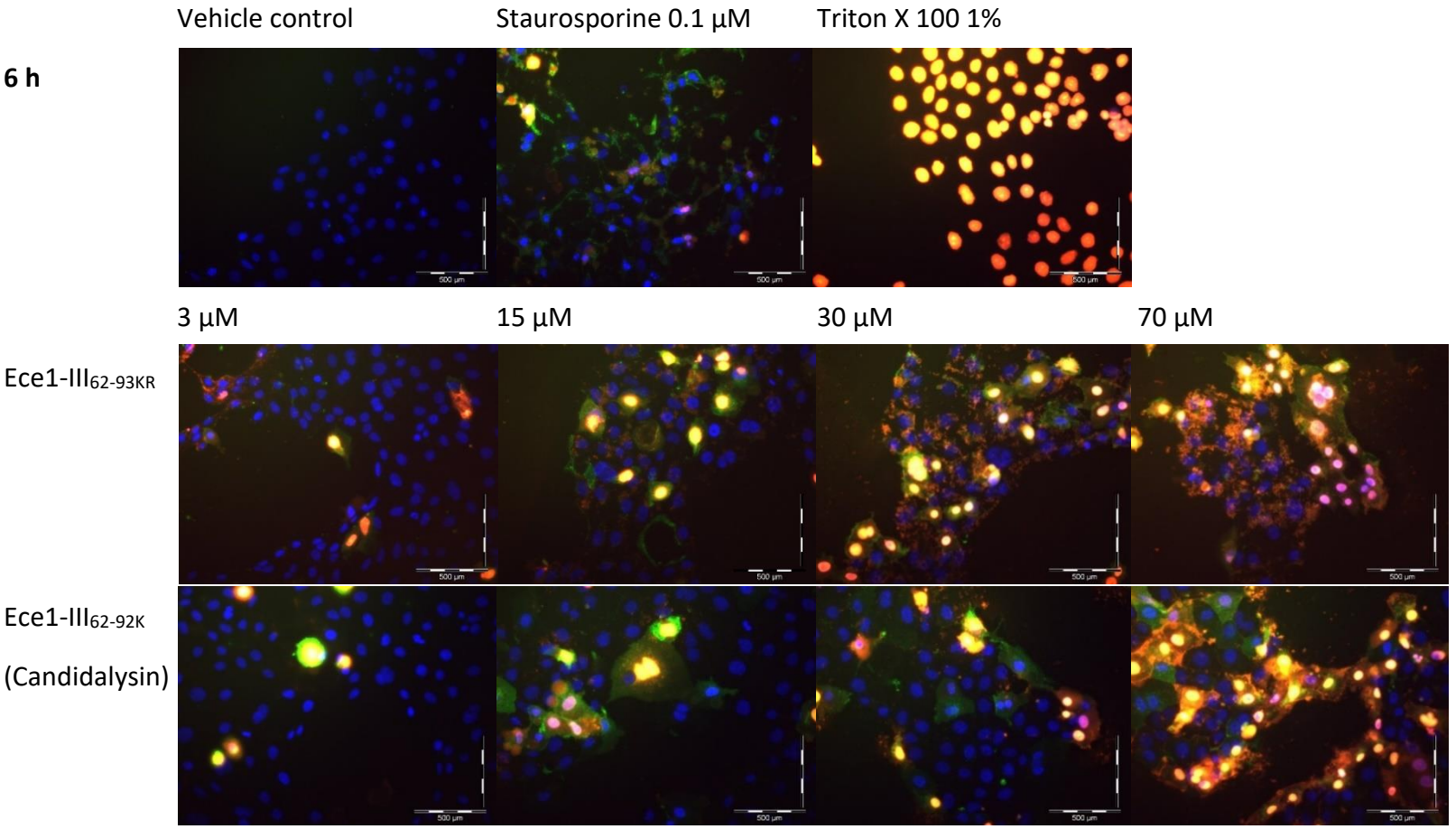

Figure 3-4. **Cell death markers induced in epithelial cells by Candidalysin peptides after 6 h.** TR146 oral epithelial cells were pre-incubated with Hoechst 33342 (blue-fluorescent staining of the entire cell population), FITC Annexin V fluorochromes (apoptotic stain: Green), Eth Homo III (necrotic stain: Red/Yellow) and incubated with Candidalysin peptides (70, 30, 15 and 3 µM) for 6 h. 0.1 µM staurosporine was used as control for Annexin V postive cells and 1% (v/v) Triton X-100 for Ethidium Homodimer III positive cells. Data are representative of three biological replicates. Images were taken with a fluorescence microscope at 100x magnification. Scale bars are 500 µm.

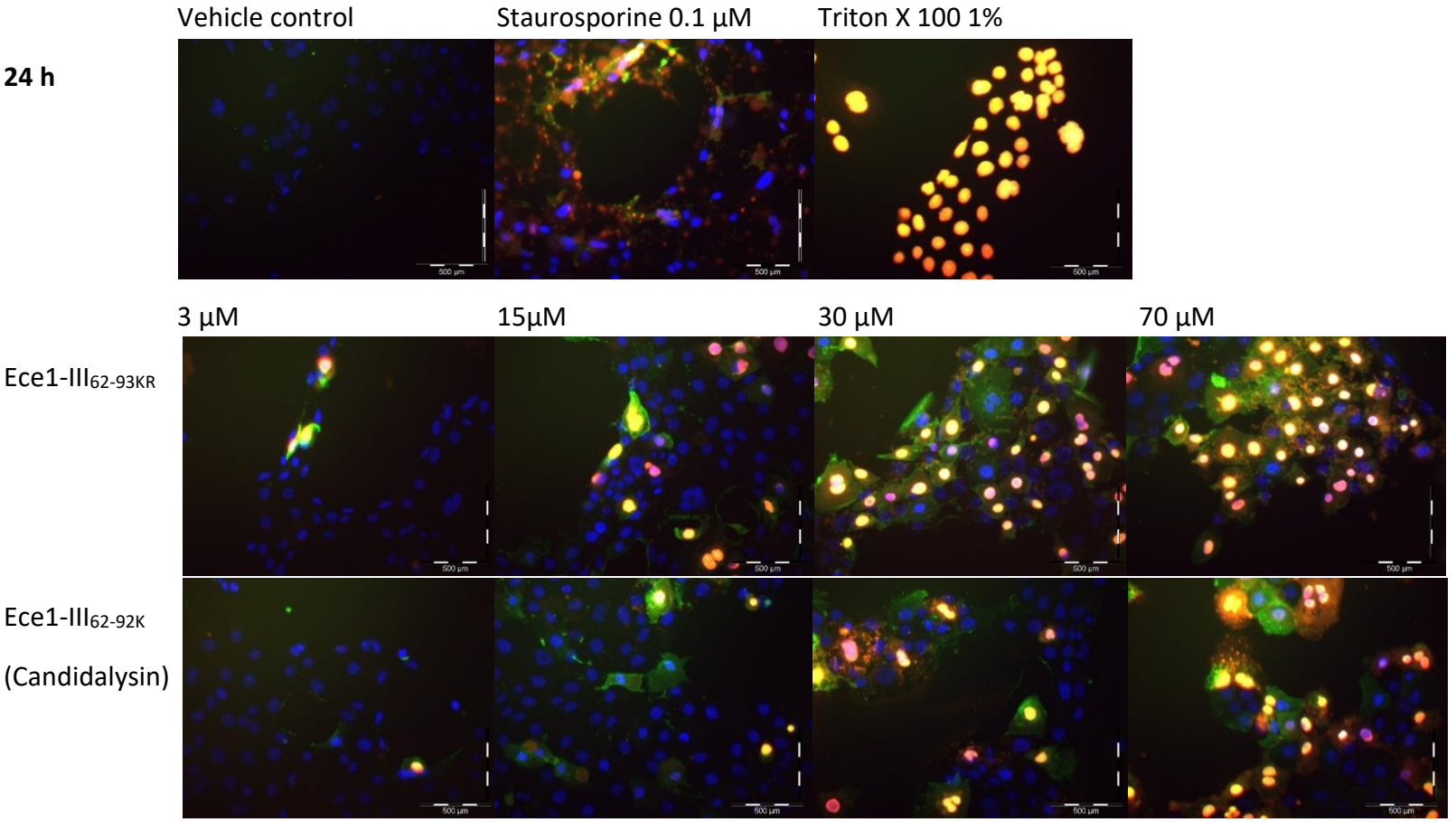

Figure 3-5. **Cell death markers induced in epithelial cells by Candidalysin peptides after 24 h.** TR146 oral epithelial cells were pre-incubated with Hoechst 33342 (blue-fluorescent staining of the entire cell population), FITC Annexin V fluorochromes (apoptotic stain: Green), Eth Homo III (necrotic stain: Red/Yellow) and incubated with Candidalysin peptides (70, 30, 15 and 3 µM) for 24 h. 0.1 µM staurosporine was used as control for Annexin V postive cells and 1% (v/v) Triton X-100 for Ethidium Homodimer III positive cells. Data are representative of three biological replicates. Images were taken with a fluorescence microscope at 100x magnification. Scale bars are 500 µm.

3.3.3 Candidalysin peptides induce loss of mitochondrial fitness in TR146 cells

During periods of cell stress, mitochondrial viability is often negatively affected and is commonly used as a robust indicator of cytotoxicity in several cell death pathways.

Given that Ece1-III$_{62\text{-}93KR}$ and Candidalysin induce epithelial cell damage and have an impact on membrane permeability, mitochondrial activity was also investigated testing mitochondrial fitness by MTT assay. The MTT assay quantifies the activity of mitochondrial NAD(P)H-dependent cellular oxidoreductase enzymes, which act as a reporter for the presence of metabolically active cells. Thus, TR146 oral epithelial cells were treated with Ece1-III$_{62\text{-}93KR}$ or Candidalysin at 70, 60, 45, 30, 15, 3 and 1.5 µM for 3 h and mitochondrial activity was assessed (Figure 3-6). 1% Triton X-100, which lyses epithelial cells, was used as a positive control.

TR146 mitochondrial fitness was negatively affected by both Candidalysin peptides in a dose-dependent manner. Notably, Candidalysin had a stronger effect on mitochondria than Ece1-III$_{62\text{-}93KR}$. Compared with untreated cells, treatment with Ece1-III$_{62\text{-}93KR}$ caused a non-significant reduction of mitochondrial activity (Figure 3-6 A), whereas exposure to Candidalysin (45 µM or higher) resulted in a significant decrease in mitochondrial fitness (Figure 3-6 B).

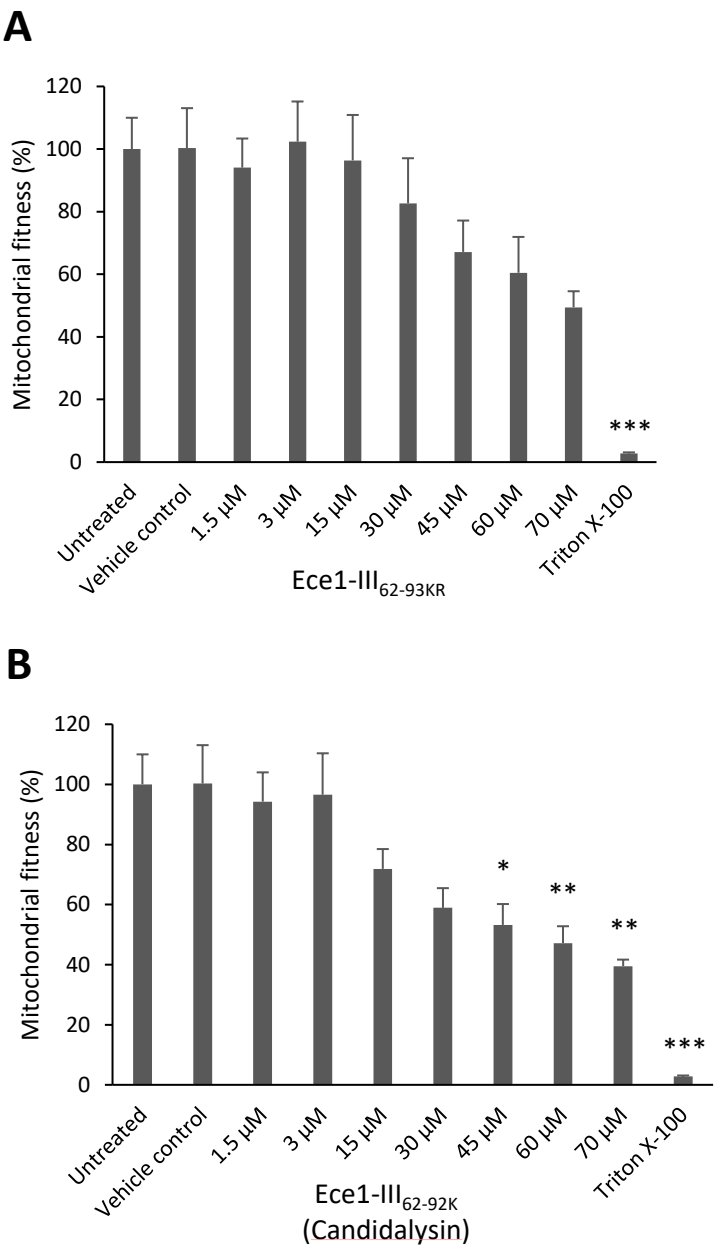

Figure 3-6. **Reduction in mitochondrial fitness in response to Candidalysin peptides.** TR146 oral epithelial cells were incubated with Ece1-III$_{62\text{-}93KR}$ (A) and Candidalysin (B) (1.5, 3, 15, 30, 45, 60, 70 µM) for 3 h and assayed for mitochondrial fitness by MTT assay. Triton X-100 (1%) was used as a positive control. Data are expressed as a percentage of mitochondrial fitness relative to untreated cells. Data are the mean of three biological replicates (+SEM). Statistical significance was calculated by one way ANOVA, * P<0.05, ** P<0.01, *** P<0.001.

Having observed a concentration-dependent effect of Candidalysin peptides on TR146 mitochondrial activity, I next assessed whether the loss of mitochondrial fitness was time-dependent. To address this, TR146 oral epithelial cells were treated with Ece1-III$_{62\text{-}93KR}$ or Candidalysin at 70 or 15 µM for 5 min, 15 min, 30 min, 1 h, 1.5 h, 2 h, 2.5 h, 3 h, 6 h and 24 h (Figure 3-7).

Compared with untreated cells, a significant 60-70% reduction in mitochondrial activity was observed in cells treated with 70 µM Ece1-III$_{62\text{-}93KR}$ at all time points tested. Treatment with 15 µM Ece1-III$_{62\text{-}93KR}$ caused a 20% reduction in mitochondrial fitness, which was not significant. Interestingly, treatment with Candidalysin caused a significant reduction in mitochondrial activity at both high (70 µM) and intermediate (15 µM) concentrations. High Candidalysin concentrations caused a significant (70%) loss of mitochondrial fitness after only 5 min of treatment. This reduction in activity was further increased from 70% to 95% in a time-dependent manner up to 24 h of exposure. Intermediate concentrations of Candidalysin reduced mitochondrial activity by 50% at all time points tested, with significance being reached from 1.5 h onwards.

In summary, these data demonstrate that Candidalysin peptides affect TR146 mitochondria in a dose- and time- dependent manner and the reduction in mitochondrial activity is particularly significant in response to Candidalysin.

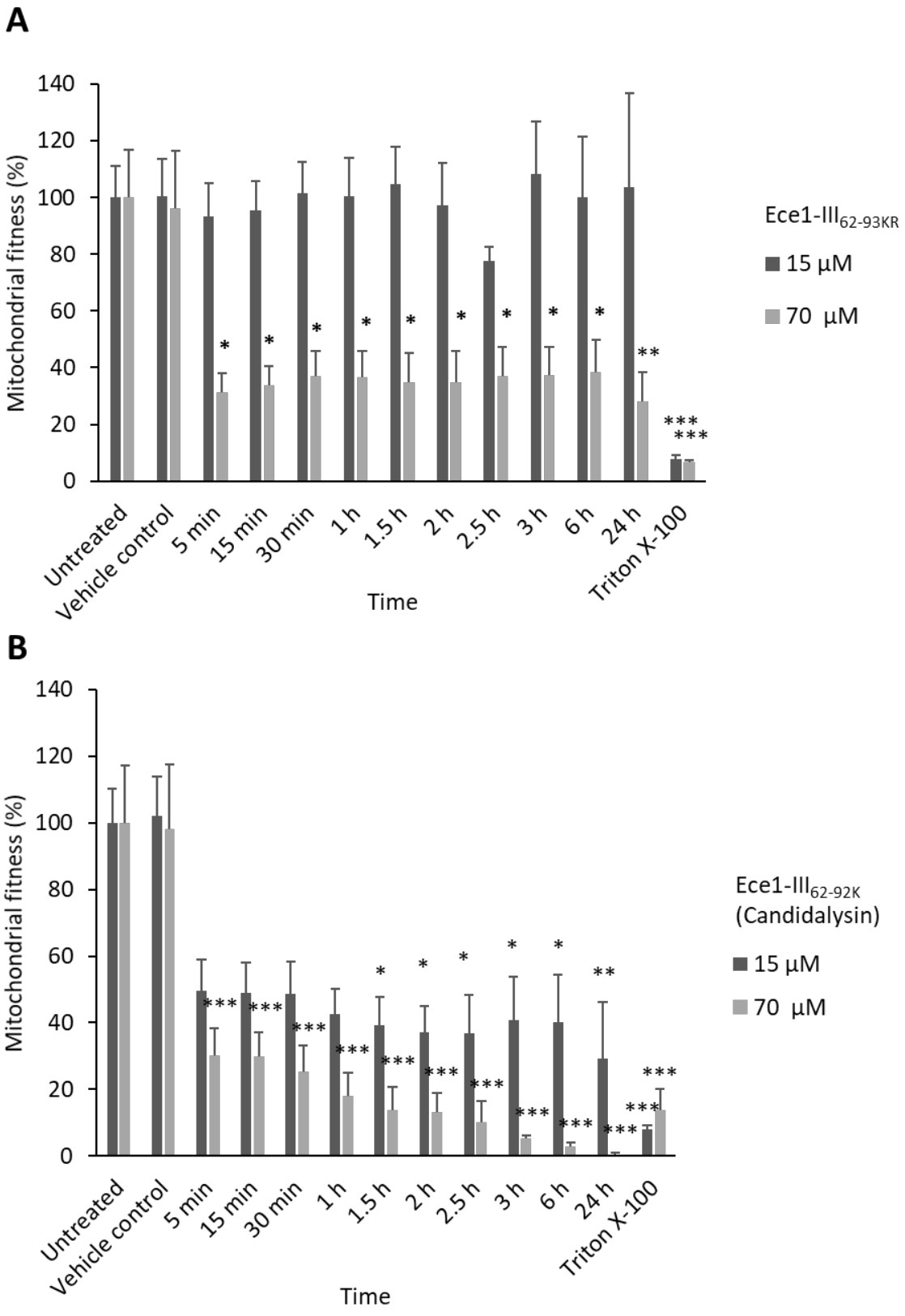

Figure 3-7. **Time-course of mitochondrial fitness following treatment with Candidalysin peptides.** TR146 oral epithelial cells were incubated with Ece1-III$_{62\text{-}93KR}$ (A) and Candidalysin (B) at 15 and 70 µM between 5 min and 6 h and assayed for mitochondrial fitness by MTT assay. 1% Triton X-100 was used as a positive control. Data are expressed as percentage of mitochondrial fitness relative to untreated cells. Data are the mean of three biological replicates (+SEM). Statistical significance was calculated by one way ANOVA, * P<0.05, ** P<0.01, *** P<0.001.

3.3.4 Candidalysin peptides induce production of intracellular ROS in TR146 cells

During cellular homeostasis, mitochondria generate low levels of reactive oxygen species (ROS). However, disruption of the electron transport chain within mitochondria can result in high levels of ROS production. The production of ROS within cells is widely considered to be a deleterious event that is responsible for damaging numerous macromolecules including nucleic acids, proteins, carbohydrates, and lipids. Cells that undergo ROS-mediated damage induce host defence/repair mechanisms, but if this response is incapable of repairing the ROS-induced damage, cell death may occur (Rahal et al., 2014).

Generation of ROS is triggered by various stimuli, including toxins (Dantas Ada et al., 2015; Rovin et al., 1990; Zhang et al., 2017; Zhang et al., 2016). Thus, to assess if Candidalysin peptides affected the production of intracellular ROS, TR146 oral epithelial cells were treated with Ece1-III$_{62\text{-}93KR}$ or Candidalysin and measurements of ROS were taken in real time over 30 min.

Both Ece1-III$_{62\text{-}93KR}$ and Candidalysin induced the generation of ROS in a dose-dependent manner (Figure 3-8). Notably, treatment with 70 µM Candidalysin produced a greater spike in levels of intracellular ROS compared to treatment with Ece1-III$_{62\text{-}93KR}$. In both cases, ROS levels were sustained and continued to increase over time.

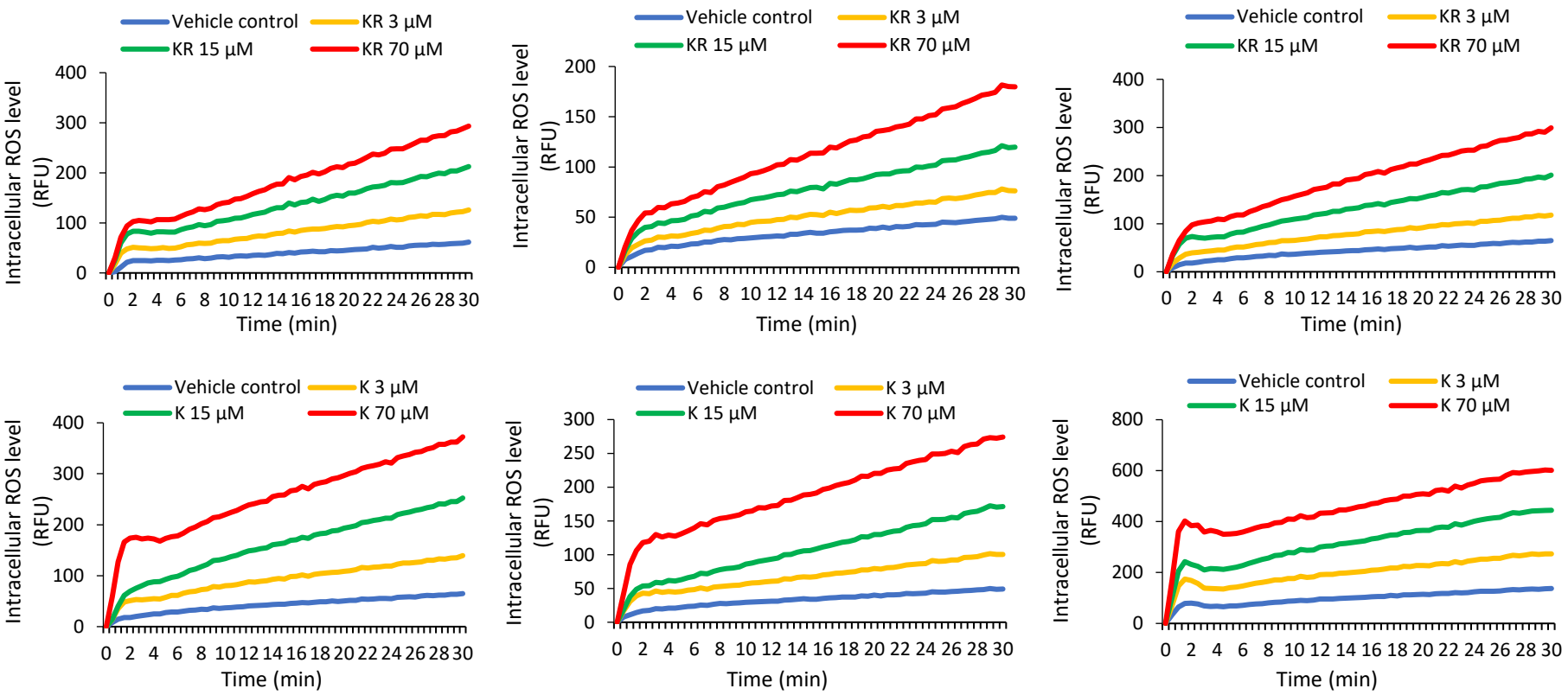

Figure 3-8. **Quantification of intracellular ROS in oral epithelial cells treated with *C. albicans* Candidalysin peptides.** TR146 oral epithelial cells were pre-incubated with DCFH-DA for 1 h and subsequently incubated with Candidalysin peptides (70, 15 and 3 µM). Fluorescence was measured in real time for up to 30 min. All three biological replicates are illustrated.

3.3.5 Candidalysin peptides cause depletion of intracellular ATP in TR146 cells

Mitochondria are essential organelles required for viability of eukaryotic cells. The primary function of mitochondria is the biosynthesis of adenosine triphosphate (ATP). Given this critical functionality, loss of general mitochondrial fitness or an inability to produce ATP can often result in a gross disruption of cellular homeostasis leading to irrecoverable damage and death.

Since treatment of epithelial cells with Candidalysin peptides was observed to cause loss of mitochondrial fitness and increases in ROS, I next quantified levels of intracellular ATP. TR146 oral epithelial cells were treated with Ece1-III$_{62\text{-}93KR}$ or Candidalysin at 70, 60, 45, 30, 15, 3 and 1.5 µM for 3 h (Figure 3-9). 1% Triton X-100 was used as a positive control.

Intracellular ATP levels were influenced by Candidalysin peptides in a dose-dependent manner but Ece1-$_{III62\text{-}93KR}$ was observed to reduce levels of intracellular ATP more strongly than Candidalysin. Compared with untreated cells, Ece1-III$_{62\text{-}93KR}$ caused a non-significant decrease in intracellular ATP at 15 µM, but a significant decrease at 30 µM and above (Figure 3.9 A). Candidalysin induced a non-significant decrease in intracellular ATP at 15 µM and 30 µM, but a significant decrease at 45 µM and above (Figure 3-9 B).

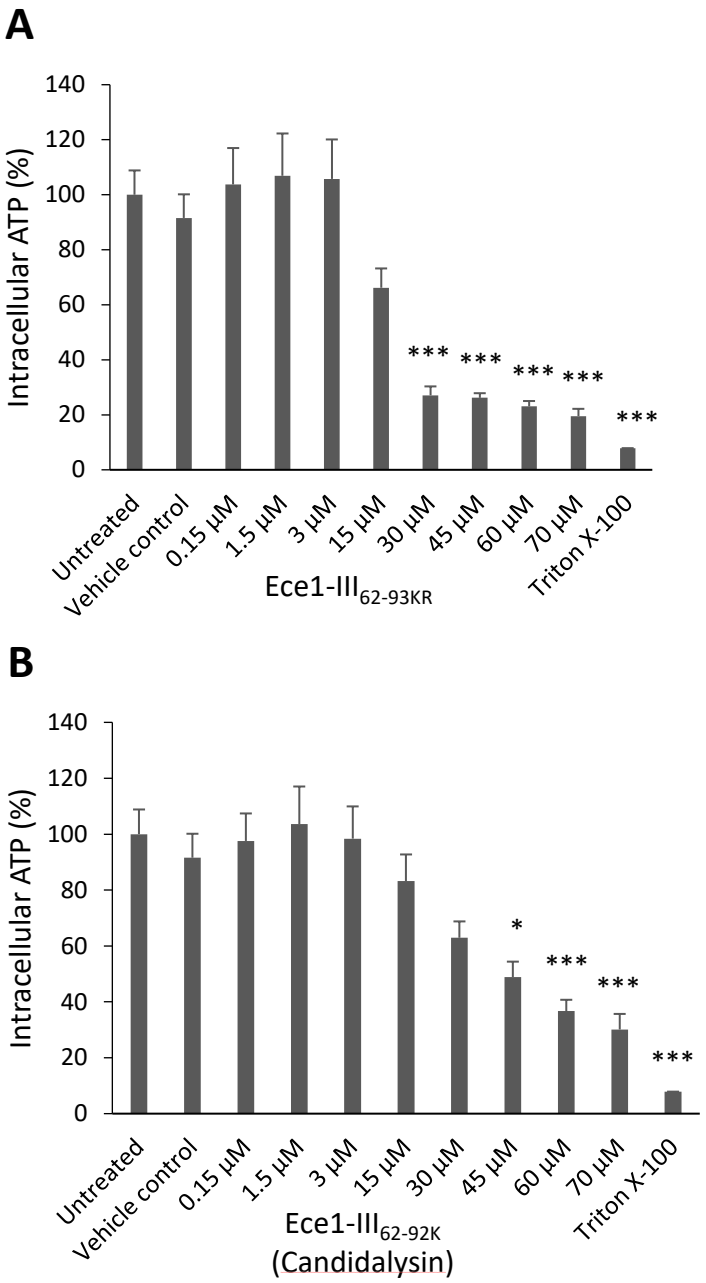

Figure 3-9. **Intracellular ATP levels following treatment with *C. albicans* Candidalysin peptides.** TR146 oral epithelial cells were incubated with Ece1-III$_{62\text{-}93KR}$ (A) and Candidalysin (B) (0.15, 1.5, 3, 15, 30, 45, 60, 70 µM) for 3 h and levels of intracellular ATP were quantified by luminescence assay. 1% (v/v) Triton X-100 was used as a positive control. Data are expressed as the percentage of intracellular ATP relative to untreated cells. Data are the mean of three biological replicates (+SEM). Statistical significance was calculated by one way ANOVA, * P<0.05, ** P<0.01, *** P<0.001.

Given that treatment of TR146 cells with Candidalysin peptides resulted in a dose-dependent reduction in intracellular ATP levels, I next investigated whether the observed decrease in ATP was time-dependent. To address this, TR146 oral epithelial cells were exposed to Ece1-III$_{62\text{-}93KR}$ or Candidalysin at 70 or 15 µM for 5 min, 15 min, 30

min, 1 h, 1.5 h, 2 h, 2.5 h, 3 h and 6 h and ATP levels quantified as described (Figure 3-10).

Compared with untreated cells, Ece1-III$_{62\text{-}93KR}$ at 70 µM caused a time-dependent decrease in intracellular ATP, which was significant from 1 h of exposure. TR146 cells treated with 15 µM Ece1-III$_{62\text{-}93KR}$ exhibited no change until 30 min. However, from 30 min to 6 h, ATP levels were observed to decrease in a time-dependent manner, reaching significance from 3 h onwards.

In general, the observed trends in ATP reduction were more pronounced in response to Ece1-III$_{62\text{-}93KR}$ than with Candidalysin. Treatment with 70 µM Candidalysin caused an initial reduction in ATP at 5 and 15 min followed by a recovery between 30 min and 2.5 h. A similar trend was also observed with 15 µM of Candidalysin. However, by 6 h, a significant (85%) reduction in ATP levels were observed in TR146 cells exposed to 70 µM Candidalysin.

In summary, these data demonstrate that Candidalysin peptides affect the level of intracellular ATP in epithelial cells in both a dose- and time-dependent manner.

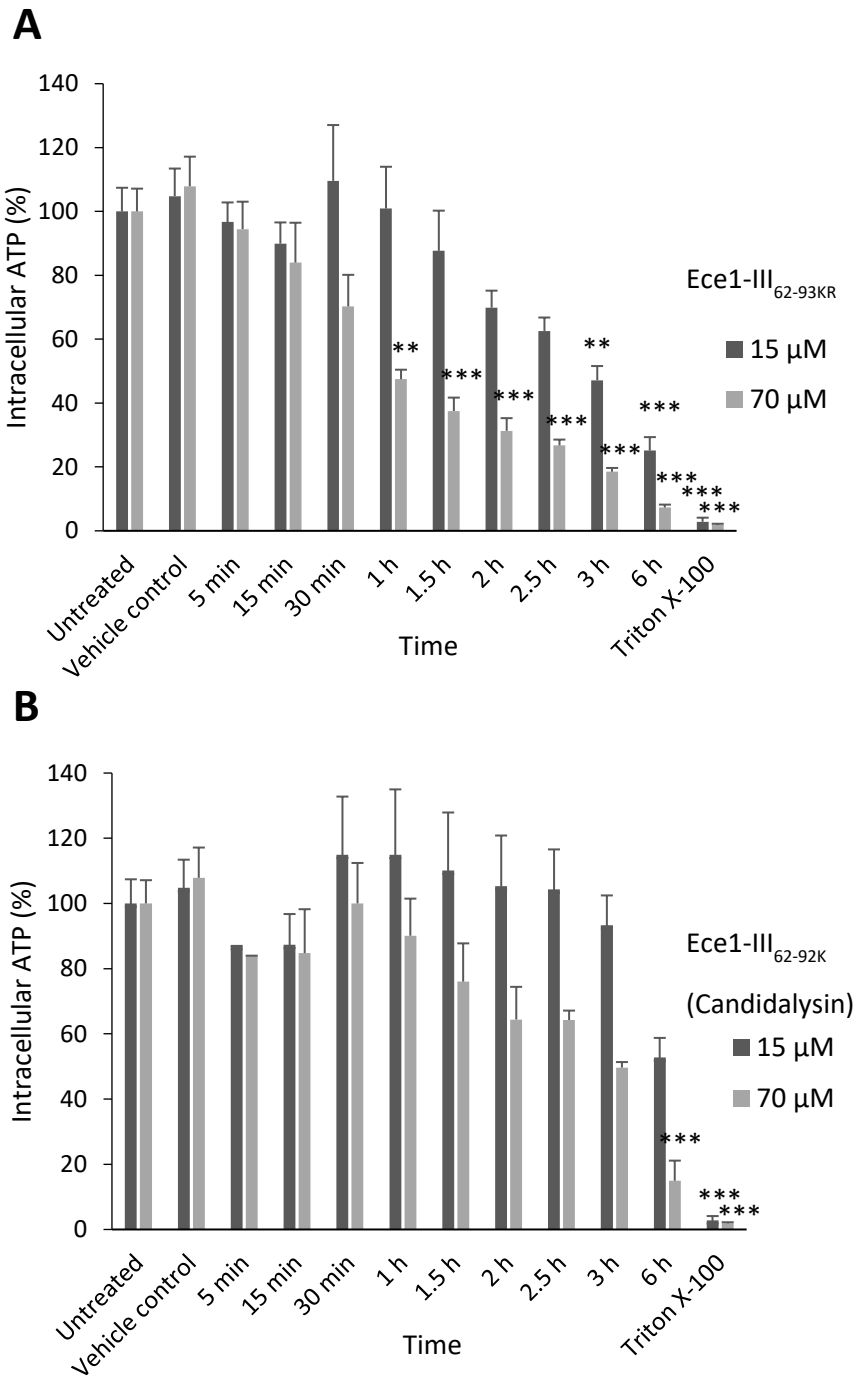

Figure 3-10. **Time-course of intracellular ATP levels following treatment with Candidalysin peptides.** TR146 oral epithelial cells were incubated with Ece1-III$_{62-93KR}$ (A) and Candidalysin (B) at 15 and 70 µM between 5 min and 6 h and assayed for intracellular ATP by luminescence assay. Triton X 100 (1%) was used as a positive control. Data are expressed as percentage of intracellular ATP relative to untreated cells. Data are the mean of three biological replicates (+SEM). Statistical significance was calculated by one way ANOVA, ** P<0.01, *** P<0.001.

3.3.6 Candidalysin induces calcium influx in TR146 cells

Calcium is an important secondary messenger involved in intra- and extracellular signaling events and plays an essential cellular role in life and death outcomes (Berridge et al., 2000). Disturbances in mitochondrial function that affect levels of intracellular ROS and ATP can interfere with calcium homeostasis and cause an accumulation of calcium ions in the cytosol (Gorlach et al., 2015; Guo et al., 2013; Heeman et al., 2011). Given that treatment of epithelial cells with Candidalysin peptides caused loss of mitochondrial fitness, production of intracellular ROS and depletion of intracellular ATP, I questioned whether Candidalysin peptides were also capable of inducing changes in cytosolic calcium levels.

Accordingly, TR146 oral epithelial cells were pre-treated with fura-2 solution and then incubated with Candidalysin peptides. Intracellular calcium levels were measured for up to 180 min post exposure.

While intermediate (15 µM) and low (3 µM, 1.5 µM) concentrations of Ece1-III$_{62\text{-}93KR}$ were not observed to affect calcium levels, high concentrations of Ece1-III$_{62\text{-}93KR}$ (70 µM) showed an immediate and significant increase in intracellular calcium (Figure 3-11).

Compared with Ece1-III$_{62\text{-}93KR}$, Candidalysin exhibited a delayed response in the increase in calcium levels. Treatment of epithelial cells with 70 µM Candidalysin caused an increase in cytosolic calcium after 15 min, which was significant at 25 min and sustained over the entire time course (180 min). Lower concentrations of Candidalysin (15, 3 and 1.5 µM) had no significant effect on intracellular calcium levels.

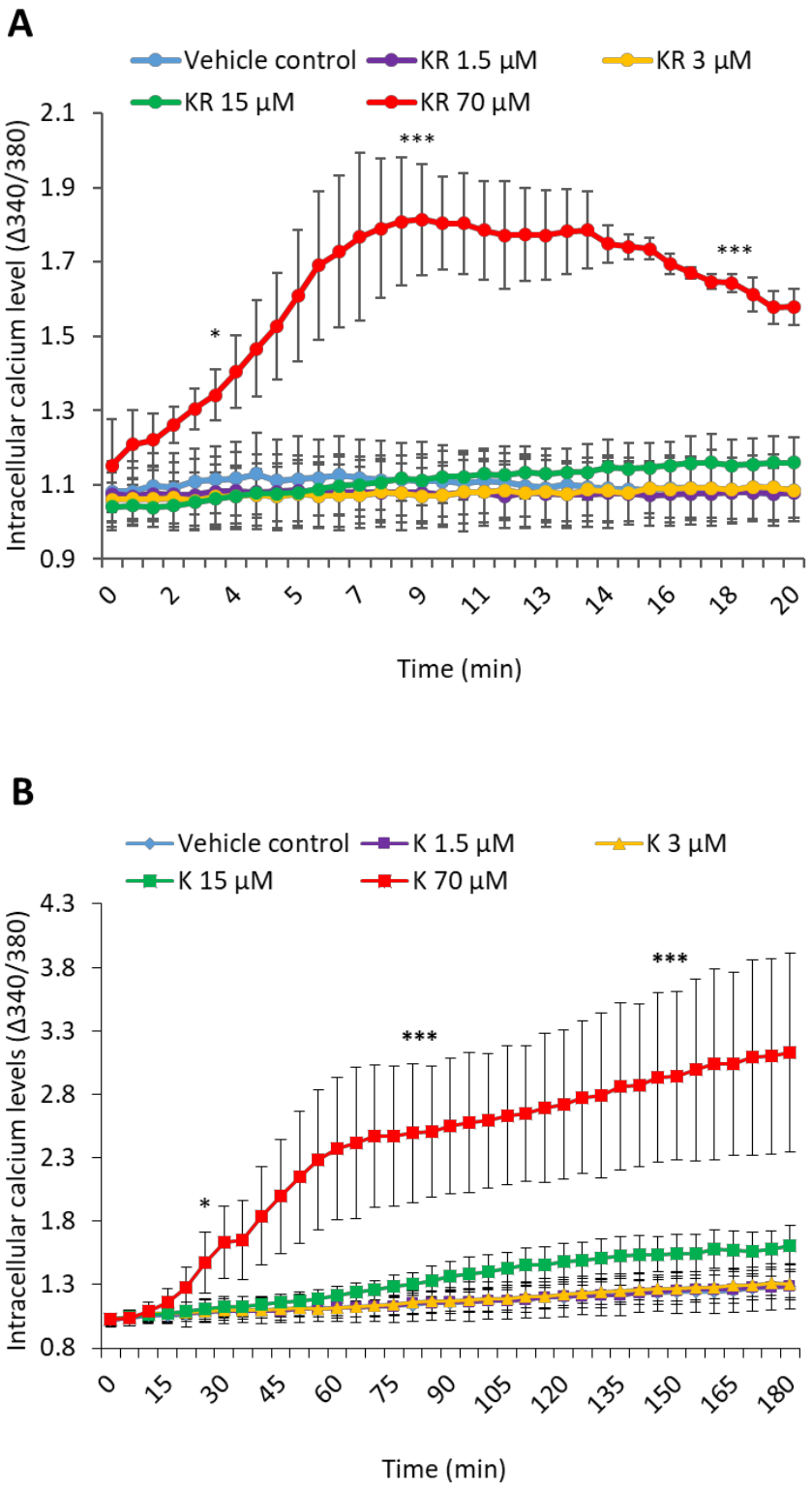

Figure 3-11. Intracellular calcium levels of oral epithelial cells in response to treatment with *C. albicans* Candidalysin peptides. TR146 oral epithelial cells were pre-incubated with Fura-2 for 1 h and subsequently incubated with Ece1-III$_{62\text{-}93KR}$ (A) and Candidalysin (B) (70, 15, 3 and 1.5 µM). Fluorescence was measured in real time for up to 3 h (180 min). Data are the mean of three biological replicates (±SEM). Statistical significance was calculated by one way ANOVA, * P<0.05, *** P<0.001.

Intracellular calcium levels are normally maintained approximately 20,000 fold lower than the extracellular compartment (Clapham, 2007). To maintain the intracellular concentration, calcium is actively pumped out of the cell and also into cytosolic organelles such as the endoplasmatic reticulum.

Treatment of epithelial cells with 70 μM Candidalysin caused a significant increase in the intracellular calcium levels (Figure 3-11). However, it was not clear whether the observed increase in intracellular calcium was due to influx from the extracellular environment or release from intracellular stores (i.e. the ER). To discern between these two possibilities, TR146 cells were incubated with Candidalysin in a calcium-free buffer and intracellular calcium levels were assessed. Ionomycin (1 μM; an ionophore that strongly induces calcium influx) in calcium-containing buffer was used as a positive control (Figure 3-12). The immediate and significant increase in intracellular calcium levels was only observed in calcium-containing buffer and was maintained throughout the experiment. In contrast, Candidalysin failed to induce an increase in intracellular calcium levels in calcium-free buffer. This strongly suggests that the increase in intracellular calcium observed in response to Candidalysin occurs as a result of calcium influx from the external environment and not from internal stores.

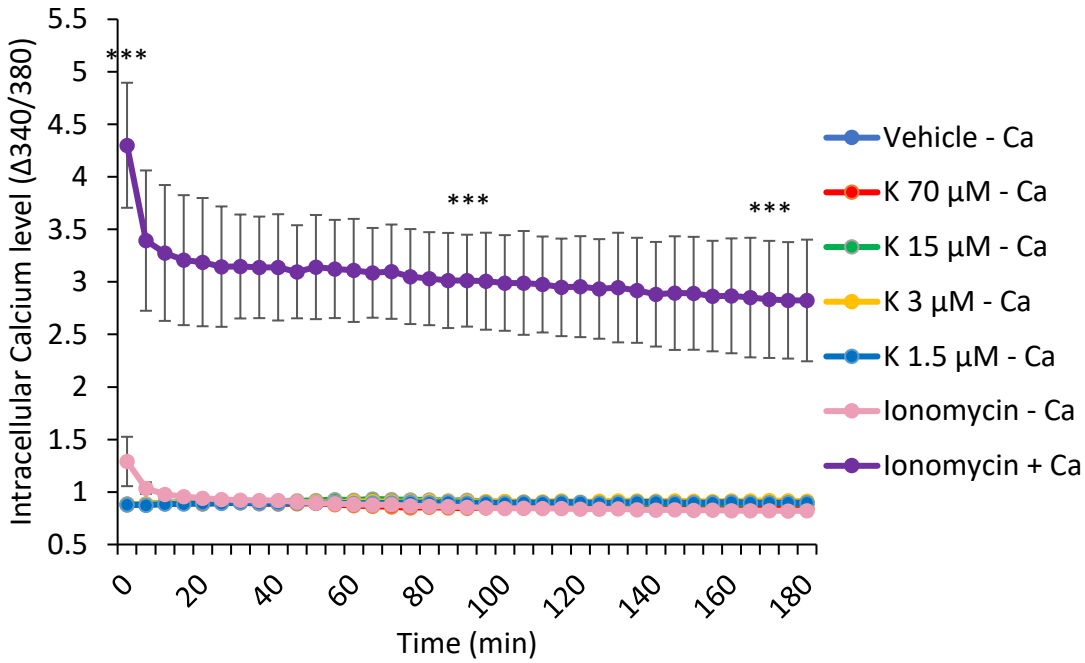

Figure 3-12. **Intracellular calcium levels of oral epithelial cells in response to treatment with Candidalysin.** TR146 oral epithelial cells were stained with Fura-2 for 1 h and subsequently incubated with Candidalysin (70, 15, 3 and 1.5 µM) in calcium-free buffer. Fluorescence was measured in real time for up to 3 h (180 min). As a positive control, cells were treated with 1 µM Ionomycin in calcium-containing medium. Data are the mean of three biological replicates (±SEM). Statistical significance was calculated by one way ANOVA, *** P<0.001.

3.4 Discussion

The ability of *C. albicans* to invade and damage the host mucosa is critical for initiating and maintaining symptomatic mucosal infection. The hyphae of *C. albicans* breach epithelial barriers using two mechanistically distinct processes; induced endocytosis and active penetration (Naglik et al., 2011), and hyphal infiltration into underlying tissues causes extensive cell stress that can culminate in cell death (Chiang et al., 2007).

The Candidalysin toxin is part of a larger 271 amino acid parental protein, Ece1p (Moyes et al., 2016). An initial computational analysis of full length Ece1p predicted cleavage of Ece1p after lysine-arginine motifs by a protease, producing eight individual peptide fragments. Ece1p is indeed cleaved by the endoproteinase Kex2p *in vitro* (Bader et al., 2008) and therefore Candidalysin (the third peptide fragment of Ece1p) was predicted to terminate with a lysine-arginine motif. Accordingly, in order to characterise the effect of Candidalysin on epithelial cells during the early stages of this study, research was

undertaken using the peptide sequence: SIIGIIMGILGNIPQVIQIIMSIVKAFKGNKR (Ece1-III$_{62\text{-}93KR}$). Subsequently, however, an analysis of secreted Candidalysin by mass spectrometry revealed that the toxin terminates with a C-terminal lysine residue, lacking the C-terminal arginine: SIIGIIMGILGNIPQVIQIIMSIVKAFKGNK (Ece1-III$_{62\text{-}92K)}$ (Moyes et al., 2016). Thus, having confirmed the amino acid sequence of Candidalysin secreted from *C. albicans* hyphae during epithelial infection, work continued using this toxin.

Microbial toxins facilitate the survival and proliferation of pathogens within an infected host by altering the cellular environment and inducing cell stresses that culminate in a range of pathologies (Los et al., 2013). Cells respond to toxin-induced stresses in various ways ranging from the activation of survival pathways to the initiation of cell death that eliminates injured cells from the host (Fulda et al., 2010). Successful activation and appropriate regulation of these mechanisms depends on the host's ability to cope with the altered physiological conditions imposed by the toxin (Fulda et al., 2010). The observation that Candidalysin induces epithelial lesions strongly suggests that it may also induce multiple stresses in epithelial cells which may result in cell death. Hence, in this study we set out to investigate the role of Candidalysin peptides (Ece1-III$_{62\text{-}93KR}$ and Candidalysin (Ece1-III$_{62\text{-}92K}$)) in inducing cell stress and cell death processes in TR146 oral epithelial cells.

Membrane permeability is widely considered to be a robust marker of cellular stress and cell death. The permeability of epithelial plasma membranes was first assessed by investigating LDH release. While TR146 oral epithelial cells infected with fungus induced significant release of LDH, cells infected with *C. albicans ECE1* mutants that are unable to synthesise and secrete Candidalysin were incapable of causing epithelial damage ((Moyes et al., 2016) and this study), confirming Candidalysin as a driver of epithelial membrane perturbation. Furthermore, epithelial cells exposed to Candidalysin peptides responded by releasing LDH in a dose-dependent manner. These observations are in agreement with studies that have demonstrated release of LDH from epithelial cells in response to other microbial toxins, such as *Streptococcus pneumoniae* pneumolysin (Hirst et al., 2002), *Clostridium difficile* Toxin B (Chumbler et al., 2012) and *Staphylococcus aureus* α-toxin (Gonzalez-Juarbe et al., 2017).

Membrane permeability was additionally observed by fluorescent microscopy, employing Eth Homo III as a marker for necrosis and Annexin V as an indicator of

apoptosis. Necrosis is a form of cell death resulting from drastic membrane rupture, facilitating access of Eth Homo III to the nucleus. Apoptosis, in contrast, is a carefully regulated process where the stoichiometry of the plasma membrane changes, allowing Annexin V to bind to phosphatidylserine residues that become exposed on the outer leaflet of the plasma membrane (Thompson, 1995). Previous studies have shown that epithelial cells respond to the presence of *C. albicans* by inducing apoptosis and necrosis (Villar et al., 2012; Villar and Zhao, 2010; Wagener et al., 2012). Treatment of oral epithelial cells with 30 and 70 μM of Candidalysin peptides induced visual phenotypes consistent with both apoptosis (Annexin V-positive staining) and necrosis (Eth Homo III-positive staining), suggesting a potential role for Candidalysin in driving these cell death mechanisms. However, the recruitment of Annexins to the site of damage caused by toxins is also closely associated with membrane repair (Romero et al., 2017). Thus, given that Annexin V-positive staining was weaker than Eth Homo III staining, it is more likely that Candidalysin-induced cell death is due to necrotic rather than apoptotic mechanisms (see Chapters 4 and 5).

In addition to membrane destabilisation, microbial toxins can also compromise the function of host cell organelles. Mitochondria are a major source of ROS and ATP, the modulation of which are important during cellular stress and the induction of cellular death (Jiang et al., 2012). The accumulation of intracellular ROS within a cell can result in damage to biological macromolecules and, if sustained, may result in cell death by apoptosis or necrosis (Trachootham et al., 2008). Dysfunction of epithelial mitochondria (as measured by MTT assay) was observed in a dose- and time-dependent manner in response to Candidalysin peptides, concomitant with the generation of intracellular ROS and depletion of intracellular ATP.

Both ROS generation and depletion of intracellular ATP levels can determine cell fate and modulate the activation of cell death pathways (Eguchi et al., 1997). The generation of ROS following severe insult contributes to the release of cytochrome c through oxidation of the mitochondrial membrane (Orrenius et al., 2007). Cytochrome c released from the mitochondria into the cytosol activates caspases to induce apoptosis (Arnoult et al., 2009). However, in addition to causing apoptosis, ROS can also circumvent the apoptotic pathway to induce death by necrosis (Samali et al., 1999). The switch from apoptosis to necrosis can also occur following the oxidation of the caspase active site by

ROS (Samali et al., 1999). All caspases contain an active site cysteine nucleophile, which is prone to oxidation through the modulation of the redox status of the cell and the oxidation of the cysteine residues in caspases (Hampton and Orrenius, 1997). The shift from apoptosis to necrosis can also occur following severe depletion of intracellular ATP caused by the failure of mitochondrial energy production by oxidants (Samali et al., 1999). Candidalysin peptides were observed to deplete intracellular ATP levels in a dose- and time-dependent manner. Given that apoptosis is an energy-dependent mechanism with ATP as key factor for the formation of the apoptosome (Apaf-1-cytochrome c complex, which cleaves and activates caspase-9 during the intrinsic apoptosis process (Jiang and Wang, 2000)), critically low levels of intracellular ATP prevent apoptosome formation, resulting in cell death via necrosis (Eguchi et al., 1997).

In addition to the observed loss of mitochondrial fitness, reduction in ATP and elevation of intracellular ROS, Candidalysin peptides were also observed to cause calcium influx. Influx of calcium ions from the extracellular environment is consistent with peptide-induced membrane permeabilisation and LDH release. Calcium signaling plays an important role in the initiation and effectuation of both apoptotic and necrotic pathways. Necrosis and apoptosis are both associated with a perturbation of intracellular calcium homeostasis (Orrenius et al., 2003).

Cytoplasmic calcium overload can lead to abnormal mitochondrial calcium uptake. Such an abnormal uptake of calcium into the mitochondria can trigger the mitohondrial permeability transition (MPT) and swelling of the organelle with release of mitochondrial proteins into the cytosol. One of these proteins is cytochrome c that, together with Apaf-1 and ATP, form the apoptosome complex which leads to apoptosis. Thus, successful activation of the apoptosome is in part dependent on the available pool of intracellular ATP; ATP is required for apoptosome activation and induction of apoptosis, whereas cells that contain insufficient levels of ATP fail to activate the apoptosome and instead undergo necrosis (Kim et al., 2003).

While Ece1-III$_{62\text{-}93KR}$ and Candidalysin appear to function through the induction of similar epithelial cell stresses, some notable differences were observed between peptide treatments. Compared with Ece1-III$_{62\text{-}93KR}$, Candidalysin was observed to be more potent in reducing mitochondrial fitness and increasing levels of intracellular ROS, whereas it

was less effective in promoting membrane permeability, increases in intracellular calcium and depletion of intracellular ATP.

Both peptides are predicted to adopt an α-helical conformation in solution as revealed by circular dichroism spectroscopy (Moyes et al., 2016). However, compared with Ece1-III$_{62\text{-}93KR}$, Candidalysin lacks a positively charged arginine (R) at its C-terminus (Moyes et al., 2016). The absence of this C-terminal arginine residue could conceivably alter the net charge of the toxin, which may result in altered interactions with components of the epithelial plasma membrane, accounting for the differeces in epithelial responses observed.

While both peptides were capable of causing epithelial damage, Ece1-III$_{62\text{-}93KR}$ was more damaging than Candidalysin, causing more efficient membrane permeabilisation concomitant with rapid calcium influx. In addition to damage, Candidalysin induced more potent intracellular toxicity compared with Ece1-III$_{62\text{-}93KR}$, by causing greater oxidative stress and affecting mitochondrial fitness.

Mitochondria are a major source of ATP (Jiang et al., 2012), however, the observed loss of mitochondrial fitness induced by peptide exposure did not correlate precisely with the observed levels of intracellular ATP depletion. Specifically, while the epithelial response to Ece1-III$_{62\text{-}93KR}$ resulted in a modest reduction in mitochondrial fitness and a significant depletion of intracellular ATP, the opposite response, comprised of a significant reduction in mitochoindrial fitness and a modest reduction in intracellular ATP was observed in response to Candidalysin.

One possibility that may explain these observations relates to the damage capacity of Ece1-III$_{62\text{-}93KR}$ when compared with Candidalysin. Ece1-III$_{62\text{-}93KR}$ is more damaging to epithelial cells when compared with Candidalysin (Moyes et al., 2016). Thus, an inverse relationship may exist between damage and the capacity to induce effective intracellular signalling; the more damaging the peptide (Ece1-III$_{62\text{-}93KR}$ compared with Candidlaysin), the less likely that effective intracellular signalling may be sustained to induce appropriate stress responses. In contrast, a peptide that has a reduced capacity to cause damage (Candidalysin compared with Ece1-III$_{62\text{-}93KR}$) may allow epithelial activation to occur sufficiently for intracellular stress responses to be induced.

Nevertheless, despite the difference in responses observed following treatment of epithelial cells with Ece1-III$_{62\text{-}93KR}$ or Candidalysin, it is Candidalysin (and not Ece1-III$_{62\text{-}93KR}$) that is detectable in the extracellular environment following infection of epithelial cells with *C. albicans* (Moyes et al., 2016). Given this observation, it is the epithelial phenotypes observed in response to Candidalysin (and not Ece1-III$_{62\text{-}93KR}$) that can be considered to be physiologically relevant in the context of fungal infection at the mucosal surface.

The data presented here demonstrate that Candidalysin triggers a variety of epithelial stress responses that are strongly associated with the common readouts and characteristics of cellular death. These characteristics include plasma membrane permeabilisation, mitochondrial dysfunction, generation of ROS, ATP depletion and calcium influx. Given the multiple and detrimental effects of these cellular stresses and their impact on the induction of cell death pathways, it is unclear which specific pathways of cell death are activated by Candidalysin. The study of these cell death pathways will be further investigated in Chapters 4 and 5.

Chapter 4: Role of Candidalysin in driving apoptotic death in human oral epithelial cells

4.1 Introduction

The interaction between *C. albicans* and oral mucosal tissues during oropharyngeal candidiasis results in epithelial cell damage and cell death. This process results in tissue dysfunction and occurs during intracellular fungal invasion when Candidalysin, a cytolytic peptide toxin of *C. albicans*, is secreted from the fungus (Moyes et al., 2016).

Apoptosis is a biological process that describes a specific, tightly-regulated form of cellular death. It is an integral component of initial tissue development and homeostasis, but also occurs in response to stress conditions such as infections (Hotchkiss et al., 2009). Apoptosis can be initiated through extrinsic and intrinsic pathways (Chapter 1, Figure 1-9).

The extrinsic pathway is activated by ligands that bind to death receptors expressed on the surface of various cells types. Upon ligand binding, several proteins are recruited to the death receptor to form Complex 1 (Chapter 1, Figure 1-7). Among these proteins, the cellular inhibitor of apoptosis proteins (cIAPs) play a critical role in the initiation of the extrinsic apoptotic pathway through negative regulation of ripoptosome formation (a protein complex that forms in the cytosol in the absence of cIAPs; Chapter 1, Figure 1-7). The ripoptosome is the death platform that permits activation of caspase-8 and propagation of the apoptotic process. The intrinsic apoptosis pathway is activated through signals that promote disruption of mitochondrial integrity. Dysfunctional mitochondria release proteins including cytochrome c that amplify an intracellular caspase cascade.

Both extrinsic and intrinsic apoptosis pathways feed into the apoptotic execution pathway, characterised by activation of caspase-3. Activated caspase-3 proteolytically degrades the cytoskeleton of the host cell and inactivates substrates essential for cell repair such as PARP. Finally, intrinsic and extrinsic apoptotic signalling culminates in cell shrinkage, DNA fragmentation, externalisation of phosphatidylserine and induction of membrane “blebbing”, which is followed by the release of apoptotic bodies into the

extracellular environment that are subsequently phagocytosed by macrophages (Taylor et al., 2008).

Previous studies have demonstrated that *C. albicans* stimulates apoptosis in oral epithelial cells (Villar and Zhao, 2010; Wagener et al., 2012). Furthermore, in Chapter 3 I showed that treatment of epithelial cells with Candidalysin resulted in cells that were weakly positive for Annexin V (binds externalised phosphatidylserine; a cellular phenotype that closely resembles apoptosis). Therefore, in this chapter I sought to determine whether Candidalysin can drive apoptotic cell death in epithelial cells.

4.2 Methods

4.2.1 Western blot

TR146 monolayers were treated with *C. albicans* strains (Table 4.1) at an MOI of 0.01 and with Ece1-III$_{62\text{-}92K}$ (Candidalysin) at 70, 30, 15, 3 μM for 24 h. Proteins were extracted, quantified and separated by size using electrophoresis. Separated proteins were transferred to a nitrocellulose membrane which was probed with anti-caspase-8, anti-caspase-3, anti-cIAP2 or anti-PARP primary antibody and detected with a HRP-conjugated secondary antibody (see Section 2.5).

4.2.2 Quantification of Caspase activity

TR146 oral epithelial cells were infected with *C. albicans* strains at a MOI of 0.01 and Ece1-III$_{62\text{-}92K}$ (Candidalysin) at 70, 30, 15 and 3 μM for 24 h. Caspase activity was assessed by adding a substrate solution and measuring luminescence after incubation for 30 min (Caspase-3) or 1 h (Caspase-8) (see section 2.4.7).

4.2.3 Quantification of cytochrome c

TR146 oral epithelial cells were infected with *C. albicans* strains at a MOI of 0.01 and Ece1-III$_{62\text{-}92K}$ (Candidalysin) at 70, 30, 15 and 3 μM for 24 h. Exhausted culture medium and epithelial cell lysate was collected and cytochrome c quantified by ELISA (Invitrogen) (see Section 2.4.8).

4.2 Results

4.2.1 Ripoptosome assembly is Candidalysin-independent

The cellular inhibitor of apoptosis protein (cIAP) plays important roles in the modulation of inflammation and apoptosis (Silke and Meier, 2013). The presence of cIAP1 and cIAP2 in particular, can repress apoptotic cell death by inhibiting the formation of the ripoptosome (Chapter 1, Figure 1-7) (Tenev et al., 2011).

Data presented here demonstrates that Candidalysin induces Annexin V positive cells (a characteristic associated with apoptotic death; Chapter 3) at 3 h, 6 h and 24 h. In addition, gene expression profiling of OKF6/TERT2 oral epithelial cells infected with *C. albicans* showed upregulation of the gene encoding cIAP2 at 8 h post-infection (Villar et al., 2012), suggesting that the ripoptosome was not formed at 8 h. I therefore investigated ripoptosome assembly at later time points (24 h) by assessing epithelial expression of cIAP2 in Candidalysin and *C. albicans* treated cells.

TR146 monolayers were incubated with Candidalysin at 70, 30, 15, 3 µM and with *C. albicans ECE1* mutant strains at a MOI of 0.01 for 24 h. Total protein was isolated and analysed by SDS-PAGE and western blotting for the presence of cIAP2 (see sections 2.5.1-2.5.4). As a positive control, 0.1 µM staurosporine was used to induce apoptosis (Nakamura-Lopez et al., 2009).

Treatment of epithelial cells with 30, 15 and 3 µM (but not 70 µM) Candidalysin appeared to result in a modest increase in cIAP2 expression when compared with the vehicle control (Figure 4-1). In contrast, staurosporine treatment (an apoptosis inducer) strongly decreased cIAP2 expression. Notably, infection of epithelial cells with the *C. albicans ECE1* mutant strains also decreased cIAP2 expression, irrespective of their ability to produce Candidalysin.

This data suggests that Candidalysin does not promote ripoptosome assembly in epithelial cells. In contrast however, challenge of epithelial cells with fungus may promote ripoptosome formation and an extrinsic pro-apoptotic response.

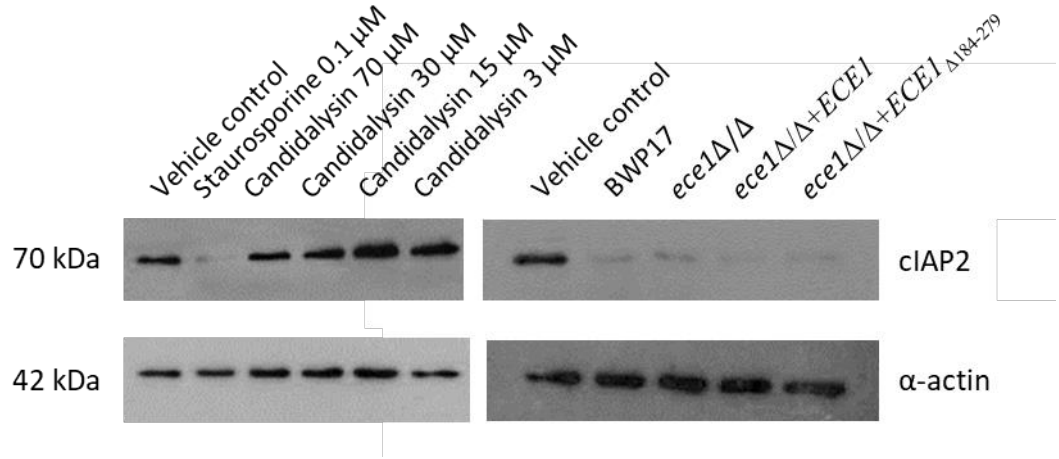

Figure 4-1. Expression of cIAP2 in oral epithelial cells in response to Candidalysin and *Candida ECE1* mutant strains. TR146 oral epithelial cells were incubated with Candidalysin (70, 30, 15 and 3 µM) and *Candida ECE1* mutant strains (MOI of 0.01) for 24 h and cell lysate assayed for cIAP2 expression by western blot. Data are representative of three biological replicates.

4.2.2 Caspase-8 activity is not induced by Candidalysin

Having observed that *C. albicans* may promote ripoptosome assembly in a Candidalysin-independent manner, I investigated activation of pro-caspase-8 (hallmark of extrinsic apoptosis) in *C. albicans* treated cells. Caspase-8 activation by Candidalysin was also investigated to confirm the non-involvement of Candidalysin in inducing extrinsic apoptosis in oral epithelial cells.

TR146 monolayers were incubated with Candidalysin at 70, 30, 15, 3 µM and with *C. albicans ECE1* mutants at a MOI of 0.01 for 24 h. Total protein was isolated and analysed by SDS-PAGE and western blotting for the presence of caspase-8 (see sections 2.5.1-2.5.4). As a positive control, 0.1 µM staurosporine was used to induce apoptosis (Nakamura-Lopez et al., 2009).

Pro-caspase-8 was observed to be expressed in vehicle treated cells, and no further increase in pro-caspase-8 expression was observed following treatment with Candidalysin or *C. albicans ECE1* mutant strains (Figure 4-2). Only TR146 epithelial cells treated with staurosporine exhibited a very modest cleavage of immature caspase-8 (57 kDa) to produce a product consistent with the molecular weight of active caspase-8 (17 kDa - white arrow).

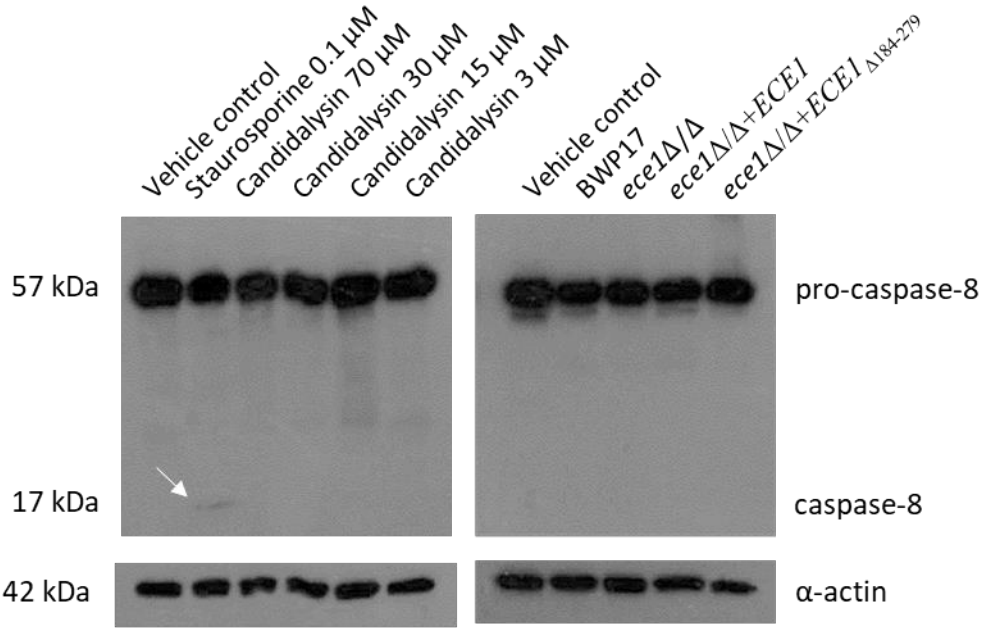

Figure 4-2. Expression of caspase-8 in oral epithelial cells in response to Candidalysin. TR146 oral epithelial cells were incubated with Candidalysin (70, 30, 15 and 3 µM) and *C. albicans ECE1* mutant strains (MOI of 0.01) for 24 h and cell lysate assayed for caspase-8 expression by western blot. Data are representative of three biological replicates.

Having detected strong expression of pro-caspase-8 in epithelial cells but only a modest activation of caspase-8 following staurosporine treatment, I decided to utilise a more sensitive luminescence-based assay to detect the generation of active caspase-8 by Candidalysin (Figure 4-3).

As with the western blot data, there was no apparent change in caspase-8 activity in epithelial cells treated with Candidalysin when compared with the vehicle control (Figure 4-3). In contrast, epithelial cells treated with staurosporine showed significant caspase-8 activity. Collectively, these data demonstrate that while TR146 oral epithelial cells express a high baseline level of pro-caspase-8, Candidalysin activity does not induce the generation of active caspase-8 from pro-caspase-8. Interestingly, however, while not significant, there was a decrease in caspase-8 activity in epithelial cells treated with the *C. albicans* strains, especially those that were able to produce Candidalysin (BWP17 and *ece1*Δ/Δ+*ECE1*).

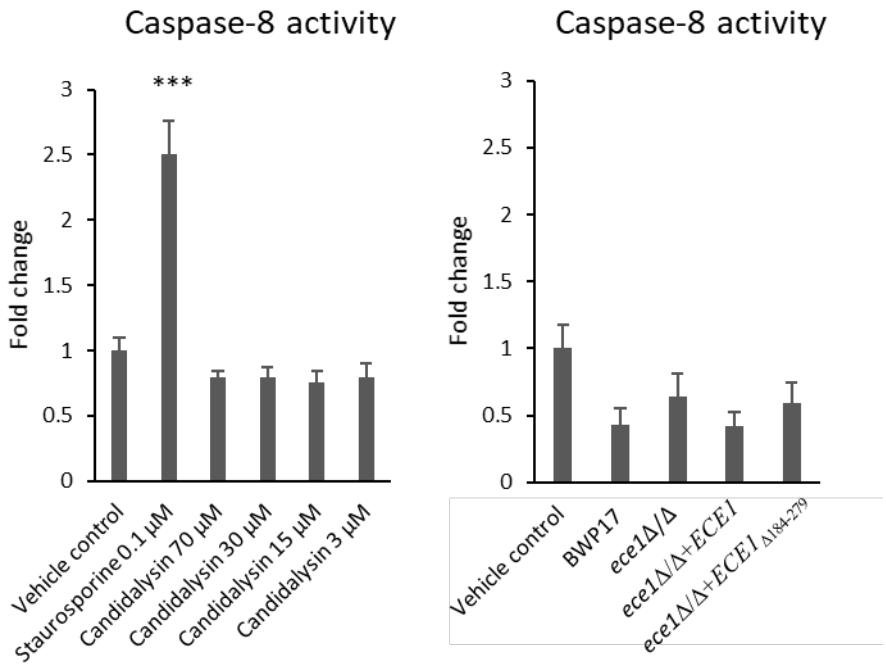

Figure 4-3. Caspase-8 activity in oral epithelial cells infected with Candidalysin and *C. albicans ECE1* mutants. TR146 oral epithelial cells were incubated with Candidalysin (70, 30, 15 and 3 µM) and *C. albicans ECE1* mutant strains (MOI of 0.01) for 24 h and cells assayed for caspase-8 activity by luminescence assay. Bars indicate caspase-8 activity relative to the vehicle control (fold change). Data are the mean of three biological replicates (+SEM). Statistical significance was calculated by one way ANOVA test, *** P<0.001.

4.2.3 Candidalysin contributes to Cytochrome c release only in the context of a fungal infection

Having discounted a role for Candidalysin in activating the extrinsic apoptotic pathway in epithelial cells, activation of the intrinsic apoptosis pathway was investigated. Activation of the intrinsic apoptotic pathway results in release of cytochrome c from mitochondria into the cytosol and/or extracellular environment, promoting the assembly of the apoptosome and propagating the apoptotic response (Arnoult et al., 2009; Renz et al., 2001) (Chapter 1, Figure 1-8).

Accordingly, TR146 oral epithelial cells were treated with Candidalysin at 70, 30, 15 and 3 µM, *C. albicans ECE1* strains at a MOI of 0.01 and staurosporine at 0.1 µM for 24 h. Epithelial cell lysates and exhausted culture medium were collected and cytochrome c was quantified by ELISA.

Treatment of epithelial cells with Candidalysin, *C. albicans ECE1* mutant strains or staurosporine did not result in a detectable increase in cytochrome c present in cell lysates when compared with the vehicle control (Figure 4-3). In contrast, Candidalysin

treatment reduced cytochrome c levels in epithelial cell lysates in a dose dependent manner, with the highest concentration of Candidalysin (70 µM) and 0.1 µM staurosporine treatment inducing similar (non-significant) reductions. Notably, significant reductions in cytochrome c levels were observed in epithelial cell lysates after treatment with all *C. albicans* strains, particularly with strains that were able to produce Candidalysin (BWP17 and *ece1*Δ/Δ+*ECE1*).

In contrast to epithelial cell lysates, significant levels of cytochrome c were detected in the exhausted culture medium of epithelial cells treated with staurosporine and with *C. albicans* strains able to produce Candidalysin (BWP17 and *ece1*Δ/Δ+*ECE1*). However, *C. albicans* strains unable to produce Candidalysin (*ece1*Δ/Δ and *ece1*Δ/Δ+*ECE1*$_{\Delta 184\text{-}279}$) did not induce cytochrome c release (Figure 4-4). Interestingly, Candidalysin treatment alone also did not induce release of cytochrome c into the medium.

These data suggest that Candidalysin is able to drive cytochrome c release from epithelial cells but only in the context of a fungal infection, not when added exogenously.

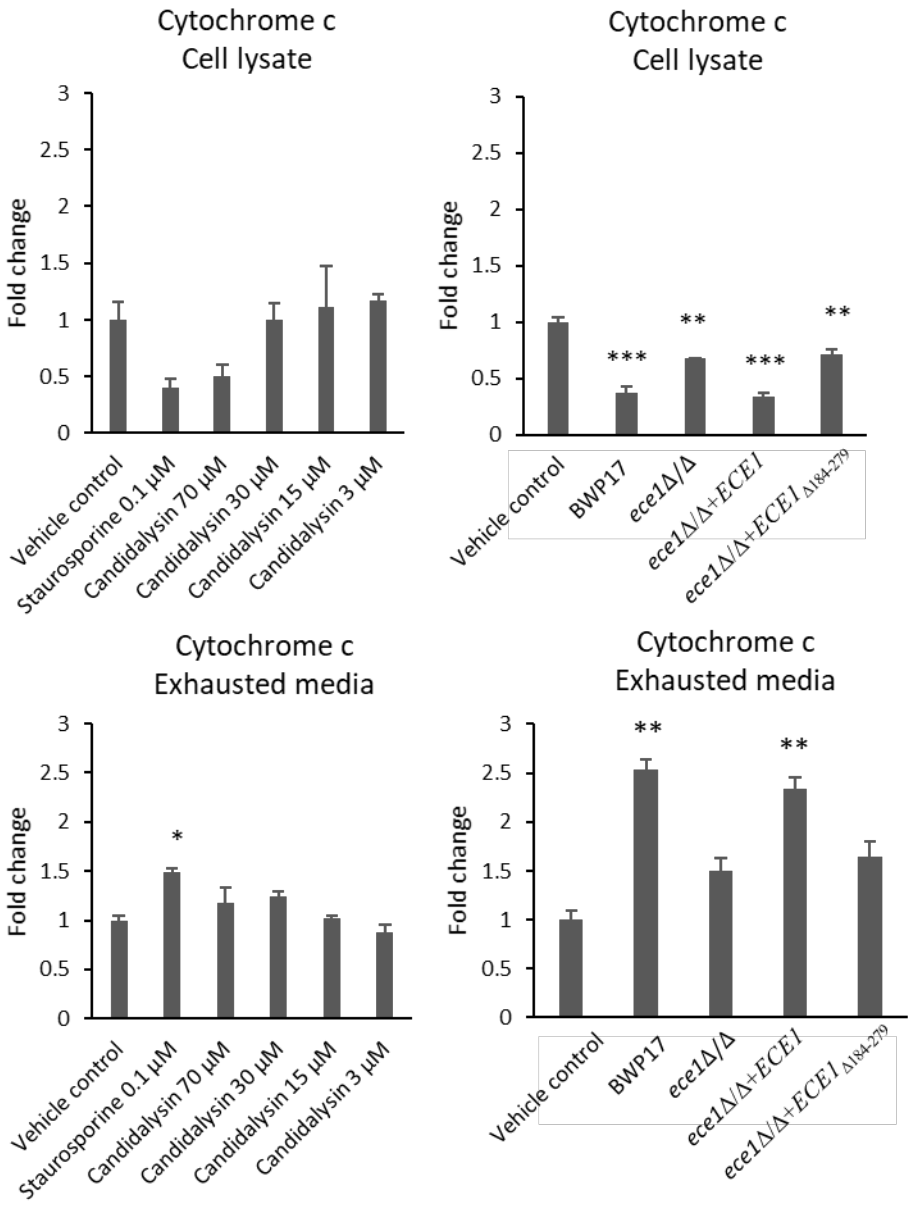

Figure 4-4. Quantification of cytochrome c release from oral epithelial cells in response to Candidalysin and *C. albicans ECE1* mutant strains. TR146 oral epithelial cells were incubated with Candidalysin (70, 30, 15 and 3 µM) and *C. albicans ECE1* mutant strains (MOI of 0.01) for 24 h. Cytochrome c was quantified in cell lysate and exhausted culture medium by ELISA. Bars represent amount of cytochrome c relative to the vehicle control (fold change). Data are the mean of three biological replicates (+SEM). Statistical significance was calculated by one way ANOVA test, * $P<0.05$, ** $P<0.01$ *** $P<0.001$.

4.2.5 Caspase-3 activity is not induced by Candidalysin

Both extrinsic and intrinsic apoptotic pathways lead to the apoptotic execution phase which is induced following activation of caspase-3 (Elmore, 2007). Having investigated activation of apoptosis through the extrinsic pathway (via cIAP2 and caspase-8) and

through the intrinsic pathway (via cytochrome c release), activation of the pro-apoptotic effector protein caspase-3 was determined.

Accordingly, TR146 monolayers were incubated with Candidalysin at 70, 30, 15, 3 µM and with *C. albicans ECE1* mutants at a MOI of 0.01 for 24 h. Total protein was isolated and analysed by SDS-PAGE and western blotting for the presence of caspase-3 (see sections 2.5.1-2.5.4). As a positive control, 0.1 µM staurosporine was used to induce apoptosis (Nakamura-Lopez et al., 2009).

Similar to pro-caspase-8 (Figure 4-2), pro-caspase-3 (31 kDa) was observed to be highly expressed in resting (vehicle control) cells. Neither an increase in pro-caspase-3 expression or cleavage of pro-caspase-3 to generate active caspase-3 (19/17 kDa – white arrows) was observed following treatment with Candidalysin or *C. albicans ECE1* mutant strains (Figure 4-5). Only staurosporine-treated epithelial cells showed a modest cleavage of pro-caspase-3 to active caspase-3.

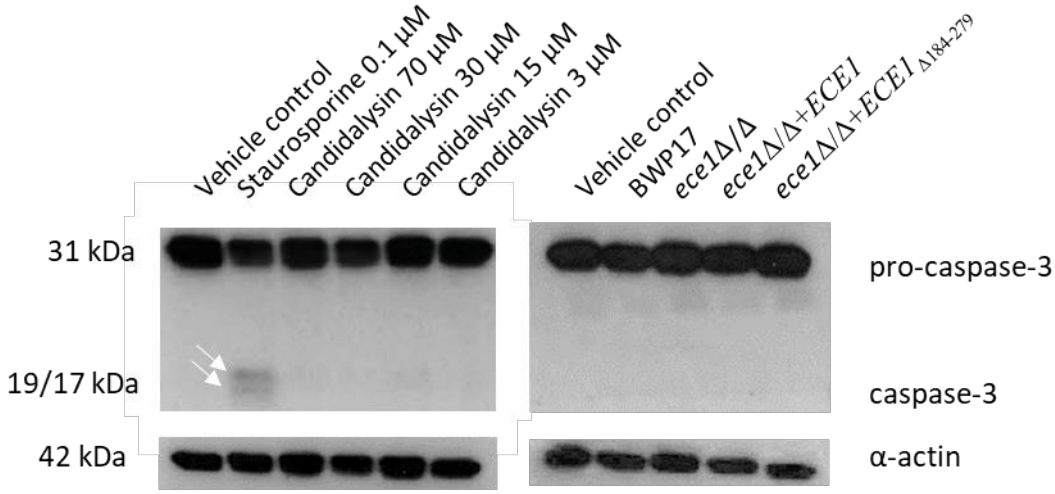

Figure 4-5. Expression of caspase-3 in oral epithelial cells in response to Candidalysin and *C. albicans ECE1* mutant strains. TR146 oral epithelial cells were incubated with Candidalysin (70, 30, 15 and 3 µM) and *C. albicans ECE1* mutant strains (MOI of 0.01) for 24 h and cell lysate assayed for caspase-3 expression by western blot. Data are representative of three biological replicates.

Having detected strong expression of pro-caspase-3 in epithelial cells and only a modest activation of caspase-3 following staurosporine treatment, we decided to utilise a more sensitive luminescence-based assay to detect the generation of active caspase-3 by Candidalysin. In agreement with the western blot analysis (Figure 4-5) incubation of

epithelial cells with Candidalysin or *C. albicans ECE1* mutants did not result in an increase in detectable caspase-3 activity when compared with the vehicle control (Figure 4-6). In contrast, treatment with staurosporine resulted in significant caspase-3 activity. It should be noted that, while not significant, as with the caspase-3 data (Figure 4-2), there was a decrease in caspase-8 activity in epithelial cells treated with the *C. albicans* strains, especially those that were able to produce Candidalysin (BWP17 and *ece1*Δ/Δ+*ECE1*).

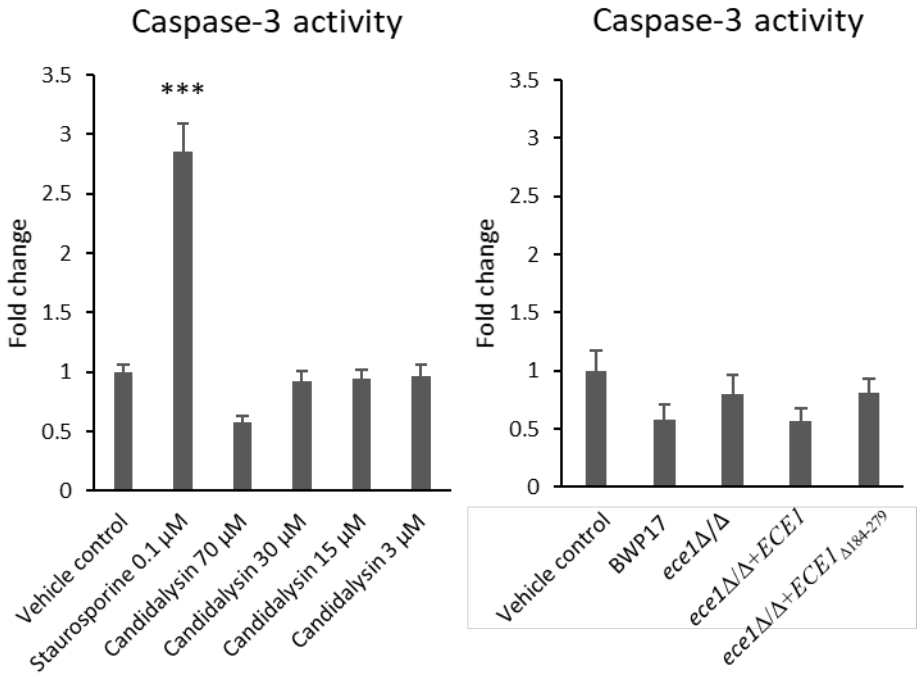

Figure 4-6. Caspase-3 activity in oral epithelial cells treated with Candidalysin and *C. albicans ECE1* mutant strains. TR146 oral epithelial cells were incubated with Candidalysin (70, 30, 15 and 3 µM) and *C. albicans ECE1* mutant strains (MOI of 0.01) for 24 h and cells assayed for caspase-3 activity by luminescence assay. Bars represent caspase-3 activity relative to vehicle control (fold change). Data are the mean of three biological replicates (+SEM). Statistical significance was calculated by one way ANOVA test, *** $p<0.001$.

4.2.6 PARP is not cleaved by Candidalysin

In addition to caspase activation and cytochrome c release, apoptosis is also characterised by cleavage of Poly-(ADP-Ribose) Polymerase (PARP) (Kaufmann et al., 1993). During apoptosis, PARP is inactivated by caspase-3-mediated cleavage, which prevents DNA repair within the cell (Kaufmann et al., 1993). PARP cleavage is thus a convenient readout of caspase-3 activity. Inactivation of PARP may also occur to prevent severe depletion of energy that is required during the later stages of apoptosis (Berger, 1985).

To investigate caspase-3 activity and address the possibility that caspase-independent cell death may be occurring in epithelial cells in response to Candidalysin and *C. albicans ECE1* mutant strains, cleavage of the surrogate marker PARP was assessed by western blot analysis.

TR146 monolayers were incubated with Candidalysin at 70, 30, 15, 3 µM and with *C. albicans ECE1* mutants at MOI of 0.01 for 24 h. Total protein was isolated and analysed by SDS-PAGE and western blotting for the presence of PARP (see sections 2.5.1-2.5.4). As a positive control, 0.1 µM staurosporine was used to induce PARP cleavage (Thuret et al., 2003).

Treatment of epithelial cells with Candidalysin or *C. albicans ECE1* mutant strains was not observed to induce PARP cleavage (Figure 4-7). However, treatment of epithelial cells with staurosporine resulted in PARP cleavage (89 kDa). Taken together, these data confirm that caspase-3 activity is not a feature of the epithelial response to Candidalysin or *C. albicans* infection *in vitro*.

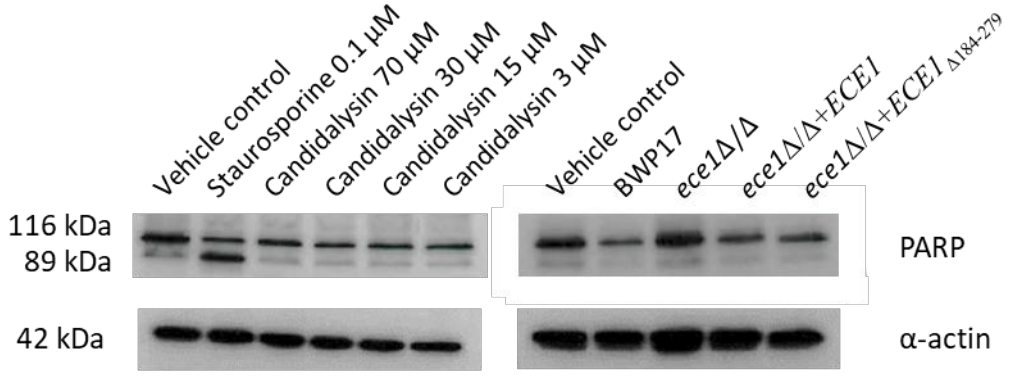

Figure 4-7. Expression of PARP in oral epithelial cells treated with Candidalysin and *C. albicans ECE1* mutant strains. TR146 oral epithelial cells were incubated with Candidalysin (70, 30, 15 and 3 µM) and *C. albicans ECE1* mutant strains (MOI of 0.01) for 24 h and cell lysate assayed for PARP expression and cleavage by western blot. Data are representative of three biological replicates.

4.3 Discussion

Candidalysin is an important driver of numerous cellular stresses in oral epithelial cells, many of which are strongly associated with characteristics of cellular death (Chapter 3). Previous *in vitro* studies have shown that *C. albicans* induces phenotypes in oral

epithelial cells that are consistent with apoptosis (Villar et al., 2012; Villar and Zhao, 2010; Wagener et al., 2012). However, it is presently unknown if apoptotic signalling occurs in epithelial cells in response to Candidalysin. Therefore, this chapter investigated the activation of apoptotic mechanisms in oral epithelial cells following treatment with Candidalysin or *C. albicans ECE1* mutant strains unable to express and secrete the toxin.

Apoptosis can be activated by extrinsic and intrinsic signals (Chapter 1, Figure 1-9). The extrinsic apoptosis pathway plays a critical role in the transmission of death-inducing signals from the extracellular environment via cell surface death receptors, ripoptosome formation, caspase-8 and caspase-3.

The extrinsic pathway is best described by the interaction between TNF-α/TNFR1 ligand-receptor pairing. Following TNF-α-TNFR1 interaction, TRADD, RIPK1, TRAF2, cIAPs and LIUBAC associate with the receptor to form Complex 1 (Chapter 1, Figure 1-7), which is essential for the activation of NF-κB signalling. In the absence of cIAP1 and cIAP2, RIPK1 dissociates from Complex 1 and recruitis FADD and pro-caspase-8 forming a ripoptosome complex in the cytosol (Figure 1-7) resulting in the autocatalytic activation of pro-caspase-8 (Kischkel et al., 1995). Once caspase-8 is activated, the execution phase of apoptosis is triggered.

Epithelial cells treated with 70 µM Candidalysin induced no change in cIAP2 expression, however a small increase in cIAP2 was observed with 30, 15 and 3 µM toxin suggesting that Candidalysin may inhibit ripoptosome formation and extrinsic apoptosis by maintaning Complex 1 integrity and promoting NF-κB signalling. High concentrations of Candidalysin (70 µM) destabilises the epithelial plasma membrane and may therefore hamper expression and recruitment of cIAP2 to the membrane receptor TFNR1.

cIAP2-mediated inhibition of apoptotic signalling has also been observed to occur in intestinal epithelial cells in response to the enterotoxin of *Bacteroides fragilis* (Kim et al., 2008). In contrast to treatment with Candidalysin, epithelial cells infected with the *C. albicans* strains showed a decrease in cIAP2 expression. While such a decrease could conceivably be associated with ripoptosome formation and apoptosis, activation of caspase-8 was not observed in epithelial cells exposed to any of the *C. albicans* strains 24 h post-infection, suggesting that even in the absence of cIAP2, extrinsic apoptosis was not activated in epithelial cells by *C. albicans*. This finding is in agreement with

previous studies that demonstrated an inability of *C. albicans* to activate caspase-8 in oral epithelial cells (Villar et al., 2012).

The intrinsic apoptotic signaling pathway can be initiated by numerous non-receptor-mediated stimuli which act directly on intracellular targets, particularly mitochondria. All of these stimuli cause changes in the permeability of the mitochondrial membrane, which triggers the release of pro-apoptotic proteins including cytochrome c (Saelens et al., 2004). In agreement with Villar et al., *C. albicans* was observed to cause significant release of cytochrome c from oral epithelial cells. Interestingly, *C. albicans* mutants that were unable to express and secrete Candidalysin were unable to induce the release of cytochrome c from epithelial cells. Likewise, treatment of epithelial cells with Candidalysin alone did not result in cytochrome c release. These data suggest that the intrinsic apoptosis pathway is initiated in epithelial cells in response to fungal infection but that Candidalysin plays no role in this process.

Thus, Candidalysin appears unable to drive the initiation of the intrinsic epithelial apoptosis pathway. These results also suggest that there are fungal factors besides Candidalysin that contribute to cytochrome c secretion. Indeed, it has been reported that fungal cell wall *N*-linked glycans (Wagener et al., 2012), proteases Sap 4-6 (Wu et al., 2013) and the the quorum sensing molecule farnesol (Scheper et al., 2008) have a role in activating apoptosis in oral epithelial cells. It is therefore conceiveable that components of the fungal cell wall and secreted factors distinct from Candidalysin affect ripoptosome formation since cIAP2 expression was reduced in response to *C. albicans* in a Candidalysin-independent manner.

Cytochrome c released from mitochondria into the cytosol binds to Apaf-1 and pro-caspase-9 in the presence of ATP to form a complex called the apoptosome (Chinnaiyan, 1999). Apoptosome formation leads to the activation of the intrinsic pathway initiator caspase-9 and subsequent activation of the executioner caspase-3 (Chinnaiyan, 1999; Hill et al., 2004). No increase in caspase-3 activity was observed in oral epithelial cells treated with Candidalysin or *C. albicans* strains after 24 h. This observation is in accordance with studies that showed no caspase-3 activity after 16 h of *C. albicans* infection (Villar et al., 2012).

Caspase-3 is a protease that cleaves multiple downstream targets essential for apoptotic progression (Janicke et al., 1998). Among these targets, cleavage of PARP is a robust indicator of caspase-3 activity within the cell and execution of apoptosis. Epithelial PARP was not cleaved following treatment with Candidalysin or infection with the *C. albicans* strains after 24 h, confirming that caspase-3 was not active within the epithelial cells. In contrast to these observations, Villar et al., reported a modest cleavage of epithelial PARP after 8 h of *C. albicans* infection, concomitant with transient activation of caspase-3 (Villar et al., 2012). The difference between the epithelial responses observed here and those reported by Villar et al. may be attributable to differences in epithelial cell lines (TR146 vs OKF6/TERT2) and the time point chosen for analysis (8 h vs 24 h). Neverthless, Villar et al. concluded that the transient activation of caspase-3 was most likely insufficient to trigger PARP cleavage observed at 8 h of *C. albicans* infection. They speculated that PARP degradation could be caused partially or entirely by lysosomal proteases (Gobeil et al., 2001). Indeed, the (early) activation of apoptosis observed at 8 h by Villar at al. failed to progress and was not detected at later time points in epithelial cells infected with *C. albicans*. It is therefore possible that apoptotic signalling may be initiated in response to *C. albicans* at earlier time points. However, data presented here demonstrate that, if activated, the apoptotic response is insufficient to drive the major death response since caspase-3 and PARP activation was not observed.

Extensive damage occurs to oral epithelial cells during the late phases of *C. albicans* infection (Chiang et al., 2007; Park et al., 2005; Villar et al., 2004). Thus, it is possible that epithelial apoptotic pathways are inhibited during the late stages of infection as a result of overwhelming microbial insult, which may promote cellular necrosis. One explanation for these observations is that apoptosis may be detrimental to the survival of *C. albicans* during infection. Cells undergoing apoptosis are known to release apoptotic bodies that stimulate recruitment of macrophages to the site of production (Taylor et al., 2008). Accordingly, it is possible that macrophage recruitment may also lead to phagocytosis of the infecting fungus and hence fungal clearance.

An interesting observation is that when compared with vehicle-treated cells, *C. albicans* mutants able to express and secrete Candidalysin caused a significant reduction in the level of intracellular cytochrome c and a non-significant decrese in caspase-8 and -3

activity. These observations suggest that Candidalysin may hamper the expression of apoptotic proteins and may instead promote necrosis (Chapter 1, Table 2).

It should also be noted that *C. albicans* and Candidalysin activate members of the NF-kB family in oral epithelial cells (Moyes et al., 2010; Moyes et al., 2016). Activation of the NF-kB signalling pathway leads to the expression of multiple genes including host cell anti-apoptotic factors, such as cIAP that block apoptotic cell death and promote necrotic cell death (Gyrd-Hansen and Meier, 2010). cIAPs play an important role in the modulation of NF-kB signalling and the caspase-independent cell death pathway necroptosis (Gyrd-Hansen and Meier, 2010). cIAP2 has been demonstrated to modulate apoptotic and necrotic cell death by promoting the assembly of an upstream cell death-inducing platform called the ripoptosome (Geserick et al., 2009). Formation of the ripoptosome, whose core components are comprised of RIPK1, FADD and pro-caspase-8, can result in the activation of pro-caspase-8 and caspase-dependent cell death. However, under circumstances where caspases are not active, the absence of cIAP2 can stimulate assembly of the necroptosome to promote necroptotic cell death (Tenev et al., 2011). Epithelial cells treated with Candidalysin were observed to express cIAP2, which can inhibit apoptosis through NF-kB signalling and the induction of anti-apoptotic factors (Silke and Meier, 2013). However, epithelial cells challenged with fungus showed reduced cIAP2 expression and no caspase-3/8 activity. This could lead to the formation of the necroptosome complex involved in necrosis (Chapter 1, Figure 1-10). Thus, the results of this work demonstrate that neither Candidalysin or *C. albicans* induced apoptosis in oral epithelial cells. Therefore, activation of regulated necrotic pathways by Candidalysin was addressed in Chapter 5.

Chapter 5: Role of Candidalysin in driving regulated necrotic cell death in human oral epithelial cells

5.1 Introduction

Programmed cell death plays an important role during host-pathogen interactions. It regulates tissue development, immune homeostasis and host defence against microbes. For a long time, apoptosis was used as a synonym for programmed cell death, whereas necrosis was considered to occur inadvertently following physiochemical insult. This viewpoint has since changed following recent discoveries that demonstrated the existence of different pathways of regulated necrosis such as necroptosis and pyroptosis (Vanden Berghe et al., 2014).

Necroptotic cell death is triggered following activation of cell death receptors, such as tumour necrosis factor receptor (TNFR) by extrinsic stimuli (Chan et al., 2003). Activation of a cell death receptor induces the recruitment of RIPK1 and several other proteins to form complex 1 (Chapter 1, Figure 1-10). Complex 1 then dissociates and RIPK1 forms a second complex in the cytosol, known as a ripoptosome, which contains RIPK1, caspase-8 and FADD (Imre et al., 2011) (Chapter 1, Figure 1-10). Activated caspase-8 cleaves and inactivates RIPK1 and RIPK3 (Lin et al., 1999) triggering the pro-apoptotic cascade. Thus, caspase-8 activity acts as a negative regulator of the necroptotic pathway. In the absence of active caspase-8, RIPK1 and RIPK3 assemble to form a necroptosome complex (Wang et al., 2008), which in turn leads to the induction of necroptosis. RIPK3 phosphorylates MLKL which translocates from the cytosol to the plasma membrane causing calcium influx and membrane lysis (Cai et al., 2014).

Pyroptosis is another form of regulated necrosis and is mechanistically distinct from apoptosis as cells undergo lysis rather than membrane blebbing and the process is pro-inflammatory. Importantly, pyroptosis differs from unregulated necrosis and necroptosis as it is mediated by inflammatory caspases such as caspase-1, -4, -5 and -11; and involves inflammasome activation (Bergsbaken et al., 2009). The canonical inflammasome is a complex of proteins formed from a NOD-like receptor (NLR), the adaptor protein ASC (apoptosis-associated speck-like protein containing a C-terminal caspase-recruitment domain (CARD)) and caspase-1. Caspase-1 processes the cytokines

pro-IL-1β and pro-IL-18 from their immature, biologically inactive form into biologically functional IL-1β and IL-18 (Fantuzzi and Dinarello, 1999) (Chapter 1, Figure 1-13). During pyroptosis, caspase-1 also cleaves gasdermin D resulting in release of the gasdermin D N-terminus which acts on plasma membranes causing pores with rapid progression of cell swelling and lytic cell death (Kayagaki et al., 2015; Shi et al., 2015).

The secreted toxins of *Bacillus anthracis* (Fink et al., 2008), *Staphylococcus aureus* (Kitur et al., 2015) and *Streptococcus pneumoniae* (Gonzalez-Juarbe et al., 2017) activate necroptosis or pyroptosis in macrophages and epithelial cells. In addition, pyroptosis and inflammasome activation is triggered in macrophages following *C. albicans* infection (Wellington et al., 2014); and there is evidence of inflammasome activation in the oral mucosa (Tomalka et al., 2011). However, the *C. albicans* factor(s) that activate pyroptosis and/or inflammasome activation in epithelial cells have not been identified. Thus, the aim of this chapter was to determine the role of Candidalysin in driving necroptosis and pyroptosis in oral epithelial cells.

5.2 Methods

5.2.1 Western blot analysis

TR146 monolayers were treated with *C. albicans* strains (Table 5.1) at a MOI of 5 and 0.01 and with 70, 30, 15 and 3 μM Candidalysin for 6 h and 24 h. Proteins were extracted, quantified and separated by size with gel electrophoresis. Separated proteins were transferred to a nitrocellulose membrane, which was probed with anti-RIPK1, anti-p-RIPK1, anti-RIPK3, anti-p-RIPK3, anti-MLKL, anti-p-MLKL, anti-NLRP3, anti-ASC, anti-caspase-1, anti-IL-1β, anti-IL-18 or anti-gasdermin D primary antibody and then with a HRP-conjugated secondary antibody (see Section 2.5).

5.2.2 Quantification of Caspase activity

TR146 oral epithelial cells were treated with *C. albicans* strains at a MOI of 5 and 0.01 and with 70, 30, 15 and 3 μM Candidalysin for 6 h and 24 h. Caspase activity was assessed by adding a substrate solution and measuring luminescence after incubating infected cells for 1 h (see section 2.4.7).

5.2.3 Quantification of IL-1β and IL-18

TR146 oral epithelial cells were treated with *C. albicans* strains at a MOI of 5 and 0.01 and with 70, 30, 15 and 3 μM Candidalysin for 6 h and 24 h. Exhausted culture medium was collected and cytokine levels were quantified using ELISA kits (Invitrogen and MLB) (see Section 2.4.8).

5.3 Results

5.3.1 Expression and phosphorylation of RIPK1 in epithelial cells treated with Candidalysin and *C. albicans ECE1* mutants

Necroptosis is a caspase-independent form of cell death and is often characterised by phosphorylation of RIPK1, RIPK3 and MLKL that propagate the signal that drives necroptotic cell death. Since treatment of epithelial cells with Candidalysin or *C. albicans* was observed to induce necrotic rather than apoptotic cell death (Chapter 4), necroptosis was first investigated by assessment of RIPK1 phosphorylation.

TR146 monolayers were incubated with 70, 30, 15 and 3 μM Candidalysin and with *C. albicans ECE1* mutants at a MOI of 5 and 0.01 for 6 h and 24 h. Total protein was isolated and analysed by SDS-PAGE and western blotting for the expression and phosphorylation of RIPK1 (see sections 2.5.1-2.5.4). No positive control for the specific induction of necroptosis in TR146 oral epithelial cells has been reported in the literature. Therefore, based on observations of necroptosis induction in HT-29 human colorectal epithelial cells and U937 human macrophages by TNF, staurosporine and ZVAD (Cai et al., 2014; Dunai et al., 2012; Su et al., 2016), 20 μg/mL TNF, 0.1 μM staurosporine and 100 μM ZVAD (T/S/Z) were used to induce necroptosis in the TR146 epithelial cell line.

RIPK1 was expressed in resting (vehicle) treated cells, and no further increase in RIPK1 expression was observed following treatment with Candidalysin or *C. albicans ECE1* mutant strains (Figure 5-1). However, a slight decrease in RIPK1 expression was observed in epithelial cells treated for 24 h with *C. albicans* strains able to express and secrete Candidalysin (BWP17 and *ECE1* reintegrant; *ece1*Δ/Δ+*ECE1*).

TR146 epithelial cells treated with T/S/Z exhibited phosphorylation of RIPK1 at 6 h (78-82 kDa) which was reduced at 24 h. Compared to the vehicle control, no increase in RIPK1 phosphorylation was observed following treatment with Candidalysin or

C. albicans ECE1 mutant strains at 6 h and 24 h, except for a slight increase in phosphorylation of RIPK1 in response to 15 µM Candidalysin at 24 h.

These data suggest that at the MOIs and time points tested, *C. albicans ECE1* mutants do not induce phosphorylation of RIPK1 in TR146 epithelial cells. However, a weak increase in phosphorylation of RIPK1 was observed in epithelial cells treated with 15 µM Candidalysin.

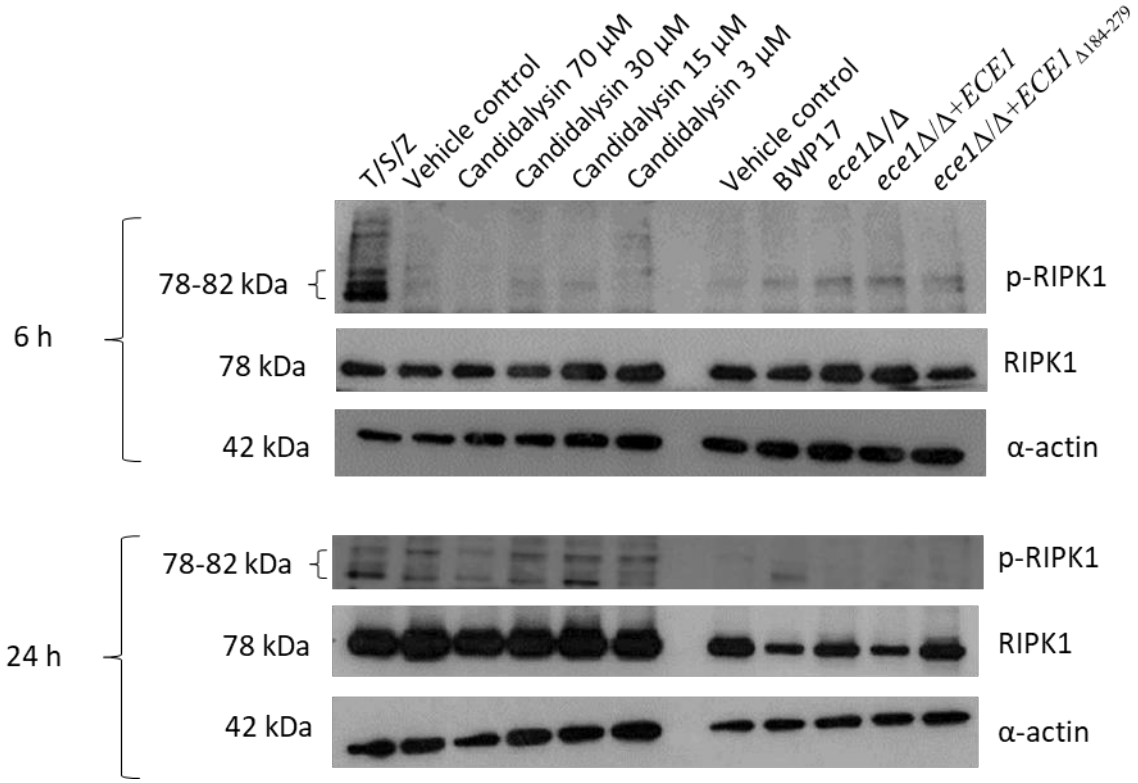

Figure 5-1. Expression and phosphorylation of RIPK1 in oral epithelial cells in response to Candidalysin and *C. albicans ECE1* mutant strains. TR146 oral epithelial cells were incubated with 70, 30, 15 and 3 µM Candidalysin or with *C. albicans ECE1* mutant strains for 6 h (MOI of 5) and 24 h (MOI of 0.01) and cell lysate assayed for p-RIPK1 and RIPK1 expression by western blot. T/S/Z was used as positive control for necroptosis. Data are representative of three biological replicates.

5.3.2 Expression and phosphorylation of RIPK3 in TR146 epithelial cells treated with Candidalysin and *C. albicans ECE1* mutants

Previous studies have shown that necroptosis can be induced independently of RIPK1 phosphorylation (Kaiser et al., 2013; Tamura et al., 2011). Necroptosis is defined as a RIPK3-dependent molecular cascade that promotes regulated necrosis (Moriwaki and

Chan, 2013). Thus, phosphorylation of RIPK3 was assessed in epithelial cells treated with Candidalysin and *C. albicans ECE1* mutants.

TR146 monolayers were incubated with 70, 30, 15 and 3 µM Candidalysin and with *C. albicans ECE1* mutants at a MOI of 5 and 0.01 for 6 h and 24 h. Total protein was isolated and analysed by SDS-PAGE and western blotting for the expression and phosphorylation of RIPK3 (see sections 2.5.1-2.5.4). T/S/Z was used as a positive control for necroptosis.

Epithelial cells exposed to the vehicle control expressed baseline levels of RIPK3, and no further increase in RIPK3 expression was observed following treatment with Candidalysin or *Candida* mutant strains (Figure 5-2). Similar to RIPK1, a decrease in RIPK3 expression was observed in epithelial cells treated for 24 h with *Candida* strains able to express and secrete Candidalysin (BWP17 and *ECE1* reintegrant; *ece1*Δ/Δ+*ECE1*).

Epithelial cells treated with Candidalysin and *C. albicans ECE1* mutants for 6 h exhibited variation in the degree of RIPK3 phosphorylation observed between biological replicates. However, a weak but reproducible phosphorylation of RIPK3 at 6 h was observed in T/S/Z treated cells (Figure 5-2). No phosphorylation of RIPK3 was detected in epithelial cells treated for 24 h.

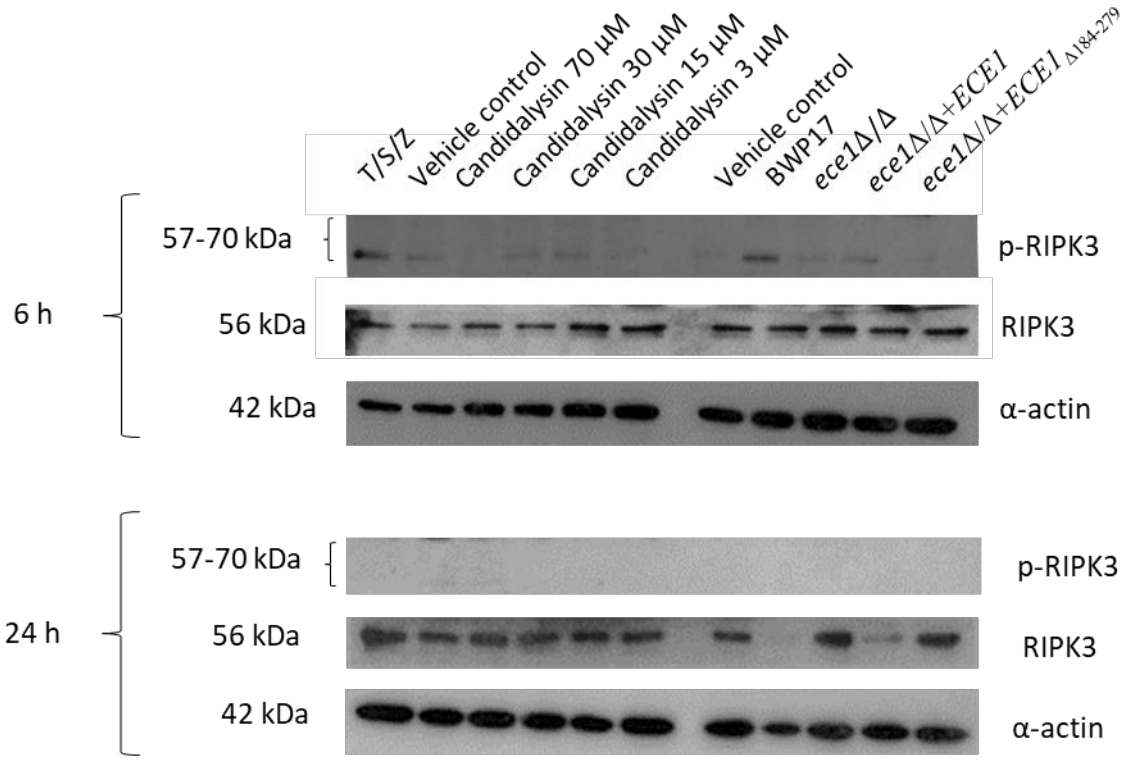

Figure 5-2. Expression and phosphorylation of RIPK3 in oral epithelial cells in response to Candidalysin and *C. albicans ECE1* mutant strains. TR146 oral epithelial cells were incubated with 70, 30, 15 and 3 µM Candidalysin or with *C. albicans ECE1* mutant strains for 6 h (MOI of 5) and 24 h (MOI of 0.01) and cell lysate assayed for p-RIPK3 and RIPK3 expression by western blot. T/S/Z was used as positive control for necroptosis. A single experiment is presented from a total of three biological replicates performed.

5.3.3 Expression and phosphorylation of MLKL in TR146 epithelial cells treated with Candidalysin and *C. albicans ECE1* mutants

During necroptosis, phosphorylation of RIPK3 causes the recruitment and phosphorylation of the necroptotic effector MLKL which translocates to the plasma membrane of the cell resulting in pore formation and cell lysis (Chapter 1, Figure 1-10). Thus, to investigate if epithelial cell death in response to Candidalysin and *C. albicans ECE1* mutants occurs by necroptosis, I also investigated phosphorylation of MLKL.

Accordingly, TR146 monolayers were incubated with 70, 30, 15 or 3 µM Candidalysin and with *Candida* mutants at a MOI of 5 and 0.01 for 6 h and 24 h. Total protein was isolated and analysed by SDS-PAGE and western blotting for the expression and phosphorylation of MLKL (see sections 2.5.1-2.5.4). T/S/Z was used as a positive control for necroptosis.

T/S/Z treated cells showed MLKL expression at 6 h, which was observed to be reduced at 24 h post treatment. MLKL expression was observed in vehicle treated cells at 6 h and 24 h. Addition of low and intermediate concentrations of Candidalysin (3-30 µM) for 6 h and 24 h induced negligible MLKL expression while 70 µM Candidalysin induced a reduction in MLKL expression when compared with vehicle-treated cells (Fig 5-3). Infection of epithelial cells for 6 h with *C. albicans ECE1* mutants again induced modest levels of MLKL expression which was not maintained at 24 h.

Treatment of epithelial cells with T/S/Z for 24 h resulted in weak, but nevertheless reproducible phosphorylation of MLKL (54 kDa), whereas treatment with Candidalysin or *C. albicans ECE1* mutant strains was not observed to stimulate MLKL phosphorylation at any time point tested.

In summary, Candidalysin and *C. albicans ECE1* mutants failed to induce MLKL phosphorylation in epithelial cells, indicating that necroptotic cell death was not induced, and suggesting that epithelial cell death in response to Candidalysin and *C. albicans ECE1* mutants may proceed through an alternative necrotic pathway.

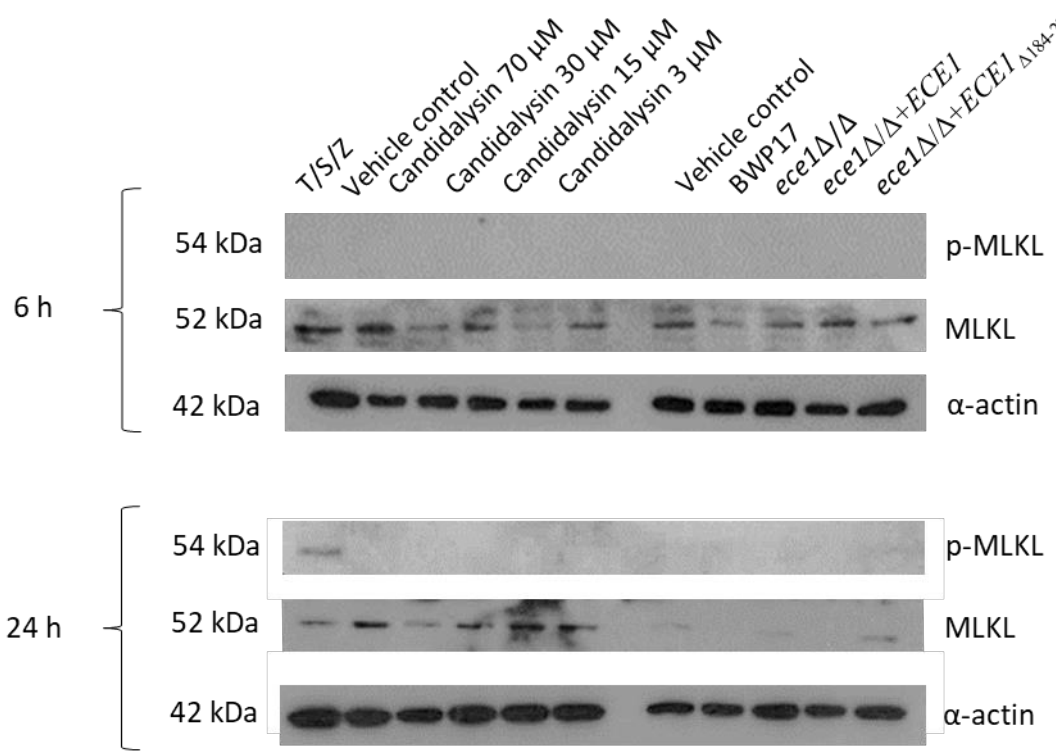

Figure 5-3. Expression and phosphorylation of MLKL in oral epithelial cells treated with Candidalysin and *C. albicans ECE1* mutants. TR146 oral epithelial cells were incubated with 70, 30, 15 and 3 µM Candidalysin or with *C. albicans ECE1* mutant strains for 6 h (MOI of 5) and 24 h (MOI of 0.01) and cell lysate assayed for expression and phosphorylation of MLKL by western blot. T/S/Z was used as a positive control for necroptosis. Data are representative of three biological replicates.

5.3.4 Secretion of IL-1β and IL-18 from TR146 oral epithelial cells in response to Candidalysin and *C. albicans ECE1* mutant strains

Having discounted the necroptotic pathway in epithelial responses to Candidalysin and *C. albicans* infection, activation of the pyroptotic cell death pathway (Chapter 1, Figure 1-13) was investigated. Pyroptosis is a cell death pathway that involves inflammasome activation and release of the cytokines IL-1β and IL-18 to activate pro-inflammatory responses. To investigate the induction of pyroptosis by Candidalysin and *C. albicans* mutant strains, IL-1β and IL-18 secretion was quantified from epithelial cells.

TR146 oral epithelial cells were treated with 70, 30, 15 and 3 µM Candidalysin or *C. albicans ECE1* mutant strains at a MOI of 5 and 0.01 for 6 h and 24 h. Exhausted culture medium was collected and IL-1β and IL-18 were quantified by ELISA.

Treatment of epithelial cells with 70 µM Candidalysin for 6 h resulted in a robust and significant increase in IL-1β secretion when compared with the vehicle control (Figure 5-4). No increase in IL-1β secretion was observed with the lower concentrations of Candidalysin (3 – 30 µM) at 6 h. Interestingly, an intermediate concentration of Candidalysin (15 µM) was observed to induce the greatest level of IL-1β secretion from epithelial cells after 24 h. However, while statistically significant, the overall level of IL-1β secretion observed at 24 h was low (0 - 18 pg/mL) when compared to secretion at 6 h (~320 pg/mL).

Epithelial cells infected with *C. albicans ECE1* mutant strains for 6 h did not secrete appreciable amounts of IL-1β when compared with the vehicle control. However, infection of epithelial cells with BWP17 or *ECE1* reintegrant (*ece1*Δ/Δ+*ECE1*) strains for 24 h caused significant secretion of IL-1β when compared with the vehicle control. In contrast, *C. albicans* mutant strains that were unable to express and secrete Candidalysin (*ece1*Δ/Δ and *ece1*Δ/Δ+*ECE1*$_{\Delta 184\text{-}279}$) were incapable of inducing significant levels of IL-1β secretion from epithelial cells. However, while statistically significant, the overall level of IL-1β secretion observed at 24 h was still low (<25 pg/mL) when compared to IL-1β levels induced at 6 h by 70 µM Candidalysin (~320 pg/mL).

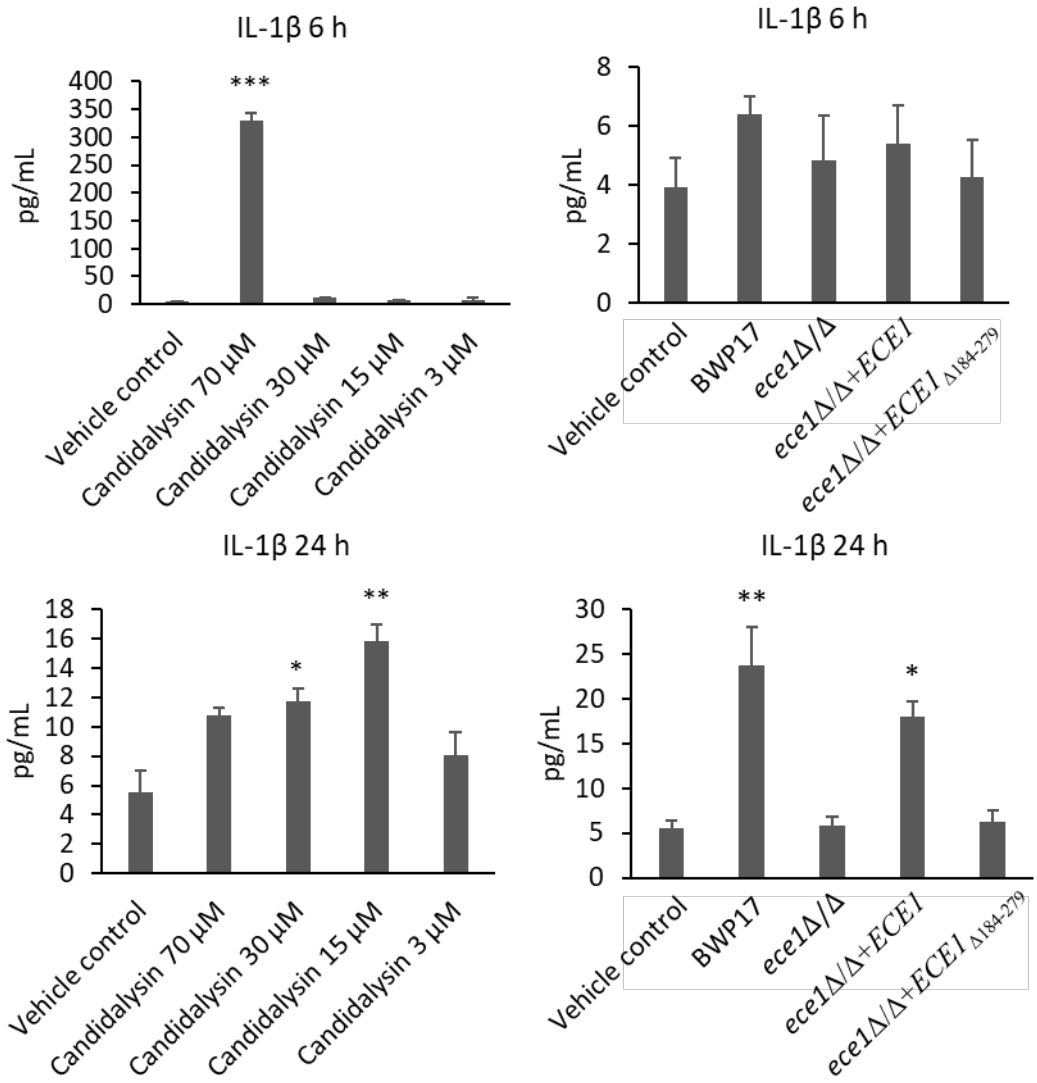

Figure 5-4. Secretion of IL-1β from TR146 oral epithelial cells treated with Candidalysin and *C. albicans ECE1* mutant strains. TR146 oral epithelial cells were incubated with 70, 30, 15 and 3 µM Candidalysin or with *C. albicans ECE1* mutant strains for 6 h (MOI of 5) and for 24 h (MOI of 0.01). IL-1β was quantified in exhausted culture medium by ELISA. Data are the mean of three biological replicates (+SEM). Statistical significance was calculated by one way ANOVA, * $p<0.05$, ** $p<0.01$ *** $p<0.001$.

During pyroptosis (and similar to IL-1β), IL-18 is also synthesised as an inactive precursor that is proteolytically processed by inflammatory caspases (a component of the inflammasome; Chapter 1, Figure 1-13) into its mature, biologically active form which is then secreted from the cell. To further investigate activation of the pyroptotic pathway, I quantified secretion of IL-18 from epithelial cells in response to Candidalysin and *C. albicans ECE1* mutant strains.

Epithelial cells were observed to secrete IL-18 in a dose-dependent manner in response to Candidalysin (Figure 5-5), with a concentration of 70 µM causing significant IL-18

secretion after 6 h. Notably, as with IL-1β, treatment of epithelial cells with Candidalysin for 24 h induced maximum IL-18 secretion when intermediate concentrations of toxin (30 μM and 15 μM) were administered.

Infection of epithelial cells with BWP17 or *ECE1* reintegrant strain (*ece1*Δ/Δ+*ECE1*) for 6 h resulted in an increase in IL-18 secretion from epithelial cells when compared with the vehicle control. The observed increase in secretion was maintained and became statistically significant at 24 h post-infection. In contrast, *C. albicans* mutant strains unable to express and secrete Candidalysin (*ece1*Δ/Δ and *ece1*Δ/Δ+*ECE1*$_{\Delta 184\text{-}279}$) were incapable of inducing significant IL-18 secretion from oral epithelial cells when compared with the vehicle control (Figure 5-5). Importantly, and unlike IL-1β, the levels of IL-18 secretion was similar in epithelial cells treated with Candidalysin and *C. albicans* strains (~60 - 150 pg/mL).

These data demonstrate that Candidalysin induces secretion of IL-18 from oral epithelial cells at 6 h and 24 h.

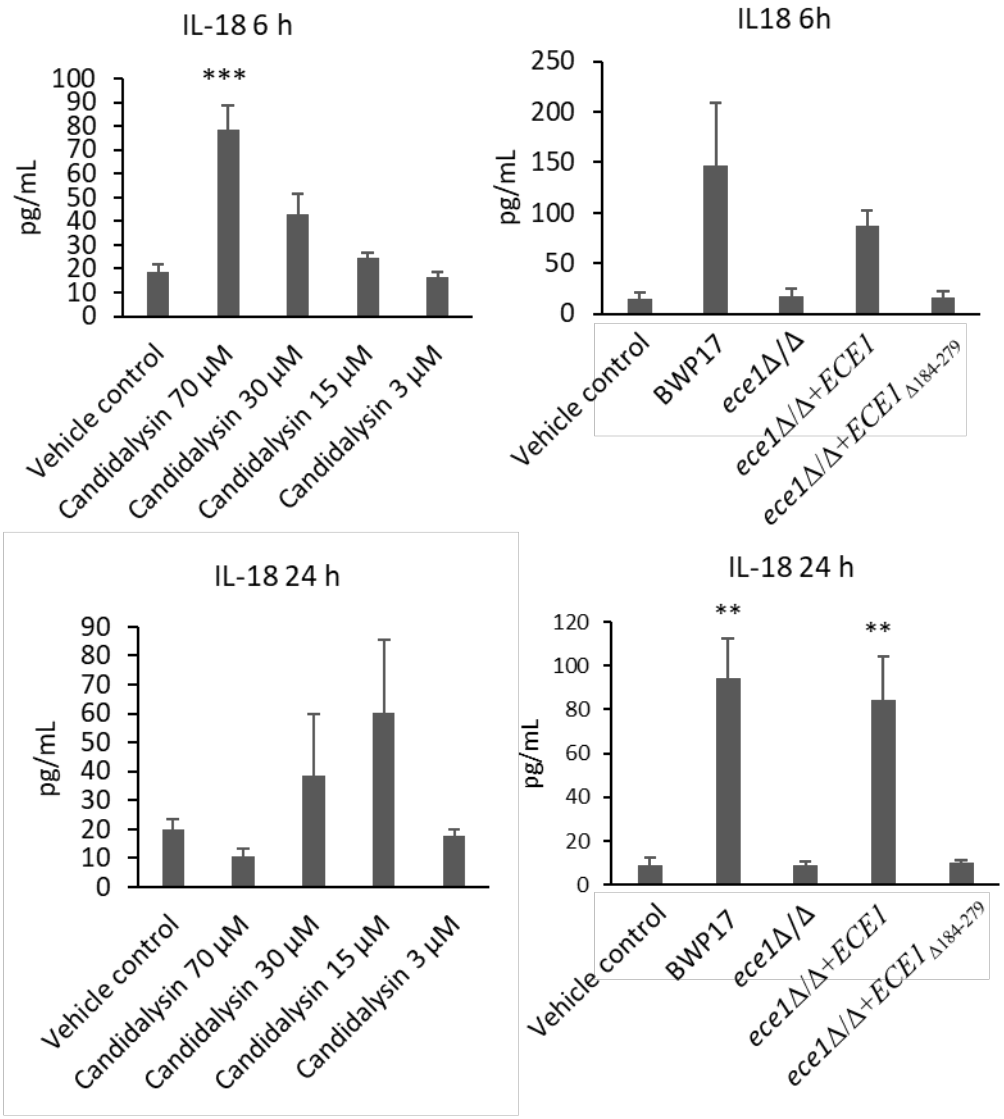

Figure 5-5. Secretion of IL-18 from oral epithelial cells treated with Candidalysin and *C. albicans ECE1* mutants. TR146 oral epithelial cells were incubated with 70, 30, 15 and 3 µM Candidalysin, or with *C. albicans ECE1* mutant strains for 6 h (MOI of 5) and for 24 h (MOI of 0.01). IL-18 was quantified in exhausted culture medium by ELISA. Data are the mean of three biological replicates (+SEM). Statistical significance was calculated by one way ANOVA, ** p<0.01 ***, p<0.001.

5.3.5 Expression of intracellular IL-1β and IL-18 in oral epithelial cells in response to Candidalysin and *C. albicans ECE1* mutant strains

While the general trend of IL-1β and IL-18 secretion from epithelial cells 24 h post infection appeared comparable, the pattern of IL-1β and IL-18 secretion observed at 6 h post infection varied between cytokines (Figures 5-4 and 5-5). In particular, *C. albicans* strains induced substantial IL-18 secretion compared to IL-1β at 6 h infection, while both cytokines were released in significant amounts at 24 h in an *ECE1*- and Candidalysin-

dependent manner, potentially suggesting that IL-18, but not IL-1β, was constitutively present within the cell ready to be secreted at 6 h infection. Thus, to understand how Candidalysin and *C. albicans ECE1* mutant strain treatment impacts on the accumulation of IL-1β and IL-18, the expression of intracellular IL-1β and IL-18 were investigated.

TR146 monolayers were incubated with 70, 30, 15 and 3 μM Candidalysin and with *Candida* mutants at a MOI of 5 and 0.01 for 6 h and 24 h respectively. Total protein was isolated and analysed by SDS-PAGE and western blotting for the presence of IL-1β and IL-18 (see sections 2.5.1-2.5.4).

Treatment of epithelial cells with Candidalysin for 6 h or 24 h resulted in an increase in pro-IL-1β expression when compared with the vehicle control (Figure 5-6).

Infection of epithelial cells with BWP17 or *ECE1* reintegrant (*ece1*Δ/Δ+*ECE1*) strain for 6 h resulted in an increase in pro-IL-1β expression when compared with the vehicle control. A slight increase in pro-IL-1β expression was also observed following treatment with *C. albicans* mutant strains unable to express and secrete Candidalysin (*ece1*Δ/Δ and *ece1*Δ/Δ+*ECE1*$_{\Delta 184\text{-}279}$) but only at 6 h. The increase in epithelial pro-IL-1β expression observed in response to BWP17 and *ECE1* reintegrant strains was less pronounced at 24 h.

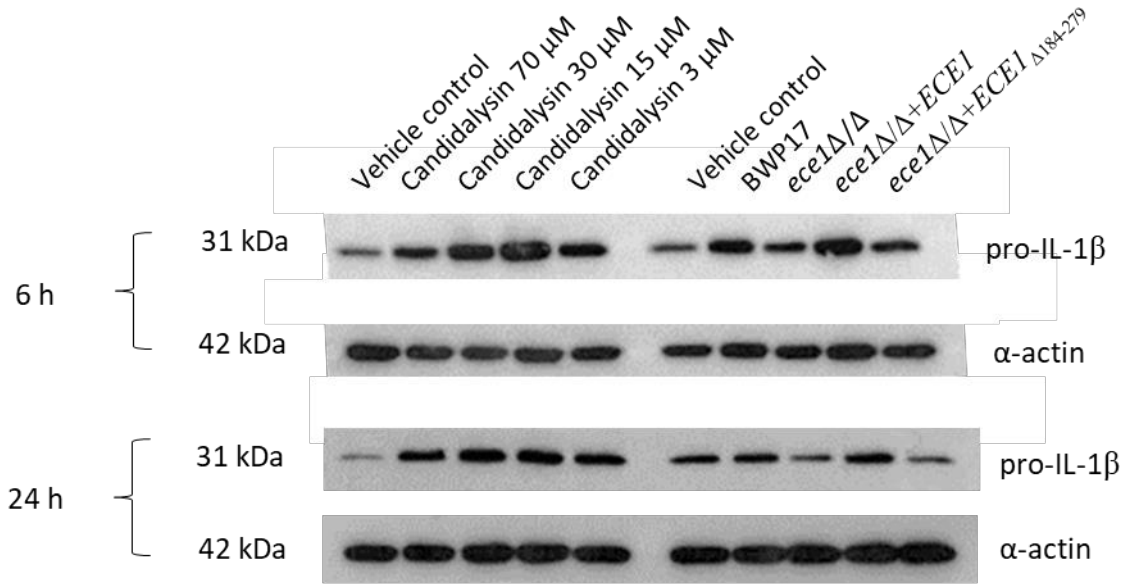

Figure 5-6. Epithelial expression of intracellular pro-IL-1β in response to Candidalysin and *C. albicans ECE1* mutant strains. TR146 oral epithelial cells were incubated with 70, 30, 15 and 3 µM Candidalysin or with *C. albicans ECE1* mutant strains for 6 h (MOI of 5) and for 24 h (MOI of 0.01) and cell lysate assayed for pro-IL-1β expression by western blot. Data are representative of three biological replicates.

Having observed an increase in the expression of intracellular pro-IL-1β in response to Candidalysin and *C. albicans* strains able to express and secrete Candidalysin, I next investigated expression of intracellular pro-IL-18.

Pro-IL-18 was observed to be expressed in vehicle treated cells, and no further increase in pro-IL-18 expression was observed following treatment with Candidalysin or *C. albicans ECE1* mutants at 6 h or 24 h (Figure 5-7) suggesting that immature IL-18 is constitutively present in epithelial cells.

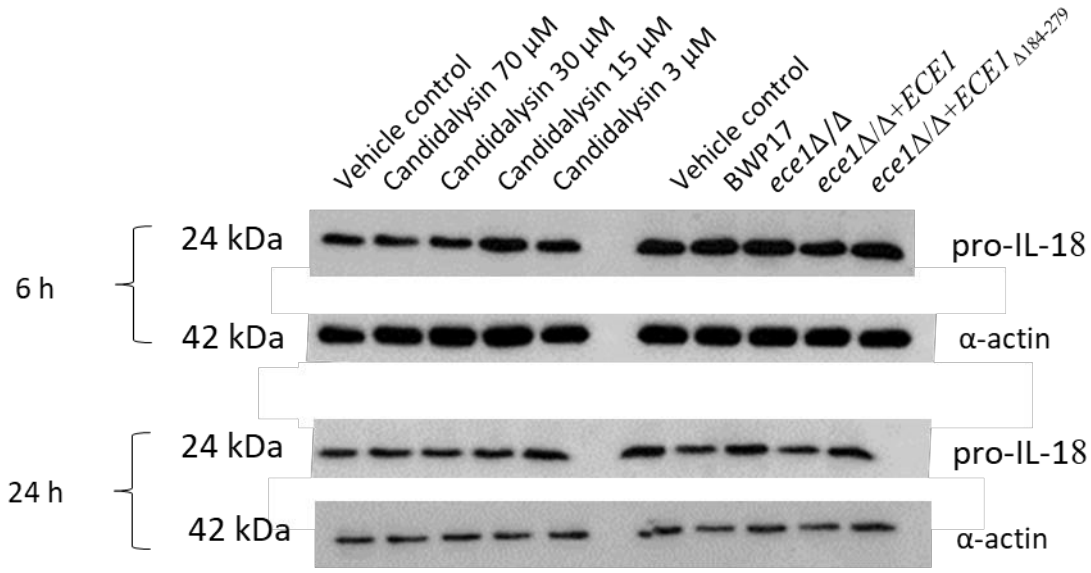

Figure 5-7. Epithelial expression of intracellular pro-IL-18 in response to Candidalysin and *C. albicans ECE1* mutants. TR146 oral epithelial cells were incubated with 70, 30, 15 and 3 µM Candidalysin or with *C. albicans ECE1* mutants for 6 h (MOI of 5) and for 24 h (MOI of 0.01) and cell lysate assayed for pro-IL-18 expression by western blot. Data are representative of three biological replicates.

5.3.6 Expression of NLRP3 in oral epithelial cells in response to Candidalysin and *C. albicans ECE1* mutants

Secretion of IL-1β and IL-18 requires the activation of the inflammasome complex which includes a NOD-like receptor, ASC adaptor protein, and caspase-1 (Martinon et al., 2002). Since IL-1β and IL-18 were secreted from epithelial cells in response to Candidalysin and *C. albicans ECE1* mutants, I investigated activation of the NLRP3 inflammasome by assessing NLRP3 expression.

TR146 monolayers were incubated with 70, 30, 15 and 3 µM Candidalysin and with *C. albicans ECE1* mutants at a MOI of 5 and 0.01 for 6 h and 24 h. Total protein was isolated and analysed by SDS-PAGE and western blotting for the presence of NLRP3 (see sections 2.5.1-2.5.4).

Treatment of epithelial cells with intermediate concentrations (30 µM and 15 µM) of Candidalysin for 6 h resulted in an increase in NLRP3 expression when compared with the vehicle control (Figure 5-8). However, treatment of cells with higher (70 µM) or lower (3 µM) concentrations of Candidalysin induced only modest NLRP3 expression. In

contrast to 6 h, treatment of epithelial cells with Candidalysin for 24 h resulted in robust, dose-dependent NLRP3 expression.

Expression of NLRP3 in response to *C. albicans* was observed to occur in an *ECE1*- and Candidalysin-dependent manner at 6 h when compared to vehicle-treated cells. In contrast to the 6 h NLRP3 expression profile, infection of epithelial cells for 24 h was not observed to induce NLRP3 expression.

These data suggest that Candidalysin induces NLRP3 expression in oral epithelial cells and that the region of *ECE1* that encodes Candidalysin is important for the expression of epithelial NLRP3 at 6 h post infection.

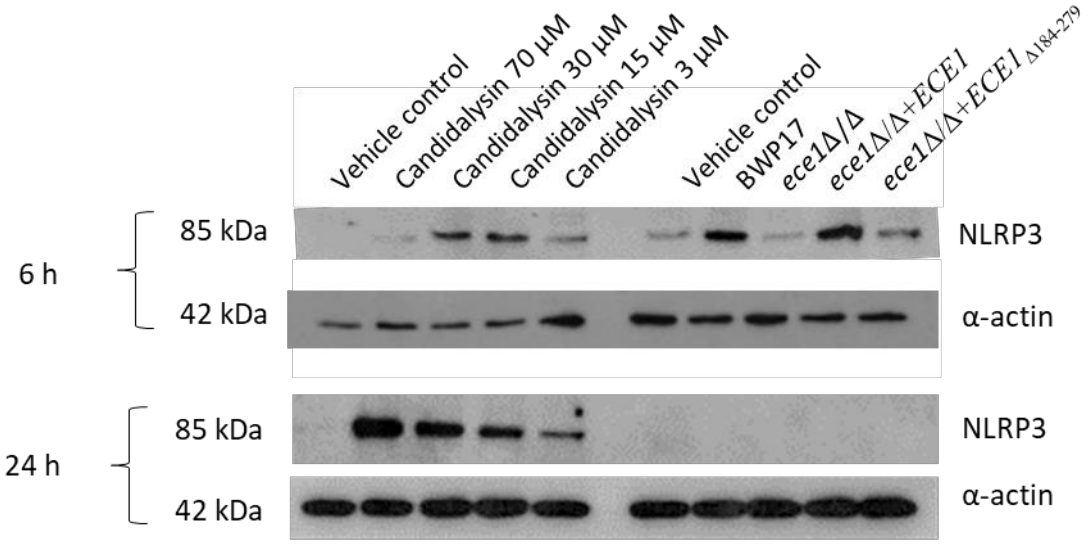

Figure 5-8. Expression of NLRP3 in epithelial cells treated with Candidalysin and *C. albicans ECE1* mutants. TR146 oral epithelial cells were incubated with 70, 30, 15 and 3 µM Candidalysin or with *C. albicans ECE1* mutants for 6 h (MOI of 5) and for 24 h (MOI of 0.01) and cell lysate assayed for NLRP3 expression by western blot. Data are representative of three biological replicates.

5.3.7 Expression of ASC in oral epithelial cells in response to Candidalysin and *C. albicans ECE1* mutants

Having observed expression of NLRP3 in epithelial cells in response to Candidalysin at both 6 h and 24 h and *C. albicans ECE1* mutants at 6 h post-treatment, expression of the adaptor protein ASC (a component of the NLRP3 inflammasome) was investigated. TR146 monolayers were incubated with 70, 30, 15 and 3 µM Candidalysin and with *C. albicans ECE1* mutant strains at a MOI of 5 and 0.01 for 6 h and 24 h, respectively.

Total protein was isolated and analysed by SDS-PAGE and western blotting for the presence of ASC (see sections 2.5.1-2.5.4).

ASC was observed to be expressed in vehicle treated cells, and no further increase in ASC expression was observed following treatment with Candidalysin or *C. albicans ECE1* mutant strains at 6 h or 24 h (Figure 5-9). These data suggest that the adaptor protein ASC is constitutively expressed in the TR146 epithelial cell line.

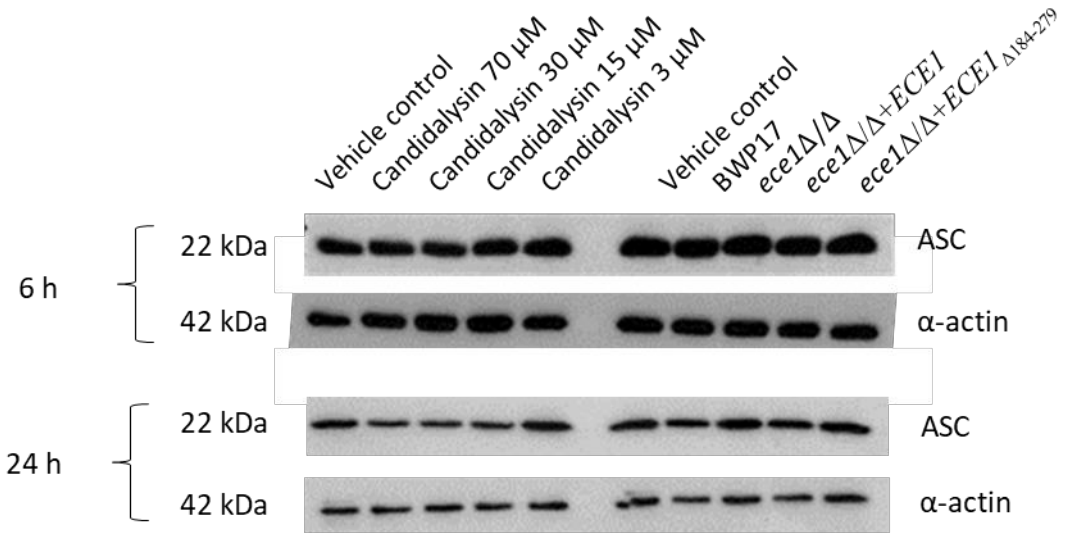

Figure 5-9. Expression of ASC in epithelial cells treated with Candidalysin and *C. albicans ECE1* mutants. TR146 oral epithelial cells were incubated with 70, 30, 15 and 3 µM Candidalysin or with *C. albicans ECE1* mutant strains for 6 h (MOI of 5) and for 24 h (MOI of 0.01) and cell lysate assayed for ASC expression by western blot. Data are representative of three biological replicates.

5.3.8 Expression and activity of caspase-1 in TR146 epithelial cells treated with Candidalysin and *C. albicans ECE1* mutants

Caspase-1 is a cysteine protease that cleaves inflammatory cytokines such as pro-IL-1β and pro-IL-18 into their mature, biologically active forms (Thornberry et al., 1992). Activation of caspase-1 occurs through a molecular platform termed the inflammasome that includes caspase-1, ASC, and NLRP3 (Martinon et al., 2002). When the inflammasome is assembled, caspase-1 undergoes autocatalytic activation, generating products between 30-48 kDa, and two active subunits of 20 kDa and 10 kDa, respectively (Alnemri et al., 1995). Having observed epithelial secretion of IL-1β, IL-18 and expression

of NLRP3 in response to Candidalysin and *C. albicans ECE1* mutant strains, expression of caspase-1 was assessed by western blot.

TR146 monolayers were incubated with 70, 30, 15 and 3 µM Candidalysin and with *C. albicans ECE1* mutants at a MOI of 5 and 0.01 for 6 h and 24 h, respectively. Total protein was isolated and analysed by SDS-PAGE and western blotting for the presence of caspase-1 (see sections 2.5.1-2.5.4).

Caspase-1 isoforms (ranging in molecular weight between 30-45 kDa) were observed to be expressed in vehicle treated epithelial cells (Figure 5-10). Treatment of epithelial cells with Candidalysin induced a dose-dependent decrease in the expression of the 30 kDa caspase-1 isoform at 6 h, which was more pronounced at 24 h post treatment. No difference in caspase-1 expression was observed in response to *C. albicans ECE1* mutants at 6 h post infection when compared to the vehicle control. In contrast, infection with *C. albicans ECE1* mutants for 24 h prevented caspase-1 (30-45 kDa) expression in epithelial cells, most notably with *C. albicans* strains able to express and secrete Candidalysin (BWP17 and *ECE1* reintegrant; *ece1*Δ/Δ+*ECE1*). Treatment of epithelial cells with Candidalysin or *C. albicans ECE1* mutants was not observed to induce expression of the active isoforms of caspase-1 (10-20 kDa) at 6 h or 24 h (Figure 5-10).

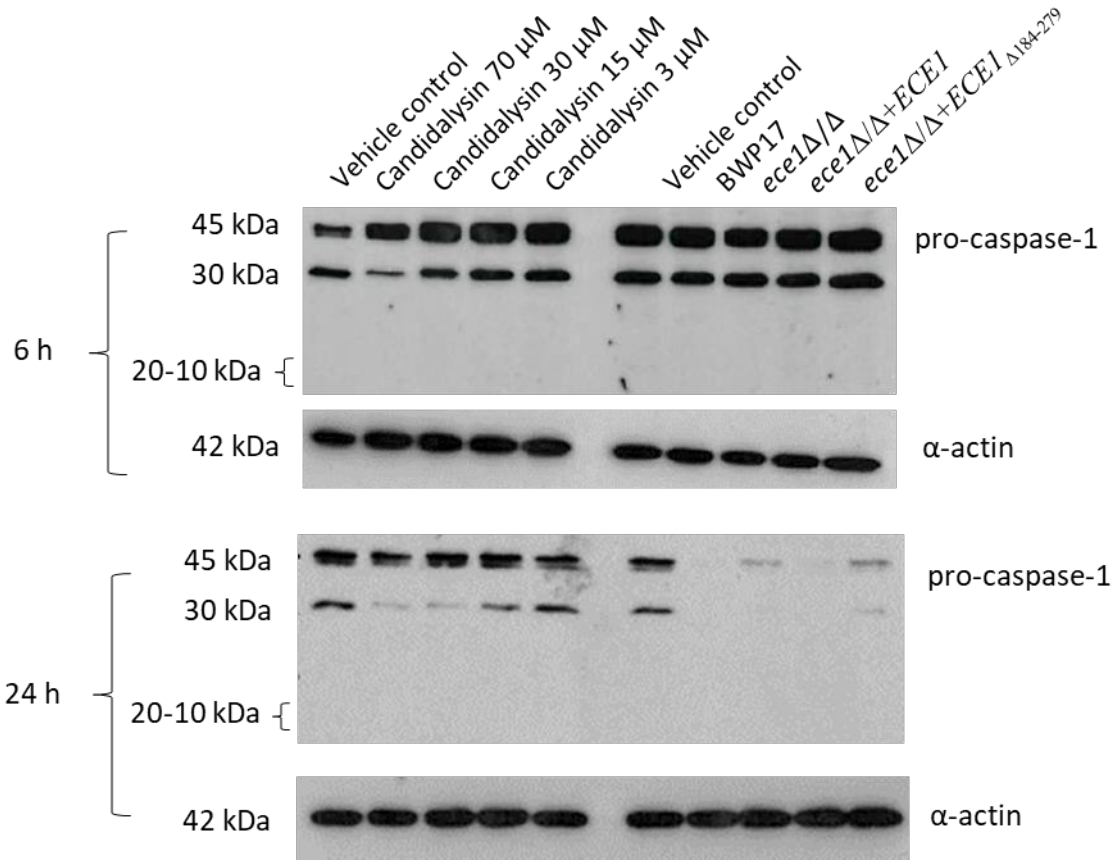

Figure 5-10. Expression of Caspase-1 in epithelial cells treated with Candidalysin and *C. albicans ECE1* mutants. TR146 oral epithelial cells were incubated with 70, 30, 15 and 3 µM Candidalysin or with *C. albicans ECE1* mutants for 6 h (MOI of 5) and for 24 h (MOI of 0.01) and cell lysate assayed for caspase-1 expression by western blot. Data are representative of three biological replicates.

Having detected strong expression of pro-caspase-1 but no expression of the active isoforms of caspase-1, I decided to utilise a more sensitive luminescence-based assay to detect the generation of active caspase-1 by Candidalysin or *Candida ECE1* mutants. In agreement with the western blot analysis, which showed no expression of active caspase-1 isoforms (10-20 kDa) (Figure 5-10), incubation of epithelial cells with Candidalysin or *Candida ECE1* mutants did not result in an increase in caspase-1 activity when compared with the vehicle control at 6 or 24 h (Figure 5-11). However, there did appear to be a (non-significant) reduction in caspase-1 activity with *C. albicans* strains able to express and secrete Candidalysin (BWP17 and *ECE1* reintegrant; *ece1*Δ/Δ+*ECE1*) at 6 h and more specifically at 24 h.

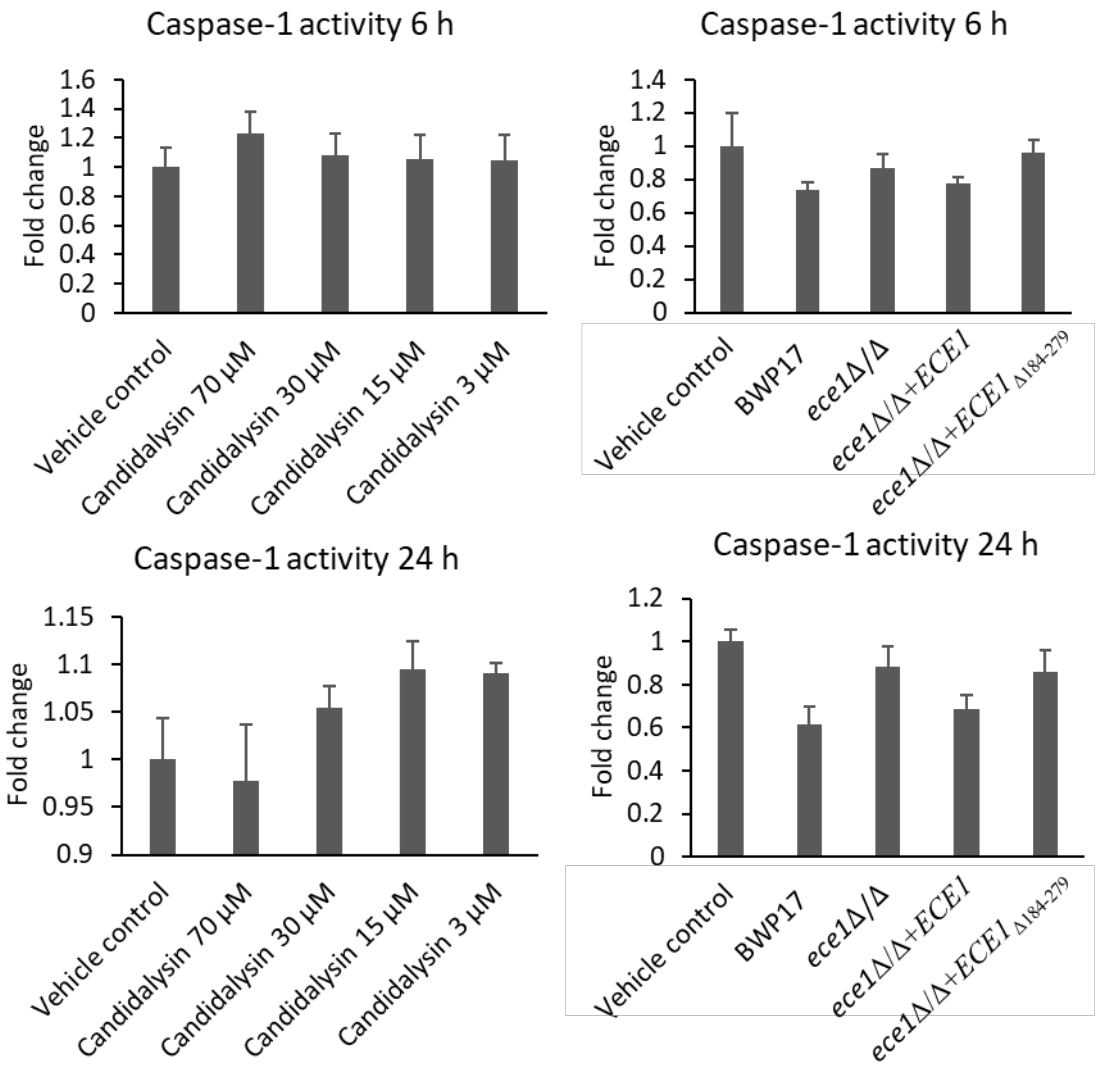

Figure 5-11. Caspase-1 activity in oral epithelial cells treated with Candidalysin and *C. albicans ECE1* mutants. TR146 oral epithelial cells were incubated with 70, 30, 15 and 3 µM Candidalysin or with *C. albicans ECE1* mutants for 6 h (MOI of 5) and for 24 h (MOI of 0.01) and cells assayed for caspase-1 activity by luminescence assay. Bars represent caspase-1 activity relative to vehicle control (fold change). Data are the mean of three biological replicates (+SEM). No statistical differences were found using one-way ANOVA.

5.3.9 Detection of IL-1β and IL-18 secreted from TR146 epithelial cells in response to Candidalysin and *C. albicans ECE1* mutants

The secretion of active IL-1β and IL-18 from cells first requires that their inactive isoforms (pro-IL-1β and pro-IL-18) are processed by proteases such as caspase-1 (inflammasome component) (Martinon et al., 2002). However, data from this study indicates that epithelial cells secrete IL-1β and IL-18 in response to Candidalysin in a caspase-1 independent manner (Figure 5-4, 5-5 and 5-11). Given the established role of caspase-1 in IL-1β and IL-18 maturation, I investigated whether the IL-1β and IL-18

secreted from epithelial cells in response to Candidalysin and *C. albicans ECE1* mutants were secreted as mature (active) or immature (inactive) isoforms.

TR146 oral epithelial cells were treated with 70, 30, 15 and 3 µM Candidalysin or *C. albicans ECE1* mutants at a MOI of 5 and 0.01 for 6 h and 24 h respectively. Exhausted culture medium was collected and secretion of IL-1β and IL-18 was determined by western blot. As a positive control for processed IL-1β and IL-18, 2.5 ng of recombinant human IL-1β and 0.2 pg of recombinant human IL-18 were included in the analysis.

Treatment of epithelial cells with Candidalysin and *C. albicans ECE1* mutants for 6 h and 24 h did not result in detectable levels of pro-IL-1β or mature IL-1β in the exhausted culture medium (Figure 5-12). Only recombinant human IL-1β (positive control) was detected at 17 kDa.

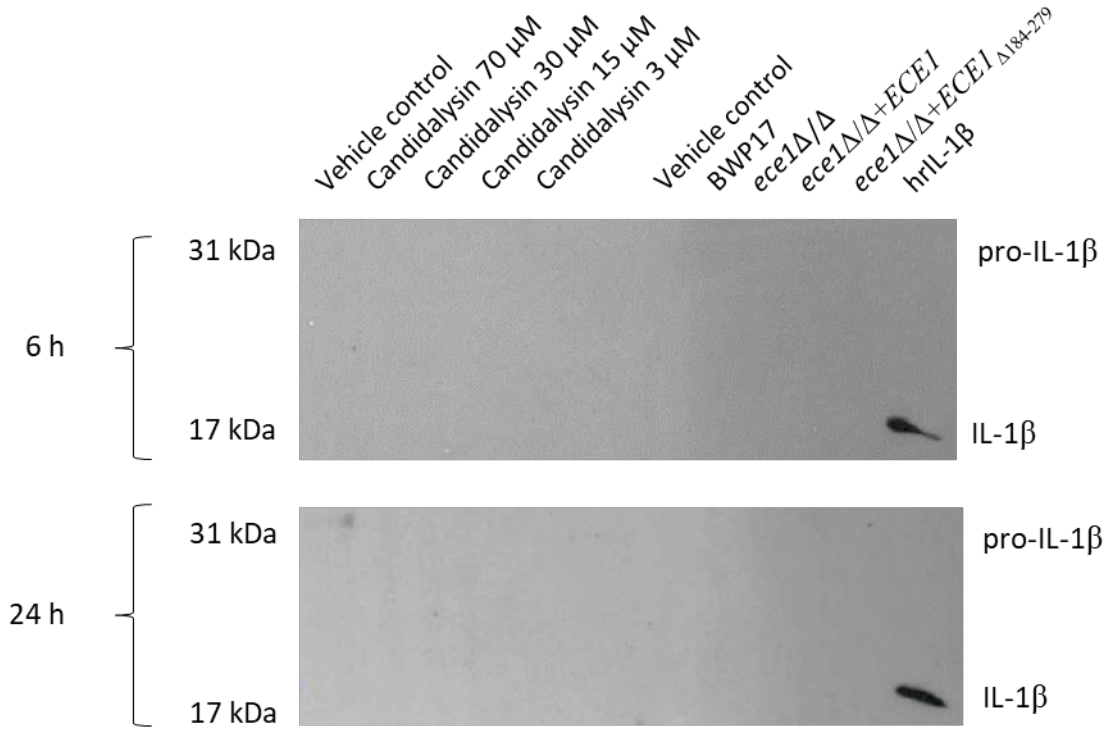

Figure 5-12. Secretion of IL-1β from epithelial cells in response to Candidalysin and *C. albicans ECE1* mutant strains. TR146 oral epithelial cells were incubated with 70, 30, 15 and 3 µM Candidalysin or with *C. albicans ECE1* mutants for 6 h (MOI of 5) and for 24 h (MOI of 0.01) and exhausted culture medium was quantified for IL-1β by western blot. Recombinant human IL-1β was used as a positive control for processed, biologically active cytokine. Data are representative of three biological replicates.

Like pro-IL-1β, pro-IL-18 must also be processed by the inflammasome in order to generate an active cytokine (Fantuzzi and Dinarello, 1999). Exhausted culture medium from epithelial cells treated with Candidalysin and *C. albicans ECE1* mutants able to secrete Candidalysin contained pro-IL-18 (24 kDa) but not mature IL-18 (17 kDa) (Figure 5-13). The human recombinant IL-18 positive control produced a band at 17 kDa (mature IL-18), suggesting that the IL-18 secreted from epithelial cells in response to Candidalysin and *C. albicans ECE1* mutants was unprocessed and therefore inactive.

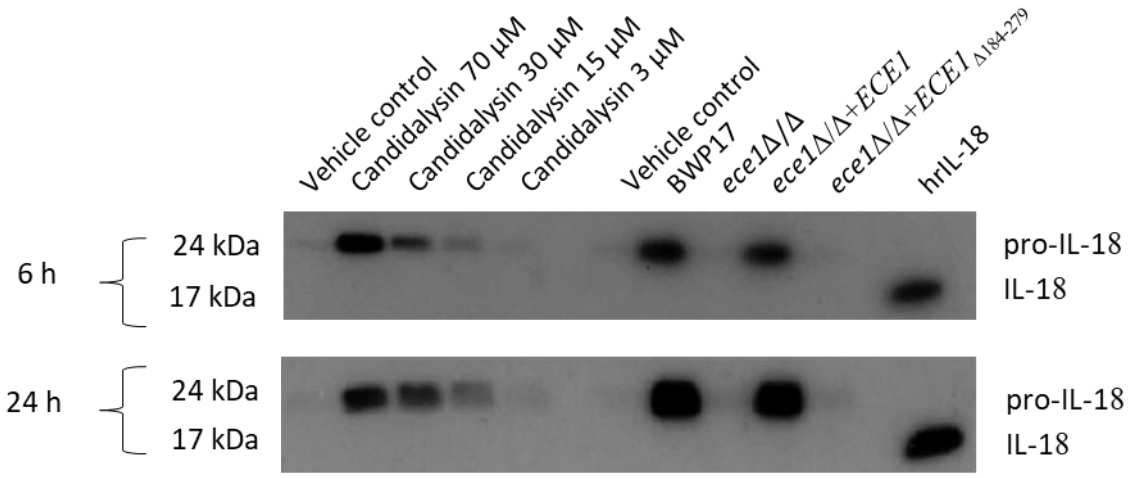

Figure 5-13. Secretion of IL-18 from epithelial cells in response to Candidalysin and *C. albicans ECE1* mutants. TR146 oral epithelial cells were incubated with 70, 30, 15 and 3 μM Candidalysin or with *C. albicans ECE1* mutants for 6 h (MOI of 5) and for 24 h (MOI of 0.01) and exhausted culture medium was quantified for IL-18 by western blot. Recombinant human IL-18 was used as a positive control for processed, biologically active cytokine. Data are representative of three biological replicates.

5.3.10 Expression of gasdermin D in epithelial cells in response to Candidalysin and *C. albicans ECE1* mutants

It was recently shown that in addition to inflammasome activation, gasdermin D is a key protein that can trigger pyroptotic cell death (Shi et al., 2015). When cleaved, gasdermin D translocates to the plasma and organelle membranes of affected cells, causing pore formation (Liu et al., 2016). Gasdermin D is cleaved by pro-inflammatory caspase-1, -4, -5 and -11 to generate N- and C- terminal products (of molecular weight 31 kDa and 22 kDa respectively), that trigger pyroptotic death and release of inflammatory cytokines such as IL-1β and IL-18 (Shi et al., 2015). Given that no appreciable caspase-1 activity was detected in epithelial cells in response to Candidalysin and *C. albicans ECE1* mutants

(Figure 5-10), I examined gasdermin D expression to determine if caspase-4, -5 and -11 were potentially activated under identical treatment conditions.

Accordingly, TR146 monolayers were incubated with 70, 30, 15, 3 µM Candidalysin and with *C. albicans ECE1* mutants at a MOI of 5 and 0.01 for 6 h and 24 h respectively. Total protein was isolated and analysed by SDS-PAGE and western blotting for the presence of gasdermin D (see sections 2.5.1-2.5.4).

Intact gasdermin D (53 kDa) was observed to be expressed in vehicle treated cells, and no further increase in gasdermin D expression was observed following treatment with Candidalysin or *C. albicans ECE1* mutant strains after 6 h (Figure 5-14). Intriguingly however, a decrease in gasdermin D expression was observed in epithelial cells treated for 24 h with *Candida* strains able to express and secrete Candidalysin (BWP17 and *ECE1* reintegrant; *ece1*Δ/Δ+*ECE1*).

These data suggest that at 6 h, epithelial cells do not respond to Candidalysin or *C. albicans ECE1* mutants by cleaving gasdermin D. While the observed lack of gasdermin D cleavage in response to Candidalysin was maintained at 24 h, expression (but not cleavage) of gasdermin D did appear to be partially influenced by the ability of *C. albicans* to express and secrete Candidalysin.

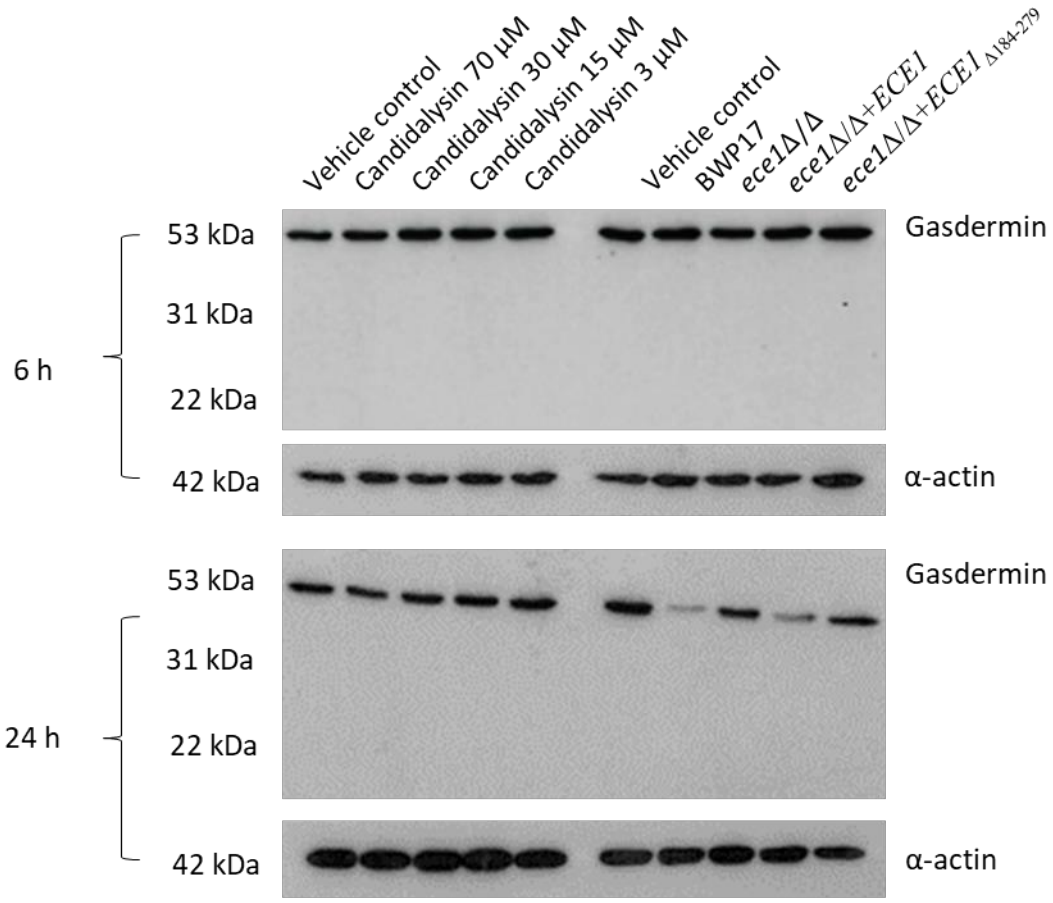

Figure 5-14. Epithelial expression of gasdermin D in response to Candidalysin and *C. albicans ECE1* mutants. TR146 oral epithelial cells were incubated with 70, 30, 15 and 3 µM Candidalysin or with *C. albicans ECE1* mutants for 6 h (MOI of 5) and for 24 h (MOI of 0.01) and cell lysate assayed for gasdermin D expression by western blot. Data are representative of three biological replicates.

5.4 Discussion

5.4.1 The epithelial necroptotic response to Candidalysin

In the past, while the traditional view of necrosis was that of a dysregulated, uncontrolled form of cell death, recent studies have now demonstrated that necrotic cell death can be a regulated event that contributes to tissue development and biological homeostasis. Among programmed cell death pathways, necroptosis (Degterev et al., 2005) and pyroptosis (Cookson and Brennan, 2001) have been used to describe models of non-apoptotic cell death that display aspects of programmed necrosis.

Necroptosis is a pro-inflammatory, caspase-independent form of cell death that is triggered following the activation of a cell death receptor by TNF family members, FAS ligand, LPS, genotoxic stress and physiochemical perturbations (Chan et al., 2003). The interaction between TNF and TNFR1 is a well-characterised activator of necroptosis that results in the recruitment of TRADD and RIPK1 to the cytoplasmic domain of the activated receptor to form complex 1 (Chapter 1, Figure 1-10). Complex 1 then dissociates, releasing RIPK1 which participates in ripoptosome formation with caspase-8 and FADD (Chapter 1, Figure 1-10) (Imre et al., 2011). Importantly however, in the absence of active caspase-8, ripoptosome assembly evolves, resulting in the formation of a necroptosome complex that drives necroptotic rather than apoptotic death (Wang et al., 2008). The necroptosome complex assembles through a series of RIPK1- and RIPK3-mediated auto- and trans-phosphorylation events that in turn lead to the induction of necroptosis (Cho et al., 2009 148).

Candidalysin and *C. albicans ECE1* mutants did not induce caspase-8 activity in epithelial cells (Chapter 4), suggesting that the toxin or fungus may induce necroptosome assembly, thereby propagating necroptotic signalling. However, RIPK1 was not phosphorylated in response to *C. albicans ECE1* mutants, and only a weak phosphorylation of RIPK1 was observed in response to 15 µM Candidalysin at 24 h. These observations suggest that the necroptotic process was not initiated by *C. albicans* despite the lack of caspase-8 activity, although it may have been transiently initiated in response to an intermediate concentration of Candidalysin.

Nevertheless, different signalling pathways are capable of inducing RIPK3 activation, and necroptotic death is known to occur independently of RIPK1 in some instances. For example, fibroblast TLR3/TLR4 can phosphorylate RIPK3 through a RIP kinase homotypic interaction motif-dependent association with TRIF (Kaiser et al., 2013). Therefore, necroptosis is defined as a RIPK3-dependent molecular cascade promoting programmed cell necrosis. Phosphorylation of RIPK3 stimulates the recruitment of MLKL, which is subsequently phosphorylated (Sun et al., 2012). Phosphorylated MLKL is the effector of necroptosis that translocates to and associates with the plasma membrane, inducing rupture, and the release of intracellular contents (Cai et al., 2014; Wang et al., 2014).

Epithelial cells treated with Candidalysin and *C. albicans ECE1* mutants for 6 h exhibited variable levels of RIPK3 phosphorylation between experiments, and phosphorylation of

RIPK3 at 24 h was not observed. Likewise, phosphorylation of MLKL was not observed in response to Candidalysin or *C. albicans ECE1* mutants at 6 h and 24 h, suggesting that transient and/or variable RIPK3 phosphorylation was insufficient to drive MLKL activation at the time points tested. Furthermore, these data demonstrate that LDH release and calcium influx caused by Candidalysin and *C. albicans ECE1* mutant strains (Chapter 3) was not induced through the formation of p-MLKL pores.

Collectively, these observations suggest that Candidaysin and *C. albicans ECE1* mutant strains do not induce necroptotic cell death in oral epithelial cells.

5.4.2 The epithelial pyroptotic response to Candidalysin

To further investigate the potential role of Candidalysin as a driver of regulated necrosis, the activation of pyroptosis was investigated. Pyroptosis is known to be induced in macrophages that phagocytose *C. albicans* yeast cells (Wellington et al., 2014). Following internalisation, the acidic environment of the phagolysosome stimulates the yeast cell to undergo morphological switching, resulting in the production of hyphal filaments that physically rupture the phagolysosome membrane and the plasma membrane of the macrophage, facilitating fungal escape (Jimenez-Lopez and Lorenz, 2013). Interestingly, the induction of pyroptosis is known to precede hyphal escape from macrophages (Uwamahoro et al., 2014). The *ECE1* gene of *C. albicans* is highly expressed during hyphal growth (Birse et al., 1993) and results in the production of Candidalysin, which is secreted from the hyphal form of the fungus (Moyes et al., 2016). Since Candidalysin is critical for the success of *C. albicans* mucosal infection *in vivo*, (Moyes et al., 2016), I hypothesised that Candidalysin may be required to activate pyroptotic responses in epithelial cells.

Induction of pyroptosis is dependent upon the activation of the inflammasome. The inflammasome has been reported to play an essential role in defences against *C. albicans* infection (Hise et al., 2009; Tomalka et al., 2011; van de Veerdonk et al., 2011). Activation of the inflammasome leads to cleavage of inactive pro-IL-1β and pro-IL-18 to produce mature, biologically active cytokines that trigger pro-inflammatory responses (Fantuzzi and Dinarello, 1999). Therefore, to determine whether inflammasome activation and pyroptosis was induced by Candidalysin and *C. albicans ECE1* mutant strains, secretion of IL-1β and IL-18 from oral epithelial cells was quantified.

Secretion of IL-1β and IL-18 was significantly increased when epithelial cells were exposed to 70 μM Candidalysin for 6 h. Interestingly, secretion of IL-1β and IL-18 at 24 h was observed to be greatest in response to 15 μM but not 70 μM Candidalysin, when compared to the vehicle control. It is possible that high concentrations of toxin may overwhelm the epithelial cell, affecting cytokine expression, and preventing assembly and activation of the inflammasome and hence secretion of mature IL-1β and IL-18. Indeed, high concentration of toxin (70 μM) induced extensive cell stress including plasma membrane permeabilisation, mitochondrial dysfunction, generation of ROS, ATP depletion and calcium influx (Chapter 3). Notably, *C. albicans* mutant strains unable to express and secrete Candidalysin (*ece1*Δ/Δ and *ece1*Δ/Δ+*ECE1*$_{\Delta 184\text{-}279}$) were unable to stimulate IL-1β and IL-18 secretion from epithelial cells. These observations demonstrate that Candidalysin is required to stimulate secretion of IL-1β and IL-18 from epithelial cells, and further confirm the role of Candidalysin as a critical inducer of pro-inflammatory epithelial responses (Moyes et al., 2016).

Robust secretion of IL-1β from epithelial cells was observed at 6 h, but an equivalent level of secretion was not maintained at 24 h, highlighting temporal differences in IL-1β secretion from epithelial cells in response to Candidalysin. Conversely, infection of epithelial cells with *C. albicans ECE1* mutant strains required more time to induce significant levels of IL-1β secretion when compared with Candidalysin alone, an observation that is most likely consistent with the lag-phase that precedes the induction of hyphal growth and the time taken to accumulate damage-inducing concentrations of Candidalysin from *C. albicans* hyphae *in vitro*.

In contrast to the observations of others that showed substantial secretion of IL-1β from macrophages at 24 h (9000 pg/mL) (Uwamahoro et al., 2014), secretion of IL-1β from epithelial cells in response to Candidalysin and *C. albicans ECE1* mutant strains was observed to be low (15 pg/mL and 24 pg/mL). The low levels of IL-1β secretion observed at 24 h could be attributed either to the fact that epithelial cells do not produce significant levels of IL-1β themselves (Bui et al., 2016; Thinwa et al., 2014), or because IL-1β can be damaging to the cell. Paradoxically, while IL-1β is essential for resistance to infections, it can nevertheless cause tissue damage (Dinarello, 2010). In view of these findings, it is plausible that the secretion of IL-1β from epithelial cells is tightly regulated in order to prevent damage to surrounding cells and tissues. Minimal IL-1β secretion

from epithelial cells in response to *C. albicans* at 24 h has been observed elsewhere (Schaller et al., 2004). Importantly, Schaller et al. showed that low IL-1β levels secreted (25 pg/mL) from epithelial cells combined with other cytokines (Interferon gamma, TNFα, IL-10, IL-6 and IL-8) were sufficient for neutrophil recruitment to the epithelium and for fungal clearance (Schaller et al., 2004). Like IL-1β, IL-6 is involved in the recruitment of neutrophils (Naglik et al., 2011) and has been shown to be secreted from TR146 oral epithelial cells in response to *C. albicans* and Candidalysin (Moyes et al., 2010; Moyes et al., 2016). It is, therefore, conceivable that the low levels of IL-1β secretion observed in response to Candidalysin and *C. albicans* may be sufficient to trigger neutrophil recruitment.

IL-18, like IL-1β, is a pro-inflammatory cytokine released during pyroptosis. Data obtained in this study demonstrates that oral epithelial cells respond to Candidalysin and *C. albicans ECE1* mutant strains by secreting substantial amounts of IL-18. While these observations corroborate previous studies that demonstrated secretion of IL-18 from oral epithelial cells infected with *C. albicans* (Rouabhia et al., 2002; Tardif et al., 2004a), the work presented here identifies Candidalysin as the fungal moiety that drives IL-18 secretion.

While the pattern of IL-1β and IL-18 secretion from epithelial cells was observed to be similar at 24 h, the pattern of IL-1β and IL-18 secretion observed at 6 h was clearly different (Figures 5-3 and 5-4). Expression of pro-IL-1β increased in response to Candidalysin and *C. albicans* strains able to express and release the toxin, whereas no increase in pro-IL-1β expression was observed following infection with *C. albicans* mutant strains unable to express and secrete Candidalysin. Expression of pro-IL-18 did not vary between untreated and treated oral epithelial cells. One possible explanation for this observation is that unlike pro-IL-1β, pro-IL-18 is constitutively present in oral epithelial cells ((Sugawara et al., 2001) and Fig 5-7) and in this regard, pro-IL-18 is similar to IL-1α and IL-33 (Moussion et al., 2008). However, like pro-IL-1β, pro-IL-18 is synthesised as an inactive precursor requiring processing by the inflammasome into a biologically active cytokine. Collectively, these observations suggest that the inflammasome might be activated in oral epithelial cells and mediates the release of pro-IL-1β and pro-IL-18 in response to Candidalysin treatment and *C. albicans* infection.

Data obtained in this study shows that TR146 oral epithelial cells respond to Candidalysin and *C. albicans* by expressing the NOD-like receptor NLRP3. These observations correlate with *in vivo* studies by others that demonstrated the importance of the NLRP3 receptor in mucosal and systemic infections caused by *C. albicans* (Hise et al., 2009; Joly et al., 2009; Tomalka et al., 2011). Importantly, the data presented here extend the findings of Hise, Joly and Tomalka by identifying a Candidalysin-dependent mechanism of NLRP3 expression. Expression of NLRP3 at 6 h was observed to increase in response to *C. albicans* strains able to express and secrete Candidalysin, whereas no increase in NLRP3 expression was observed in response to strains compromised for toxin production.

Interestingly, no expression of NLRP3 was observed in epithelial cells infected with *C. albicans ECE1* mutant strains at 24 h suggesting that NLRP3 may be degraded by other proteins late during the infection. Indeed, it has been reported that chronic TLR stimulation (12-24 h) by LPS dampens NLRP3 expression through IL-10 autocrine NLRP3 regulation in macrophages (Gurung et al., 2015). Another study showed that TLR2/TLR4 engagement resulted in upregulation of plasminogen activator inhibitor type 2 (PAI-2), which promoted autophagy and a subsequent reduction in NLRP3 expression (Chuang et al., 2013). Fungal cell wall components are known to interact with host TLRs, in particular TLR2 and TLR4 (Gow et al., 2011). Given that Candidalysin alone induced NLRP3 expression very clearly at 24 h, it is conceivable that longer term infections with *C. albicans* induces the activation of NLRP3 degradation mechanisms via fungal cell wall-host PRR interaction. Thus, the finding that NLRP3 expression is Candidalysin-dependent during early stages of infection (Figure 5-8) suggests that the NLRP3 inflammasome is first activated by the toxin, but then later other fungal-mediated mechanisms might promote NLRP3 degradation.

The adaptor protein ASC plays a central role in NLRP3 inflammasome assembly. The NLRP3 receptor does not contain a CARD domain, and so cannot directly interact with caspase-1. However, the pyrin domain of NLRP3 is capable of binding to the ASC adaptor protein, forming a heterodimeric complex, which in turn interacts directly with caspase-1 to form the NLRP3 inflammasome (Martinon et al., 2002). Expression of ASC was observed in vehicle, Candidalysin and *C. albicans ECE1* mutant-treated cells and no alteration in ASC expression was observed between treatment groups, suggesting that

ASC is constitutively expressed in TR146 oral epithelial cells to enable inflammasome assembly without the need for upregulation. Given this observation, ASC is presumed to be available to participate in inflammasome formation at 6 h and 24 h post-treatment with Candidalysin and *C. albicans ECE1* mutants.

The interaction of NLRP3 with ASC creates a protein complex into which caspase-1 is first recruited, and then subsequently activated through an autocatalytic mechanism (Martinon et al., 2002). Epithelial cells exposed to Candidalysin or *C. albicans ECE1* mutants exhibited baseline expression of pro-caspase-1, and only treatment with a high concentration of toxin (70 μM), or infection with *C. albicans* strains for 24 h prevented pro-caspase-1 expression in epithelial cells. A decrease in epithelial pro-caspase-1 expression in response to *C. albicans* 24 h infection has been observed elsewhere (Rouabhia et al., 2002). It is possible that during the course of a *C. albicans* infection where *ECE1* expression is robustly induced and maintained, Candidalysin reaches concentrations capable of causing significant cell stress (Chapter 3) which may subsequently activate mechanisms that degrade caspase-1. Nevertheless, neither Candidalysin nor *C. albicans* strains induced caspase-1 activity.

A previous study demonstrated that expression and secretion of IL-1β in response to *C. albicans* is dependent on the NLRP3 inflammasome (Hise et al., 2009). However, the essential role of the NLRP3 inflammasome and caspase-1 in particular against *C. albicans* infection is controversial. Indeed, another group reported that caspase-1 is not indispensable for the release of mature IL-1β in a systemic murine model of candidiasis (Mencacci et al., 2000), suggesting that release of active IL-1β during *C. albicans* infection can proceed through different mechanisms.

Data from this study collectively suggest that release of IL-1β and IL-18 from TR146 oral epithelial cells occurred through a caspase-1-independent mechanism. It is therefore conceivable that a non-canonical inflammasome (Kayagaki et al., 2011) might be activated in oral epithelial cells in response to Candidalysin and *C. albicans ECE1* mutants.

Activation of the canonical NLRP3 inflammasome leads to pro-IL-1β and pro-IL-18 processing and release of mature cytokines. In contrast, the non-canonical NLRP3 inflammasome is unable to cleave pro-IL-1β and pro-IL-18 (Kayagaki et al., 2011). Data

from this study show that IL-18 secreted from epithelial cells challenged with Candidalysin and *C. albicans ECE1* mutants was not proteolytically cleaved or activated. Only inactive IL-18 (24 kDa) was detected in the exhausted culture medium of treated cells. Although inactive, release of immature cytokines following cell death may not be biologically irrelevant. Indeed, several studies have demonstrated that inactive IL-1β and IL-18 can be processed by extracellular proteases produced from other cells *in vivo* (Beausejour et al., 1998; Joosten et al., 2009). For instance, proteinase 3 derived from infiltrating neutrophils drives the extracellular processing of IL-18 secreted from oral epithelial cells (Sugawara et al., 2001).

Previous work has shown that *C. albicans* strains able to secrete Candidalysin (BWP17 and *ECE1* reintegrant) caused neutrophil infiltration into infected tongue tissues. Contrarily, tongue tissue infected with *C. albicans* strains unable to secrete Candidalysin showed no inflammatory infiltrates (Moyes et al., 2016). It is thus conceivable that a non-canonical inflammasome is activated in epithelial cells in response to Candidalysin and *C. albicans* strains that stimulates secretion of pro-IL-1β and pro-IL-18, which are then subjected to extracellular processing by proteinase 3, neutrophil elastase and cathepsin G secreted from neutrophils recruited to the site of fungal infection (Afonina et al., 2015; Joosten et al., 2009).

In addition to inflammasome activation, cleavage of gasdermin D is required to trigger pyroptosis (Kayagaki et al., 2015; Shi et al., 2015). Cleavage of gasdermin D can be initiated by canonical and non-canonical inflammasomes, which release the gasdermin D N-terminal domain that associates and damages the host cell plasma membrane by forming pores (Liu et al., 2016). If affected cells are unable to repair the damage inflicted by pore formation, pyroptotic death is initiated as a means to control damage that could potentially induce long term deleterious consequences to cells and tissues if permitted to continue unchecked (Jorgensen et al., 2017).

Gasdermin D cleavage was not observed in epithelial cells exposed to Candidalysin or *C. albicans ECE1* mutant strains. Full-length (unprocessed) gasdermin D was expressed in vehicle-treated cells with no further change in expression following exposure to Candidalysin. However, epithelial cells infected for 24 h with *C. albicans ECE1* mutant strains able to secrete Candidalysin exhibited a decrease in the expression of full-length gasdermin D. It is therefore conceivable that infection of epithelial cells with *C. albicans*

induces the degradation of gasdermin D 24 h post-infection, although the mechanism underpinning this observation is currently unknown.

Interestingly, Candidalysin produced in the context of a fungal infection prevented expression of most proteins involved in necroptosis and pyroptosis pathways at 24 h. The expression and activation of proteins involved in regulated necrosis pathways may be detrimental to the fungus because they trigger pro-inflammatory responses facilitating fungal clearance. To avoid this, it is possible that long term *C. albicans* infections may prevent the activation of regulated necrosis pathways by inducing degradation mechanisms that have yet to be identified.

In summary, the work in this chapter suggests that Candidalysin does not induce classical necroptotic or pyroptotic cell death pathways in oral epithelial cells. However, Candidalysin appears to play an essential role in inducing the expression of NLRP3, IL-1β and IL-18, and the subsequent secretion of pro-IL-1β and pro-IL-18 from the epithelial cell, which may then be processed into their active forms by other host enzymes. Indeed, Candidalysin plays an essential role in neutrophil recruitment to the site of infection (Moyes et al., 2016). Thus, the Candidalysin-dependent release of immature cytokines from epithelial cells may occur in order to prevent overreaction of the immune response to *C. albicans*.

Chapter 6: General discussion

Candidiasis is the most prevalent fungal infection of humans, and is a frequent cause of morbidity in healthy individuals and mortality in patients with a wide spectrum of immune deficiencies (Fidel, 2006; Hasan et al., 2009). *C. albicans* has an asymptomatic carriage rate of approximately 60% in the human population and is the most pathogenic *Candida* species. The morphological plasticity of *C. albicans* is a major virulence trait, enabling the fungus to invade mucosal surfaces causing infection.

A key virulence factor of *C. albicans* hyphae is Candidalysin, a cytolytic peptide toxin derived from the hypha-associated gene *ECE1* (Moyes et al., 2016). Candidalysin causes epithelial damage and activates epithelial immunity, resulting in the production of immune modulators that recruit immune cells to the site of infection, which facilitate fungal clearance (Verma et al., 2017). Given this striking effect on epithelial cells, it is likely that detection of Candidalysin activity is the trigger for the host to determine when this normally commensal fungus has turned into a potentially dangerous pathogen.

This thesis investigated the hypothesis that Candidalysin triggers specific cellular responses that promote the death of oral epithelial cells. To characterise these events, the activation of epithelial cell stress and death pathways in response to Candidalysin was investigated.

6.1 Epithelial cell death responses to Candidalysin

Cell death can occur following periods of cell stress, injury and/or infection, and is linked to tissue damage and progression of disease. During oropharyngeal candidiasis, fungal invasion through the mucosal barrier and into underlying tissues is accompanied by damage and destruction of oral epithelial cells, which present as erosions and ulcerations of the buccal mucosa. Hypha-induced tissue damage causes localised discomfort, altered taste sensation, dysphagia and may also contribute to malnutrition, further impacting quality of life.

Microbial infection places cells under considerable stress and can induce signalling cascades that trigger apoptosis and necrosis. Sources of stress and stress signals, can be derived from the extracellular environment (damage, PAMPs and/or DAMPs), and from

intracellular sources (mitochondrial damage, oxidative stress and ATP/calcium fluctuations) (Fulda et al., 2010).

Since Candidalysin is a virulence factor that is essential for epithelial damage during mucosal infection by *C. albicans*, we hypothesised that Candidalysin may induce cell stress and cell death responses when applied to oral epithelial cells. Accordingly, the activation of Candidalysin peptide-dependent stress responses associated with cell death was investigated in TR146 oral epithelial cells.

Several oral epithelial cell lines have been used in the study of *C. albicans* infection and *C. albicans*-induced cell death, including FaDu pharyngeal cells (Park et al., 2005), OKF6/TERT-2 oral epithelial cells (Villar et al., 2012; Zhu et al., 2012) and SCC15 tongue cells (Villar and Zhao, 2010). The data presented in this study were derived from the TR146 oral epithelial cell line which can form stratified layers, thereby mimicking the human buccal mucosa (Rupniak et al., 1985). The TR146 cell line was used previously to characterise epithelial responses to Candidalysin (Moyes et al., 2016) and is representative of cells that are typically infected by *C. albicans* during oropharyngeal candidiasis.

During the course of characterising Candidalysin (Moyes et al., 2016), computational analysis of *C. albicans* Ece1p predicted that Kex2p-mediated proteolysis would result in the production of several peptide fragments, each terminating with a C-terminal lysine-arginine (KR) motif. Therefore, to characterise cell death responses to Candidalysin, epithelial cells were initially treated with a peptide composed of the following amino acid sequence; SIIGIIMGILGNIPQVIQIIMSIVKAFKGNKR (Ece1-III$_{62\text{-}93KR}$). However, subsequent mass spectroscopy analysis of Candidalysin secreted from the hyphae of *C. albicans* revealed that the toxin was in fact comprised of the following sequence; SIIGIIMGILGNIPQVIQIIMSIVKAFKGNK (Ece1-III$_{62\text{-}92K}$) (Moyes et al., 2016). Accordingly, work continued using this toxin sequence exclusively.

The present study demonstrates that oral epithelial cells respond to Candidalysin peptides by eliciting a range of cellular stress responses that are strongly associated with cell death. Cellular stress responses included membrane permeability, loss of mitochondrial fitness, generation of intracellular ROS, loss of intracellular ATP and calcium influx (Chapter 3).

Interestingly, differences were observed in some of the epithelial responses to Ece1-III$_{62-93KR}$ and Candidalysin sequences. While Ece1-III$_{62-93KR}$ was observed to be more damaging to epithelial cells, Candidalysin induced stronger intracellular toxicity. However, despite these intriguing observations, Candidalysin (Ece1-III$_{62-92K}$) but not Ece1-III$_{62-93KR}$ is secreted from the hyphae of infecting *C. albicans*, and is therefore the most physiologically relevant molecule in the context of fungal infection (Moyes et al., 2016).

An interesting question that arises from these observations is "why does *C. albicans* secrete a virulence factor that induces less cellular damage but more intracellular toxicity?" One possible explanation for these observations may lie in the general mechanism of mucosal infection caused by the fungus. Following adhesion of *C. albicans* yeast to the epithelial surface, the transcriptional machinery induces numerous genes required for the yeast-to-hypha morphological transition, and for expression of adhesins and secreted virulence factors, including Candidalysin. Once the morphological transition is activated, germ tubes are typically produced within 90 min, and continue to develop into hyphae, resulting in enhanced adhesion of the fungus to the mucosal surface. During these early stages of infection, it may not be advantageous to secrete a virulence factor that induces potent inflammatory and immune-stimulatory responses, as this may lead to a heightened host response to the infiltrating fungus, resulting in rapid clearance from the body.

Indeed, oral epithelial cells have evolved an exquisitely sensitive mechanism of morphological discrimination (Chapter 1, Figure 1-4), which is dependent upon hyphal burden/Candidalysin secretion. Accordingly, a toxin that elicits a less robust response may facilitate persistence during the early stages of infection, allowing the fungus to establish a niche from which a more severe infection can be initiated.

Epithelial cells respond to Candidalysin with potent intracellular alarm signals, which activate host defences against the infecting fungus. These responses are most likely a product of host pathogen co-evolution, and are thus likely to influence fungal pathogenicity and host defence strategies simultaneously.

This study has identified numerous Candidalysin-induced epithelial cell stress responses that contribute to cell death. Although this work was conducted entirely *in vitro* with an oral epithelial cell line, it nevertheless provides a robust and reproducible model for the

study of oral epithelial cell responses to Candidalysin. However, additional research should also be conducted using primary cells and organotypic models (and eventually animal models) to further confirm the importance of these experimental observations.

6.2 Epithelial apoptotic responses to Candidalysin

Given the multiple and detrimental effects of epithelial cellular stresses in response to Candidalysin and their impact on the induction of cell death pathways, I first investigated epithelial apoptotic responses to Candidalysin. Apoptosis contributes to several biological processes including maintenance of cellular homeostasis and morphogenesis, but can also occur in response to stress conditions such as damage or intracellular stress. The data presented in this study (Chapter 4) clearly demonstrate that oral epithelial cells do not undergo apoptosis in response to Candidalysin and *C. albicans*.

It is possible that epithelial cells may have evolved to induce particular forms of cell death other than apoptosis to promote specific biological outcomes in response to microbial insult. Apoptosis does not elicit pro-inflammatory responses, and thus the value of apoptotic death in response to microbial infection may be limited. Thus necrosis, which induces a robust pro-inflammatory response, may be a preferred form of cell death, as the pro-inflammatory molecules that are released from the infected cell will persist in the extracellular environment and continue to recruit immune cells to the site of infection following death of the infected cell.

6.3 Epithelial necrotic responses to Candidalysin

Given the essential role of Candidalysin in driving epithelial cell damage and stress responses, and having observed that epithelial cells treated with Candidalysin do not undergo apoptosis, I investigated the induction of regulated necrotic processes in response to Candidalysin. Necroptosis and pyroptosis are well-characterised forms of regulated necrosis and both are activated by microbes and pore-forming toxins to induce cell death (Fink et al., 2008; Gonzalez-Juarbe et al., 2017; Kitur et al., 2015), and reviewed in (Ashida et al., 2011). Thus, I investigated the activation of necroptotic and pyroptotic events in epithelial cells in response to Candidalysin.

6.3.1 Epithelial necroptotic responses to Candidalysin

Historically, cellular necrosis was considered to occur as a consequence of inflammation. More recently, however, the concept that cell death may precede or augment inflammatory responses has gained increasing attention. In this regard, necroptosis has been proposed to occur as a means of positively reinforcing the inflammatory response through the release of DAMPs from damaged or stressed cells (Kaczmarek et al., 2013). However, necroptosis may also influence inflammation through a number of alternative mechanisms including the disruption of epithelial plasma membranes and weakening of mucosal barrier function, which may trigger microbe-induced immune responses. The release of DAMPs has been suggested to enhance non-resolving inflammatory conditions and contribute to the pathogenesis of inflammatory conditions including Crohn's disease, ulcerative colitis and allergic colitis (Pierdomenico et al., 2014).

Necroptotic responses to *C. albicans* infection have yet to be characterised. However, previous studies have demonstrated the release of epithelial DAMPs (including IL-1α, S100A8 and S100A9) in response to *C. albicans* and Candidalysin (Moyes et al., 2010; Moyes et al., 2014; Moyes et al., 2016). Accordingly, I investigated Candidalysin-induced epithelial signalling events that are associated with the necroptotic pathway.

The data presented in this study demonstrates that epithelial cells do not respond to *C. albicans* or Candidalysin by activating the necroptosis pathway (Chapter 5), suggesting that the DAMPs that were observed to be released following *C. albicans* and Candidalysin treatment were released through an alternative necrotic pathway. Given these observations, I next investigated pyroptosis, an additional regulated necrotic cell death pathway that culminates in cell lysis and the release of immune modulators, including DAMPs.

6.3.2 Epithelial pyroptotic responses to Candidalysin

Similar to necroptosis, pyroptosis is also a pro-inflammatory regulated form of cell death. However, unlike necroptosis, pyroptosis is characterised by inflammasome activation. *C. albicans* activates the NLRP3 inflammasome, the non-canonical inflammasome and pyroptosis in macrophages. Importantly, the pyroptotic machinery is also expressed in epithelial cells (Liu and Lieberman, 2017; Nadatani et al., 2016), suggesting that pyroptotic responses may also occur at mucosal surfaces.

Inflammasome activation has been studied extensively in immune cells. Typically, activation of the inflammasome requires two signals that can be provided simultaneously (Juliana et al., 2012). The first of these activator signals is a priming event, in which stimuli-mediated receptor signalling and/or stimuli-mediated cellular stress drive the activation of the transcription factor NF-κB. The activation of NF-κB is critical for the transcription of both pro-IL-1β and NLRP3, as pro-IL-1β is not constitutively expressed and basal levels of NLRP3 are not sufficient for inflammasome formation (Bauernfeind et al., 2009). In contrast, transcriptional induction of ASC, pro-caspase-1 or pro-IL-18 is not required, as these factors are present in sufficient quantities for inflammasome assembly in steady-state cells (Bauernfeind et al., 2009).

The second activator signal is provided by agonists including exogenous ATP and pore-forming toxins, that trigger NLRP3 activation, assembly of the inflammasome complex, and activation of pro-caspase-1 (Nomura et al., 2015; Zha et al., 2016). Inflammasome activation results in IL-1β and IL-18 secretion, which trigger pro-inflammatory responses, and processing of gasdermin D, which causes plasma membrane damage and pyroptotic cell death (Liu et al., 2016).

Given that Candidalysin induces epithelial stress responses and damages epithelial plasma membranes (Chapter 3), I investigated whether Candidalysin was capable of simultaneously providing both of the activator signals required for inflammasome activation. This study reveals for the first time that Candidalysin is essential for inducing the expression of NLRP3 and pro-IL-1β in oral epithelial cells (Chapter 5, Figure 5-6 and Figure 5-8). However, notably, Candidalysin does not induce the processing of pro-IL-1β and pro-IL-18 into its active forms prior to secretion from the cell. Thus, Candidalysin appears to drive the secretion of pro-IL-1β and pro-IL-18 from epithelial cells.

Importantly, a key consequence of Candidalysin activity is the recruitment of neutrophils to the mucosal site of infection (Moyes et al., 2016; Richardson et al., 2017). Neutrophils secrete proteinase 3, elastase and cathepsin G, proteinases that can cleave pro-IL-1β and pro-IL-18 to produce active IL-1β and IL-18, which in turn trigger innate and adaptive Th17 and Th1 responses against *C. albicans* infection (Afonina et al., 2015; Joosten et al., 2009; Robertson et al., 2006). Therefore, it is plausible that secretion of Candidalysin from *C. albicans* hyphae induces the release of pro-IL-1β and pro-IL-18 from epithelial cells, which are then subsequently activated by secreted proteinases produced by

infiltrating neutrophils. This mechanism might be highly advantageous to the host, as secretion of inactive inflammatory mediators into the extracellular environment would avoid premature and unnecessary localised innate immune responses, which could result in destruction of the mucosal barrier and facilitate microbial invasion from the resident commensal flora. However, further studies are required to investigate how pro-IL-1β and pro-IL-18 are activated once secreted from epithelial cells.

The present study also demonstrates that, despite inducing NLRP3 expression, oral epithelial cells do not respond to Candidalysin or *C. albicans* by activating the inflammasome or gasdermin D processing (Chapter 5). These observations suggest that oral epithelial cells do not undergo classical pyroptosis in response to fungal challenge. Further studies of the epithelial response to Candidalysin should therefore focus on alternative pathways of regulated necrosis.

6.4 Conclusions

Recent research has advanced our understanding of the complex molecular events involved in the interaction between *C. albicans* and the oral mucosa. Epithelial cells are typically the first point of contact between host and pathogen, and are actively involved in orchestrating mucosal immunity by secreting antimicrobial, pro-inflammatory and immune-modulatory molecules that can recruit and activate immune cells. It is becoming increasingly clear that in addition to classical immune responses, the process of cell death contributes to host defence during infection. The aims of this project were to determine the role of Candidalysin in activating oral epithelial cell death responses by investigating classical hallmarks of cellular stress; and to investigate oral epithelial apoptotic, necrotic, necroptotic and pyroptotic responses to Candidalysin. This study demonstrates that oral epithelial cells respond to the secreted fungal toxin Candidalysin by inducing cell stress responses, which are intimately linked with cell death. Epithelial cells treated with Candidalysin were observed to undergo necrotic, but not apoptotic, necroptotic or pyroptotic death, and promoted inflammation through a mechanism involving necrosis-dependent pro-IL-1β and pro-IL-18 release. Unravelling the specific mechanism of epithelial necrosis in response to Candidalysin may ultimately result in

the development of new therapeutics to manipulate host signalling pathways to promote protection during *C. albicans* infections.

References

Afonina, I.S., Muller, C., Martin, S.J., and Beyaert, R. (2015). Proteolytic Processing of Interleukin-1 Family Cytokines: Variations on a Common Theme. Immunity *42*, 991-1004.

Alnemri, E.S., Fernandes-Alnemri, T., and Litwack, G. (1995). Cloning and expression of four novel isoforms of human interleukin-1 beta converting enzyme with different apoptotic activities. J Biol Chem *270*, 4312-4317.

Arendorf, T.M., Walker, D.M., Kingdom, R.J., Roll, J.R., and Newcombe, R.G. (1983). Tobacco smoking and denture wearing in oral candidal leukoplakia. Br Dent J *155*, 340-343.

Arnoult, D., Carneiro, L., Tattoli, I., and Girardin, S.E. (2009). The role of mitochondria in cellular defense against microbial infection. Semin Immunol *21*, 223-232.

Ashida, H., Mimuro, H., Ogawa, M., Kobayashi, T., Sanada, T., Kim, M., and Sasakawa, C. (2011). Cell death and infection: a double-edged sword for host and pathogen survival. J Cell Biol *195*, 931-942.

Ashkenazi, A., and Dixit, V.M. (1998). Death receptors: signaling and modulation. Science *281*, 1305-1308.

Backhed, F., and Hornef, M. (2003). Toll-like receptor 4-mediated signaling by epithelial surfaces: necessity or threat? Microbes Infect *5*, 951-959.

Bader, O., Krauke, Y., and Hube, B. (2008). Processing of predicted substrates of fungal Kex2 proteinases from *Candida albicans*, *C. glabrata*, *Saccharomyces cerevisiae* and *Pichia pastoris*. BMC Microbiol *8*, 116.

Bauernfeind, F.G., Horvath, G., Stutz, A., Alnemri, E.S., MacDonald, K., Speert, D., Fernandes-Alnemri, T., Wu, J., Monks, B.G., Fitzgerald, K.A.*, et al.* (2009). Cutting edge: NF-kappaB activating pattern recognition and cytokine receptors license NLRP3 inflammasome activation by regulating NLRP3 expression. J Immunol *183*, 787-791.

Beausejour, A., Grenier, D., Goulet, J.P., and Deslauriers, N. (1998). Proteolytic activation of the interleukin-1beta precursor by *Candida albicans*. Infect Immun *66*, 676-681.

Ben-Sasson, S.Z., Hu-Li, J., Quiel, J., Cauchetaux, S., Ratner, M., Shapira, I., Dinarello, C.A., and Paul, W.E. (2009). IL-1 acts directly on CD4 T cells to enhance their antigen-driven expansion and differentiation. Proc Natl Acad Sci U S A *106*, 7119-7124.

Berger, N.A. (1985). Poly(ADP-ribose) in the cellular response to DNA damage. Radiat Res *101*, 4-15.

Bergsbaken, T., Fink, S.L., and Cookson, B.T. (2009). Pyroptosis: host cell death and inflammation. Nat Rev Microbiol *7*, 99-109.

Berridge, M.J., Lipp, P., and Bootman, M.D. (2000). The versatility and universality of calcium signalling. Nat Rev Mol Cell Biol *1*, 11-21.

Bianchi, K., and Meier, P. (2009). A tangled web of ubiquitin chains: breaking news in TNF-R1 signaling. Mol Cell *36*, 736-742.

Birse, C.E., Irwin, M.Y., Fonzi, W.A., and Sypherd, P.S. (1993). Cloning and characterization of *ECE1*, a gene expressed in association with cell elongation of the dimorphic pathogen *Candida albicans*. Infect Immun *61*, 3648-3655.

Bischofberger, M., Iacovache, I., and van der Goot, F.G. (2012). Pathogenic pore-forming proteins: function and host response. Cell Host Microbe *12*, 266-275.

Bokor-Bratic, M., Cankovic, M., and Dragnic, N. (2013). Unstimulated whole salivary flow rate and anxiolytics intake are independently associated with oral *Candida* infection in patients with oral lichen planus. Eur J Oral Sci *121*, 427-433.

Boulares, A.H., Zoltoski, A.J., Yakovlev, A., Xu, M., and Smulson, M.E. (2001). Roles of DNA fragmentation factor and poly(ADP-ribose) polymerase in an amplification phase of tumor necrosis factor-induced apoptosis. J Biol Chem *276*, 38185-38192.

Brand, M.D., Affourtit, C., Esteves, T.C., Green, K., Lambert, A.J., Miwa, S., Pakay, J.L., and Parker, N. (2004). Mitochondrial superoxide: production, biological effects, and activation of uncoupling proteins. Free Radic Biol Med *37*, 755-767.

Bratton, D.L., Fadok, V.A., Richter, D.A., Kailey, J.M., Guthrie, L.A., and Henson, P.M. (1997). Appearance of phosphatidylserine on apoptotic cells requires calcium-mediated nonspecific flip-flop and is enhanced by loss of the aminophospholipid translocase. J Biol Chem *272*, 26159-26165.

Bromuro, C., Romano, M., Chiani, P., Berti, F., Tontini, M., Proietti, D., Mori, E., Torosantucci, A., Costantino, P., Rappuoli, R*., et al.* (2010). Beta-glucan-CRM197 conjugates as candidates antifungal vaccines. Vaccine *28*, 2615-2623.

Brown, G.D., Denning, D.W., Gow, N.A., Levitz, S.M., Netea, M.G., and White, T.C. (2012). Hidden killers: human fungal infections. Sci Transl Med *4*, 165rv113.

Brown, G.D., and Gordon, S. (2001). Immune recognition. A new receptor for beta-glucans. Nature *413*, 36-37.

Broz, P., and Monack, D.M. (2013). Newly described pattern recognition receptors team up against intracellular pathogens. Nat Rev Immunol *13*, 551-565.

Brune, B. (2005). The intimate relation between nitric oxide and superoxide in apoptosis and cell survival. Antioxid Redox Signal *7*, 497-507.

Buffo, J., Herman, M.A., and Soll, D.R. (1984). A characterization of pH-regulated dimorphism in *Candida albicans*. Mycopathologia *85*, 21-30.

Bui, F.Q., Johnson, L., Roberts, J., Hung, S.C., Lee, J., Atanasova, K.R., Huang, P.R., Yilmaz, O., and Ojcius, D.M. (2016). Fusobacterium nucleatum infection of gingival epithelial cells leads to NLRP3 inflammasome-dependent secretion of IL-1beta and the danger signals ASC and HMGB1. Cell Microbiol *18*, 970-981.

Cai, Z., Jitkaew, S., Zhao, J., Chiang, H.C., Choksi, S., Liu, J., Ward, Y., Wu, L.G., and Liu, Z.G. (2014). Plasma membrane translocation of trimerized MLKL protein is required for TNF-induced necroptosis. Nat Cell Biol *16*, 55-65.

Cambi, A., Gijzen, K., de Vries l, J., Torensma, R., Joosten, B., Adema, G.J., Netea, M.G., Kullberg, B.J., Romani, L., and Figdor, C.G. (2003). The C-type lectin DC-SIGN (CD209) is an antigen-uptake receptor for *Candida albicans* on dendritic cells. Eur J Immunol *33*, 532-538.

Carafoli, E. (2002). Calcium signaling: a tale for all seasons. Proc Natl Acad Sci U S A *99*, 1115-1122.

Casadevall, A., and Pirofski, L.A. (2014). Microbiology: Ditch the term pathogen. Nature *516*, 165-166.

Chahoud, J., Kanafani, Z.A., and Kanj, S.S. (2013). Management of candidaemia and invasive candidiasis in critically ill patients. Int J Antimicrob Agents *42 Suppl*, S29-35.

Chan, F.K., Shisler, J., Bixby, J.G., Felices, M., Zheng, L., Appel, M., Orenstein, J., Moss, B., and Lenardo, M.J. (2003). A role for tumor necrosis factor receptor-2 and receptor-interacting protein in programmed necrosis and antiviral responses. J Biol Chem *278*, 51613-51621.

Chen, J.J., Bertrand, H., and Yu, B.P. (1995). Inhibition of adenine nucleotide translocator by lipid peroxidation products. Free Radic Biol Med *19*, 583-590.

Chen, X., Li, W., Ren, J., Huang, D., He, W.T., Song, Y., Yang, C., Li, W., Zheng, X., Chen, P.*, et al.* (2014). Translocation of mixed lineage kinase domain-like protein to plasma membrane leads to necrotic cell death. Cell Res *24*, 105-121.

Cheng, S.C., Joosten, L.A., Kullberg, B.J., and Netea, M.G. (2012). Interplay between *Candida albicans* and the mammalian innate host defense. Infect Immun *80*, 1304-1313.

Chiang, L.Y., Sheppard, D.C., Bruno, V.M., Mitchell, A.P., Edwards, J.E., Jr., and Filler, S.G. (2007). *Candida albicans* protein kinase CK2 governs virulence during oropharyngeal candidiasis. Cell Microbiol *9*, 233-245.

Chinnaiyan, A.M. (1999). The apoptosome: heart and soul of the cell death machine. Neoplasia *1*, 5-15.

Cho, Y.S., Challa, S., Moquin, D., Genga, R., Ray, T.D., Guildford, M., and Chan, F.K. (2009). Phosphorylation-driven assembly of the RIP1-RIP3 complex regulates programmed necrosis and virus-induced inflammation. Cell *137*, 1112-1123.

Chuang, S.Y., Yang, C.H., Chou, C.C., Chiang, Y.P., Chuang, T.H., and Hsu, L.C. (2013). TLR-induced PAI-2 expression suppresses IL-1beta processing via increasing autophagy and NLRP3 degradation. Proc Natl Acad Sci U S A *110*, 16079-16084.

Chumbler, N.M., Farrow, M.A., Lapierre, L.A., Franklin, J.L., Haslam, D.B., Goldenring, J.R., and Lacy, D.B. (2012). *Clostridium difficile* Toxin B causes epithelial cell necrosis through an autoprocessing-independent mechanism. PLoS Pathog *8*, e1003072.

Clapham, D.E. (2007). Calcium signaling. Cell *131*, 1047-1058.

Colina, A.R., Aumont, F., Deslauriers, N., Belhumeur, P., and de Repentigny, L. (1996). Evidence for degradation of gastrointestinal mucin by *Candida albicans* secretory aspartyl proteinase. Infect Immun *64*, 4514-4519.

Conti, H.R., Shen, F., Nayyar, N., Stocum, E., Sun, J.N., Lindemann, M.J., Ho, A.W., Hai, J.H., Yu, J.J., Jung, J.W.*, et al.* (2009). Th17 cells and IL-17 receptor signaling are essential for mucosal host defense against oral candidiasis. J Exp Med *206*, 299-311.

Contreras, L., Drago, I., Zampese, E., and Pozzan, T. (2010). Mitochondria: the calcium connection. Biochim Biophys Acta *1797*, 607-618.

Cookson, B.T., and Brennan, M.A. (2001). Pro-inflammatory programmed cell death. Trends Microbiol *9*, 113-114.

Correia, A., Lermann, U., Teixeira, L., Cerca, F., Botelho, S., da Costa, R.M., Sampaio, P., Gartner, F., Morschhauser, J., Vilanova, M.*, et al.* (2010). Limited role of secreted aspartyl proteinases Sap1 to Sap6 in *Candida albicans* virulence and host immune response in murine hematogenously disseminated candidiasis. Infect Immun *78*, 4839-4849.

Cory, S., and Adams, J.M. (2002). The Bcl2 family: regulators of the cellular life-or-death switch. Nat Rev Cancer *2*, 647-656.

Csank, C., Schroppel, K., Leberer, E., Harcus, D., Mohamed, O., Meloche, S., Thomas, D.Y., and Whiteway, M. (1998). Roles of the *Candida albicans* mitogen-activated protein kinase homolog, Cek1p, in hyphal development and systemic candidiasis. Infect Immun *66*, 2713-2721.

da Silva Dantas, A., Lee, K.K., Raziunaite, I., Schaefer, K., Wagener, J., Yadav, B., and Gow, N.A. (2016). Cell biology of *Candida albicans*-host interactions. Curr Opin Microbiol *34*, 111-118.

Dalle, F., Wachtler, B., L'Ollivier, C., Holland, G., Bannert, N., Wilson, D., Labruere, C., Bonnin, A., and Hube, B. (2010). Cellular interactions of *Candida albicans* with human oral epithelial cells and enterocytes. Cell Microbiol *12*, 248-271.

Dantas Ada, S., Day, A., Ikeh, M., Kos, I., Achan, B., and Quinn, J. (2015). Oxidative stress responses in the human fungal pathogen, *Candida albicans*. Biomolecules *5*, 142-165.

De Bernardis, F., Amacker, M., Arancia, S., Sandini, S., Gremion, C., Zurbriggen, R., Moser, C., and Cassone, A. (2012). A virosomal vaccine against candidal vaginitis: immunogenicity, efficacy and safety profile in animal models. Vaccine *30*, 4490-4498.

De Luca, A., Zelante, T., D'Angelo, C., Zagarella, S., Fallarino, F., Spreca, A., Iannitti, R.G., Bonifazi, P., Renauld, J.C., Bistoni, F.*, et al.* (2010). IL-22 defines a novel immune pathway of antifungal resistance. Mucosal Immunol *3*, 361-373.

Degterev, A., Huang, Z., Boyce, M., Li, Y., Jagtap, P., Mizushima, N., Cuny, G.D., Mitchison, T.J., Moskowitz, M.A., and Yuan, J. (2005). Chemical inhibitor of nonapoptotic cell death with therapeutic potential for ischemic brain injury. Nat Chem Biol *1*, 112-119.

Dethlefsen, L., McFall-Ngai, M., and Relman, D.A. (2007). An ecological and evolutionary perspective on human-microbe mutualism and disease. Nature *449*, 811-818.

Dias, A.P., and Samaranayake, L.P. (1995). Clinical, microbiological and ultrastructural features of angular cheilitis lesions in Southern Chinese. Oral Dis *1*, 43-48.

Dickens, L.S., Powley, I.R., Hughes, M.A., and MacFarlane, M. (2012). The 'complexities' of life and death: death receptor signalling platforms. Exp Cell Res *318*, 1269-1277.

Dinarello, C.A. (1996). Biologic basis for interleukin-1 in disease. Blood *87*, 2095-2147.

Dinarello, C.A. (2010). Anti-inflammatory Agents: Present and Future. Cell *140*, 935-950.

Dinarello, C.A., Novick, D., Kim, S., and Kaplanski, G. (2013). Interleukin-18 and IL-18 binding protein. Front Immunol *4*, 289.

Dondelinger, Y., Declercq, W., Montessuit, S., Roelandt, R., Goncalves, A., Bruggeman, I., Hulpiau, P., Weber, K., Sehon, C.A., Marquis, R.W.*, et al.* (2014). MLKL compromises plasma membrane integrity by binding to phosphatidylinositol phosphates. Cell Rep *7*, 971-981.

Drago, L., Mombelli, B., De Vecchi, E., Bonaccorso, C., Fassina, M.C., and Gismondo, M.R. (2000). *Candida albicans* cellular internalization: a new pathogenic factor? Int J Antimicrob Agents *16*, 545-547.

Dunai, Z.A., Imre, G., Barna, G., Korcsmaros, T., Petak, I., Bauer, P.I., and Mihalik, R. (2012). Staurosporine induces necroptotic cell death under caspase-compromised conditions in U937 cells. PLoS One *7*, e41945.

Eggimann, P., and Pittet, D. (2014). *Candida* colonization index and subsequent infection in critically ill surgical patients: 20 years later. Intensive Care Med *40*, 1429-1448.

Eguchi, Y., Shimizu, S., and Tsujimoto, Y. (1997). Intracellular ATP levels determine cell death fate by apoptosis or necrosis. Cancer Res *57*, 1835-1840.

Elliott, M.R., and Ravichandran, K.S. (2010). Clearance of apoptotic cells: implications in health and disease. J Cell Biol *189*, 1059-1070.

Elmore, S. (2007). Apoptosis: a review of programmed cell death. Toxicol Pathol *35*, 495-516.

Enache, E., Eskandari, T., Borja, L., Wadsworth, E., Hoxter, B., and Calderone, R. (1996). *Candida albicans* adherence to a human oesophageal cell line. Microbiology *142 (Pt 10)*, 2741-2746.

Enari, M., Sakahira, H., Yokoyama, H., Okawa, K., Iwamatsu, A., and Nagata, S. (1998). A caspase-activated DNase that degrades DNA during apoptosis, and its inhibitor ICAD. Nature *391*, 43-50.

Eyerich, K., Eyerich, S., Hiller, J., Behrendt, H., and Traidl-Hoffmann, C. (2010). Chronic mucocutaneous candidiasis, from bench to bedside. Eur J Dermatol *20*, 260-265.

Ezekowitz, R.A., Sastry, K., Bailly, P., and Warner, A. (1990). Molecular characterization of the human macrophage mannose receptor: demonstration of multiple carbohydrate recognition-like domains and phagocytosis of yeasts in Cos-1 cells. J Exp Med *172*, 1785-1794.

Fadeel, B., and Xue, D. (2009). The ins and outs of phospholipid asymmetry in the plasma membrane: roles in health and disease. Crit Rev Biochem Mol Biol *44*, 264-277.

Fadok, V.A., de Cathelineau, A., Daleke, D.L., Henson, P.M., and Bratton, D.L. (2001). Loss of phospholipid asymmetry and surface exposure of phosphatidylserine is required for phagocytosis of apoptotic cells by macrophages and fibroblasts. J Biol Chem *276*, 1071-1077.

Fadok, V.A., Voelker, D.R., Campbell, P.A., Cohen, J.J., Bratton, D.L., and Henson, P.M. (1992). Exposure of phosphatidylserine on the surface of apoptotic lymphocytes triggers specific recognition and removal by macrophages. J Immunol *148*, 2207-2216.

Fan, T., Lu, H., Hu, H., Shi, L., McClarty, G.A., Nance, D.M., Greenberg, A.H., and Zhong, G. (1998). Inhibition of apoptosis in chlamydia-infected cells: blockade of mitochondrial cytochrome c release and caspase activation. J Exp Med *187*, 487-496.

Fantuzzi, G., and Dinarello, C.A. (1999). Interleukin-18 and interleukin-1 beta: two cytokine substrates for ICE (caspase-1). J Clin Immunol *19*, 1-11.

Feng, S., Yang, Y., Mei, Y., Ma, L., Zhu, D.E., Hoti, N., Castanares, M., and Wu, M. (2007). Cleavage of RIP3 inactivates its caspase-independent apoptosis pathway by removal of kinase domain. Cell Signal *19*, 2056-2067.

Feoktistova, M., Geserick, P., Panayotova-Dimitrova, D., and Leverkus, M. (2012). Pick your poison: the Ripoptosome, a cell death platform regulating apoptosis and necroptosis. Cell Cycle *11*, 460-467.

Ferrer, J. (2000). Vaginal candidosis: epidemiological and etiological factors. Int J Gynaecol Obstet *71 Suppl 1*, S21-27.

Festjens, N., Vanden Berghe, T., and Vandenabeele, P. (2006). Necrosis, a well-orchestrated form of cell demise: signalling cascades, important mediators and concomitant immune response. Biochim Biophys Acta *1757*, 1371-1387.

Fidel, P.L., Jr. (2006). Candida-host interactions in HIV disease: relationships in oropharyngeal candidiasis. Adv Dent Res *19*, 80-84.

Fink, S.L., Bergsbaken, T., and Cookson, B.T. (2008). *Anthrax* lethal toxin and *Salmonella* elicit the common cell death pathway of caspase-1-dependent pyroptosis via distinct mechanisms. Proc Natl Acad Sci U S A *105*, 4312-4317.

Fu, Y., Luo, G., Spellberg, B.J., Edwards, J.E., Jr., and Ibrahim, A.S. (2008). Gene overexpression/suppression analysis of candidate virulence factors of *Candida albicans*. Eukaryot Cell *7*, 483-492.

Fulda, S., Gorman, A.M., Hori, O., and Samali, A. (2010). Cellular stress responses: cell survival and cell death. Int J Cell Biol *2010*, 214074.

Gabrielli, E., Pericolini, E., Luciano, E., Sabbatini, S., Roselletti, E., Perito, S., Kasper, L., Hube, B., and Vecchiarelli, A. (2015). Induction of caspase-11 by aspartyl proteinases of *Candida albicans* and implication in promoting inflammatory response. Infect Immun *83*, 1940-1948.

Gacser, A., Stehr, F., Kroger, C., Kredics, L., Schafer, W., and Nosanchuk, J.D. (2007). Lipase 8 affects the pathogenesis of *Candida albicans*. Infect Immun *75*, 4710-4718.

Gasparoto, T.H., Gaziri, L.C., Burger, E., de Almeida, R.S., and Felipe, I. (2004). Apoptosis of phagocytic cells induced by *Candida albicans* and production of IL-10. FEMS Immunol Med Microbiol *42*, 219-224.

Genestra, M. (2007). Oxyl radicals, redox-sensitive signalling cascades and antioxidants. Cell Signal *19*, 1807-1819.

Geserick, P., Hupe, M., Moulin, M., Wong, W.W., Feoktistova, M., Kellert, B., Gollnick, H., Silke, J., and Leverkus, M. (2009). Cellular IAPs inhibit a cryptic CD95-induced cell death by limiting RIP1 kinase recruitment. J Cell Biol *187*, 1037-1054.

Ghannoum, M.A. (2000). Potential role of phospholipases in virulence and fungal pathogenesis. Clin Microbiol Rev *13*, 122-143, table of contents.

Gillum, A.M., Tsay, E.Y., and Kirsch, D.R. (1984). Isolation of the *Candida albicans* gene for orotidine-5'-phosphate decarboxylase by complementation of *S. cerevisiae* ura3 and *E. coli* pyrF mutations. Mol Gen Genet *198*, 179-182.

Gobeil, S., Boucher, C.C., Nadeau, D., and Poirier, G.G. (2001). Characterization of the necrotic cleavage of poly(ADP-ribose) polymerase (PARP-1): implication of lysosomal proteases. Cell Death Differ *8*, 588-594.

Gonzalez-Juarbe, N., Bradley, K.M., Shenoy, A.T., Gilley, R.P., Reyes, L.F., Hinojosa, C.A., Restrepo, M.I., Dube, P.H., Bergman, M.A., and Orihuela, C.J. (2017). Pore-forming toxin-mediated ion dysregulation leads to death receptor-independent necroptosis of lung epithelial cells during bacterial pneumonia. Cell Death Differ *24*, 917-928.

Gorlach, A., Bertram, K., Hudecova, S., and Krizanova, O. (2015). Calcium and ROS: A mutual interplay. Redox Biol *6*, 260-271.

Gow, N.A., van de Veerdonk, F.L., Brown, A.J., and Netea, M.G. (2011). *Candida albicans* morphogenesis and host defence: discriminating invasion from colonization. Nat Rev Microbiol *10*, 112-122.

Granger, B.L., Flenniken, M.L., Davis, D.A., Mitchell, A.P., and Cutler, J.E. (2005). Yeast wall protein 1 of *Candida albicans*. Microbiology *151*, 1631-1644.

Gross, O., Poeck, H., Bscheider, M., Dostert, C., Hannesschlager, N., Endres, S., Hartmann, G., Tardivel, A., Schweighoffer, E., Tybulewicz, V.*, et al.* (2009). Syk kinase signalling couples to the Nlrp3 inflammasome for anti-fungal host defence. Nature *459*, 433-436.

Guo, C., Sun, L., Chen, X., and Zhang, D. (2013). Oxidative stress, mitochondrial damage and neurodegenerative diseases. Neural Regen Res *8*, 2003-2014.

Gurung, P., Li, B., Subbarao Malireddi, R.K., Lamkanfi, M., Geiger, T.L., and Kanneganti, T.D. (2015). Chronic TLR Stimulation Controls NLRP3 Inflammasome Activation through IL-10 Mediated Regulation of NLRP3 Expression and Caspase-8 Activation. Sci Rep *5*, 14488.

Gyrd-Hansen, M., and Meier, P. (2010). IAPs: from caspase inhibitors to modulators of NF-kappaB, inflammation and cancer. Nat Rev Cancer *10*, 561-574.

Haas, T.L., Emmerich, C.H., Gerlach, B., Schmukle, A.C., Cordier, S.M., Rieser, E., Feltham, R., Vince, J., Warnken, U., Wenger, T.*, et al.* (2009). Recruitment of the linear ubiquitin chain assembly complex stabilizes the TNF-R1 signaling complex and is required for TNF-mediated gene induction. Mol Cell *36*, 831-844.

Hagar, J.A., Powell, D.A., Aachoui, Y., Ernst, R.K., and Miao, E.A. (2013). Cytoplasmic LPS activates caspase-11: implications in TLR4-independent endotoxic shock. Science *341*, 1250-1253.

Hampton, M.B., and Orrenius, S. (1997). Dual regulation of caspase activity by hydrogen peroxide: implications for apoptosis. FEBS Lett *414*, 552-556.

Hasan, F., Xess, I., Wang, X., Jain, N., and Fries, B.C. (2009). Biofilm formation in clinical *Candida* isolates and its association with virulence. Microbes Infect *11*, 753-761.

Heeman, B., Van den Haute, C., Aelvoet, S.A., Valsecchi, F., Rodenburg, R.J., Reumers, V., Debyser, Z., Callewaert, G., Koopman, W.J., Willems, P.H.*, et al.* (2011). Depletion of *PINK1* affects mitochondrial metabolism, calcium homeostasis and energy maintenance. J Cell Sci *124*, 1115-1125.

Hernandez-Santos, N., Huppler, A.R., Peterson, A.C., Khader, S.A., McKenna, K.C., and Gaffen, S.L. (2013). Th17 cells confer long-term adaptive immunity to oral mucosal *Candida albicans* infections. Mucosal Immunol *6*, 900-910.

Hibino, K., Samaranayake, L.P., Hagg, U., Wong, R.W., and Lee, W. (2009). The role of salivary factors in persistent oral carriage of *Candida* in humans. Arch Oral Biol *54*, 678-683.

Hill, M.M., Adrain, C., Duriez, P.J., Creagh, E.M., and Martin, S.J. (2004). Analysis of the composition, assembly kinetics and activity of native Apaf-1 apoptosomes. EMBO J *23*, 2134-2145.

Hirsiger, S., Simmen, H.P., Werner, C.M., Wanner, G.A., and Rittirsch, D. (2012). Danger signals activating the immune response after trauma. Mediators Inflamm *2012*, 315941.

Hirst, R.A., Yesilkaya, H., Clitheroe, E., Rutman, A., Dufty, N., Mitchell, T.J., O'Callaghan, C., and Andrew, P.W. (2002). Sensitivities of human monocytes and epithelial cells to pneumolysin are different. Infect Immun *70*, 1017-1022.

Hise, A.G., Tomalka, J., Ganesan, S., Patel, K., Hall, B.A., Brown, G.D., and Fitzgerald, K.A. (2009). An essential role for the NLRP3 inflammasome in host defense against the human fungal pathogen *Candida albicans*. Cell Host Microbe *5*, 487-497.

Holler, N., Zaru, R., Micheau, O., Thome, M., Attinger, A., Valitutti, S., Bodmer, J.L., Schneider, P., Seed, B., and Tschopp, J. (2000). Fas triggers an alternative, caspase-8-independent cell death pathway using the kinase RIP as effector molecule. Nat Immunol *1*, 489-495.

Hotchkiss, R.S., Strasser, A., McDunn, J.E., and Swanson, P.E. (2009). Cell death. N Engl J Med *361*, 1570-1583.

Hoyer, L.L. (2001). The ALS gene family of *Candida albicans*. Trends Microbiol *9*, 176-180.

Huang, W., Na, L., Fidel, P.L., and Schwarzenberger, P. (2004). Requirement of interleukin-17A for systemic anti-*Candida albicans* host defense in mice. J Infect Dis *190*, 624-631.

Hube, B., Stehr, F., Bossenz, M., Mazur, A., Kretschmar, M., and Schafer, W. (2000). Secreted lipases of *Candida albicans*: cloning, characterisation and expression analysis of a new gene family with at least ten members. Arch Microbiol *174*, 362-374.

Ibata-Ombetta, S., Idziorek, T., Trinel, P.A., Poulain, D., and Jouault, T. (2003). *Candida albicans* phospholipomannan promotes survival of phagocytosed yeasts through modulation of bad phosphorylation and macrophage apoptosis. J Biol Chem *278*, 13086-13093.

Ibrahim, A.S., Spellberg, B.J., Avanesian, V., Fu, Y., and Edwards, J.E., Jr. (2006). The anti-*Candida* vaccine based on the recombinant N-terminal domain of Als1p is broadly active against disseminated candidiasis. Infect Immun *74*, 3039-3041.

Imre, G., Larisch, S., and Rajalingam, K. (2011). Ripoptosome: a novel IAP-regulated cell death-signalling platform. J Mol Cell Biol *3*, 324-326.

Janicke, R.U., Sprengart, M.L., Wati, M.R., and Porter, A.G. (1998). Caspase-3 is required for DNA fragmentation and morphological changes associated with apoptosis. J Biol Chem *273*, 9357-9360.

Jiang, J.H., Tong, J., and Gabriel, K. (2012). Hijacking mitochondria: bacterial toxins that modulate mitochondrial function. IUBMB Life *64*, 397-401.

Jiang, X., and Wang, X. (2000). Cytochrome c promotes caspase-9 activation by inducing nucleotide binding to Apaf-1. J Biol Chem *275*, 31199-31203.

Jimenez-Lopez, C., and Lorenz, M.C. (2013). Fungal immune evasion in a model host-pathogen interaction: *Candida albicans* versus macrophages. PLoS Pathog *9*, e1003741.

Jimenez-Lucho, V., Ginsburg, V., and Krivan, H.C. (1990). *Cryptococcus neoformans*, *Candida albicans*, and other fungi bind specifically to the glycosphingolipid lactosylceramide (Gal beta 1-4Glc beta 1-1Cer), a possible adhesion receptor for yeasts. Infect Immun *58*, 2085-2090.

Joly, S., Ma, N., Sadler, J.J., Soll, D.R., Cassel, S.L., and Sutterwala, F.S. (2009). Cutting edge: *Candida albicans* hyphae formation triggers activation of the Nlrp3 inflammasome. J Immunol *183*, 3578-3581.

Joly, S., and Sutterwala, F.S. (2010). Fungal pathogen recognition by the NLRP3 inflammasome. Virulence *1*, 276-280.

Joosten, L.A., Netea, M.G., Fantuzzi, G., Koenders, M.I., Helsen, M.M., Sparrer, H., Pham, C.T., van der Meer, J.W., Dinarello, C.A., and van den Berg, W.B. (2009). Inflammatory arthritis in caspase 1 gene-deficient mice: contribution of proteinase 3 to caspase 1-independent production of bioactive interleukin-1beta. Arthritis Rheum *60*, 3651-3662.

Jorgensen, I., Rayamajhi, M., and Miao, E.A. (2017). Programmed cell death as a defence against infection. Nat Rev Immunol *17*, 151-164.

Jouault, T., El Abed-El Behi, M., Martinez-Esparza, M., Breuilh, L., Trinel, P.A., Chamaillard, M., Trottein, F., and Poulain, D. (2006). Specific recognition of *Candida albicans* by macrophages requires galectin-3 to discriminate *Saccharomyces cerevisiae* and needs association with TLR2 for signaling. J Immunol *177*, 4679-4687.

Jouault, T., Ibata-Ombetta, S., Takeuchi, O., Trinel, P.A., Sacchetti, P., Lefebvre, P., Akira, S., and Poulain, D. (2003). *Candida albicans* phospholipomannan is sensed through toll-like receptors. J Infect Dis *188*, 165-172.

Juliana, C., Fernandes-Alnemri, T., Kang, S., Farias, A., Qin, F., and Alnemri, E.S. (2012). Non-transcriptional priming and deubiquitination regulate NLRP3 inflammasome activation. J Biol Chem *287*, 36617-36622.

Kabir, J., Lobo, M., and Zachary, I. (2002). Staurosporine induces endothelial cell apoptosis via focal adhesion kinase dephosphorylation and focal adhesion disassembly independent of focal adhesion kinase proteolysis. Biochem J *367*, 145-155.

Kaczmarek, A., Vandenabeele, P., and Krysko, D.V. (2013). Necroptosis: the release of damage-associated molecular patterns and its physiological relevance. Immunity *38*, 209-223.

Kaiser, W.J., Sridharan, H., Huang, C., Mandal, P., Upton, J.W., Gough, P.J., Sehon, C.A., Marquis, R.W., Bertin, J., and Mocarski, E.S. (2013). Toll-like receptor 3-mediated necrosis via TRIF, RIP3, and MLKL. J Biol Chem *288*, 31268-31279.

Kamai, Y., Kubota, M., Kamai, Y., Hosokawa, T., Fukuoka, T., and Filler, S.G. (2001). New model of oropharyngeal candidiasis in mice. Antimicrob Agents Chemother *45*, 3195-3197.

Kamai, Y., Kubota, M., Kamai, Y., Hosokawa, T., Fukuoka, T., and Filler, S.G. (2002). Contribution of *Candida albicans* ALS1 to the pathogenesis of experimental oropharyngeal candidiasis. Infect Immun *70*, 5256-5258.

Kaufmann, S.H., Desnoyers, S., Ottaviano, Y., Davidson, N.E., and Poirier, G.G. (1993). Specific proteolytic cleavage of poly(ADP-ribose) polymerase: an early marker of chemotherapy-induced apoptosis. Cancer Res *53*, 3976-3985.

Kayagaki, N., Stowe, I.B., Lee, B.L., O'Rourke, K., Anderson, K., Warming, S., Cuellar, T., Haley, B., Roose-Girma, M., Phung, Q.T.*, et al.* (2015). Caspase-11 cleaves gasdermin D for non-canonical inflammasome signalling. Nature *526*, 666-671.

Kayagaki, N., Warming, S., Lamkanfi, M., Vande Walle, L., Louie, S., Dong, J., Newton, K., Qu, Y., Liu, J., Heldens, S.*, et al.* (2011). Non-canonical inflammasome activation targets caspase-11. Nature *479*, 117-121.

Kayagaki, N., Wong, M.T., Stowe, I.B., Ramani, S.R., Gonzalez, L.C., Akashi-Takamura, S., Miyake, K., Zhang, J., Lee, W.P., Muszynski, A.*, et al.* (2013). Noncanonical inflammasome activation by intracellular LPS independent of TLR4. Science *341*, 1246-1249.

Khelef, N., Zychlinsky, A., and Guiso, N. (1993). *Bordetella pertussis* induces apoptosis in macrophages: role of adenylate cyclase-hemolysin. Infect Immun *61*, 4064-4071.

Kim, J.M., Lee, J.Y., and Kim, Y.J. (2008). Inhibition of apoptosis in *Bacteroides fragilis* enterotoxin-stimulated intestinal epithelial cells through the induction of c-IAP-2. Eur J Immunol *38*, 2190-2199.

Kim, J.S., He, L., and Lemasters, J.J. (2003). Mitochondrial permeability transition: a common pathway to necrosis and apoptosis. Biochem Biophys Res Commun *304*, 463-470.

Kischkel, F.C., Hellbardt, S., Behrmann, I., Germer, M., Pawlita, M., Krammer, P.H., and Peter, M.E. (1995). Cytotoxicity-dependent APO-1 (Fas/CD95)-associated proteins form a death-inducing signaling complex (DISC) with the receptor. EMBO J *14*, 5579-5588.

Kitur, K., Parker, D., Nieto, P., Ahn, D.S., Cohen, T.S., Chung, S., Wachtel, S., Bueno, S., and Prince, A. (2015). Toxin-induced necroptosis is a major mechanism of *Staphylococcus aureus* lung damage. PLoS Pathog *11*, e1004820.

Knodler, L.A., Crowley, S.M., Sham, H.P., Yang, H., Wrande, M., Ma, C., Ernst, R.K., Steele-Mortimer, O., Celli, J., and Vallance, B.A. (2014). Noncanonical inflammasome activation of caspase-4/caspase-11 mediates epithelial defenses against enteric bacterial pathogens. Cell Host Microbe *16*, 249-256.

Kwon, C.H., Wheeldon, I., Kachouie, N.N., Lee, S.H., Bae, H., Sant, S., Fukuda, J., Kang, J.W., and Khademhosseini, A. (2011). Drug-eluting microarrays for cell-based screening of chemical-induced apoptosis. Anal Chem *83*, 4118-4125.

Labbe, K., and Saleh, M. (2008). Cell death in the host response to infection. Cell Death Differ *15*, 1339-1349.

Lamkanfi, M., and Dixit, V.M. (2010). Manipulation of host cell death pathways during microbial infections. Cell Host Microbe *8*, 44-54.

Lei-Leston, A.C., Murphy, A.G., and Maloy, K.J. (2017). Epithelial Cell Inflammasomes in Intestinal Immunity and Inflammation. Front Immunol *8*, 1168.

Leibovitz, E., Iuster-Reicher, A., Amitai, M., and Mogilner, B. (1992). Systemic candidal infections associated with use of peripheral venous catheters in neonates: a 9-year experience. Clin Infect Dis *14*, 485-491.

Lermann, U., and Morschhauser, J. (2008). Secreted aspartic proteases are not required for invasion of reconstituted human epithelia by Candida albicans. Microbiology *154*, 3281-3295.

Lewis, L.E., Bain, J.M., Lowes, C., Gillespie, C., Rudkin, F.M., Gow, N.A., and Erwig, L.P. (2012). Stage specific assessment of *Candida albicans* phagocytosis by macrophages identifies cell wall composition and morphogenesis as key determinants. PLoS Pathog *8*, e1002578.

Li, F., and Palecek, S.P. (2003). *EAP1*, a *Candida albicans* gene involved in binding human epithelial cells. Eukaryot Cell *2*, 1266-1273.

Li, F., and Palecek, S.P. (2008). Distinct domains of the *Candida albicans* adhesin Eap1p mediate cell-cell and cell-substrate interactions. Microbiology *154*, 1193-1203.

Li, J., McQuade, T., Siemer, A.B., Napetschnig, J., Moriwaki, K., Hsiao, Y.S., Damko, E., Moquin, D., Walz, T., McDermott, A.*, et al.* (2012). The RIP1/RIP3 necrosome forms a functional amyloid signaling complex required for programmed necrosis. Cell *150*, 339-350.

Lin, L., Ibrahim, A.S., Xu, X., Farber, J.M., Avanesian, V., Baquir, B., Fu, Y., French, S.W., Edwards, J.E., Jr., and Spellberg, B. (2009). Th1-Th17 cells mediate protective adaptive immunity against *Staphylococcus aureus* and *Candida albicans* infection in mice. PLoS Pathog *5*, e1000703.

Lin, Y., Devin, A., Rodriguez, Y., and Liu, Z.G. (1999). Cleavage of the death domain kinase RIP by caspase-8 prompts TNF-induced apoptosis. Genes Dev *13*, 2514-2526.

Linden, S.K., Sutton, P., Karlsson, N.G., Korolik, V., and McGuckin, M.A. (2008). Mucins in the mucosal barrier to infection. Mucosal Immunol *1*, 183-197.

Liu, H., Kohler, J., and Fink, G.R. (1994). Suppression of hyphal formation in *Candida albicans* by mutation of a *STE12* homolog. Science *266*, 1723-1726.

Liu, X., and Lieberman, J. (2017). A Mechanistic Understanding of Pyroptosis: The Fiery Death Triggered by Invasive Infection. Adv Immunol *135*, 81-117.

Liu, X., Zhang, Z., Ruan, J., Pan, Y., Magupalli, V.G., Wu, H., and Lieberman, J. (2016). Inflammasome-activated gasdermin D causes pyroptosis by forming membrane pores. Nature *535*, 153-158.

Liu, Y., Shetty, A.C., Schwartz, J.A., Bradford, L.L., Xu, W., Phan, Q.T., Kumari, P., Mahurkar, A., Mitchell, A.P., Ravel, J.*, et al.* (2015). New signaling pathways govern the host response to *C. albicans* infection in various niches. Genome Res *25*, 679-689.

Lo, H.J., Kohler, J.R., DiDomenico, B., Loebenberg, D., Cacciapuoti, A., and Fink, G.R. (1997). Nonfilamentous *C. albicans* mutants are avirulent. Cell *90*, 939-949.

Locksley, R.M., Killeen, N., and Lenardo, M.J. (2001). The TNF and TNF receptor superfamilies: integrating mammalian biology. Cell *104*, 487-501.

Los, F.C., Randis, T.M., Aroian, R.V., and Ratner, A.J. (2013). Role of pore-forming toxins in bacterial infectious diseases. Microbiol Mol Biol Rev *77*, 173-207.

Luo, G., Ibrahim, A.S., Spellberg, B., Nobile, C.J., Mitchell, A.P., and Fu, Y. (2010). *Candida albicans* Hyr1p confers resistance to neutrophil killing and is a potential vaccine target. J Infect Dis *201*, 1718-1728.

Luo, X., Budihardjo, I., Zou, H., Slaughter, C., and Wang, X. (1998). Bid, a Bcl2 interacting protein, mediates cytochrome c release from mitochondria in response to activation of cell surface death receptors. Cell *94*, 481-490.

Magalhaes, J.G., Tattoli, I., and Girardin, S.E. (2007). The intestinal epithelial barrier: how to distinguish between the microbial flora and pathogens. Semin Immunol *19*, 106-115.

Mardon, D., Balish, E., and Phillips, A.W. (1969). Control of dimorphism in a biochemical variant of *Candida albicans*. J Bacteriol *100*, 701-707.

Martinon, F., Burns, K., and Tschopp, J. (2002). The inflammasome: a molecular platform triggering activation of inflammatory caspases and processing of proIL-beta. Mol Cell *10*, 417-426.

McGreal, E.P., Rosas, M., Brown, G.D., Zamze, S., Wong, S.Y., Gordon, S., Martinez-Pomares, L., and Taylor, P.R. (2006). The carbohydrate-recognition domain of Dectin-2 is a C-type lectin with specificity for high mannose. Glycobiology *16*, 422-430.

Mencacci, A., Bacci, A., Cenci, E., Montagnoli, C., Fiorucci, S., Casagrande, A., Flavell, R.A., Bistoni, F., and Romani, L. (2000). Interleukin 18 restores defective Th1 immunity to *Candida albicans* in caspase 1-deficient mice. Infect Immun *68*, 5126-5131.

Miyazato, A., Nakamura, K., Yamamoto, N., Mora-Montes, H.M., Tanaka, M., Abe, Y., Tanno, D., Inden, K., Gang, X., Ishii, K.*, et al.* (2009). Toll-like receptor 9-dependent activation of myeloid dendritic cells by Deoxynucleic acids from *Candida albicans*. Infect Immun *77*, 3056-3064.

Mogensen, T.H. (2009). Pathogen recognition and inflammatory signaling in innate immune defenses. Clin Microbiol Rev *22*, 240-273, Table of Contents.

Moreno-Ruiz, E., Galan-Diez, M., Zhu, W., Fernandez-Ruiz, E., d'Enfert, C., Filler, S.G., Cossart, P., and Veiga, E. (2009). *Candida albicans* internalization by host cells is mediated by a clathrin-dependent mechanism. Cell Microbiol *11*, 1179-1189.

Morimoto, H., and Bonavida, B. (1992). *Diphtheria* toxin- and *Pseudomonas* A toxin-mediated apoptosis. ADP ribosylation of elongation factor-2 is required for DNA fragmentation and cell lysis and synergy with tumor necrosis factor-alpha. J Immunol *149*, 2089-2094.

Moriwaki, K., and Chan, F.K. (2013). RIP3: a molecular switch for necrosis and inflammation. Genes Dev *27*, 1640-1649.

Moriwaki, K., and Chan, F.K. (2014). Necrosis-dependent and independent signaling of the RIP kinases in inflammation. Cytokine Growth Factor Rev *25*, 167-174.

Moussion, C., Ortega, N., and Girard, J.P. (2008). The IL-1-like cytokine IL-33 is constitutively expressed in the nucleus of endothelial cells and epithelial cells in vivo: a novel 'alarmin'? PLoS One *3*, e3331.

Moyes, D.L., Richardson, J.P., and Naglik, J.R. (2015). *Candida albicans*-epithelial interactions and pathogenicity mechanisms: scratching the surface. Virulence *6*, 338-346.

Moyes, D.L., Runglall, M., Murciano, C., Shen, C., Nayar, D., Thavaraj, S., Kohli, A., Islam, A., Mora-Montes, H., Challacombe, S.J*., et al.* (2010). A biphasic innate immune MAPK response discriminates between the yeast and hyphal forms of *Candida albicans* in epithelial cells. Cell Host Microbe *8*, 225-235.

Moyes, D.L., Shen, C., Murciano, C., Runglall, M., Richardson, J.P., Arno, M., Aldecoa-Otalora, E., and Naglik, J.R. (2014). Protection against epithelial damage during *Candida albicans* infection is mediated by PI3K/Akt and mammalian target of rapamycin signaling. J Infect Dis *209*, 1816-1826.

Moyes, D.L., Wilson, D., Richardson, J.P., Mogavero, S., Tang, S.X., Wernecke, J., Hofs, S., Gratacap, R.L., Robbins, J., Runglall, M*., et al.* (2016). Candidalysin is a fungal peptide toxin critical for mucosal infection. Nature *532*, 64-68.

Muller, V., Viemann, D., Schmidt, M., Endres, N., Ludwig, S., Leverkus, M., Roth, J., and Goebeler, M. (2007). *Candida albicans* triggers activation of distinct signaling pathways to establish a proinflammatory gene expression program in primary human endothelial cells. J Immunol *179*, 8435-8445.

Murphy, J.M., Czabotar, P.E., Hildebrand, J.M., Lucet, I.S., Zhang, J.G., Alvarez-Diaz, S., Lewis, R., Lalaoui, N., Metcalf, D., Webb, A.I*., et al.* (2013). The pseudokinase MLKL mediates necroptosis via a molecular switch mechanism. Immunity *39*, 443-453.

Nadatani, Y., Huo, X., Zhang, X., Yu, C., Cheng, E., Zhang, Q., Dunbar, K.B., Theiss, A., Pham, T.H., Wang, D.H*., et al.* (2016). NOD-Like Receptor Protein 3 Inflammasome Priming and Activation in Barrett's Epithelial Cells. Cell Mol Gastroenterol Hepatol *2*, 439-453.

Naglik, J.R., Challacombe, S.J., and Hube, B. (2003). *Candida albicans* secreted aspartyl proteinases in virulence and pathogenesis. Microbiol Mol Biol Rev *67*, 400-428, table of contents.

Naglik, J.R., Konig, A., Hube, B., and Gaffen, S.L. (2017). *Candida albicans*-epithelial interactions and induction of mucosal innate immunity. Curr Opin Microbiol *40*, 104-112.

Naglik, J.R., and Moyes, D. (2011). Epithelial cell innate response to *Candida albicans*. Adv Dent Res *23*, 50-55.

Naglik, J.R., Moyes, D., Makwana, J., Kanzaria, P., Tsichlaki, E., Weindl, G., Tappuni, A.R., Rodgers, C.A., Woodman, A.J., Challacombe, S.J*., et al.* (2008). Quantitative expression of the *Candida albicans* secreted aspartyl proteinase gene family in human oral and vaginal candidiasis. Microbiology *154*, 3266-3280.

Naglik, J.R., Moyes, D.L., Wachtler, B., and Hube, B. (2011). *Candida albicans* interactions with epithelial cells and mucosal immunity. Microbes Infect *13*, 963-976.

Nakamura-Lopez, Y., Sarmiento-Silva, R.E., Moran-Andrade, J., and Gomez-Garcia, B. (2009). Staurosporine-induced apoptosis in P388D1 macrophages involves both extrinsic and intrinsic pathways. Cell Biol Int *33*, 1026-1031.

Netea, M.G., Brown, G.D., Kullberg, B.J., and Gow, N.A. (2008). An integrated model of the recognition of *Candida albicans* by the innate immune system. Nat Rev Microbiol *6*, 67-78.

Netea, M.G., Gow, N.A., Munro, C.A., Bates, S., Collins, C., Ferwerda, G., Hobson, R.P., Bertram, G., Hughes, H.B., Jansen, T.*, et al.* (2006). Immune sensing of *Candida albicans* requires cooperative recognition of mannans and glucans by lectin and Toll-like receptors. J Clin Invest *116*, 1642-1650.

Nomura, J., So, A., Tamura, M., and Busso, N. (2015). Intracellular ATP Decrease Mediates NLRP3 Inflammasome Activation upon Nigericin and Crystal Stimulation. J Immunol *195*, 5718-5724.

Nudel, K., Massari, P., and Genco, C.A. (2015). *Neisseria gonorrhoeae* Modulates Cell Death in Human Endocervical Epithelial Cells through Export of Exosome-Associated cIAP2. Infect Immun *83*, 3410-3417.

O'Meara, T.R., Veri, A.O., Ketela, T., Jiang, B., Roemer, T., and Cowen, L.E. (2015). Global analysis of fungal morphology exposes mechanisms of host cell escape. Nat Commun *6*, 6741.

Odds, F.C. (1988). *Candida* and Candidosis. Philadelphia, Bailliere Tindall.

Odds, F.C., Brown, A.J., and Gow, N.A. (2003). Antifungal agents: mechanisms of action. Trends Microbiol *11*, 272-279.

Orrenius, S., Gogvadze, V., and Zhivotovsky, B. (2007). Mitochondrial oxidative stress: implications for cell death. Annu Rev Pharmacol Toxicol *47*, 143-183.

Orrenius, S., Zhivotovsky, B., and Nicotera, P. (2003). Regulation of cell death: the calcium-apoptosis link. Nat Rev Mol Cell Biol *4*, 552-565.

Ostrosky-Zeichner, L., Casadevall, A., Galgiani, J.N., Odds, F.C., and Rex, J.H. (2010). An insight into the antifungal pipeline: selected new molecules and beyond. Nat Rev Drug Discov *9*, 719-727.

Ott, M., Robertson, J.D., Gogvadze, V., Zhivotovsky, B., and Orrenius, S. (2002). Cytochrome c release from mitochondria proceeds by a two-step process. Proc Natl Acad Sci U S A *99*, 1259-1263.

Park, H., Myers, C.L., Sheppard, D.C., Phan, Q.T., Sanchez, A.A., J, E.E., and Filler, S.G. (2005). Role of the fungal Ras-protein kinase A pathway in governing epithelial cell interactions during oropharyngeal candidiasis. Cell Microbiol *7*, 499-510.

Pasparakis, M., and Vandenabeele, P. (2015). Necroptosis and its role in inflammation. Nature *517*, 311-320.

Pfaller, M.A., Diekema, D.J., Procop, G.W., and Rinaldi, M.G. (2007). Multicenter comparison of the VITEK 2 antifungal susceptibility test with the CLSI broth microdilution reference method for testing amphotericin B, flucytosine, and voriconazole against *Candida* spp. J Clin Microbiol *45*, 3522-3528.

Phan, Q.T., Myers, C.L., Fu, Y., Sheppard, D.C., Yeaman, M.R., Welch, W.H., Ibrahim, A.S., Edwards, J.E., Jr., and Filler, S.G. (2007). Als3 is a *Candida albicans* invasin that binds to cadherins and induces endocytosis by host cells. PLoS Biol *5*, e64.

Pierdomenico, M., Negroni, A., Stronati, L., Vitali, R., Prete, E., Bertin, J., Gough, P.J., Aloi, M., and Cucchiara, S. (2014). Necroptosis is active in children with inflammatory bowel disease and contributes to heighten intestinal inflammation. Am J Gastroenterol *109*, 279-287.

Pietrella, D., Pandey, N., Gabrielli, E., Pericolini, E., Perito, S., Kasper, L., Bistoni, F., Cassone, A., Hube, B., and Vecchiarelli, A. (2013). Secreted aspartic proteases of *Candida albicans* activate the NLRP3 inflammasome. Eur J Immunol *43*, 679-692.

Puel, A., Cypowyj, S., Bustamante, J., Wright, J.F., Liu, L., Lim, H.K., Migaud, M., Israel, L., Chrabieh, M., Audry, M*., et al.* (2011). Chronic mucocutaneous candidiasis in humans with inborn errors of interleukin-17 immunity. Science *332*, 65-68.

Rahal, A., Kumar, A., Singh, V., Yadav, B., Tiwari, R., Chakraborty, S., and Dhama, K. (2014). Oxidative stress, prooxidants, and antioxidants: the interplay. Biomed Res Int *2014*, 761264.

Raska, M., Belakova, J., Wudattu, N.K., Kafkova, L., Ruzickova, K., Sebestova, M., Kolar, Z., and Weigl, E. (2005). Comparison of protective effect of protein and DNA vaccines hsp90 in murine model of systemic candidiasis. Folia Microbiol (Praha) *50*, 77-82.

Rath, P.C., and Aggarwal, B.B. (1999). TNF-induced signaling in apoptosis. J Clin Immunol *19*, 350-364.

Reales-Calderon, J.A., Sylvester, M., Strijbis, K., Jensen, O.N., Nombela, C., Molero, G., and Gil, C. (2013). *Candida albicans* induces pro-inflammatory and anti-apoptotic signals in macrophages as revealed by quantitative proteomics and phosphoproteomics. J Proteomics *91*, 106-135.

Reichart, P.A., Samaranayake, L.P., and Philipsen, H.P. (2000). Pathology and clinical correlates in oral candidiasis and its variants: a review. Oral Dis *6*, 85-91.

Renz, A., Berdel, W.E., Kreuter, M., Belka, C., Schulze-Osthoff, K., and Los, M. (2001). Rapid extracellular release of cytochrome c is specific for apoptosis and marks cell death in vivo. Blood *98*, 1542-1548.

Richardson, J.P., Willems, H.M.E., Moyes, D.L., Shoaie, S., Barker, K.S., Tan, S.L., Palmer, G.E., Hube, B., Naglik, J.R., and Peters, B.M. (2017). Candidalysin drives epithelial signaling, neutrophil recruitment, and immunopathology at the vaginal mucosa. Infect Immun.

Robertson, S.E., Young, J.D., Kitson, S., Pitt, A., Evans, J., Roes, J., Karaoglu, D., Santora, L., Ghayur, T., Liew, F.Y.*, et al.* (2006). Expression and alternative processing of IL-18 in human neutrophils. Eur J Immunol *36*, 722-731.

Rogers, N.C., Slack, E.C., Edwards, A.D., Nolte, M.A., Schulz, O., Schweighoffer, E., Williams, D.L., Gordon, S., Tybulewicz, V.L., Brown, G.D.*, et al.* (2005). Syk-dependent cytokine induction by Dectin-1 reveals a novel pattern recognition pathway for C type lectins. Immunity *22*, 507-517.

Romero, M., Keyel, M., Shi, G., Bhattacharjee, P., Roth, R., Heuser, J.E., and Keyel, P.A. (2017). Intrinsic repair protects cells from pore-forming toxins by microvesicle shedding. Cell Death Differ *24*, 798-808.

Rotstein, D., Parodo, J., Taneja, R., and Marshall, J.C. (2000). Phagocytosis of *Candida albicans* induces apoptosis of human neutrophils. Shock *14*, 278-283.

Rouabhia, M., Ross, G., Page, N., and Chakir, J. (2002). Interleukin-18 and gamma interferon production by oral epithelial cells in response to exposure to *Candida albicans* or lipopolysaccharide stimulation. Infect Immun *70*, 7073-7080.

Rovin, B.H., Wurst, E., and Kohan, D.E. (1990). Production of reactive oxygen species by tubular epithelial cells in culture. Kidney Int *37*, 1509-1514.

Ruchel, R., Ritter, B., and Schaffrinski, M. (1990). Modulation of experimental systemic murine candidosis by intravenous pepstatin. Zentralbl Bakteriol *273*, 391-403.

Ruiz Gaitan, A.C., Moret, A., Lopez Hontangas, J.L., Molina, J.M., Aleixandre Lopez, A.I., Cabezas, A.H., Mollar Maseres, J., Arcas, R.C., Gomez Ruiz, M.D., Chiveli, M.A.*, et al.* (2017). Nosocomial fungemia by *Candida auris*: First four reported cases in continental Europe. Rev Iberoam Micol *34*, 23-27.

Rupniak, H.T., Rowlatt, C., Lane, E.B., Steele, J.G., Trejdosiewicz, L.K., Laskiewicz, B., Povey, S., and Hill, B.T. (1985). Characteristics of four new human cell lines derived from squamous cell carcinomas of the head and neck. J Natl Cancer Inst *75*, 621-635.

Saelens, X., Festjens, N., Vande Walle, L., van Gurp, M., van Loo, G., and Vandenabeele, P. (2004). Toxic proteins released from mitochondria in cell death. Oncogene *23*, 2861-2874.

Sakahira, H., Enari, M., and Nagata, S. (1998). Cleavage of CAD inhibitor in CAD activation and DNA degradation during apoptosis. Nature *391*, 96-99.

Samali, A., Nordgren, H., Zhivotovsky, B., Peterson, E., and Orrenius, S. (1999). A comparative study of apoptosis and necrosis in HepG2 cells: oxidant-induced caspase inactivation leads to necrosis. Biochem Biophys Res Commun *255*, 6-11.

Sandin, R.L., Rogers, A.L., Patterson, R.J., and Beneke, E.S. (1982). Evidence for mannose-mediated adherence of *Candida albicans* to human buccal cells in vitro. Infect Immun *35*, 79-85.

Sanglard, D. (2016). Emerging Threats in Antifungal-Resistant Fungal Pathogens. Front Med (Lausanne) *3*, 11.

Sardi, J.C., Scorzoni, L., Bernardi, T., Fusco-Almeida, A.M., and Mendes Giannini, M.J. (2013). *Candida* species: current epidemiology, pathogenicity, biofilm formation, natural antifungal products and new therapeutic options. J Med Microbiol *62*, 10-24.

Sato, K., Yang, X.L., Yudate, T., Chung, J.S., Wu, J., Luby-Phelps, K., Kimberly, R.P., Underhill, D., Cruz, P.D., Jr., and Ariizumi, K. (2006). Dectin-2 is a pattern recognition receptor for fungi that couples with the Fc receptor gamma chain to induce innate immune responses. J Biol Chem *281*, 38854-38866.

Saville, S.P., Lazzell, A.L., Chaturvedi, A.K., Monteagudo, C., and Lopez-Ribot, J.L. (2008). Use of a genetically engineered strain to evaluate the pathogenic potential of yeast cell and filamentous forms during *Candida albicans* systemic infection in immunodeficient mice. Infect Immun *76*, 97-102.

Saville, S.P., Lazzell, A.L., Chaturvedi, A.K., Monteagudo, C., and Lopez-Ribot, J.L. (2009). Efficacy of a genetically engineered *Candida albicans* tet-NRG1 strain as an experimental live attenuated vaccine against hematogenously disseminated candidiasis. Clin Vaccine Immunol *16*, 430-432.

Schaller, M., Boeld, U., Oberbauer, S., Hamm, G., Hube, B., and Korting, H.C. (2004). Polymorphonuclear leukocytes (PMNs) induce protective Th1-type cytokine epithelial responses in an in vitro model of oral candidosis. Microbiology *150*, 2807-2813.

Schaller, M., Korting, H.C., Schafer, W., Bastert, J., Chen, W., and Hube, B. (1999). Secreted aspartic proteinase (Sap) activity contributes to tissue damage in a model of human oral candidosis. Mol Microbiol *34*, 169-180.

Scheper, M.A., Shirtliff, M.E., Meiller, T.F., Peters, B.M., and Jabra-Rizk, M.A. (2008). Farnesol, a fungal quorum-sensing molecule triggers apoptosis in human oral squamous carcinoma cells. Neoplasia *10*, 954-963.

Schmidt, C.S., White, C.J., Ibrahim, A.S., Filler, S.G., Fu, Y., Yeaman, M.R., Edwards, J.E., Jr., and Hennessey, J.P., Jr. (2012). NDV-3, a recombinant alum-adjuvanted vaccine for *Candida* and *Staphylococcus aureus*, is safe and immunogenic in healthy adults. Vaccine *30*, 7594-7600.

Sganga, G., Bianco, G., Frongillo, F., Lirosi, M.C., Nure, E., and Agnes, S. (2014). Fungal infections after liver transplantation: incidence and outcome. Transplant Proc *46*, 2314-2318.

Shaykhiev, R., Behr, J., and Bals, R. (2008). Microbial patterns signaling via Toll-like receptors 2 and 5 contribute to epithelial repair, growth and survival. PLoS One *3*, e1393.

Shi, J., Zhao, Y., Wang, K., Shi, X., Wang, Y., Huang, H., Zhuang, Y., Cai, T., Wang, F., and Shao, F. (2015). Cleavage of GSDMD by inflammatory caspases determines pyroptotic cell death. Nature *526*, 660-665.

Silke, J., and Meier, P. (2013). Inhibitor of apoptosis (IAP) proteins-modulators of cell death and inflammation. Cold Spring Harb Perspect Biol *5*.

Simonetti, N., Strippoli, V., and Cassone, A. (1974). Yeast-mycelial conversion induced by N-acetyl-D-glucosamine in *Candida albicans*. Nature *250*, 344-346.

Singleton, D.R., Fidel, P.L., Jr., Wozniak, K.L., and Hazen, K.C. (2005). Contribution of cell surface hydrophobicity protein 1 (Csh1p) to virulence of hydrophobic *Candida albicans* serotype A cells. FEMS Microbiol Lett *244*, 373-377.

Slee, E.A., Adrain, C., and Martin, S.J. (2001). Executioner caspase-3, -6, and -7 perform distinct, non-redundant roles during the demolition phase of apoptosis. J Biol Chem *276*, 7320-7326.

Sobel, J.D. (2007). Vulvovaginal candidosis. Lancet *369*, 1961-1971.

Sokol-Anderson, M.L., Brajtburg, J., and Medoff, G. (1986). Amphotericin B-induced oxidative damage and killing of *Candida albicans*. J Infect Dis *154*, 76-83.

Solis, N.V., Swidergall, M., Bruno, V.M., Gaffen, S.L., and Filler, S.G. (2017). The Aryl Hydrocarbon Receptor Governs Epithelial Cell Invasion during Oropharyngeal Candidiasis. MBio *8*.

Soll, D.R., Herman, M.A., and Staebell, M.A. (1985). The involvement of cell wall expansion in the two modes of mycelium formation of *Candida albicans*. J Gen Microbiol *131*, 2367-2375.

Soloviev, D.A., Fonzi, W.A., Sentandreu, R., Pluskota, E., Forsyth, C.B., Yadav, S., and Plow, E.F. (2007). Identification of pH-regulated antigen 1 released from *Candida albicans* as the major ligand for leukocyte integrin alphaMbeta2. J Immunol *178*, 2038-2046.

Staab, J.F., Bahn, Y.S., Tai, C.H., Cook, P.F., and Sundstrom, P. (2004). Expression of transglutaminase substrate activity on *Candida albicans* germ tubes through a coiled, disulfide-bonded N-terminal domain of Hwp1 requires C-terminal glycosylphosphatidylinositol modification. J Biol Chem *279*, 40737-40747.

Staab, J.F., Bradway, S.D., Fidel, P.L., and Sundstrom, P. (1999). Adhesive and mammalian transglutaminase substrate properties of *Candida albicans* Hwp1. Science *283*, 1535-1538.

Steele, C., and Fidel, P.L., Jr. (2002). Cytokine and chemokine production by human oral and vaginal epithelial cells in response to *Candida albicans*. Infect Immun *70*, 577-583.

Stennicke, H.R., and Salvesen, G.S. (2000). Caspases - controlling intracellular signals by protease zymogen activation. Biochim Biophys Acta *1477*, 299-306.

Stoldt, V.R., Sonneborn, A., Leuker, C.E., and Ernst, J.F. (1997). Efg1p, an essential regulator of morphogenesis of the human pathogen *Candida albicans*, is a member of a conserved class of bHLH proteins regulating morphogenetic processes in fungi. EMBO J *16*, 1982-1991.

Su, Z., Yang, Z., Xie, L., DeWitt, J.P., and Chen, Y. (2016). Cancer therapy in the necroptosis era. Cell Death Differ *23*, 748-756.

Sudbery, P.E. (2001). The germ tubes of *Candida albicans* hyphae and pseudohyphae show different patterns of septin ring localization. Mol Microbiol *41*, 19-31.

Sudbery, P.E. (2011). Growth of *Candida albicans* hyphae. Nat Rev Microbiol *9*, 737-748.

Sugawara, S., Uehara, A., Nochi, T., Yamaguchi, T., Ueda, H., Sugiyama, A., Hanzawa, K., Kumagai, K., Okamura, H., and Takada, H. (2001). Neutrophil proteinase 3-mediated induction of bioactive IL-18 secretion by human oral epithelial cells. J Immunol *167*, 6568-6575.

Sun, J.N., Solis, N.V., Phan, Q.T., Bajwa, J.S., Kashleva, H., Thompson, A., Liu, Y., Dongari-Bagtzoglou, A., Edgerton, M., and Filler, S.G. (2010). Host cell invasion and virulence mediated by *Candida albicans* Ssa1. PLoS Pathog *6*, e1001181.

Sun, L., Wang, H., Wang, Z., He, S., Chen, S., Liao, D., Wang, L., Yan, J., Liu, W., Lei, X.*, et al.* (2012). Mixed lineage kinase domain-like protein mediates necrosis signaling downstream of RIP3 kinase. Cell *148*, 213-227.

Sun, X., Yin, J., Starovasnik, M.A., Fairbrother, W.J., and Dixit, V.M. (2002). Identification of a novel homotypic interaction motif required for the phosphorylation of receptor-interacting protein (RIP) by RIP3. J Biol Chem *277*, 9505-9511.

Sundstrom, P., Balish, E., and Allen, C.M. (2002). Essential role of the *Candida albicans* transglutaminase substrate, hyphal wall protein 1, in lethal oroesophageal candidiasis in immunodeficient mice. J Infect Dis *185*, 521-530.

Swidergall, M., Solis, N.V., Lionakis, M.S., and Filler, S.G. (2017). EphA2 is an epithelial cell pattern recognition receptor for fungal beta-glucans. Nat Microbiol.

Tada, H., Nemoto, E., Shimauchi, H., Watanabe, T., Mikami, T., Matsumoto, T., Ohno, N., Tamura, H., Shibata, K., Akashi, S.*, et al.* (2002). *Saccharomyces cerevisiae*- and *Candida albicans*-derived mannan induced production of tumor necrosis factor alpha by human monocytes in a CD14- and Toll-like receptor 4-dependent manner. Microbiol Immunol *46*, 503-512.

Tamura, Y., Chiba, Y., Tanioka, T., Shimizu, N., Shinozaki, S., Yamada, M., Kaneki, K., Mori, S., Araki, A., Ito, H.*, et al.* (2011). NO donor induces Nec-1-inhibitable, but RIP1-independent, necrotic cell death in pancreatic beta-cells. FEBS Lett *585*, 3058-3064.

Tang, S.X., Moyes, D.L., Richardson, J.P., Blagojevic, M., and Naglik, J.R. (2016). Epithelial discrimination of commensal and pathogenic *Candida albicans*. Oral Dis *22 Suppl 1*, 114-119.

Tardif, F., Goulet, J.P., Zakrazewski, A., Chauvin, P., and Rouabhia, M. (2004a). Involvement of interleukin-18 in the inflammatory response against oropharyngeal candidiasis. Med Sci Monit *10*, BR239-249.

Tardif, F., Ross, G., and Rouabhia, M. (2004b). Gingival and dermal fibroblasts produce interleukin-1 beta converting enzyme and interleukin-1 beta but not interleukin-18 even after stimulation with lipopolysaccharide. J Cell Physiol *198*, 125-132.

Taschdjian, C.L., Burchall, J.J., and Kozinn, P.J. (1960). Rapid identification of *Candida albicans* by filamentation on serum and serum substitutes. AMA J Dis Child *99*, 212-215.

Taylor, P.R., Tsoni, S.V., Willment, J.A., Dennehy, K.M., Rosas, M., Findon, H., Haynes, K., Steele, C., Botto, M., Gordon, S.*, et al.* (2007). Dectin-1 is required for beta-glucan recognition and control of fungal infection. Nat Immunol *8*, 31-38.

Taylor, R.C., Cullen, S.P., and Martin, S.J. (2008). Apoptosis: controlled demolition at the cellular level. Nat Rev Mol Cell Biol *9*, 231-241.

Tenev, T., Bianchi, K., Darding, M., Broemer, M., Langlais, C., Wallberg, F., Zachariou, A., Lopez, J., MacFarlane, M., Cain, K.*, et al.* (2011). The Ripoptosome, a signaling platform that assembles in response to genotoxic stress and loss of IAPs. Mol Cell *43*, 432-448.

Thinwa, J., Segovia, J.A., Bose, S., and Dube, P.H. (2014). Integrin-mediated first signal for inflammasome activation in intestinal epithelial cells. J Immunol *193*, 1373-1382.

Thompson, C.B. (1995). Apoptosis in the pathogenesis and treatment of disease. Science *267*, 1456-1462.

Thornberry, N.A., Bull, H.G., Calaycay, J.R., Chapman, K.T., Howard, A.D., Kostura, M.J., Miller, D.K., Molineaux, S.M., Weidner, J.R., Aunins, J.*, et al.* (1992). A novel heterodimeric cysteine protease is required for interleukin-1 beta processing in monocytes. Nature *356*, 768-774.

Thuret, G., Chiquet, C., Herrag, S., Dumollard, J.M., Boudard, D., Bednarz, J., Campos, L., and Gain, P. (2003). Mechanisms of staurosporine induced apoptosis in a human corneal endothelial cell line. Br J Ophthalmol *87*, 346-352.

Tomalka, J., Ganesan, S., Azodi, E., Patel, K., Majmudar, P., Hall, B.A., Fitzgerald, K.A., and Hise, A.G. (2011). A novel role for the NLRC4 inflammasome in mucosal defenses against the fungal pathogen *Candida albicans*. PLoS Pathog *7*, e1002379.

Tortorano, A.M., Kibbler, C., Peman, J., Bernhardt, H., Klingspor, L., and Grillot, R. (2006). Candidaemia in Europe: epidemiology and resistance. Int J Antimicrob Agents *27*, 359-366.

Tortorano, A.M., Peman, J., Bernhardt, H., Klingspor, L., Kibbler, C.C., Faure, O., Biraghi, E., Canton, E., Zimmermann, K., Seaton, S.*, et al.* (2004). Epidemiology of candidaemia in Europe: results of 28-month European Confederation of Medical Mycology (ECMM) hospital-based surveillance study. Eur J Clin Microbiol Infect Dis *23*, 317-322.

Trachootham, D., Lu, W., Ogasawara, M.A., Nilsa, R.D., and Huang, P. (2008). Redox regulation of cell survival. Antioxid Redox Signal *10*, 1343-1374.

Upton, J.W., Kaiser, W.J., and Mocarski, E.S. (2010). Virus inhibition of RIP3-dependent necrosis. Cell Host Microbe *7*, 302-313.

Urban, C.F., Reichard, U., Brinkmann, V., and Zychlinsky, A. (2006). Neutrophil extracellular traps capture and kill *Candida albicans* yeast and hyphal forms. Cell Microbiol *8*, 668-676.

Uwamahoro, N., Verma-Gaur, J., Shen, H.H., Qu, Y., Lewis, R., Lu, J., Bambery, K., Masters, S.L., Vince, J.E., Naderer, T.*, et al.* (2014). The pathogen *Candida albicans* hijacks pyroptosis for escape from macrophages. MBio *5*, e00003-00014.

van de Veerdonk, F.L., Joosten, L.A., Shaw, P.J., Smeekens, S.P., Malireddi, R.K., van der Meer, J.W., Kullberg, B.J., Netea, M.G., and Kanneganti, T.D. (2011). The inflammasome drives protective Th1 and Th17 cellular responses in disseminated candidiasis. Eur J Immunol *41*, 2260-2268.

van Meer, G. (1989). Lipid traffic in animal cells. Annu Rev Cell Biol *5*, 247-275.

Vanden Berghe, T., Linkermann, A., Jouan-Lanhouet, S., Walczak, H., and Vandenabeele, P. (2014). Regulated necrosis: the expanding network of non-apoptotic cell death pathways. Nat Rev Mol Cell Biol *15*, 135-147.

Verma, A.H., Richardson, J.P., Zhou, C., Coleman, B.M., Moyes, D.L., Ho, J., Huppler, A.R., Ramani, K., McGeachy, M.J., Mufazalov, I.A.*, et al.* (2017). Oral epithelial cells orchestrate innate type 17 responses to *Candida albicans* through the virulence factor candidalysin. Sci Immunol *2*.

Villar, C.C., Chukwuedum Aniemeke, J., Zhao, X.R., and Huynh-Ba, G. (2012). Induction of apoptosis in oral epithelial cells by *Candida albicans*. Mol Oral Microbiol *27*, 436-448.

Villar, C.C., Kashleva, H., and Dongari-Bagtzoglou, A. (2004). Role of *Candida albicans* polymorphism in interactions with oral epithelial cells. Oral Microbiol Immunol *19*, 262-269.

Villar, C.C., Kashleva, H., Mitchell, A.P., and Dongari-Bagtzoglou, A. (2005). Invasive phenotype of *Candida albicans* affects the host proinflammatory response to infection. Infect Immun *73*, 4588-4595.

Villar, C.C., Kashleva, H., Nobile, C.J., Mitchell, A.P., and Dongari-Bagtzoglou, A. (2007). Mucosal tissue invasion by *Candida albicans* is associated with E-cadherin degradation, mediated by transcription factor Rim101p and protease Sap5p. Infect Immun *75*, 2126-2135.

Villar, C.C., and Zhao, X.R. (2010). Candida albicans induces early apoptosis followed by secondary necrosis in oral epithelial cells. Mol Oral Microbiol *25*, 215-225.

Wachtler, B., Citiulo, F., Jablonowski, N., Forster, S., Dalle, F., Schaller, M., Wilson, D., and Hube, B. (2012). *Candida albicans*-epithelial interactions: dissecting the roles of active penetration, induced endocytosis and host factors on the infection process. PLoS One *7*, e36952.

Wagener, J., Weindl, G., de Groot, P.W., de Boer, A.D., Kaesler, S., Thavaraj, S., Bader, O., Mailander-Sanchez, D., Borelli, C., Weig, M*., et al.* (2012). Glycosylation of *Candida albicans* cell wall proteins is critical for induction of innate immune responses and apoptosis of epithelial cells. PLoS One *7*, e50518.

Wallach, D., Kang, T.B., and Kovalenko, A. (2014). Concepts of tissue injury and cell death in inflammation: a historical perspective. Nat Rev Immunol *14*, 51-59.

Wang, A., Raniga, P.P., Lane, S., Lu, Y., and Liu, H. (2009). Hyphal chain formation in *Candida albicans*: Cdc28-Hgc1 phosphorylation of Efg1 represses cell separation genes. Mol Cell Biol *29*, 4406-4416.

Wang, H., Sun, L., Su, L., Rizo, J., Liu, L., Wang, L.F., Wang, F.S., and Wang, X. (2014). Mixed lineage kinase domain-like protein MLKL causes necrotic membrane disruption upon phosphorylation by RIP3. Mol Cell *54*, 133-146.

Wang, L., Du, F., and Wang, X. (2008). TNF-alpha induces two distinct caspase-8 activation pathways. Cell *133*, 693-703.

Wei, M.C., Zong, W.X., Cheng, E.H., Lindsten, T., Panoutsakopoulou, V., Ross, A.J., Roth, K.A., MacGregor, G.R., Thompson, C.B., and Korsmeyer, S.J. (2001). Proapoptotic BAX and BAK: a requisite gateway to mitochondrial dysfunction and death. Science *292*, 727-730.

Weindl, G., Naglik, J.R., Kaesler, S., Biedermann, T., Hube, B., Korting, H.C., and Schaller, M. (2007). Human epithelial cells establish direct antifungal defense through TLR4-mediated signaling. J Clin Invest *117*, 3664-3672.

Weinlich, R., Oberst, A., Beere, H.M., and Green, D.R. (2017). Necroptosis in development, inflammation and disease. Nat Rev Mol Cell Biol *18*, 127-136.

Wellington, M., Koselny, K., Sutterwala, F.S., and Krysan, D.J. (2014). *Candida albicans* triggers NLRP3-mediated pyroptosis in macrophages. Eukaryot Cell *13*, 329-340.

Wells, C.A., Salvage-Jones, J.A., Li, X., Hitchens, K., Butcher, S., Murray, R.Z., Beckhouse, A.G., Lo, Y.L., Manzanero, S., Cobbold, C*., et al.* (2008). The macrophage-inducible C-type lectin, mincle, is an essential component of the innate immune response to *Candida albicans*. J Immunol *180*, 7404-7413.

Williams, D., and Lewis, M. (2011). Pathogenesis and treatment of oral candidosis. J Oral Microbiol *3*.

Wilson, D., Thewes, S., Zakikhany, K., Fradin, C., Albrecht, A., Almeida, R., Brunke, S., Grosse, K., Martin, R., Mayer, F*., et al.* (2009). Identifying infection-associated genes of *Candida albicans* in the postgenomic era. FEMS Yeast Res *9*, 688-700.

Wu, H., Downs, D., Ghosh, K., Ghosh, A.K., Staib, P., Monod, M., and Tang, J. (2013). *Candida albicans* secreted aspartic proteases 4-6 induce apoptosis of epithelial cells by a novel Trojan horse mechanism. FASEB J *27*, 2132-2144.

Xin, H., Dziadek, S., Bundle, D.R., and Cutler, J.E. (2008). Synthetic glycopeptide vaccines combining beta-mannan and peptide epitopes induce protection against candidiasis. Proc Natl Acad Sci U S A *105*, 13526-13531.

Yadev, N.P., Murdoch, C., Saville, S.P., and Thornhill, M.H. (2011). Evaluation of tissue engineered models of the oral mucosa to investigate oral candidiasis. Microb Pathog *50*, 278-285.

Yu, L., Lee, K.K., Sheth, H.B., Lane-Bell, P., Srivastava, G., Hindsgaul, O., Paranchych, W., Hodges, R.S., and Irvin, R.T. (1994). Fimbria-mediated adherence of *Candida albicans* to glycosphingolipid receptors on human buccal epithelial cells. Infect Immun *62*, 2843-2848.

Zakikhany, K., Naglik, J.R., Schmidt-Westhausen, A., Holland, G., Schaller, M., and Hube, B. (2007). In vivo transcript profiling of *Candida albicans* identifies a gene essential for interepithelial dissemination. Cell Microbiol *9*, 2938-2954.

Zamaraev, A.V., Kopeina, G.S., Prokhorova, E.A., Zhivotovsky, B., and Lavrik, I.N. (2017). Post-translational Modification of Caspases: The Other Side of Apoptosis Regulation. Trends Cell Biol *27*, 322-339.

Zha, Q.B., Wei, H.X., Li, C.G., Liang, Y.D., Xu, L.H., Bai, W.J., Pan, H., He, X.H., and Ouyang, D.Y. (2016). ATP-Induced Inflammasome Activation and Pyroptosis Is Regulated by AMP-Activated Protein Kinase in Macrophages. Front Immunol *7*, 597.

Zhang, P., Hong, J., Yoon, I.N., Kang, J.K., Hwang, J.S., and Kim, H. (2017). *Clostridium difficile* Toxin A Induces Reactive Oxygen Species Production and p38 MAPK Activation to Exert Cellular Toxicity in Neuronal Cells. J Microbiol Biotechnol *27*, 1163-1170.

Zhang, Y., Han, J., Zhu, C.C., Tang, F., Cui, X.S., Kim, N.H., and Sun, S.C. (2016). Exposure to HT-2 toxin causes oxidative stress induced apoptosis/autophagy in porcine oocytes. Sci Rep *6*, 33904.

Zhao, X., Oh, S.H., Cheng, G., Green, C.B., Nuessen, J.A., Yeater, K., Leng, R.P., Brown, A.J., and Hoyer, L.L. (2004). ALS3 and ALS8 represent a single locus that encodes a *Candida albicans* adhesin; functional comparisons between Als3p and Als1p. Microbiology *150*, 2415-2428.

Zhao, X., Oh, S.H., and Hoyer, L.L. (2007). Deletion of ALS5, ALS6 or ALS7 increases adhesion of *Candida albicans* to human vascular endothelial and buccal epithelial cells. Med Mycol *45*, 429-434.

Zhao, X., Oh, S.H., Yeater, K.M., and Hoyer, L.L. (2005). Analysis of the *Candida albicans* Als2p and Als4p adhesins suggests the potential for compensatory function within the Als family. Microbiology *151*, 1619-1630.

Zhivotovsky, B., and Orrenius, S. (2011). Calcium and cell death mechanisms: a perspective from the cell death community. Cell Calcium *50*, 211-221.

Zhu, W., Phan, Q.T., Boontheung, P., Solis, N.V., Loo, J.A., and Filler, S.G. (2012). EGFR and HER2 receptor kinase signaling mediate epithelial cell invasion by *Candida albicans* during oropharyngeal infection. Proc Natl Acad Sci U S A *109*, 14194-14199.

Zitvogel, L., Kepp, O., and Kroemer, G. (2010). Decoding cell death signals in inflammation and immunity. Cell *140*, 798-804.

Appendix A: Published papers

The experimental research presented in this thesis was acknowledged as an important contribution to several conceptual advances in our understanding of Candidalysin biology. Specifically, data obtained during the course of my research was published in the journal Nature (Figure 2c and 4g of Moyes et al., 2016), a publication in which I was listed as a co-author.

ARTICLE

doi:10.1038/nature17625

Candidalysin is a fungal peptide toxin critical for mucosal infection

David L. Moyes[1]*, Duncan Wilson[2]†*, Jonathan P. Richardson[1]*, Selene Mogavero[2]*, Shirley X. Tang[1], Julia Wernecke[3,4], Sarah Höfs[2], Remi L. Gratacap[5], Jon Robbins[6], Manohursingh Runglall[1]†, Celia Murciano[1]†, Mariana Blagojevic[1], Selvam Thavaraj[1], Toni M. Förster[2], Betty Hebecker[2,7], Lydia Kasper[2], Gema Vizcay[8], Simona I. Iancu[1], Nessim Kichik[1,9], Antje Häder[10], Oliver Kurzai[10], Ting Luo[11], Thomas Krüger[11], Olaf Kniemeyer[11], Ernesto Cota[9], Oliver Bader[12], Robert T. Wheeler[5], Thomas Gutsmann[3], Bernhard Hube[2,13,14] & Julian R. Naglik[1]

Cytolytic proteins and peptide toxins are classical virulence factors of several bacterial pathogens which disrupt epithelial barrier function, damage cells and activate or modulate host immune responses. Such toxins have not been identified previously in human pathogenic fungi. Here we identify the first, to our knowledge, fungal cytolytic peptide toxin in the opportunistic pathogen *Candida albicans*. This secreted toxin directly damages epithelial membranes, triggers a danger response signalling pathway and activates epithelial immunity. Membrane permeabilization is enhanced by a positive charge at the carboxy terminus of the peptide, which triggers an inward current concomitant with calcium influx. *C. albicans* strains lacking this toxin do not activate or damage epithelial cells and are avirulent in animal models of mucosal infection. We propose the name 'Candidalysin' for this cytolytic peptide toxin; a newly identified, critical molecular determinant of epithelial damage and host recognition of the clinically important fungus, *C. albicans*.

The ability of mucosal surfaces to discriminate between commensal and pathogenic microbes is essential to human health. The fungus *Candida albicans* is normally a benign member of the human microbiota, but is also responsible for millions of mucosal infections each year in immunocompromised hosts, often with severe morbidity[1]. A defining feature of *C. albicans* pathogenesis is the transition from yeast to invasive filamentous hyphae[2]. Hyphae damage mucosal epithelia and induce activation of the activating protein-1 (AP-1) transcription factor, c-Fos (via p38-MAPK) and the MAPK phosphatase MKP1 (via ERK1/2-MAPK), which trigger pro-inflammatory cytokine responses[3–7]. These signalling events constitute a 'danger response' against invasive hyphae, thus serving as a sensor of pathogenic *C. albicans* invasion[8–14]. However, it is unclear how *C. albicans* hyphae induce epithelial inflammatory responses and cell damage during mucosal infections. Here we identify and characterize Candidalysin, the first, to our knowledge, cytolytic peptide toxin isolated from any human fungal pathogen, as the hyphal factor critical for epithelial immune activation and *C. albicans* mucosal infection.

Ece1p is vital for epithelial activation and damage

Despite the well-known association between filamentation and virulence, the molecular mechanism underlying hypha-driven epithelial activation and mucosal damage has remained obscure. To elucidate this mechanism, we screened a panel of *C. albicans* gene deletion mutants that targeted key processes, pathways and proteins known or predicted to be associated with the yeast–hyphal transition and pathogenicity (62 strains). Only hypha-producing strains induced MKP1 phosphorylation (p-MKP1), c-Fos, cytokines (IL-1α, IL-6, G-CSF) and damage in oral epithelial cells (Extended Data Table 1). However, one *C. albicans* mutant (*ece1*Δ/Δ)[15] formed normal hyphae but was incapable of inducing these epithelial danger responses. The *C. albicans* extent of cell elongation 1 gene (*ECE1*) is highly expressed by hyphae during epithelial infection (Extended Data Fig. 1a, b), and is predicted to encode a secreted protein[16]. To probe its function, we generated a panel of *C. albicans ECE1* mutants (Extended Data Table 2). The *ece1*Δ/Δ strain formed normal hyphae on (Extended Data Fig. 1c), and adhered to and invaded human epithelial cells similarly to wild-type *C. albicans* (Extended Data Fig. 1d, e). The strain *ece1*Δ/Δ was capable of extensive epithelial invasion, penetrating through multiple epithelial cells (Extended Data Fig. 1f). Despite this, invasive *ece1*Δ/Δ hyphae did not damage epithelia or induce p-MKP1/c-Fos-mediated danger responses or cytokine secretion (Fig. 1a–d). Thus, Ece1p is critical for epithelial damage and innate recognition of *C. albicans* hyphae *in vitro*.

Ece1p is critical for mucosal pathogenesis

We next assessed the role of *ECE1* in two *in vivo* models of *C. albicans* mucosal infection. In murine oropharyngeal candidiasis (OPC)[17], mice infected with *C. albicans* wild-type or *ECE1* re-integrant (*ece1*Δ/Δ + *ECE1*) strains exhibited disease symptoms, including extensive hyphal invasion of the tongue epithelium, micro-abscesses of infiltrating neutrophils and tissue damage (Fig. 1e, f, h, i). In contrast, tongue tissue from *ece1*Δ/Δ-infected animals ($n = 17/20$) showed no invasive fungi and no inflammatory infiltrates or damage (Fig. 1g). We detected very low numbers of *ece1*Δ/Δ cells in only 3/20 mice

[1]Mucosal & Salivary Biology Division, Dental Institute, King's College London SE1 1UL, UK. [2]Department of Microbial Pathogenicity Mechanisms, Hans Knöll Institute, D-07745 Jena, Germany. [3]Research Center Borstel, Division of Biophysics, D-23845 Borstel, Germany. [4]Deutsches Elektronen-Synchrotron DESY, D-22607 Hamburg, Germany. [5]Department of Molecular & Biomedical Sciences, University of Maine, Orono, Maine 04469, USA. [6]Wolfson CARD, King's College London, Guy's Campus, London SE1 1UL, UK. [7]Research Group Microbial Immunology, Hans Knöll Institute, D-07745 Jena, Germany. [8]Centre for Ultrastructural Imaging, King's College London, London SE1 1UL, UK. [9]Department of Life Sciences, Imperial College London, London SW7 2AZ, UK. [10]Septomics Research Center, Hans-Knöll Institute and Friedrich Schiller University, D-07745 Jena, Germany. [11]Department of Molecular and Applied Microbiology, Hans Knöll Institute, D-07745 Jena, Germany. [12]Institute for Medical Microbiology, University Medical Center Göttingen, D-37075 Göttingen, Germany. [13]Friedrich Schiller University, D-07737 Jena, Germany. [14]Integrated Research and Treatment Center, Center for Sepsis Control and Care, D-07747 Jena, Germany. †Present addresses: Aberdeen Fungal Group, School of Medicine, Medical Sciences and Nutrition, University of Aberdeen, Aberdeen AB25 2ZD, UK (D.W.); NIHR Biomedical Research Centre, Guy's and St Thomas' NHS Foundation Trust, London SE1 1UL, UK (M.R.); ERI Biotecmed & Microbiology and Ecology Department, University of Valencia, Valencia 46100, Spain (C.M.).
*These authors contributed equally to this work.

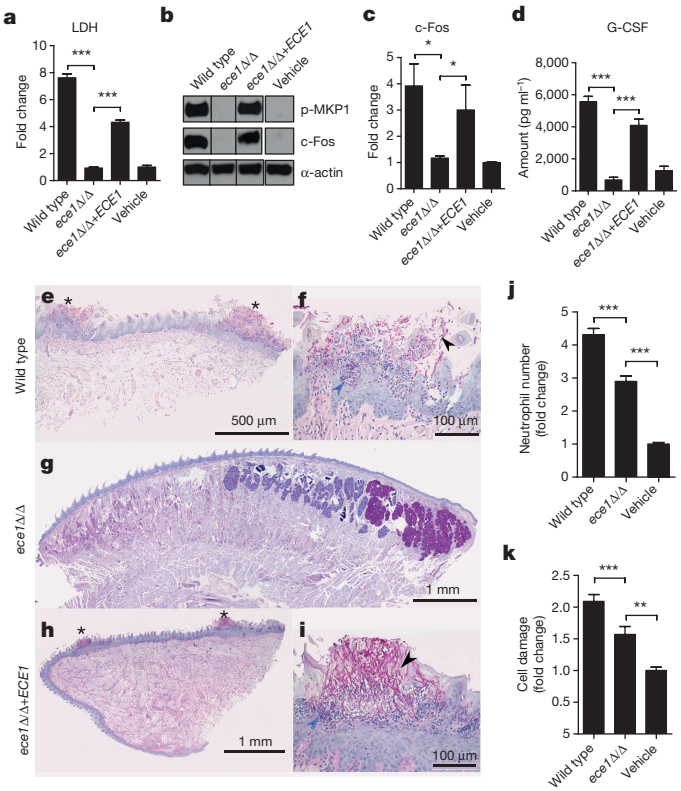

Figure 1 | *ECE1* is required for epithelial activation and *C. albicans* infection. TR146 cells were infected with the indicated *C. albicans* strains. **a**, LDH release 24 h post-infection (p.i.) (MOI = 0.1). **b**, Induction of p-MKP-1 and c-Fos at 2 h p.i. (MOI = 10). **c**, c-Fos DNA binding at 3 h p.i. (MOI = 10). **d**, G-CSF production at 24 h p.i. (MOI = 0.01). **e–i**, PAS-stained tongues from mice subjected to OPC 2 days p.i. Whole-mount (×25) (**e**, **g**, **h**) and high-magnification (**f**, **i**) (×200) views of PAS-stained tongues of mice infected with *C. albicans* wild type (**e**, **f**), *ece1*Δ/Δ (**g**) and *ece1*Δ/Δ + *ECE1* (**h**, **i**). Invading hyphae (black arrowhead) and inflammatory cells (blue arrowhead) are indicated. **j**, Quantification of neutrophils in zebrafish swimbladder following infection with wild-type *C. albicans* (number of fish (n) = 47), *ece1*Δ/Δ (n = 53) or PBS (n = 40). **k**, Quantification of damaged cells in zebrafish swimbladder after infection with *C. albicans* wild-type (n = 73) or *ece1*Δ/Δ strains (n = 59) or vehicle (n = 63). Data are representative (**b**, **e–i**) or the mean (**a**, **c**, **d**, **j**, **k**) of three biological replicates. Error bars ± s.e.m. Data were analysed by one-way ANOVA (**a**, **d**), paired t-test (**c**) or Kruskal–Wallis test (**j**, **k**). $^{*}P < 0.05$, $^{**}P < 0.01$, $^{***}P < 0.001$. For gel image, see Supplementary Fig. 1.

(Extended Data Fig. 2a), which showed no evidence of local epithelial damage (data not shown). Quantification of histology sections indicated that the percentage of epithelial surface infected was significantly greater with the wild-type and *ECE1* re-integrant strains (Extended Data Fig. 2b). In a zebrafish swimbladder model of mucosal infection[18,19], neutrophil recruitment and tissue damage were both significantly lower following *ece1*Δ/Δ infection as compared with the wild-type strain (Fig. 1j, k and Extended Data Fig. 2c, d). Therefore, *C. albicans* Ece1p is critical for mucosal pathogenesis and is an innate immune activator *in vivo*.

Ece1p encodes a cytolytic peptide toxin

Ece1p is an *in vitro* substrate for Kex2p, a Golgi-located protease that cleaves proteins after lysine–arginine (KR) motifs[20]. Ece1p contains seven KR-processing sites, suggesting it has the potential to produce eight secreted peptides from *C. albicans*[20] (Extended Data Fig. 3a, b). Liquid chromatography–tandem mass spectrometry (LC-MS/MS) analysis confirmed that recombinant Kex2p (rKex2p) processes recombinant Ece1p (rEce1p), and that all eight peptides generated terminated in KR (and fragments thereof, showing that less efficient processing occurs also after a single K or R) (Supplementary Information). The importance of Kex2p-mediated Ece1p processing was demonstrated using a *kex2*Δ/Δ null strain[21], which was unable to damage oral epithelia or induce p-MKP1/c-Fos-mediated danger responses or cytokine secretion (Extended Data Table 1). To determine which Ece1p peptide(s) were responsible for epithelial activation and damage, oral epithelial cells were incubated with peptides Ece1-I–VIII (1.5–70 μM). Only Ece1-III$_{62–93}$ induced p-MKP1, c-Fos, cytokines and damage (Fig. 2a–c, Extended Data Fig. 3c–e). Notably, low Ece1-III$_{62–93}$ concentrations (1.5–15 μM) were sufficient to induce c-Fos DNA binding (Fig. 2d), G-CSF and GM-CSF (Fig. 2c and Extended Data Fig. 3c), whereas high Ece1-III$_{62–93}$ concentrations (70 μM) were required to induce damage (Fig. 2e) and the damage-associated cytokines IL-1α and IL-6, respectively (Extended Data Fig. 3d, e). Ece1-III$_{62–93}$ could also directly lyse multiple human epithelial cell types and induce haemolysis of red blood cells, a classical test for cytotoxin activity (not shown). Neither the N-terminal hydrophobic region (Ece1-III$_{62–85}$) nor the C-terminal hydrophilic region (Ece1-III$_{86–93}$) induced p-MKP1, c-Fos, cytokines or damage of epithelial cells, either individually or in combination (Extended Data Fig. 3f–h), demonstrating that the peptide containing both regions is required for activity. Therefore, Ece1-III$_{62–93}$ is the active region of Ece1p, acting as an epithelial immune activator and a cytolytic agent.

To confirm that Ece1-III$_{62–93}$ drives epithelial activation and fungal pathogenicity, we generated a *C. albicans* strain lacking only the Ece1-III$_{62–93}$ region (*ece1*Δ/Δ + *ECE1*$_{Δ184–279}$). LC-MS/MS analysis showed that the modified protein in this strain is stable, secreted and processed into each of the predicted peptide fragments, with the exception of the deleted peptide toxin (Supplementary Information). Like *ece1*Δ/Δ, *ece1*Δ/Δ + *ECE1*$_{Δ184–279}$ efficiently formed invasive hyphae (not shown). However, *ece1*Δ/Δ + *ECE1*$_{Δ184–279}$ was unable to induce p-MKP1, c-Fos DNA binding, cytokines, or damage epithelia (Extended Data Fig. 3i–l). In murine OPC, unlike the *ece1*Δ/Δ + *ECE1* complemented strain, *ece1*Δ/Δ + *ECE1*$_{Δ184–279}$-infected mice demonstrated absent (n = 4/10) or low (n = 6/10) fungal burdens, with no evidence of inflammatory infiltrates or local epithelial damage (Fig. 2f–h and Extended Data Fig. 4a, b). Likewise, *ece1*Δ/Δ + *ECE1*$_{Δ184–279}$ did not induce full damage in the zebrafish swimbladder model (Fig. 2i and Extended Data Fig. 4c). In contrast, injection of lytic doses of Ece1-III$_{62–93}$ into the swimbladder induced epithelial damage (Fig. 2j, k). Thus, Ece1-III$_{62–93}$ is both necessary and sufficient for epithelial immune activation, damage and mucosal infection *in vivo*.

The amphipathic properties of Ece1-III$_{62–93}$ (SIIGIIMGILGNIPQ VIQIIMSIVKAFKGNKR) coupled with the α-helical structure of the N-terminal hydrophobic region (Extended Data Fig. 5a, b) indicated that this fungal peptide may act similarly to cationic antimicrobial peptides and peptide toxins such as melittin[22] (honey bee), magainin 2 (ref. 23) (African clawed frog) and alamethicin[24] (*Trichoderma viride*). Cytolytic peptide toxins have not previously been found in human pathogenic fungi, but bacterial cytolytic toxins are known to induce lesions after binding to target cell membranes[25,26]. To investigate the importance of lipid composition for Ece1-III$_{62–93}$-mediated cytolysis, we used Förster resonance energy transfer (FRET) and electrical impedance spectroscopy to analyse the interactions of Ece1-III$_{62–93}$ with model membranes comprised of lipid bilayers of dioleoylphosphatidylcholine (DOPC) with or without cholesterol. Although Ece1-III$_{62–93}$ was able to efficiently intercalate into DOPC membranes (Extended Data Fig. 5c), Ece1-III$_{62–93}$ permeabilization was enhanced in the presence of cholesterol (Fig. 3a). Ece1-III$_{62–93}$-induced lesions were heterogeneous and transient (Extended Data Fig. 5d), indicating that the peptide may damage target membranes through a 'carpet-like' mechanism[27]. Patch-clamp analysis of epithelial cells demonstrated that lesion formation by Ece1-III$_{62–93}$ is rapid and causes an inward current (Fig. 3b), associated with calcium influx (Fig. 3c). Similar phenomena occur with bacterial cytolytic toxins, which are known to trigger cell activation[25,26,28].

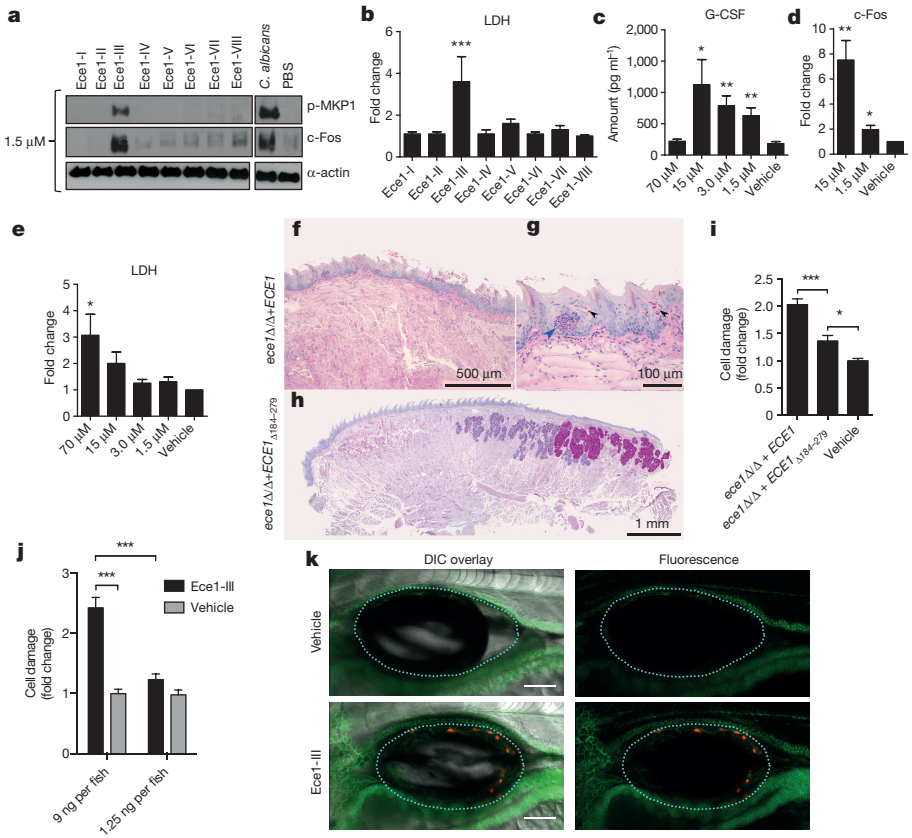

Figure 2 | Ece1-III$_{62–93}$ is the active region of Ece1p and is required for TR146 cell activation and mucosal *C. albicans* infection. **a**, Induction of p-MKP-1 and c-Fos 2 h post-stimulation (p.s.) with Ece1 peptides at 1.5 μM. **b**, LDH release 24 h p.s. with 70 μM Ece1 peptides. **c**, Induction of G-CSF 24 h p.s. with Ece1-III$_{62–93}$. **d**, c-Fos DNA binding induction 3 h p.s. with sub-lytic concentrations of Ece1-III$_{62–93}$. **e**, LDH release 24 h p.s. with Ece1-III$_{62–93}$. **f–h**, PAS-stained tongue sections from mice subjected to OPC, 2 days p.i. with *C. albicans ece1*Δ/Δ + *ECE1* (×25 and ×200) (**f**, **g**) or *ece1*Δ/Δ + *ECE1*$_{Δ184–279}$ (**h**). Invading hyphae (black arrowheads) and infiltrating inflammatory cells (blue arrowhead) are shown. **i**, Damaged cells in a zebrafish swimbladder 24 h p.i. with *C. albicans ece1*Δ/Δ + *ECE1* (number of fish (n) = 44), *ece1*Δ/Δ + *ECE1*$_{Δ184–279}$ (n = 58) or vehicle (n = 58). **j**, Damaged cells in zebrafish swimbladders after stimulation with 9 ng (n = 51) or 1.25 ng (n = 56) Ece1-III$_{62-93,}$ or vehicle (40% DMSO, n = 54 and 5% DMSO, n = 55). **k**, Co-localization of adherens junctions (α-catenin-citrine) with Ece1-III$_{62–93}$-damaged cells (Sytox Orange-positive cells) in a zebrafish swimbladder. Scale bar, 100 μm. Data are representative (**a**, **f–h**, **k**) or mean (**b–e**, **i**, **j**) of three biological replicates (**a–d**) or ten mice or fish (**f–h**, **k**). Error bars show ± s.e.m. Data were analysed by one-way ANOVA (**b**, **c**, **e**) paired *t*-test (**d**) or Kruskal–Wallis (**i**, **j**). $*P < 0.05$, $**P < 0.01$, $***P < 0.001$ (compared with vehicle control unless otherwise indicated). For gel image, see Supplementary Fig. 1.

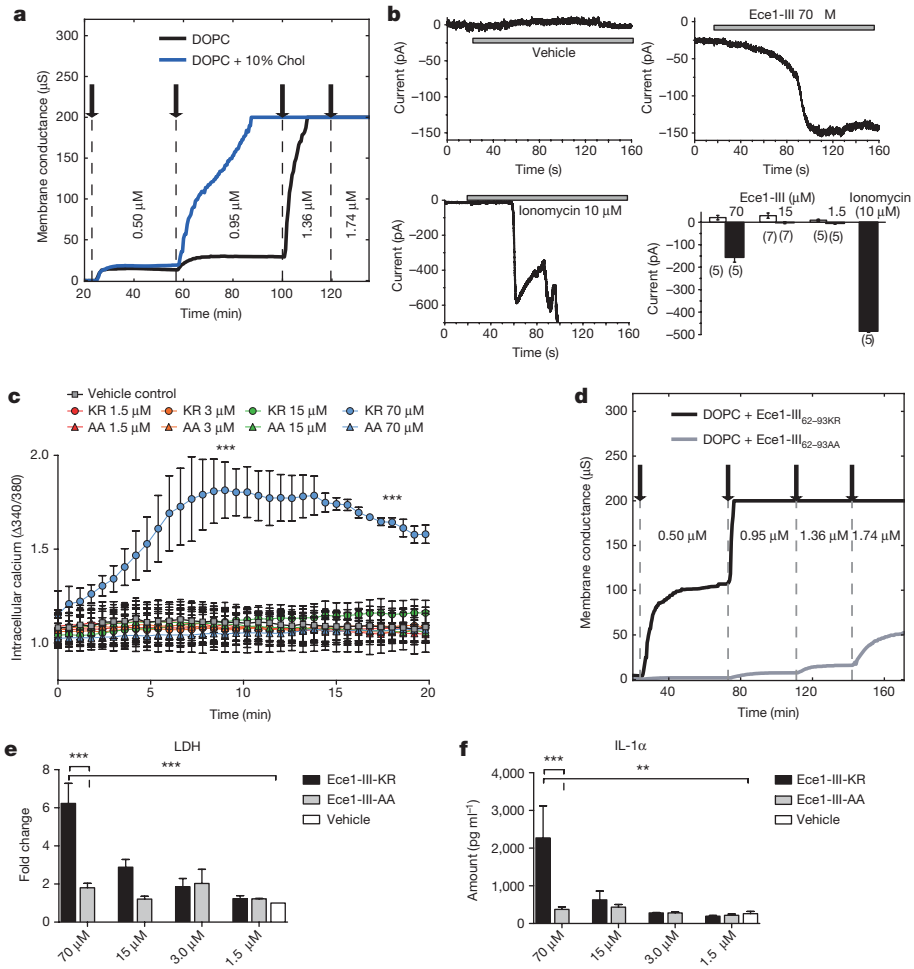

Figure 3 | Ece1-III$_{62–93}$ functions as a cytolytic peptide toxin. **a**, Kinetic changes in conductance of tethered lipid membranes after exposure to different concentrations of Ece1-III$_{62–93}$. **b**, Evoked inward current at a membrane potential of −60 mV in TR146 cells post-addition of Ece1-III$_{62–93}$ or ionomycin (positive control); individual (representative) and cumulative changes (bar chart indicates number of cells analysed below each bar) shown. **c**, Intracellular calcium level kinetics in TR146 cells post-stimulation (p.s.) with Ece1-III$_{62–93}$ wild type (Ece1-III$_{62–93KR}$) or Ece1-III$_{62–93}$ AA C-terminal substitution (Ece1-III$_{62–93AA}$). **d**, Kinetic changes in conductance of tethered DOPC membranes after exposure to different concentrations of Ece1-III$_{62-93KR}$ and Ece1-III$_{62–93AA}$. **e**, **f**, LDH release (**e**) and secretion of IL-1α (**f**) from TR146 cells 24 h p.s. with Ece1-III$_{62–93KR}$ or Ece1-III$_{62–93AA}$. Data shown are representative (**a**, **d**) or mean (**b**, **c**, **e**, **f**) of three biological replicates. Error bars show ± s.e.m. Data were analysed by one-way ANOVA (**c**, **e** and **f**). $**P < 0.01$, $***P < 0.001$.

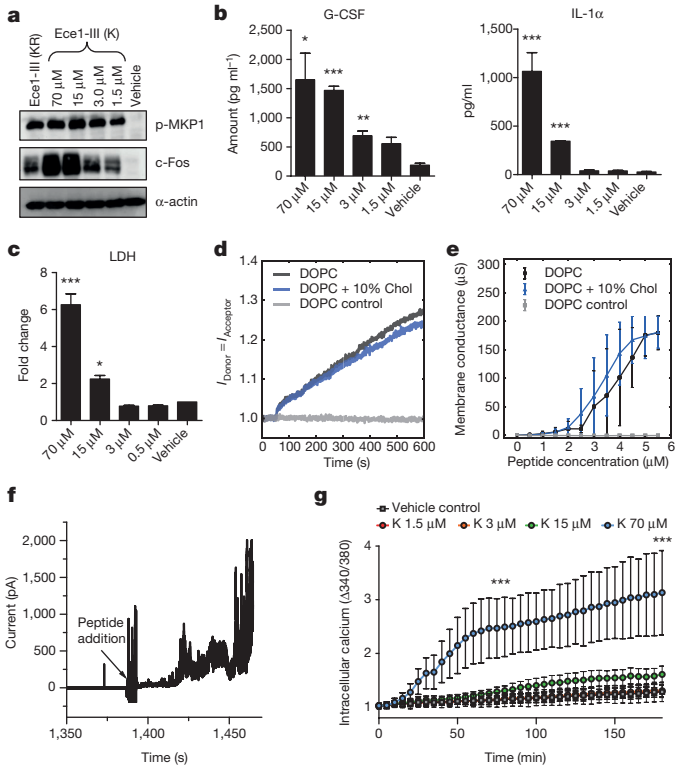

Figure 4 | Ece1-III$_{62–92K}$ functions as a cytolytic peptide toxin that activates and damages epithelial cells. a–c, Induction of p-MKP-1 and c-Fos 2 h post-stimulation (p.s.) (**a**), secretion of G-CSF and IL-1-α 24 h p.s. (**b**), and LDH release 24 h p.s. of TR146 cells with Ece1-III$_{62–92K}$ (**c**). **d**, Förster resonance energy transfer (FRET) showing intercalation of Ece1-III$_{62–92K}$ (10 μM) into lipid liposomes. **e**, Average peptide concentration-dependent changes in conductance of tethered lipid membranes. **f**, Ece1-III$_{62–92K}$ (4 μM) induced permeabilization of planar lipid membranes showing heterogeneous and transient lesions leading to membrane rupture. **g**, Intracellular calcium level kinetics in TR146 cells p.s. with Ece1-III$_{62–92K}$. Data shown are representative (**a**, **d**, **f**) or mean (**b**, **c**, **e**, **g**) of three biological replicates. Error bars show ± s.e.m. Data are analysed by one-way ANOVA (**b**, **c**). $*P < 0.05$, $**P < 0.01$, $***P < 0.001$ (compared with vehicle control). For gel image, see Supplementary Fig. 1.

We postulated that the positively-charged C-terminal KR residues of Ece1-III$_{62–93}$ might be critical for interacting with negatively-charged components of host membranes to promote lesion formation. Substitution of the KR motif to AA (alanine–alanine; Ece1-III$_{62–93AA}$) did not affect membrane intercalation (not shown) but significantly reduced the peptide's ability to permeabilize membranes, damage epithelial cells and induce calcium influx (Fig. 3c–e). Thus, the positive C terminus of Ece1-III$_{62–93}$ is critical for lesion formation and damage induction in epithelial membranes. Notably, Ece1-III$_{62–93AA}$ still induced p-MKP1, c-Fos and the non-damage associated cytokine G-CSF (Extended Data Fig. 5e, f), but not the damage-associated cytokine IL-1α (Fig. 3f), suggesting that Ece1-III$_{62–93AA}$ can be recognized by epithelial immunity without damaging cells. The importance of this finding is that it means epithelial cells are not only responding to damage, but have evolved to specifically recognize the peptide.

Ece1-III$_{62–92K}$ is a secreted cytolytic peptide toxin

To demonstrate that Ece1-III is generated during epithelial infection, we performed LC-MS/MS analysis on the secretome from wild-type *C. albicans* hyphae grown in the presence and absence of epithelial cells (Supplementary Information). Notably, Ece1-III was the only peptide detected in the presence of epithelial cells, indicating that the fungus secretes this toxin during mucosal infection. However, the predominant form of secreted Ece1-III terminated in a K residue (SIIGIIMGILGNIPQVIQIIMSIVKAFKGNK; Ece1-III$_{62–92K}$) and not KR (SIIGIIMGILGNIPQVIQIIMSIVKAFKGNKR; Ece1-III$_{62–93KR}$) (Extended Data Table 3). In fungi, it is known that following Kex2p processing, many proteins are subsequently cleaved by Kex1p[29] (also in the Golgi), removing the C-terminal R. LC-MS/MS analysis on the hyphal secretome of a *kex1*Δ/Δ mutant demonstrated that the predominant peptide secreted terminates in KR (not K) (Supplementary Information). Therefore, Ece1p is also subject to ordered Kex2p/Kex1p processing. Accordingly, we confirmed that Ece1-III$_{62–92K}$ functioned similarly to Ece1-III$_{62–93KR}$ with respect to epithelial cell activation. Specifically, Ece1-III$_{62-92K}$ is also α-helical (not shown) and induces c-Fos, p-MKP1, cytokines (IL-1α, G-CSF), damage (LDH), membrane intercalation and permeabilization, and calcium influx (Fig. 4a–g). Thus, the dominant peptide secreted from *C. albicans* hyphae during mucosal infection is Ece1-III$_{62–92K}$, which acts as a cytolytic peptide toxin that activates epithelial cells.

Based on these data, we propose a model of *C. albicans* mucosal infection whereby invasive hyphae secrete Ece1-III$_{62-92K}$ into a membrane-bound 'invasion pocket'[30,31], facilitating peptide accumulation (Extended Data Fig. 6). During early stages of infection, sub-lytic concentrations of Ece1-III$_{62–92K}$ induce epithelial immunity by activating the 'danger response' pathway (p-MKP1/c-Fos), alerting the host to the transition from colonizing yeast to invasive, toxin-producing hyphae. As infection progresses, Ece1-III$_{62–92K}$ levels accumulate and elicit direct tissue damage. Mechanistically, we propose that the asymmetric distribution of charge along the α-helix of Ece1-III$_{62–92K}$ facilitates correct peptide orientation relative to the host membrane, enabling intercalation, permeabilization and calcium influx. Our data identifies *C. albicans* Ece1-III$_{62–92K}$ as the first cytolytic peptide toxin in a human fungal pathogen and reveals the molecular mechanisms of epithelial damage and host recognition of this clinically important fungus. We propose the name 'Candidalysin' for this newly discovered fungal toxin.

Online Content Methods, along with any additional Extended Data display items and Source Data, are available in the online version of the paper; references unique to these sections appear only in the online paper.

Received 23 July 2015; accepted 26 February 2016.
Published online 30 March 2016.

1. Brown, G. D. *et al. Hidden killers: human fungal infections. Sci. Transl Med.* **4,** 165rv113 (2012).
2. Jacobsen, I. D. *et al. Candida albicans* dimorphism as a therapeutic target. *Expert Rev. Anti Infect. Ther.* **10,** 85–93 (2012).
3. Moyes, D. L. *et al.* A biphasic innate immune MAPK response discriminates between the yeast and hyphal forms of *Candida albicans* in epithelial cells. *Cell Host Microbe* **8,** 225–235 (2010).
4. Moyes, D. L. *et al. Candida albicans* yeast and hyphae are discriminated by MAPK signaling in vaginal epithelial cells. *PLoS ONE* **6,** e26580 (2011).
5. Murciano, C. *et al. Candida albicans* cell wall glycosylation may be indirectly required for activation of epithelial cell proinflammatory responses. *Infect. Immun.* **79,** 4902–4911 (2011).
6. Moyes, D. L. *et al.* Activation of MAPK/c-Fos induced responses in oral epithelial cells is specific to *Candida albicans* and *Candida dubliniensis* hyphae. *Med. Microbiol. Immunol. (Berl.)* **201,** 93–101 (2012).
7. Murciano, C. *et al.* Evaluation of the role of *Candida albicans* agglutinin-like sequence (Als) proteins in human oral epithelial cell interactions. *PLoS ONE* **7,** e33362 (2012).
8. Moyes, D. L. & Naglik, J. R. Mucosal immunity and *Candida albicans* infection. *Clin. Dev. Immunol.* **2011,** 346307 (2011).
9. Naglik, J. R. & Moyes, D. Epithelial cell innate response to *Candida albicans*. *Adv. Dent. Res.* **23,** 50–55 (2011).
10. Naglik, J. R., Moyes, D. L., Wachtler, B. & Hube, B. *Candida albicans* interactions with epithelial cells and mucosal immunity. *Microbes Infect.* **13,** 963–976 (2011).
11. Hebecker, B., Naglik, J. R., Hube, B. & Jacobsen, I. D. Pathogenicity mechanisms and host response during oral *Candida albicans* infections. *Expert Rev. Anti Infect. Ther.* **12,** 867–879 (2014).
12. Naglik, J. R. *Candida* immunity. *New J. Science* **2014,** 390241 (2014).
13. Naglik, J. R., Richardson, J. P. & Moyes, D. L. *Candida albicans* Pathogenicity and epithelial immunity. *PLoS Pathog.* **10,** e1004257 (2014).
14. Moyes, D. L., Richardson, J. P. & Naglik, J. R. *Candida albicans*—epithelial interactions and pathogenicity mechanisms: scratching the surface. *Virulence* **6,** 338–346 (2015).

15. Birse, C. E., Irwin, M. Y., Fonzi, W. A. & Sypherd, P. S. Cloning and characterization of *ECE1*, a gene expressed in association with cell elongation of the dimorphic pathogen *Candida albicans*. *Infect. Immun.* **61,** 3648–3655 (1993).
16. Röhm, M. *et al.* A family of secreted pathogenesis-related proteins in *Candida albicans*. *Mol. Microbiol.* **87,** 132–151 (2013).
17. Kamai, Y., Kubota, M., Hosokawa, T., Fukuoka, T. & Filler, S. G. New model of oropharyngeal candidiasis in mice. *Antimicrob. Agents Chemother.* **45,** 3195–3197 (2001).
18. Brothers, K. M. *et al.* NADPH oxidase-driven phagocyte recruitment controls *Candida albicans* filamentous growth and prevents mortality. *PLoS Pathog.* **9,** e1003634 (2013).
19. Gratacap, R. L., Rawls, J. F. & Wheeler, R. T. Mucosal candidiasis elicits NF-κB activation, proinflammatory gene expression and localized neutrophilia in zebrafish. *Dis. Model. Mech.* **6,** 1260–1270 (2013).
20. Bader, O., Krauke, Y. & Hube, B. Processing of predicted substrates of fungal Kex2 proteinases from *Candida albicans, C. glabrata, Saccharomyces cerevisiae* and *Pichia pastoris*. *BMC Microbiol.* **8,** 116 (2008).
21. Newport, G. & Agabian, N. *KEX2* influences *Candida albicans* proteinase secretion and hyphal formation. *J. Biol. Chem.* **272,** 28954–28961 (1997).
22. Liu, P., Huang, X., Zhou, R. & Berne, B. J. Observation of a dewetting transition in the collapse of the melittin tetramer. *Nature* **437,** 159–162 (2005).
23. Bechinger, B. & Salnikov, E. S. The membrane interactions of antimicrobial peptides revealed by solid-state NMR spectroscopy. *Chem. Phys. Lipids* **165,** 282–301 (2012).
24. Pieta, P., Mirza, J. & Lipkowski, J. Direct visualization of the alamethicin pore formed in a planar phospholipid matrix. *Proc. Natl Acad. Sci. USA* **109,** 21223–21227 (2012).
25. Bischofberger, M., Iacovache, I. & van der Goot, F. G. Pathogenic pore-forming proteins: function and host response. *Cell Host Microbe* **12,** 266–275 (2012).
26. Los, F. C., Randis, T. M., Aroian, R. V. & Ratner, A. J. Role of pore-forming toxins in bacterial infectious diseases. *Microbiol. Mol. Biol. Rev.* **77,** 173–207 (2013).
27. Oren, Z. & Shai, Y. Selective lysis of bacteria but not mammalian cells by diastereomers of melittin: structure-function study. *Biochemistry* **36,** 1826–1835 (1997).
28. Walev, I. *et al.* Delivery of proteins into living cells by reversible membrane permeabilization with streptolysin-O. *Proc. Natl Acad. Sci. USA* **98,** 3185–3190 (2001).
29. Schmitt, M. J. & Breinig, F. Yeast viral killer toxins: lethality and self-protection. *Nature Rev. Microbiol.* **4,** 212–221 (2006).
30. Zakikhany, K. *et al. In vivo* transcript profiling of *Candida albicans* identifies a gene essential for interepithelial dissemination. *Cell. Microbiol.* **9,** 2938–2954 (2007).
31. Wächtler, B. *et al. Candida albicans*-epithelial interactions: dissecting the roles of active penetration, induced endocytosis and host factors on the infection process. *PLoS ONE* **7,** e36952 (2012).

Supplementary Information is available in the online version of the paper.

Acknowledgements We thank S. Gaffen, B. Klein, C. Hertweck, A. Tucker, J. Green and S. Challacombe for comments on the manuscript. For experimental assistance, we thank S. Bevan and D. Andersson (calcium assays), D. Nayar (histology), D. Rahman and M. Mistry (murine model), M. Nilan (zebrafish model), S. Groth (FRET spectroscopy), N. Gebauer (Impedance experiments), D. Schulz (*kex1*Δ/Δ strain) and our colleagues for supplying fungal mutant strains. This work was supported by grants from the Medical Research Council (MR/J008303/1, MR/M011372/1), Biotechnology & Biological Sciences Research Council (BB/J015261/1), FP7-PEOPLE-2013-Initial Training Network (606786) to J.R.N.; Wellcome Trust Strategic Award for Medical Mycology and Fungal Immunology (097377/Z/11/Z) to J.R.N. and D.W.; Sir Henry Dale Fellowship jointly funded by the Wellcome Trust and the Royal Society (102549/Z/13/Z) to D.W.; Deutsche Forschungsgemeinschaft CRC/TR124 FungiNet Project C1 and Z2, Deutsche Forschungsgemeinschaft SPP 1580 (Hu 528/17-1) and CSCC, German Federal Ministry of Education and Health (BMBF) 01EO1002 to B.Hu.; Cluster of Excellence 'Inflammation at interfaces' and Deutsche Forschungsgemeinschaft SPP1580 project GU 568/5-1 to T.G.; National Institutes of Health (R15AI094406) and the Burroughs Wellcome Fund to R.T.W.

Author Contributions D.L.M., J.P.R., S.X.T., M.R., C.M., M.B., S.I.I. and N.K. performed signalling, transcription factor, calcium and cytokine assays, and murine work; D.W., S.H., S.M., T.M.F., B.He., L.K. A.H., O.B. and O.Ku. created fungal strains and performed fluorescent microscopy, adhesion, invasion, gene expression and damage assays; R.L.G. and R.T.W. performed zebrafish experiments; J.W. and T.G. performed biophysical analysis with artificial membranes; J.R. performed whole patch clamp analysis; G.V. performed electron microscopy; S.T. performed histological analysis; S.M., T.L., T.K. and O.Kn. performed LC-MS analyses; J.R.N., B.Hu., D.L.M., J.P.R. and D.W. wrote the paper; J.R.N., B.Hu. and E.C. supervised the project.

Author Information Reprints and permissions information is available at www.nature.com/reprints. The authors declare no competing financial interests. Readers are welcome to comment on the online version of the paper. Correspondence and requests for materials should be addressed to B.Hu. (bernhard.hube@leibniz-hki.de).

METHODS

Data reporting. No statistical methods were used to predetermine sample size. The experiments were not randomized. The investigators were not blinded to allocation during experiments and outcome assessment.

Cell lines, reagents and *Candida* strains. Experiments were carried out using the TR146 buccal epithelial squamous cell carcinoma line[32] obtained from the European Collection of Authenticated Cell Cultures (ECACC) and grown in Dulbecco's Modified Eagle's Medium (DMEM, Sigma-Aldrich) supplemented with 10% fetal bovine serum (FBS) and 1% penicillin-streptomycin. Cells were routinely tested for mycoplasma contamination using mycoplasma-specific primers and were found to be negative. Prior to stimulation, confluent TR146 cells were serum-starved overnight, and all experiments were carried out in serum-free DMEM. *C. albicans* wild-type strains included the autotrophic strain BWP17 + CIp30 (ref. 33) and the parental strain SC5314 (ref. 34). Other *C. albicans* strains used and their sources are listed in Extended Data Tables 1 and 2. *C. albicans* cultures were grown in YPD medium (1% yeast extract, 2% peptone, 2% dextrose) at 30 °C overnight. Cultures were washed in sterile PBS and adjusted to the required cell density. Antibodies to phospho-MKP1 and c-Fos were from Cell Signalling Technologies (New England Biolabs UK), mouse anti-human α-actin was from Millipore (UK), and goat anti-mouse and anti-rabbit horseradish peroxidase (HRP)-conjugated antibodies were from Jackson Immunologicals (Stratech Scientific, UK). Ece1p peptides were synthesized commercially (Proteogenix (France) or Peptide Synthetics (UK).

Generation of *C. albicans ECE1* mutant strains. *ECE1* deletion was performed as previously described[35]. Deletion cassettes were generated by PCR[36]. Primers ECE1-FG and ECE1-RG were used to amplify pFA-HIS1 and pFA-ARG4 -based markers. *C. albicans* BWP17 (ref. 37), was sequentially transformed[38] with the *ECE1*-HIS1 and *ECE1*-ARG4 deletion cassettes and then transformed with CIp10 (ref. 39), yielding the *ece1*Δ/Δ deletion strain. For complementation, the *ECE1* gene plus upstream and downstream intergenic regions were amplified with primers ECE1-RecF3k and ECE1-RecR and cloned into plasmid CIp10 at MluI and SalI sites. This plasmid was transformed into the uridine auxotrophic *ece1*Δ/Δ strain, yielding the *ece1*Δ/Δ + *ECE1* complemented strain. For generation of the *ece1*Δ/Δ + $ECE1_{\Delta 184-279}$ strain, the CIp10-*ECE1* was amplified with primers Pep3-F1 and Pep3-R1, digested with ClaI and re-ligated, yielding the CIp10 + $ECE1_{\Delta 184-279}$ plasmid. This plasmid was transformed into the uridine auxotrophic *ece1*Δ/Δ strain, yielding the *ece1*Δ/Δ + $ECE1_{\Delta 184-279}$ strain. All integrations were confirmed by PCR/sequencing and at least two independent isogenic transformants were created to confirm results. *KEX1* deletion was performed exactly as the *ECE1* deletion but using primers KEX1-FG and KEX1-RG for creating the deletion cassette. Fluorescent strains of *ece1*Δ/Δ and BWP17 were constructed as previously described[40]. Briefly, the *ece1*Δ/Δ and BWP17 strains were transformed with the pENO1-dTom-NATr plasmid. Primers used to clone and construct the *ECE1* genes and intragenic regions are listed in Extended Data Table 4. Strains are listed in Extended Data Table 2.

Construction of *C. albicans ECE1* promoter–GFP strain. *ECE1* promoter (primers 5′*ECE1*prom–NarI / 3′*ECE1*prom–XhoI) and terminator (5′*ECE1*term–SacII / 5′*ECE1*term–SacI) were amplified and cloned into pADH1-GFP. Resulting pSK-p*ECE1*-GFP was verified by sequencing. *C. albicans* SC5314 was transformed with the *pECE1-GFP* transformation cassette[38]. Resistance to nourseothricin was used as selective marker and correct integration of GFP into the *ECE1* locus was verified by PCR. Primers for cloning and validation are listed in Extended Data Table 4. Strains are listed in Extended Data Table 2.

RNA isolation and real-time PCR analysis. *C. albicans* cells grown on TR146 epithelial cells were collected into RNA pure (PeqLab), centrifuged and the pellet resuspended in 400 μl AE buffer (50 mM Na-acetate pH 5.3, 10 mM EDTA, 1% SDS). Samples were vortexed (30 s), and an equal volume of phenol/chloroform/isoamyl alcohol (25:24:1) was added and incubated for 5 min (65 °C) before subjected to 2× freeze-thawing. Lysates were clarified by centrifugation and the RNA precipitated with isopropyl alcohol/0.3 M sodium acetate by incubating for 1 h at −20 °C. Precipitated pellets were washed (2× 1 ml 70% ice-cold ethanol), resuspended in DEPC-treated water and stored at −80 °C. RNA integrity and concentration was confirmed using a Bioanalyzer (Agilent). RNA (500 ng) was treated with DNase (Epicentre) and cDNA synthesized using Reverse Transcriptase Superscript III (Invitrogen). cDNA samples were used for qPCR with EVAgreen mix (Bio&Sell). Primers (ACT1-F and ACT1-R for actin, ECE1-F and ECE1-R for *ECE1* Extended Data Table 4) were used at a final concentration of 500 nM. qPCR amplifications were performed using a Biorad CFX96 thermocycler. Data was evaluated using Bio-Rad CFX Manager 3.1 (Bio-Rad) with *ACT1* as the reference gene and t_0 as the control sample.

Western blotting. TR146 cells were lysed using a modified RIPA lysis buffer (50 mM Tris-HCl pH 7.4, 150 mM NaCl, 1 mM EDTA, 1% Triton X-100, 1% sodium deoxycholate, 0.1% SDS) containing protease (Sigma-Aldrich) and phosphatase (Perbio Science) inhibitors[41], left on ice (30 min) and then clarified (10 min) in a refrigerated microfuge. Lysate total protein content was determined using the BCA protein quantitation kit (Perbio Science). 20 μg of total protein was separated on 12% SDS–PAGE gels before transfer to nitrocellulose membranes (GE Healthcare). After probing with primary (1:1,000) and secondary (1:10,000) antibodies, membranes were developed using Immobilon chemiluminescent substrate (Millipore) and exposed to X-ray film (Fuji film). Human α-actin was used as a loading control.

Transcription factor DNA binding assay. DNA binding activity of transcription factors was assessed using the TransAM transcription factor ELISA system (Active Motif) as previously described[41,42]. Serum-starved TR146 epithelial cells were treated for 3 h before being differentially lysed to recover nuclear proteins using a nuclear protein extraction kit (Active Motif) according to the manufacturer's protocol. Protein concentration was determined (BCA protein quantitation kit (Perbio Science)) and 5 μg of nuclear extract was assayed in the TransAM system according to the manufacturer's protocol. Data was expressed as fold-change in $A_{450\,nm}$ relative to resting cells.

Cytokine determination. Cytokine levels in cell culture supernatants were determined using the Performance magnetic Fluorokine MAP cytokine multiplex kit (Bio-techne) and a Bioplex 200 machine. The data were analysed using Bioplex Manager 6.1 software to determine analyte concentrations.

Cell damage assay. Following incubation, culture supernatant was collected and assayed for lactate dehydrogenase (LDH) activity using the Cytox 96 Non-Radioactive Cytotoxicity Assay kit (Promega) according to the manufacturer's instructions. Recombinant porcine LDH (Sigma-Aldrich) was used to generate a standard curve.

Epithelial adhesion assay. Quantification of *C. albicans* adherence to TR146 epithelial cells was performed as described previously[43]. Briefly, TR146 cells were grown to confluence on glass coverslips for 48 h in tissue culture plates in DMEM medium. *C. albicans* yeast cells (2 × 105) were added into 1 ml serum-free DMEM, incubated for 60 min (37 °C/5% CO_2) and non-adherent *C. albicans* cells removed by aspiration. Following washing (3× 1 ml PBS), cells were fixed with 4% paraformaldehyde (Roth) and adherent *C. albicans* cells stained with Calcofluor White and quantified using fluorescence microscopy. The number of adherent cells was determined by counting 100 high-magnification fields of 200 μm × 200 μm size. Exact total cell numbers were calculated based on the quantified areas and the total size of the cover slip.

Epithelial invasion assay. *C. albicans* invasion of epithelial cells was determined as described previously[43]. Briefly, TR146 epithelial cells were grown to confluence on glass coverslips for 48 h and then infected with *C. albicans* yeast cells (1×10^5), for 3 h in a humidified incubator (37 °C/5% CO_2). Following washing (3× PBS), the cells were fixed with 4% paraformaldehyde. All surface adherent fungal cells were stained for 1 h with a rabbit anti-*Candida* antibody and subsequently with a goat anti-rabbit-Alexa Fluor 488 antibody. After rinsing with PBS, epithelial cells were permeabilized (0.1% Triton X-100 in PBS for 15 min) and fungal cells (invading and non-invading) were stained with Calcofluor White. Following rinsing with water, coverslips were visualized using fluorescence microscopy. The percentage of invading *C. albicans* cells was determined by dividing the number of (partially) internalized cells by the total number of adherent cells. At least 100 fungal cells were counted on each coverslip.

Imaging of *C. albicans* growth and invasion of epithelial cells. TR146 cells (10^5 per ml) seeded on glass coverslips in DMEM/10% FBS were infected with *C. albicans* (2.5×10^4 cfu per ml) in DMEM and incubated for 6 h (37 °C/5% CO_2). Cells were washed with PBS, fixed overnight (4 °C in 4% paraformaldehyde) and stained with Concanavalin A-Alexa Fluor 647 in PBS (10 μg ml^{-1}) for 45 min at room temperature in the dark with gentle shaking (70 r.p.m.) to stain the fungal cell wall. Epithelial cells were permeabilized with 0.1% Triton X-100 for 15 min at 37 °C in the dark, then washed and stained with 10 μg ml^{-1} Calcofluor White (0.1 M Tris-HCl pH 9.5) for 20 min at room temperature in the dark with gentle shaking. Cells were rinsed in water and mounted on slides with 6 μl of ProLong Gold anti-fade reagent, before air drying for 2 h in the dark. Fluorescence microscopy was performed on a Zeiss Axio Observer Z1 microscope, and 5 phase images were taken per picture.

Scanning electron microscopy. For scanning electron microscopy (SEM) analysis, TR146 cells were grown to confluence on Transwell inserts (Greiner) and serum starved overnight in serum-free DMEM. After 5 h of *C. albicans* incubation on epithelial cells at an MOI of 0.01, cell media was removed and samples were fixed overnight at 4 °C with 2.5% (v/v) glutaraldehyde in 0.05 M HEPES buffer (pH 7.2) and post-fixed in 1% (w/v) osmium tetroxide for 1 h at room temperature. After washing, samples were dehydrated through a graded ethanol series before being critical point dried (Polaron E3000, Quorum Technologies). Dried samples were

mounted using carbon double side sticky discs (TAAB) on aluminium pins (TAAB) and gold coated in an Emitech K550X sputter coater (Quorum Technologies Ltd). Samples were examined and images recorded using a FEI Quanta 200 field emission scanning electron microscope operated at 3.5 kV in high vacuum mode.

Zebrafish swimbladder mucosal infection model. Zebrafish infections were performed in accordance with NIH guidelines under Institutional Animal Care and Use Committee (IACUC) protocol A2009-11-01 at the University of Maine. To determine sample size, a power calculation was done for all experiments based on two-tailed *t*-tests in order to detect a minimum effect size of 0.8, with an alpha error probability of 0.05 and a power (1 – beta error probability) of 0.95. This gave a minimum number of 42 fish for each group. The fish selected for the experiments were randomly assigned to the different groups by picking them from a pool without bias and the groups were injected in different orders. No blinding was used to read the results. Ten to twenty zebrafish per group per experiment were maintained at 33 °C in E3 + PTU and used as previously described[40]. Briefly, 4 days post-fertilization (dpf) larvae were treated with 20 μg ml^{-1} dexamethasone dissolved in 0.1% DMSO 1 h before infection and thereafter. For tissue damage and neutrophil recruitment, individual AB or *mpo:GFP* fish (respectively) were injected into the swimbladder with 4 nl of PBS with or without 25–40 *C. albicans* yeast cells of *ece1*Δ/Δ-*dTomato*, *ece1*Δ/Δ + *ECE1* + *dTomato*, *ece1*Δ/Δ + *ECE1*$_{\Delta 184-279}$ + *dTomato* or BWP17-*dTomato*. For tissue damage, 1 nl of Sytox green (0.05 mM in 1% DMSO) was injected at 20 h post-infection into the swimbladder and fish were imaged by confocal microscopy at 24 h post-infection. For neutrophil recruitment, fish were imaged at 24 h post-injection. For synthetic peptide damage, AB or α-catenin:citrine[44] fish were injected with 2 nl of peptide (9 ng or 1.25 ng per fish) or vehicle (40% DMSO or 5% DMSO) + SytoxGreen (0.05 mM in 1% DMSO) or SytoxOrange (0.5 mM in 10% DMSO) and the fish imaged by confocal microscopy 4 h later. Numbers of neutrophils and damaged cells observed were counted and tabulated for each fish.

Zebrafish swimbladder fluorescence microscopy. Live zebrafish imaging was carried out as previously described[40]. Briefly, fish were anaesthetized in Tris-buffered Tricaine (200 μg ml^{-1}, Western Chemicals) and further immobilized in a solution of 0.4% low-melting-point agarose (LMA, Lonza) in E3 + Tricaine in a 96-well plate glass-bottom imaging dish (Greiner Bio-On). Confocal imaging was carried out using an Olympus IX-81 inverted microscope with an FV-1000 laser scanning confocal system (Olympus). Images were collected and processed using Fluoview (Olympus) and Photoshop (Adobe Systems). Panels are either a single slice for the differential interference contrast channel (DIC) with maximum projection overlays of fluorescence image channels (red-green), or maximum projection overlays of fluorescence channels. The number of slices for each maximum projection is specified in the legend of individual figures.

Murine oropharyngeal candidiasis model. Murine infections were performed under UK Home Office Project Licence PPL 70/7598 in dedicated animal facilities at King's College London. No statistical method was used to pre-determine sample size. No method of randomization was used to allocate animals to experimental groups. Mice in the same cage were part of the same treatment. The investigators were not blinded during outcome assessment. A previously described murine model of oropharyngeal candidiasis using female BALB/c mice[45] was modified to use for investigating early infection events. Briefly, mice were treated subcutaneously with 3 mg per mouse (in 200 μl PBS with 0.5% Tween 80) of cortisone acetate on days −1 and +1 post-infection. On day 0, mice were sedated for ~75 min with an intra-peritoneal injection of 110 mg per kg ketamine and 8 mg per kg xylazine, and a swab soaked in a 10^7 cfu per ml of *C. albicans* yeast culture in sterile saline was placed sublingually for 75 min. After 2 days, mice were euthanized, the tongue excised and divided longitudinally in half. One half was weighed, homogenized and cultured to derive quantitative *Candida* counts. The other half was processed for histopathology and immunohistochemistry.

Immunohistochemistry of murine tissue. *C. albicans*-infected murine tongues were fixed in 10% (v/v) formal-saline before being embedded and processed in paraffin wax using standard protocols. For each tongue, 5-μm sections were prepared using a Leica RM2055 microtome and silane coated slides. Sections were dewaxed using xylene, before *C. albicans* and infiltrating inflammatory cells were visualized by staining using Periodic Acid-Schiff (PAS) stain and counterstaining with haematoxylin. Sections were then examined by light microscopy. Histological quantification of infection was undertaken by measuring the area of infected epithelium and expressed as a percentage relative to the entire epithelial area.

Whole cell patch clamp. TR146 epithelial cells were grown in 35-mm Petri dishes (Nunc) for 48 h before recordings at low cell density (10–30% confluence). Cells were superfused with a modified Krebs solution (120 mM NaCl, 3 mM KCl, 2.5 mM $CaCl_2$, 1.2 mM $MgCl_2$, 22.6 mM $NaHCO_2$, 11.1 mM glucose, 5 mM HEPES pH 7.4). Isolated cells were recorded at room temperature (21–23 °C) in whole cell mode using microelectrodes (5–7 MΩ) containing 90 mM potassium acetate, 20 mM KCl, 40 mM HEPES, 3 mM EGTA, 3 mM $MgCl_2$, 1 mM $CaCl_2$ (free Ca^{2+} 40 nM), pH 7.4. Cells were voltage clamped at −60 mV using an Axopatch 200A amplifier (Axon Instruments) and current/voltage curves were generated by 1 s steps between −100 to +50 mV. Treatments were applied to the superfusate to produce the final required concentration, with vehicle controls similarly applied. Data was recorded using Clampex software (PClamp 6, Axon Instrument) and analysed with Clampfit 10.

Calcium flux. TR146 cells were grown in a 96-well plate overnight until confluent. The medium was removed and 50 μl of a Fura-2 solution (5 μl Fura-2 (Life Technologies) (2.5 mM in 50% Pluronic F-127 (Life Technologies):50% DMSO), 5 μl probenecid (Sigma) in 5 ml saline solution (NaCl (140 mM), KCl (5 mM), $MgCl_2$ (1 mM), $CaCl_2$ (2 mM), glucose (10 mM) and HEPES (10 mM), adjusted to pH 7.4)) was added and the plate incubated for 1 h at 37 °C/5% CO_2. The Fura-2 solution was replaced with 50 μl saline solution and baseline fluorescence readings (excitation 340 nm/emission 520 nm) taken for 10 min using a FlexStation 3 (Molecular Devices). Ece1 peptides were added at different concentrations and readings immediately taken for up to 3 h. The data was analysed using Softmax Pro software to determine calcium present in the cell cytosol and expressed as the ratio between excitation and emission spectra.

Impedance spectroscopy of tethered bilayer lipid membranes (tBLMs). tBLMs with 10% tethering lipids and 90% spacer lipids (T10 slides) were formed using the solvent exchange technique[46,47] according to the manufacturer's instructions (SDx Tethered Membranes Pty Ltd, Sydney, Australia). Briefly, 8 μl of 3 mM lipid solutions in ethanol were added, incubated for 2 min and then 93.4 μl buffer (100 mM KCl, 5 mM HEPES, pH 7.0) was added. After rinsing 3× with 100 μl buffer the conductance and capacitance of the membranes were measured for 20 min before injection of Ece1 peptides at different concentrations. All experiments were performed at room temperature. Signals were measured using the tethaPod (SDx Tethered Membranes Pty, Sydney, Australia).

FRET intercalation experiments. Intercalation of Ece1 peptides into phospholipid liposomes was determined by FRET spectroscopy applied as a probe-dilution assay[48]. Phospholipids mixed with each 1% (mol/mol) of the donor dye NBD-phosphatidylethanolamine (NBD-PE) and of the acceptor dye rhodamine-PE, were dissolved in chloroform, dried, solubilized in 1 ml buffer (100 mM KCl, 5 mM HEPES, pH 7.0) by vortexing, sonicated with a titan tip (30 W, Branson sonifier, cell disruptor B15), and subjected to three cycles of heating to 60 °C and cooling down to 4 °C, each for 30 min. Lipid samples were stored at 4 °C for at least 12 h before use. Ece1 peptide was added to liposomes and intercalation was monitored as the increase of the quotient between the donor fluorescence intensity I_D at 531 nm and the acceptor intensity I_A at 593 nm (FRET signal) independent of time.

Circular Dichroism spectroscopy. CD measurements were performed using a Jasco J-720 spectropolarimeter (Japan Spectroscopic Co., Japan), calibrated as described previously[49]. CD spectra represent the average of four scans obtained by collecting data at 1 nm intervals with a bandwidth of 2 nm. The measurements were performed in 100 mM KCl, 5 mM HEPES, pH 7.0 at 25 °C and 40 °C in a 1.0 mm quartz cuvette. The Ece1-III concentration was 15 μM.

Planar lipid bilayers. Planar lipid bilayers were prepared using the Montal-Mueller technique[50] as described previously[51]. All measurements were performed in 5 mM HEPES, 100 mM KCl, pH 7.0 (specific electrical conductivity 17.2 mS per cm) at 37 °C.

Hyphal secretome preparation for LC-MS/MS analysis. *Candida* strains were cultured for 18 h in hyphae inducing conditions (YNB medium containing 2% sucrose, 75 mM MOPSO buffer pH 7.2, 5 mM *N*-acetyl-D-glucosamine, 37 °C). Hyphal supernatants were collected by filtering through a 0.2 μm PES filter, and peptides were enriched by solid phase extraction (SPE) using first C4 and subsequently C18 columns on the C4 flowthrough. After drying in a vacuum centrifuge, samples were resolubilized in loading solution (0.2% formic acid in 71:27:2 ACN/H_2O/DMSO (v/v/v)) and filtered through a 10 kDa MWCO filter. The filtrate was transferred into HPLC vials and injected into the LC-MS/MS system. LC-MS/MS analysis was carried out on an Ultimate 3000 nano RSLC system coupled to a QExactive Plus mass spectrometer (ThermoFisher Scientific). Peptide separation was performed based on a direct injection setup without peptide trapping using an Accucore C4 column as stationary phase and a column oven temperature of 50 °C. The binary mobile phase consisting of A) 0.2% (v/v) formic acid in 95:5 H_2O/DMSO (v/v) and B) 0.2% (v/v) formic acid in 85:10:5 ACN/H_2O/DMSO (v/v/v) was applied for a 60 min gradient elution: 0–1.5 min at 60% B, 35–45 min at 96% B, 45.1–60 min at 60% B. The Nanospray Flex Ion Source (ThermoFisher Scientific) provided with a stainless steel emitter was used to generate positively charged ions at 2.2 kV spray voltage. Precursor ions were measured in full scan mode within a mass range of *m*/z 300–1600 at a resolution of 70k FWHM using a maximum injection time of 120 ms and an automatic gain control target of 1e6. For data-dependent acquisition, up to 10 most abundant precursor ions per scan cycle with an assigned charge state of $z = 2–6$ were selected in the quadrupole for

further fragmentation using an isolation width of m/z 2.0. Fragment ions were generated in the HCD cell at a normalized collision energy of 30 V using nitrogen gas. Dynamic exclusion of precursor ions was set to 20 s. Fragment ions were monitored at a resolution of 17.5k (FWHM) using a maximum injection time of 120 ms and an AGC target of 2e5.

Protein database search. Thermo raw files were processed by the Proteome Discoverer (PD) software v1.4.0.288 (Thermo). Tandem mass spectra were searched against the Candida Genome Database (http://www.candidagenome.org/download/sequence/C_albicans_SC5314/Assembly22/current/C_albicans_SC5314_A22_current_orf_trans_all.fasta.gz; status: 2015/05/03) using the Sequest HT search algorithm. Mass spectra were searched for both unspecific cleavages (no enzyme) and tryptic peptides with up to 4 missed cleavages. The precursor mass tolerance was set to 10 p.p.m. and the fragment mass tolerance to 0.02 Da. Target Decoy PSM Validator node and a reverse decoy database was used for (q value) validation of the peptide spectral matches (PSMs) using a strict target false discovery (FDR) rate of $<1\%$. Furthermore, we used the score versus charge state function of the Sequest engine to filter out insignificant peptide hits (xcorr of 2.0 for $z=2$, 2.25 for $z=3$, 2.5 for $z=4$, 2.75 for $z=5$, 3.0 for $z=6$). At least two unique peptides per protein were required for positive protein hits.

Statistics. TransAM and patch clamp data were analysed using a paired t-test while cytokines, LDH and calcium influx data were analysed using one-way ANOVA with all compared groups passing an equal variance test. Murine *in vivo* data was analysed using the Mann–Whitney test. Zebrafish data was analysed using the Kruskal–Wallis test with Dunn's multiple comparison correction. In all cases, $P<0.05$ was taken to be significant.

32. Rupniak, H. T. *et al.* Characteristics of four new human cell lines derived from squamous cell carcinomas of the head and neck. *J. Natl. Cancer Inst.* **75,** 621–635 (1985).
33. Mayer, F. L. *et al.* The novel *Candida albicans* transporter Dur31 is a multi-stage pathogenicity factor. *PLoS Pathog.* **8,** e1002592 (2012).
34. Gillum, A. M., Tsay, E. Y. & Kirsch, D. R. Isolation of the *Candida albicans* gene for orotidine-5′-phosphate decarboxylase by complementation of *S. cerevisiae* ura3 and *E. coli* pyrF mutations. *Mol. Gen. Genet.* **198,** 179–182 (1984).
35. Citiulo, F. *et al. Candida albicans* scavenges host zinc via Pra1 during endothelial invasion. *PLoS Pathog.* **8,** e1002777 (2012).
36. Gola, S., Martin, R., Walther, A., Dunkler, A. & Wendland, J. New modules for PCR-based gene targeting in *Candida albicans*: rapid and efficient gene targeting using 100 bp of flanking homology region. *Yeast* **20,** 1339–1347 (2003).
37. Wilson, R. B., Davis, D. & Mitchell, A. P. Rapid hypothesis testing with *Candida albicans* through gene disruption with short homology regions. *J. Bacteriol.* **181,** 1868–1874 (1999).
38. Walther, A. & Wendland, J. An improved transformation protocol for the human fungal pathogen *Candida albicans*. *Curr. Genet.* **42,** 339–343 (2003).
39. Murad, A. M., Lee, P. R., Broadbent, I. D., Barelle, C. J. & Brown, A. J. Clp10, an efficient and convenient integrating vector for *Candida albicans*. *Yeast* **16,** 325–327 (2000).
40. Gratacap, R. L., Rawls, J. F. & Wheeler, R. T. Mucosal candidiasis elicits NF-κB activation, proinflammatory gene expression and localized neutrophilia in zebrafish. *Dis. Model. Mech.* **6,** 1260–1270 (2013).
41. Moyes, D. L. *et al.* A biphasic innate immune MAPK response discriminates between the yeast and hyphal forms of *Candida albicans* in epithelial cells. *Cell Host Microbe* **8,** 225–235 (2010).
42. Moyes, D. L. *et al. Candida albicans* yeast and hyphae are discriminated by MAPK signaling in vaginal epithelial cells. *PLoS ONE* **6,** e26580 (2011).
43. Wächtler, B., Wilson, D., Haedicke, K., Dalle, F. & Hube, B. From attachment to damage: defined genes of *Candida albicans* mediate adhesion, invasion and damage during interaction with oral epithelial cells. *PLoS ONE* **6,** e17046 (2011).
44. Trinh L, A. *et al.* A versatile gene trap to visualize and interrogate the function of the vertebrate proteome. *Genes Dev.* **25,** 2306–2320 (2011).
45. Solis, N. V. & Filler, S. G. Mouse model of oropharyngeal candidiasis. *Nature Protocols* **7,** 637–642 (2012).
46. Cranfield, C., Carne, S., Martinac, B. & Cornell, B. The assembly and use of tethered bilayer lipid membranes (tBLMs). *Methods Mol. Biol.* **1232,** 45–53 (2015).
47. Cranfield, C. G. *et al.* Transient potential gradients and impedance measures of tethered bilayer lipid membranes: pore-forming peptide insertion and the effect of electroporation. *Biophys. J.* **106,** 182–189 (2014).
48. Schromm, A. B. *et al.* Lipopolysaccharide-binding protein mediates CD14-independent intercalation of lipopolysaccharide into phospholipid membranes. *FEBS Lett.* **399,** 267–271 (1996).
49. Chen, G. C. & Yang, J. T. 2-Point calibration of circular dichrometer with D-10-camphorsulfonic acid. *Anal. Lett.* **10,** 1195–1207 (1977).
50. Montal, M. & Mueller, P. Formation of bimolecular membranes from lipid monolayers and a study of their electrical properties. *Proc. Natl Acad. Sci. USA* **69,** 3561–3566 (1972).
51. Gutsmann, T., Heimburg, T., Keyser, U., Mahendran, K. R. & Winterhalter, M. Protein reconstitution into freestanding planar lipid membranes for electrophysiological characterization. *Nature Protocols* **10,** 188–198 (2015).
52. Gillum, A. M., Tsay, E. Y. & Kirsch, D. R. Isolation of the *Candida albicans* gene for orotidine-5′-phosphate decarboxylase by complementation of *S. cerevisiae* ura3 and *E. coli* pyrF mutations. *Mol. Gen. Genet.* **198,** 179–182 (1984).
53. Wilson, R. B., Davis, D. & Mitchell, A. P. Rapid hypothesis testing with *Candida albicans* through gene disruption with short homology regions. *J. Bacteriol.* **181,** 1868–1874 (1999).
54. Fonzi, W. A. & Irwin, M. Y. Isogenic strain construction and gene mapping in *Candida albicans*. *Genetics* **134,** 717–728 (1993).
55. Davis, D., Wilson, R. B. & Mitchell, A. P. *RIM101*-dependent and-independent pathways govern pH responses in *Candida albicans*. *Mol. Cell. Biol.* **20,** 971–978 (2000).
56. Braun, B. R. & Johnson, A. D. *TUP1*, *CPH1* and *EFG1* make independent contributions to filamentation in *Candida albicans*. *Genetics* **155,** 57–67 (2000).
57. Lo, H. J. *et al.* Nonfilamentous *C. albicans* mutants are avirulent. *Cell* **90,** 939–949 (1997).
58. Moyes, D. L. *et al.* A biphasic innate immune MAPK response discriminates between the yeast and hyphal forms of *Candida albicans* in epithelial cells. *Cell Host Microbe* **8,** 225–235 (2010).
59. Zakikhany, K. *et al.* In vivo transcript profiling of *Candida albicans* identifies a gene essential for interepithelial dissemination. *Cell. Microbiol.* **9,** 2938–2954 (2007).
60. Cao, F. *et al.* The Flo8 transcription factor is essential for hyphal development and virulence in *Candida albicans*. *Mol. Biol. Cell* **17,** 295–307 (2006).
61. Bockmühl, D. P., Krishnamurthy, S., Gerads, M., Sonneborn, A. & Ernst, J. F. Distinct and redundant roles of the two protein kinase A isoforms Tpk1p and Tpk2p in morphogenesis and growth of *Candida albicans*. *Mol. Microbiol.* **42,** 1243–1257 (2001).
62. Sonneborn, A. *et al.* Protein kinase A encoded by TPK2 regulates dimorphism of *Candida albicans*. *Mol. Microbiol.* **35,** 386–396 (2000).
63. Palmer, G. E., Cashmore, A. & Sturtevant, J. *Candida albicans VPS11* is required for vacuole biogenesis and germ tube formation. *Eukaryot. Cell* **2,** 411–421 (2003).
64. Zou, H., Fang, H. M., Zhu, Y. & Wang, Y. *Candida albicans* Cyr1, Cap1 and G-actin form a sensor/effector apparatus for activating cAMP synthesis in hyphal growth. *Mol. Microbiol.* **75,** 579–591 (2010).
65. Bates, S. *et al.* Outer chain *N*-glycans are required for cell wall integrity and virulence of *Candida albicans*. *J. Biol. Chem.* **281,** 90–98 (2006).
66. Murciano, C. *et al. Candida albicans* cell wall glycosylation may be indirectly required for activation of epithelial cell proinflammatory responses. *Infect. Immun.* **79,** 4902–4911 (2011).
67. Newport, G. & Agabian, N. *KEX2* influences *Candida albicans* proteinase secretion and hyphal formation. *J. Biol. Chem.* **272,** 28954–28961 (1997).
68. Murad, A. M. *et al. NRG1* represses yeast-hypha morphogenesis and hypha-specific gene expression in *Candida albicans*. *EMBO J.* **20,** 4742–4752 (2001).
69. Liu, H., Kohler, J. & Fink, G. R. Suppression of hyphal formation in *Candida albicans* by mutation of a *STE12* homolog. *Science* **266,** 1723–1726 (1994).
70. Lane, S., Zhou, S., Pan, T., Dai, Q. & Liu, H. The basic helix-loop-helix transcription factor Cph2 regulates hyphal development in *Candida albicans* partly via *TEC1*. *Mol. Cell. Biol.* **21,** 6418–6428 (2001).
71. White, S. J. *et al.* Self-regulation of *Candida albicans* population size during GI colonization. *PLoS Pathog.* **3,** e184 (2007).
72. Brown, D. H., Jr, Giusani, A. D., Chen, X. & Kumamoto, C. A. Filamentous growth of *Candida albicans* in response to physical environmental cues and its regulation by the unique *CZF1* gene. *Mol. Microbiol.* **34,** 651–662 (1999).
73. Kadosh, D. & Johnson, A. D. Rfg1, a protein related to the *Saccharomyces cerevisiae* hypoxic regulator Rox1, controls filamentous growth and virulence in *Candida albicans*. *Mol. Cell. Biol.* **21,** 2496–2505 (2001).
74. San José, C., Monge, R. A., Perez-Diaz, R., Pla, J. & Nombela, C. The mitogen-activated protein kinase homolog *HOG1* gene controls glycerol accumulation in the pathogenic fungus *Candida albicans*. *J. Bacteriol.* **178,** 5850–5852 (1996).
75. Firon, A. *et al.* The *SUN41* and *SUN42* genes are essential for cell separation in *Candida albicans*. *Mol. Microbiol.* **66,** 1256–1275 (2007).
76. de Boer, A. D. *et al.* The *Candida albicans* cell wall protein Rhd3/Pga29 is abundant in the yeast form and contributes to virulence. *Yeast* **27,** 611–624 (2010).
77. Mühlschlegel, F. A. & Fonzi, W. A. *PHR2* of *Candida albicans* encodes a functional homolog of the pH-regulated gene *PHR1* with an inverted pattern of pH-dependent expression. *Mol. Cell. Biol.* **17,** 5960–5967 (1997).
78. Martin, R. *et al.* A core filamentation response network in *Candida albicans* is restricted to eight genes. *PLoS ONE* **8,** e58613 (2013).
79. Birse, C. E., Irwin, M. Y., Fonzi, W. A. & Sypherd, P. S. Cloning and characterization of *ECE1*, a gene expressed in association with cell elongation of the dimorphic pathogen *Candida albicans*. *Infect. Immun.* **61,** 3648–3655 (1993).
80. Navarro-García, F., Sanchez, M., Pla, J. & Nombela, C. Functional characterization of the *MKC1* gene of *Candida albicans*, which encodes a mitogen-activated protein kinase homolog related to cell integrity. *Mol. Cell. Biol.* **15,** 2197–2206 (1995).

81. Hausauer, D. L., Gerami-Nejad, M., Kistler-Anderson, C. & Gale, C. A. Hyphal guidance and invasive growth in *Candida albicans* require the Ras-like GTPase Rsr1p and its GTPase-activating protein Bud2p. *Eukaryot. Cell* **4,** 1273–1286 (2005).
82. Sentandreu, M., Elorza, M. V., Sentandreu, R. & Fonzi, W. A. Cloning and characterization of *PRA1*, a gene encoding a novel pH-regulated antigen of *Candida albicans*. *J. Bacteriol.* **180,** 282–289 (1998).
83. Pardini, G. *et al.* The *CRH* family coding for cell wall glycosylphosphatidylinositol proteins with a predicted transglycosidase domain affects cell wall organization and virulence of *Candida albicans*. *J. Biol. Chem.* **281,** 40399–40411 (2006).
84. Braun, B. R., Head, W. S., Wang, M. X. & Johnson, A. D. Identification and characterization of *TUP1*-regulated genes in *Candida albicans*. *Genetics* **156,** 31–44 (2000).
85. Fradin, C. *et al.* Granulocytes govern the transcriptional response, morphology and proliferation of *Candida albicans* in human blood. *Mol. Microbiol.* **56,** 397–415 (2005).
86. Staab, J. F., Bradway, S. D., Fidel, P. L. & Sundstrom, P. Adhesive and mammalian transglutaminase substrate properties of *Candida albicans* Hwp1. *Science* **283,** 1535–1538 (1999).
87. Bailey, D. A., Feldmann, P. J., Bovey, M., Gow, N. A. & Brown, A. J. The *Candida albicans HYR1* gene, which is activated in response to hyphal development, belongs to a gene family encoding yeast cell wall proteins. *J. Bacteriol.* **178,** 5353–5360 (1996).
88. Sandini, S., La Valle, R., De Bernardis, F., Macri, C. & Cassone, A. The 65 kDa mannoprotein gene of *Candida albicans* encodes a putative β-glucanase adhesin required for hyphal morphogenesis and experimental pathogenicity. *Cell. Microbiol.* **9,** 1223–1238 (2007).
89. Csank, C. *et al.* Roles of the *Candida albicans* mitogen-activated protein kinase homolog, Cek1p, in hyphal development and systemic candidiasis. *Infect. Immun.* **66,** 2713–2721 (1998).
90. Hube, B. *et al.* Disruption of each of the secreted aspartyl proteinase genes *SAP1, SAP2*, and *SAP3* of *Candida albicans* attenuates virulence. *Infect. Immun.* **65,** 3529–3538 (1997).
91. Taylor, B. N. *et al.* Induction of *SAP7* correlates with virulence in an intravenous infection model of candidiasis but not in a vaginal infection model in mice. *Infect. Immun.* **73,** 7061–7063 (2005).
92. Schild, L. *et al.* Proteolytic cleavage of covalently linked cell wall proteins by *Candida albicans* Sap9 and Sap10. *Eukaryot. Cell* **10,** 98–109 (2011).
93. Zhao, X. *et al. ALS3* and *ALS8* represent a single locus that encodes a *Candida albicans* adhesin; functional comparisons between Als3p and Als1p. *Microbiol.* **150,** 2415–2428 (2004).
94. Murciano, C. *et al.* Evaluation of the role of *Candida albicans* agglutinin-like sequence (Als) proteins in human oral epithelial cell interactions. *PLoS ONE* **7,** e33362 (2012).
95. Zhao, X., Oh, S. H., Yeater, K. M. & Hoyer, L. L. Analysis of the *Candida albicans* Als2p and Als4p adhesins suggests the potential for compensatory function within the Als family. *Microbiol.* **151,** 1619–1630 (2005).
96. Zhao, X., Oh, S. H. & Hoyer, L. L. Deletion of *ALS5, ALS6* or *ALS7* increases adhesion of *Candida albicans* to human vascular endothelial and buccal epithelial cells. *Med. Mycol.* **45,** 429–434 (2007).
97. Zhao, X., Oh, S. H. & Hoyer, L. L. Unequal contribution of *ALS9* alleles to adhesion between *Candida albicans* and human vascular endothelial cells. *Microbiol.* **153,** 2342–2350 (2007).
98. Timpel, C., Strahl-Bolsinger, S., Ziegelbauer, K. & Ernst, J. F. Multiple functions of Pmt1p-mediated protein *O*-mannosylation in the fungal pathogen *Candida albicans*. *J. Biol. Chem.* **273,** 20837–20846 (1998).
99. Bates, S. *et al. Candida albicans* Pmr1p, a secretory pathway P-type Ca^{2+}/Mn^{2+}-ATPase, is required for glycosylation and virulence. *J. Biol. Chem.* **280,** 23408–23415 (2005).
100. Hobson, R. P. *et al.* Loss of cell wall mannosylphosphate in *Candida albicans* does not influence macrophage recognition. *J. Biol. Chem.* **279,** 39628–39635 (2004).
101. Southard, S. B., Specht, C. A., Mishra, C., Chen-Weiner, J. & Robbins, P. W. Molecular analysis of the *Candida albicans* homolog of *Saccharomyces cerevisiae MNN9*, required for glycosylation of cell wall mannoproteins. *J. Bacteriol.* **181,** 7439–7448 (1999).
102. Munro, C. A. *et al.* Mnt1p and Mnt2p of *Candida albicans* are partially redundant α-1,2-mannosyltransferases that participate in *O*-linked mannosylation and are required for adhesion and virulence. *J. Biol. Chem.* **280,** 1051–1060 (2005).
103. Mio, T. *et al.* Role of three chitin synthase genes in the growth of *Candida albicans*. *J. Bacteriol.* **178,** 2416–2419 (1996).
104. Mille, C. *et al.* Inactivation of *CaMIT1* inhibits *Candida albicans* phospholipomannan β-mannosylation, reduces virulence, and alters cell wall protein β-mannosylation. *J. Biol. Chem.* **279,** 47952–47960 (2004).
105. Mille, C. *et al.* Identification of a new family of genes involved in β-1,2-mannosylation of glycans in *Pichia pastoris* and *Candida albicans*. *J. Biol. Chem.* **283,** 9724–9736 (2008).
106. Mille, C. *et al.* Members 5 and 6 of the Candida albicans *BMT* family encode enzymes acting specifically on β-mannosylation of the phospholipomannan cell-wall glycosphingolipid. *Glycobiol.* **22,** 1332–1342 (2012).
107. Mio, T. *et al.* Cloning of the *Candida albicans* homolog of *Saccharomyces cerevisiae GSC1/FKS1* and its involvement in β-1,3-glucan synthesis. *J. Bacteriol.* **179,** 4096–4105 (1997).
108. Mio, T. *et al.* Isolation of the *Candida albicans* homologs of *Saccharomyces cerevisiae KRE6* and *SKN1*: expression and physiological function. *J. Bacteriol.* **179,** 2363–2372 (1997).
109. Staab, J. F. & Sundstrom, P. *URA3* as a selectable marker for disruption and virulence assessment of *Candida albicans* genes. *Trends Microbiol.* **11,** 69–73 (2003).
110. Murad, A. M., Lee, P. R., Broadbent, I. D., Barelle, C. J. & Brown, A. J. Clp10, an efficient and convenient integrating vector for *Candida albicans*. *Yeast* **16,** 325–327 (2000).

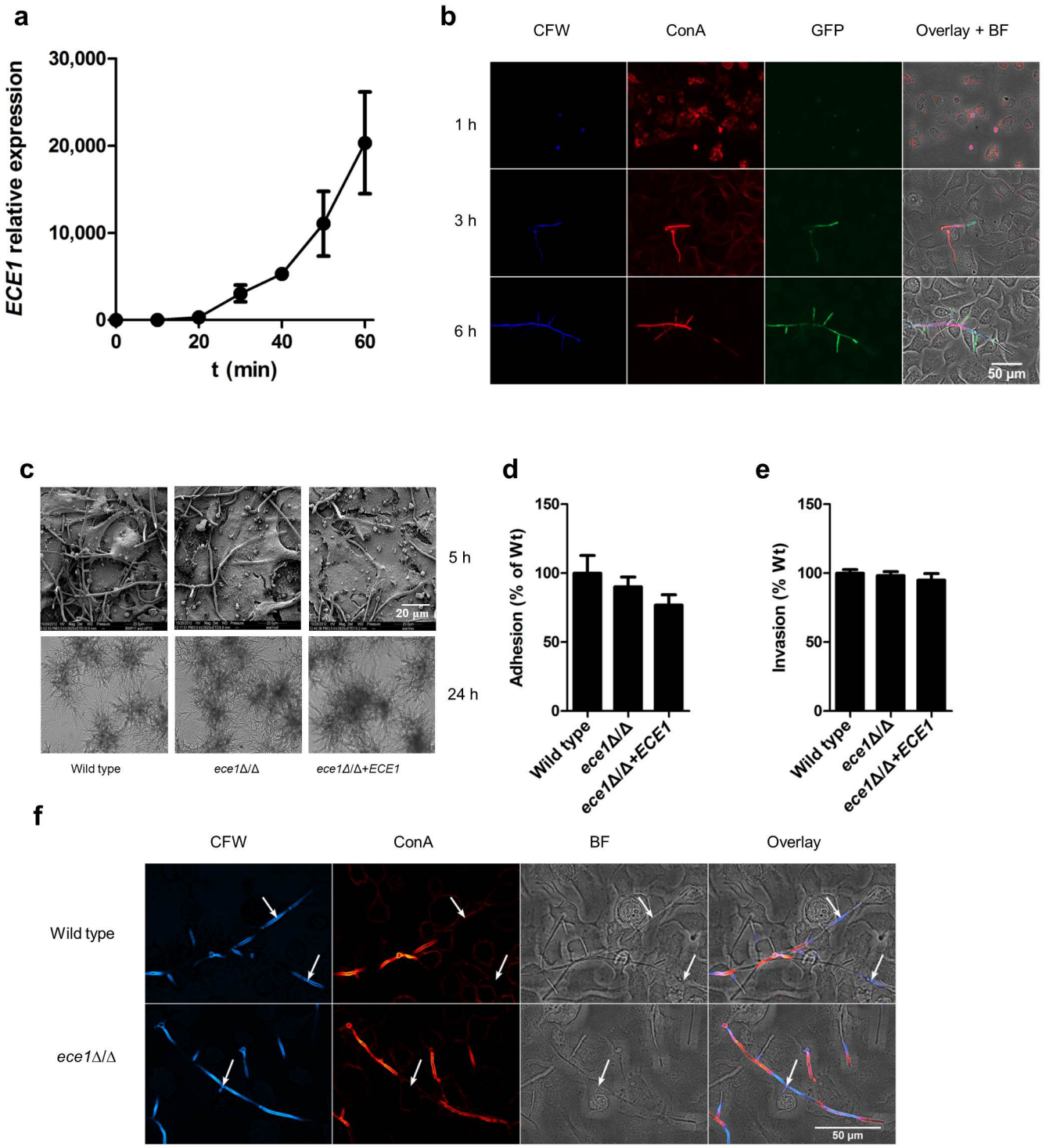

Extended Data Figure 1 | *C. albicans ECE1* expression and phenotypic effects of *ECE1* gene deletion. a, Relative expression (vs $t = 0$) of *ECE1* in *C. albicans* wild type over time after addition of yeast cells to TR146 epithelial cells as measured by RT-qPCR. **b**, Imaging confirmation of *ECE1* expression over time within *C. albicans* wild-type strain. *C. albicans* cells expressing GFP under the control of the *ECE1* 5′ intragenic region, containing the *ECE1* promoter, were grown on TR146 epithelial cells and stained with calcofluor white (CFW, post-permeabilization) to show cell wall chitin and Alexa-Fluor-647-labelled concanavalin A (ConA, pre-permeabilization) to show carbohydrates. A composite image showing CFW, ConA, GFP and the brightfield (BF) image is shown. **c**, Scanning electron micrographs (top panels, 5 h) and light microscopy (bottom panels, 24 h) showing no gross abnormalities in hypha formation between *C. albicans* wild-type (BWP17 + CIp30), *ECE1*-deletion (*ece1*Δ/Δ) and *ECE1* re-integrant (*ece1*Δ/Δ + *ECE1*) strains after infection of TR146 epithelial cells. **d**, No difference in adhesion of *C. albicans* wild-type, *ece1*Δ/Δ and *ece1*Δ/Δ + *ECE1* strains to TR146 epithelial cells after 60 min. **e**, No difference in invasion of *C. albicans* wild-type, *ece1*Δ/Δ and *ece1*Δ/Δ + *ECE1* strains into TR146 epithelial cells after 3 h. **f,** Fluorescence staining of *C. albicans* wild-type and *ece1*Δ/Δ hyphae invading through TR146 epithelial cells. Fungal cells are stained with calcofluor white (CFW, post-permeabilization) and Alexa-Fluor-647-labelled concanavalin A (ConA, pre-permeabilization) to show cell wall chitin and carbohydrates, respectively, and to distinguish between invading hyphae (only stained after permeabilization) and non-invading hyphae (stained both pre- and post-permeabilization). Levels of chitin and β-glucan are comparable in both strains. White arrows indicate invasion into epithelial cells. Data shown are representative (**b**, **c**, **f**) or the mean (**a**, **d**, **e**) of three biological replicates. Error bars show ± s.e.m.

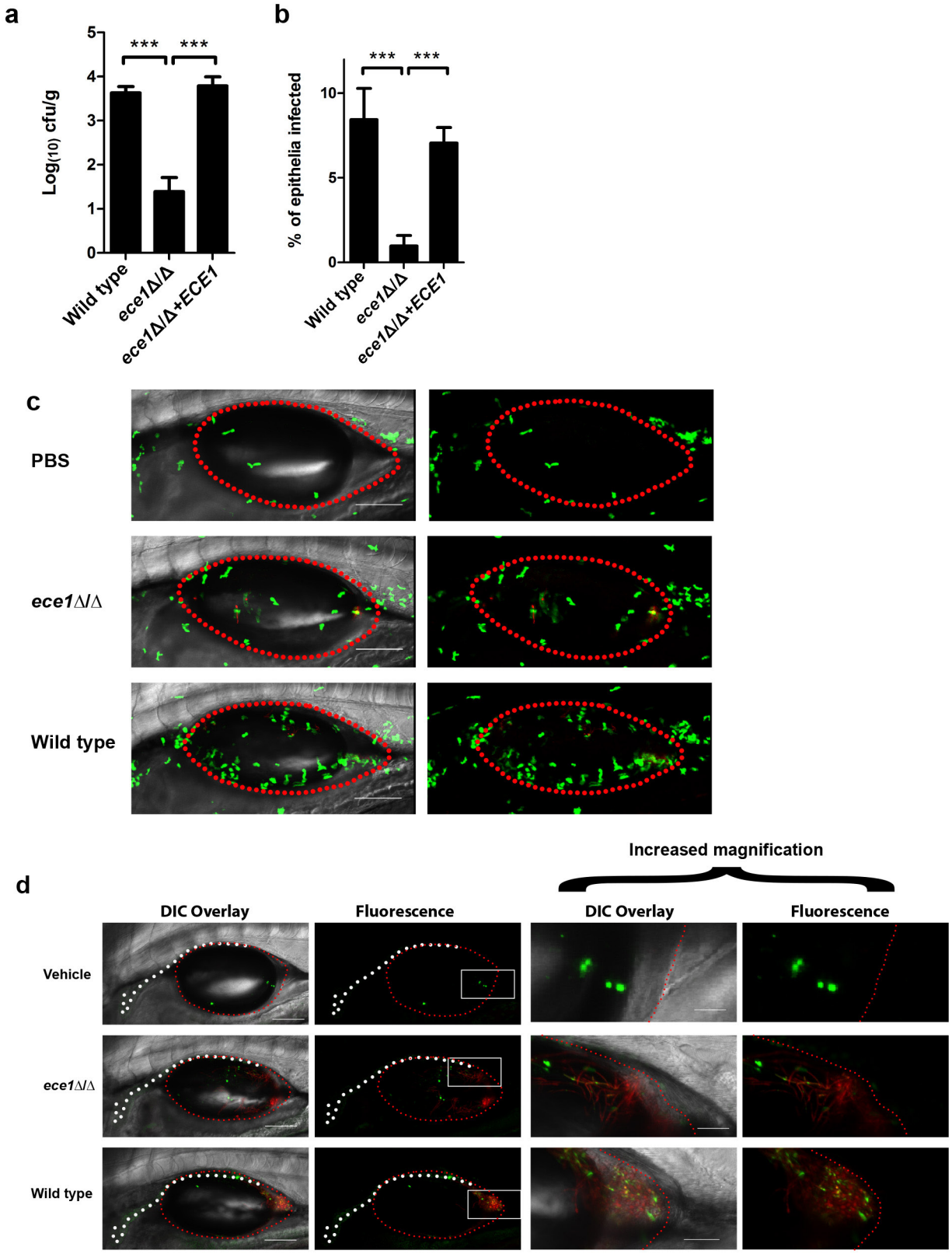

Extended Data Figure 2 | See next page for caption.

Extended Data Figure 2 | *C. albicans* Ece1p is critical for mucosal virulence *in vivo*. **a**, Fungal burdens recovered from the tongues of mice infected with *C. albicans* wild-type (BWP17 + CIp30) (number of mice(n) = 13), *ECE1*-deletion (*ece1*Δ/Δ) ($n = 20$) and *ECE1* re-integrant (*ece1*Δ/Δ + *ECE1*) ($n = 24$) strains after a 2-day oropharyngeal infection. **b**, Average percentage of the entire tongue epithelium area infected in different groups of mice infected with the different *C. albicans* strains. **c**, Confocal imaging of 4-day post-fertilization (dpf) *mpo-gfp* transgenic zebrafish swimbladders infected with *C. albicans* wild-type (BWP17 + CIp30 + *dTomato*), *ECE1*-deletion (*ece1*Δ/Δ + *dTomato*) and *ECE1* re-integrant (*ece1*Δ/Δ + *ECE1* + *dTomato*) strains for 24 h. *C. albicans* cells appear red while neutrophils appear green. Red dots outline the swimbladder. Images are composites of maximum projections in the red and green channels (25 slices each, approximately 100 μm depth) with (left) or without (right) a single slice in the DIC channel overlay. Scale bars represent 100 μm. **d**, Confocal imaging of 4 dpf zebrafish swimbladders infected with *C. albicans* wild-type (BWP17 + CIp30 + *dTomato*), *ECE1*-deletion (*ece1*Δ/Δ + *dTomato*) and *ECE1* re-integrant (*ece1*Δ/Δ + *ECE1* + *dTomato*) strains for 24 h stained with the fluorescent exclusion dye Sytox Green. *C. albicans* cells appear red and damaged epithelial cells appear green. White dots outline the pronephros and red dots outline the swimbladder. Images are composites of maximum projections in the red and green channels (25 slices each, approximately 100 μm depth) with (left) or without (right) a single slice in the DIC channel overlay. High magnification images of the white boxes are shown. Scale bars (bottom right) represent 100 μm (low magnification) and 30 μm (high magnification). Data shown are the mean (**a**, **b**) or representative (**c**, **d**) of at least three biological replicates. Error bars show ± s.e.m. Data were analysed by Mann–Whitney U-test. ***$P < 0.001$.

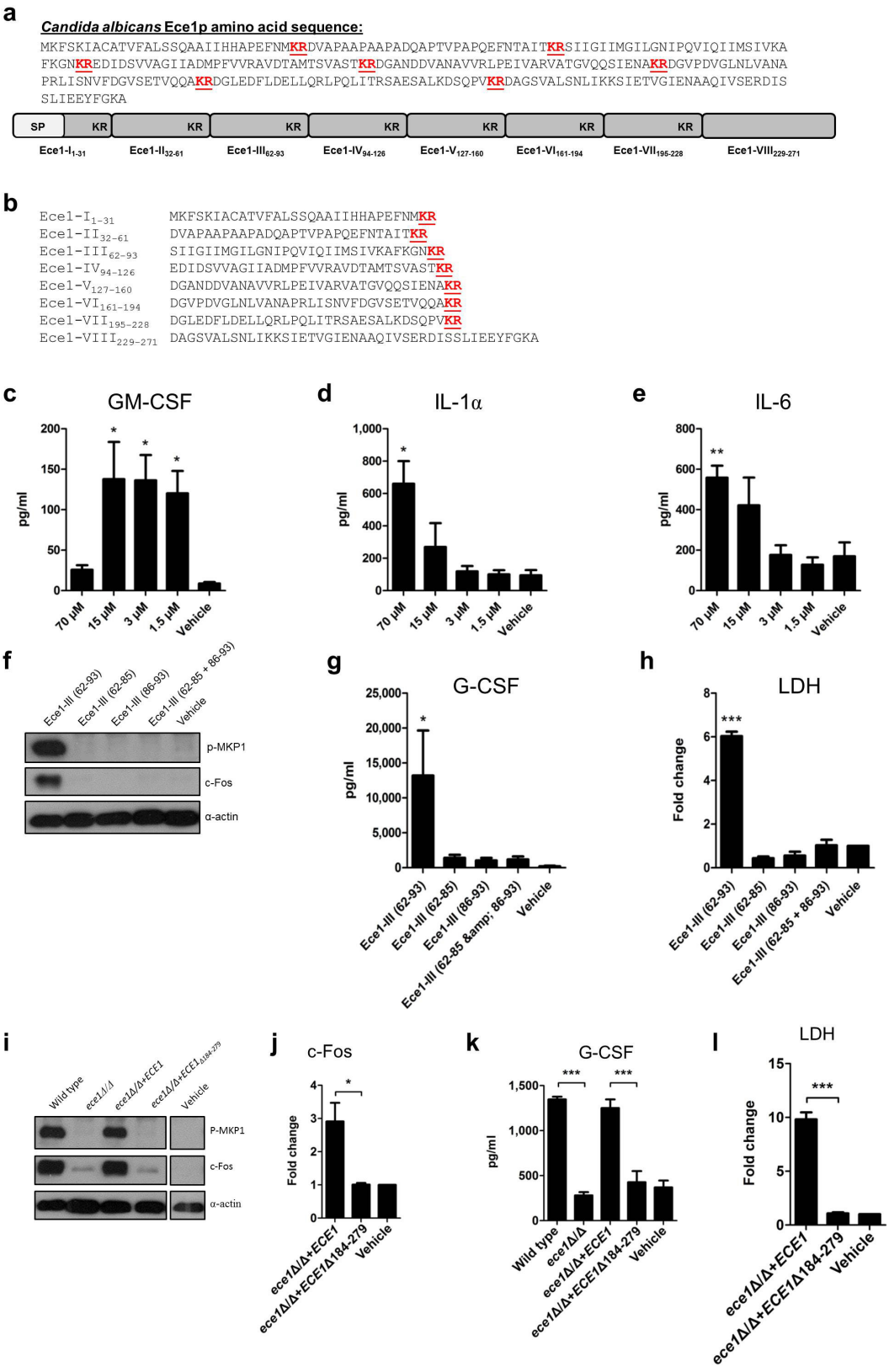

Extended Data Figure 3 | See next page for caption.

Extended Data Figure 3 | Ece1-III$_{62–93}$ is the active region of Ece1p. **a**, Amino acid sequence of Ece1p and a schematic of the protein, indicating the signal peptide (SP), lysine-arginine motifs (KR) at the C terminus of each peptide, and the processed peptides (Ece1-I–VIII) produced by Kex2p cleavage. **b**, Amino acid sequences of the processed peptides (Ece1-I–VIII) produced by Kex2p cleavage. **c**–**e**, Induction of GM-CSF (**c**), IL-1α (**d**) and IL-6 (**e**) secreted after stimulation of TR146 epithelial cells for 24 h with varying concentrations of Ece1-III$_{62–93}$ (1.5–70 μM). **f**, Phosphorylation of MKP-1 and c-Fos production after 2 h treatment of TR146 epithelial cells with 15 μM of Ece1-III$_{62–85}$ (hydrophobic region), Ece1-III$_{86–93}$ (hydrophillic region), Ece1-III$_{62–85}$ and Ece1-III$_{86–93}$ together, or Ece1-III$_{62–93}$ alone. **g**, Induction of G-CSF secretion after 24 h treatment of TR146 epithelial cells with 15 μM of Ece1-III$_{62–85}$, Ece1-III$_{86–93}$, Ece1-III$_{62–85}$ and Ece1-III$_{86–93}$ together, or Ece1-III$_{62–93}$ alone. **h**, Fold change induction of LDH release after 24 h treatment of TR146 epithelial cells with 70 μM of Ece1-III$_{62-85}$, Ece1-III$_{86-93}$, Ece1-III$_{62–85}$ and Ece1-III$_{86–93}$ together, or Ece1-III$_{62–93}$ alone. **i**, Induction of p-MKP-1 and c-Fos 2 h post-infection (p.i.) with the indicated *C. albicans* strains (MOI = 10). **j**, c-Fos DNA binding induction 3 h p.i. with indicated *C. albicans* strains (MOI = 10). **k**, G-CSF secretion and **l**, LDH release 24 h p.i. with indicated *C. albicans* strains (MOI = 0.01). Data shown are representative (**f**, **i**) or the mean (**c**–**e**, **g**, **h**, **j**–**l**) of three biological replicates. Error bars show ± s.e.m. Data were analysed by one-way ANOVA (**c**–**e**, **g, h, k**–**l**) or *t*-test (**j**). $*P < 0.05$, $**P < 0.01$, $***P < 0.001$ (compared with vehicle control). For gel image, see Supplementary Fig. 1.

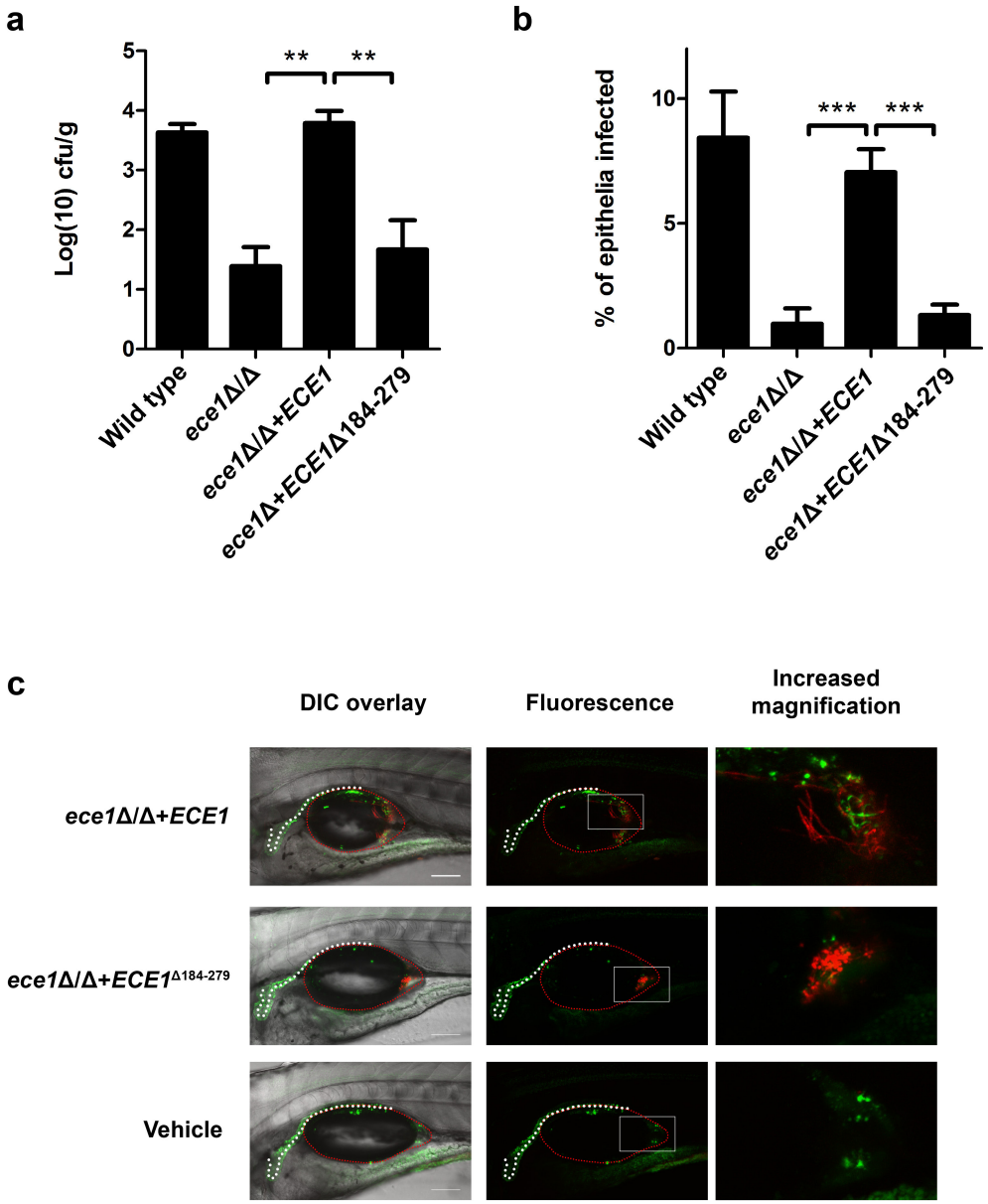

Extended Data Figure 4 | Ece1-III$_{62–93}$ is required for *C. albicans* mucosal infection. a, Fungal burdens recovered from the tongues of mice infected with *C. albicans* wild-type (BWP17 + CIp30) (number of mice (n) = 13), *ECE1*-deletion (*ece1Δ/Δ*) (n = 20), *ECE1* re-integrant (*ece1Δ/Δ + ECE1*) (n = 24) and Ece1-III$_{62–93}$ deletion (*ece1Δ/Δ + ECE1*$_{Δ184–279}$) (n = 10) strains after 2-day oropharyngeal infection. **b**, Average percentage of the entire tongue epithelium area infected in different groups of mice infected with the different *C. albicans* strains. **c**, Confocal imaging of 4 dpf zebrafish swimbladders infected with *C. albicans* Ece1-III$_{62–93}$ deletion (*ece1Δ/Δ + ECE1*$_{Δ184–279}$ + *dTomato*) and *ECE1* re-integrant (*ece1Δ/Δ + ECE1 + dTomato*) strains for 24 h stained with the fluorescent exclusion dye Sytox Green. *C. albicans* cells appear red and damaged cells appear green. White dots outline the pronephros and red dots outline the swimbladder. Images are composites of maximum projections in the red and green channels (25 slices each, approximately 100 μm depth) with (left) or without (right) a single slice in the DIC channel overlay. Scale bars (bottom right) represent 100 μm. Data shown are the mean (**a**, **b**) or representative (**c**), of at least three biological replicates. Error bars show ± s.e.m. Data were analysed by Mann–Whitney *U*-test. $^{**}P < 0.01$, $^{***}P < 0.001$.

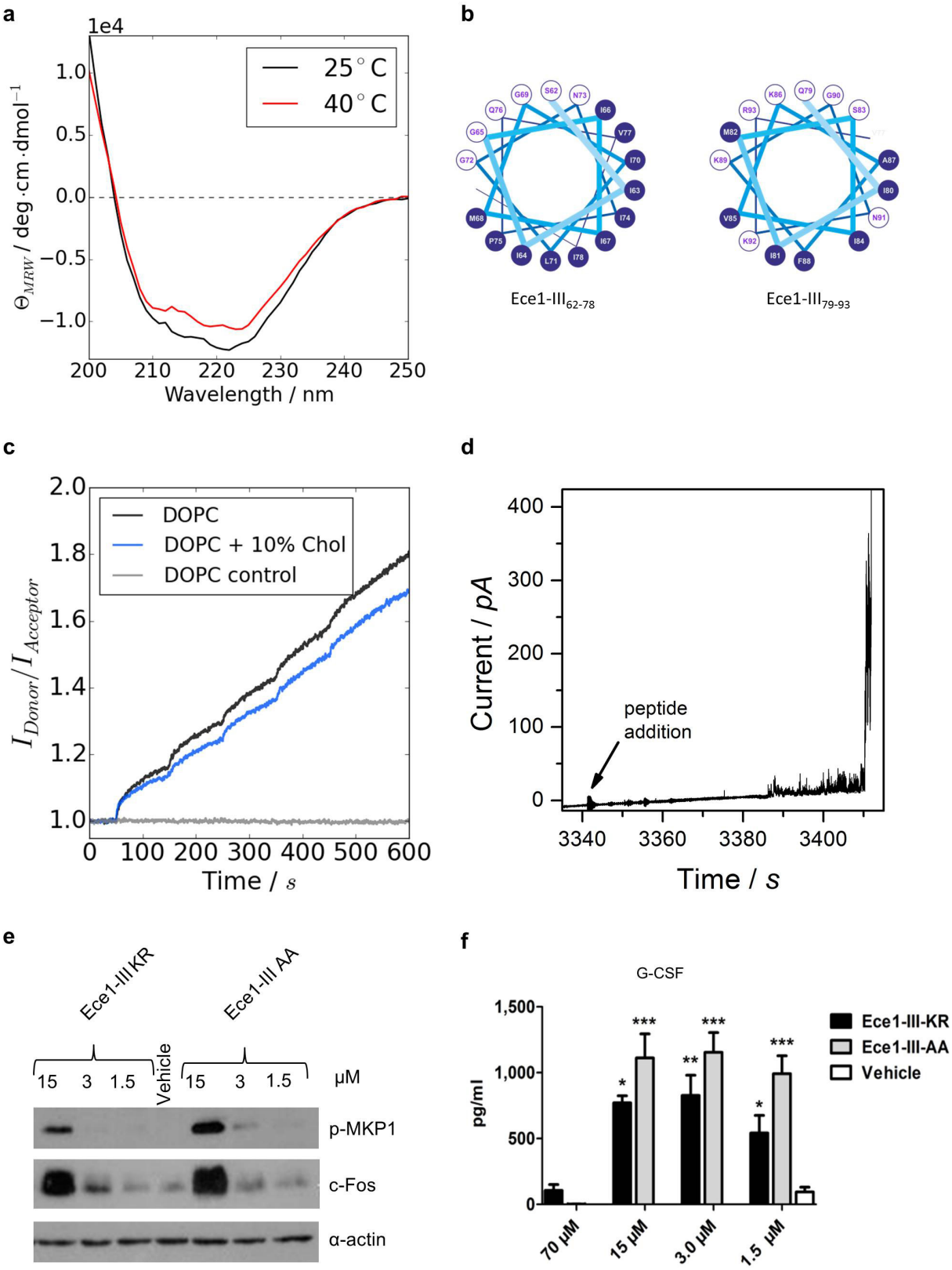

Extended Data Figure 5 | See next page for caption.

Extended Data Figure 5 | Ece1-III$_{62–93}$ is a cytolytic α-helical peptide. **a**, Circular dichroism spectra showing the α-helical conformation of Ece1-III$_{62–93}$ in buffer (100 mM KCl, 5 mM HEPES, pH 7). Increasing the temperature from 25 °C to 40 °C did not affect the stability of the α-helical structure. **b**, Diagram to illustrate the amphipathic nature of Ece1-III$_{62–93}$ (residues 62–78, left panel; residues 79–93, right panel). Residues with hydrophobic or polar/charged side chains are displayed with a blue and white background, respectively. Modified from output generated in PEPWHEEL (http://emboss.bioinformatics.nl/cgi-bin/emboss/pepwheel). **c**, Förster resonance energy transfer (FRET) experiments show the intercalation of Ece1-III$_{62–93}$ into lipid liposomes (10 μM) composed of DOPC in the absence or presence of cholesterol. Peptide titration of Ece1-III$_{62–93}$ to liposomes showed slightly enhanced intercalation for pure DOPC. **d**, Ece1-III$_{62–93}$ induced the permeabilization of planar lipid membranes composed of DOPC. The graph shows heterogeneous and transient lesions leading finally to a rupture of the membrane. Ece1-III$_{62–93}$ concentration was 0.125 μM. **e**, Induction of p-MKP-1 and c-Fos 2 h in TR146 cells post stimulation (p.s.) with Ece1-III$_{62–93KR}$ or Ece1-III$_{62–93AA}$. **f**, Secretion of G-CSF from TR146 cells 24 h p.s. with Ece1-III$_{62–93KR}$ or Ece1-III$_{62–93AA}$. Data shown are representative (**a**–**e**) or mean (**f**) of at least three biological replicates. Error bars show ± s.e.m. Data were analysed by one-way ANOVA (**f**). $*P < 0.05$, $**P < 0.01$, $***P < 0.001$ (compared with vehicle control). For gel images, see Supplementary Fig. 1.

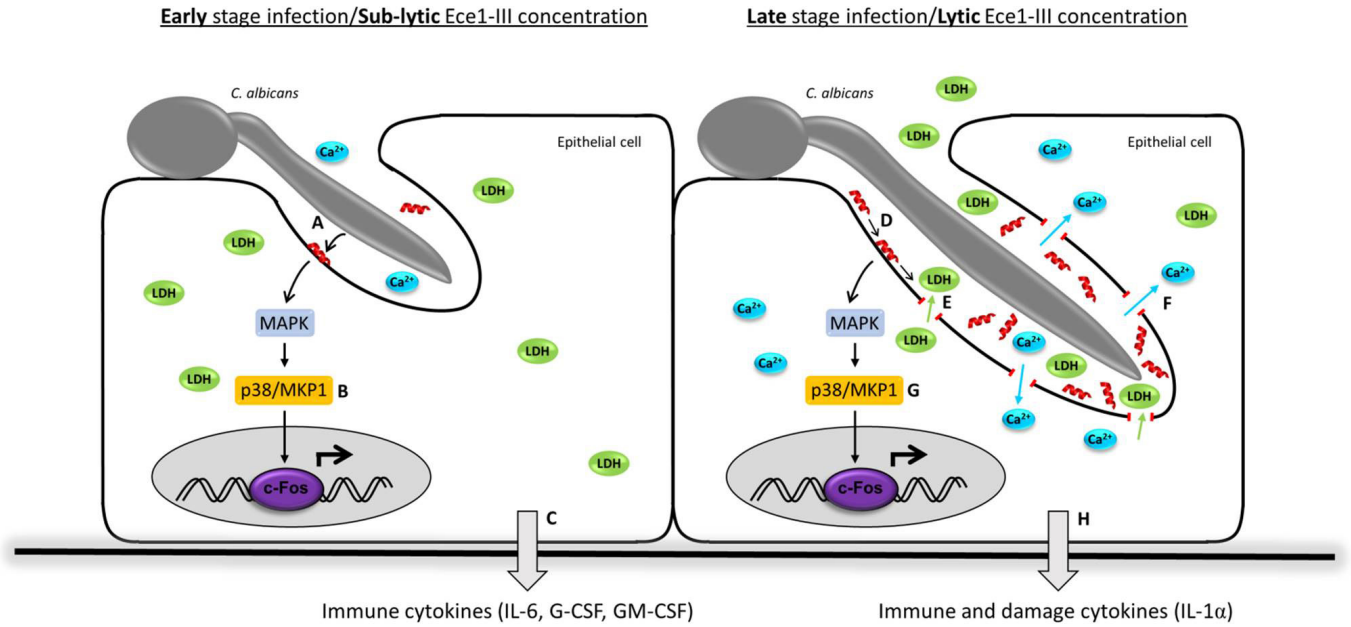

Extended Data Figure 6 | Schematic of the role of Ece1-III in *C. albicans* infection of epithelial cells. a–h, During early stage infection of the mucosal surface by *C. albicans*, Ece1-III (red α-helix) is secreted into the invasion pocket created by the invading hypha (**a**), Sub-lytic concentrations of Ece1-III trigger epithelial signal transduction through MAPK, p38/MKP-1 and c-Fos (**b**), resulting in the production of immune regulatory cytokines (**c**), As the severity of the infection increases, Ece1-III accumulates (**d**), and once lytic concentrations are reached, causes membrane damage and the release of lactate dehydrogenase from the host epithelium (**e**), concomitant with calcium influx (**f**). Epithelial signal transduction is maintained (**g**), and additionally induces the release of damage associated cytokines, such as IL-1α (**h**). Ece1-III may also have activity on the epithelial surface outside of the invasion pocket and on neighbouring cells not in contact with hyphae if Ece1-III is produced in sufficient concentrations.

Extended Data Table 1 | *C. albicans* strains used in this study

Strain name	Strain/Gene Function	Strain Reference	Morphology*	Phospho-MKP1†	c-Fos†	Cytokines‡	Damage§	Phenotype Reference
Controls								
SC5314	Wild type	[52]	Hyphae	Yes	Yes	Yes	Yes	This study
BWP17 & Clp30	Parental strain	[53]	Hyphae	Yes	Yes	Yes	Yes	This study
CAI-4 & Clp10	Parental strain	[54]	Hyphae	Yes	Yes	Yes	Yes	This study
CAF2-1	Parental strain	[54]	Hyphae	Yes	Yes	Yes	Yes	This study
DAY286	Parental strain	[55]	Hyphae	Yes	Yes	Yes	Yes	This study
Yeast-locked								
efg1Δ/Δ	*Transcription factor*	[56]	Yeast	No	No	No	No	This study
efg1/cph1Δ/Δ	*Transcription factor/ Transcription factor*	[57]	Yeast	No	No	No	No	[58]/This study
eed1Δ/Δ	*RNA polymerase II regulator*	[59]	Yeast	No	No	No	No	[58]/This study
flo8Δ/Δ	*Transcription factor*	[60]	Yeast	No	No	No	No	This study
tpk1Δ/Δ	*cAMP-dependent protein kinase*	[61]	Yeast	No	No	No	No	This study
tpk2Δ/Δ	*cAMP-dependent protein kinase*	[62]	Yeast	No	No	No	No	This study
vps11Δ/Δ	*Protein trafficking*	[63]	Yeast	No	No	No	No	This study
cap1Δ/Δ	*Transcription factor*	[64]	Yeast	No	No	Yes	No	This study
och1Δ/Δ	Alpha-1,6-mannosyltransferase	[65]	Yeast	No	No	No	No	[66]
kex2Δ/Δ	Processing enzyme	[67]	Yeast	No	No	No	No	This study
Hypha-producing								
nrg1Δ/Δ	Transcriptional corepressor	[68]	Hyphae	Yes	Yes	Yes	Yes	[58]/This study
cph1Δ/Δ	*Transcription factor*	[69]	Hyphae	Yes	Yes	Yes	Yes	This study
cph2Δ/Δ	*Transcription factor*	[70]	Hyphae	Yes	Yes	Yes	Yes	This study
efh1Δ/Δ	*Transcription factor*	[71]	Hyphae	Yes	Yes	Yes	Yes	This study
czf1Δ/Δ	*Transcription factor*	[72]	Hyphae	Yes	Yes	Yes	Yes	This study
rfg1Δ/Δ	Transcriptional repressor	[73]	Hyphae	Yes	Yes	Yes	Yes	This study
hog1Δ/Δ	*MAP kinase*	[74]	Hyphae	Yes	Yes	Yes	Yes	This study
sun42Δ/Δ	*Adhesin-like protein*	[75]	Hyphae	Yes	Yes	Yes	Yes	This study
pga29Δ/Δ	*GPI-anchored yeast-associated protein*	[76]	Hyphae	Yes	Yes	Yes	Yes	This study
phr2Δ/Δ	*Glycosidase*	[77]	Hyphae	Yes	Yes	Yes	Yes	This study
pga36Δ/Δ	*GPI-anchored protein*	[78]	Hyphae	Yes	Yes	Yes	Yes	This study
ece1Δ/Δ	***Hypha-associated protein***	**[79]‖**	**Hyphae**	**No**	**No**	**No**	**No**	**This study**
mkc1Δ/Δ	*MAP kinase*	[80]	Hyphae	Yes	Yes	Yes	Yes	This study
bud2Δ/Δ	*GTPase activating protein*	[81]	Hyphae	Yes	Yes	Yes	Yes	This study
pra1Δ/Δ	*Zinc binding protein*	[82]	Hyphae	Yes	Yes	Yes	Yes	This study
utr2/crh11/crh12Δ/Δ	*Putative wall glycosidase/transglycosylase*	[83]	Hyphae	Yes	Yes	Yes	Yes	This study
wap1Δ/Δ	*Surface antigen on hyphae/buds*	[84]	Hyphae	Yes	Yes	Yes	Yes	This study
sod5Δ/Δ	*Superoxide dismutase*	[85]	Hyphae	Yes	Yes	Yes	Yes	This study
hwp1Δ/Δ	*Adhesin*	[86]	Hyphae	Yes	Yes	Yes	Yes	This study
rbt1Δ/Δ	*Putative GPI-modified cell wall protein*	[84]	Hyphae	Yes	Yes	Yes	Yes	This study
rbt5Δ/Δ	*Heme binding*	[84]	Hyphae	Yes	Yes	Yes	Yes	This study
hyr1Δ/Δ	*GPI-anchored hyphal cell wall protein*	[87]	Hyphae	Yes	Yes	Yes	Yes	This study
mp65Δ/Δ	*Cell surface mannoprotein*	[88]	Hyphae	Yes	Yes	yes	Yes	This study
cek1Δ/Δ	*ERK-family protein kinase*	[89]	Hyphae	Yes	Yes	Yes	Yes	This study
sap2Δ/Δ	*Secreted aspartyl protease*	[90]	Hyphae	Yes	Yes	Yes	Yes	This study
sap7Δ/Δ	*Secreted aspartyl protease*	[91]	Hyphae	Yes	Yes	Yes	Yes	This study
sap9/sap10Δ/Δ	*Secreted aspartyl proteases*	[92]	Hyphae	Yes	Yes	Yes	Yes	This study
als1Δ/Δ	*Agglutinin-like sequence protein*	[93]	Hyphae	Yes	Yes	Yes	Yes	[94]
als2Δ/ P_{MAL}-ALS2	*Agglutinin-like sequence protein*	[95]	Hyphae	Yes	Yes	Yes	Yes	[94]
als3Δ/Δ	*Adhesin*	[93]	Hyphae	Yes	Yes	Partial¶	Partial¶	[94]
als4Δ/Δ	*Agglutinin-like sequence protein*	[95]	Hyphae	Yes	Yes	Yes	Yes	[94]
als5Δ/Δ	*Agglutinin-like sequence protein*	[96]	Hyphae	Yes	Yes	Yes	Yes	[94]
als6Δ/Δ	*Agglutinin-like sequence protein*	[96]	Hyphae	Yes	Yes	Yes	Yes	[94]
als7Δ/Δ	*Agglutinin-like sequence protein*	[96]	Hyphae	Yes	Yes	Yes	Yes	[94]
als9Δ/Δ	*Agglutinin-like sequence protein*	[97]	Hyphae	Yes	Yes	Yes	Yes	[94]
pmt1Δ/Δ	*Mannosyltransferase*	[98]	Hyphae	Partial¶	Partial¶	Partial¶	Partial¶	[66]
pmr1Δ/Δ	*Secretory pathway ATPase*	[99]	Hyphae	Partial¶	Partial¶	Partial¶	Partial¶	[66]
mnn4Δ/Δ	Regulator of mannosylphosphorylation	[100]	Hyphae	Yes	Yes	Yes	Yes	[66]
mnn9Δ/Δ	Putative mannosyltransferase	[101]	Hyphae	Yes	Yes	Yes	Yes	[66]
mnt1/mnt2Δ/Δ	Mannosyltransferases	[102]	Hyphae	Yes	Yes	Yes	Yes	[66]
chs2/chs3Δ/Δ	Chitin synthase/ Chitin synthase	[103]	Hyphae	Yes	Yes	Yes	Yes	This study
mit1Δ/Δ	Mannose:Inositolphosphoceramide mannose transferase	[104]	Hyphae	Yes	Yes	Yes	Yes	[66]
bmt1Δ/Δ	Beta-mannosyltransferase	[105]	Hyphae	Yes	Yes	Yes	Yes	[66]
bmt2Δ/Δ	Putative beta-mannosyltransferase	[105]	Hyphae	Yes	Yes	Yes	Yes	[66]
bmt3Δ/Δ	Beta-mannosyltransferase	[105]	Hyphae	Yes	Yes	Yes	Yes	[66]
bmt4Δ/Δ	Beta-mannosyltransferase	[105]	Hyphae	Yes	Yes	Yes	Yes	[66]
bmt5Δ/Δ	Putative beta-mannosyltransferase	[106]	Hyphae	Yes	Yes	Yes	Yes	[66]
bmt6Δ/Δ	Beta-mannosyltransferase	[106]	Hyphae	Yes	Yes	Yes	Yes	[66]
gsc1Δ/GSC1	Beta-1,3-glucan synthase catalytic subunit	[107]	Hyphae	Yes	Yes	Yes	Yes	[66]
gsl1Δ/Δ	Beta-1,3-glucan synthase subunit	[107]	Hyphae	Yes	Yes	Yes	Yes	[66]
gsl2Δ/Δ	Beta-1,3-glucan synthase subunit	[107]	Hyphae	Yes	Yes	Yes	Yes	[66]
kre6Δ/KRE6	Beta-1,6-glucan synthase subunit	[108]	Hyphae	Yes	Yes	Yes	Yes	This study

References 52–108 are cited in this table.

*Morphology recorded 2 h post-infection on TR146 buccal cell monolayers; hyphae includes pseudohyphae.

†Data based on western blotting.

‡Cytokines include IL-1α, IL-6 and G-CSF.

§Damage measured by LDH assay.

‖ New *ece1*Δ/Δ also created in this study (see Extended Data Table 2). Original mutant (in red) produced by ref. 27 using the URA-blaster protocol[3]. A set of *ece1* mutants, including partial deletion of *ECE1* and a revertant, was produced in this study in the same genetic background using strain BWP17 to avoid a URA3 effect based on genomic location[109,110].

¶Partial activation is due to lack of adhesion.

Extended Data Table 2 | *C. albicans* mutant strains constructed and used in this study

Strain description	Strain name	Genotype
BWP17+CIp30	M1477	*ura3::λimm434/ura3::λimm434 iro1::λimm434/iro1::λimm434 his1::hisG/his1::hisG arg4::hisG/arg4::hisG RPS1/rps1::(URA3-HIS1-ARG4)*
*ece1*Δ/Δ	M2057	*ura3::λimm434/ura3::λimm434 iro1::λimm434/iro1::λimm434 his1::hisG/his1::hisG arg4::hisG/arg4::hisG ece1::HIS1/ece1::ARG4 RPS1/rps1::URA3*
*ece1*Δ/Δ+*ECE1*	M2059	*ura3::λimm434/ura3::λimm434 iro1::λimm434/iro1::λimm434 his1::hisG/his1::hisG arg4::hisG/arg4::hisG ece1::HIS1/ece1::ARG4 RPS1/rps1::(URA3-ECE1)*
*ece1*Δ/Δ+$ECE1_{\Delta 184\text{-}279}$	M2174	*ura3::λimm434/ura3::λimm434 iro1::λimm434/iro1::λimm434 his1::hisG/his1::hisG arg4::hisG/arg4::hisG ece1::HIS1/ece1::ARG4 RPS1/rps1::(URA3-*$ECE1^{\Delta 184\text{-}279}$*)*
*kex1*Δ/Δ	M2258	*ura3::λimm434/ura3::λimm434 iro1::λimm434/iro1::λimm434 his1::hisG/his1::hisG arg4::hisG/arg4::hisG kex1::HIS1/kex1::ARG4 RPS1/rps1::URA3*
SC5314+*pECE1-GFP* (*ECE1* promoter-GFP)	CA58	*ECE1/ece1::GFP-SAT1*
BWP17+CIp30+*pENO1-dTom* (*ENO1* promoter-dTom)	RWC83	*ura3::λimm434/ura3::λimm434 iro1::λimm434/iro1::λimm434 his1::hisG/his1::hisG arg4::hisG/arg4::hisG RPS1/rps1::(URA3-HIS1-ARG4) ENO1/eno1::dTom-SAT1*
*ece1*Δ/Δ+*pENO1*-dTom (*ENO1* promoter-dTom)	RWC84	*ura3::λimm434/ura3::λimm434 iro1::λimm434/iro1::λimm434 his1::hisG/his1::hisG arg4::hisG/arg4::hisG ece1::HIS1/ece1::ARG4 RPS1/rps1::URA3 ENO1/eno1::dTom-SAT1*
*ece1*Δ/Δ+*ECE1* + dTomato	RWC85	*ura3::λimm434/ura3::λimm434 iro1::λimm434/iro1::λimm434 his1::hisG/his1::hisG arg4::hisG/arg4::hisG ece1::HIS1/ece1::ARG4 RPS1/rps1::(URA3-ECE1) ENO1/eno1::dTomato-NAT*^{r}
*ece1*Δ/Δ+$ECE1_{\Delta 184\text{-}279}$ + dTomato	RWC86	*ura3::λimm434/ura3::λimm434 iro1::λimm434/iro1::λimm434 his1::hisG/his1::hisG arg4::hisG/arg4::hisG ece1::HIS1/ece1::ARG4 RPS1/rps1::(URA3-*$ECE1^{\Delta 184\text{-}279}$*) ENO1/eno1::dTomato-NAT*^{r}

Extended Data Table 3 | LC-MS/MS analysis of *C. albicans* Ece1-III

Ece1-III sequence	PSM Value* (% total Ece1-III†) (% total Ece1p‡)				
	Wild Type	*ece1Δ/Δ+ECE1*	TR146+Wild type	rEce1p+rKex2p	*kex1Δ/Δ*
SIIGIIMGILGNIPQVIQIIMSIVKAFKGNK	699 (86%) (41%)	477 (89%) (35%)	79 (97.5%) (97.5%)	n/d§	49 (13.3%) (3.6%)
SIIGIIMGILGNIPQVIQIIMSIVKAFKGNKR	1 (0.1%) (0.06%)	1 (0.2%) (0.07%)	2 (2.5%) (2.5%)	248 (80%) (1.5%)	291 (78.9%) (21%)

*The number of peptide spectrum matches. Data for *ece1*Δ/Δ and *ece1*Δ/Δ + *ECE1*$_{\Delta 184-279}$ are not included as no Ece1-III peptides were detected in either strain, as expected.
†Percentage of SIIGIIMGILGNIPQVIQIIMSIVKAFKGNK or SIIGIIMGILGNIPQVIQIIMSIVKAFKGNKR detected amongst all Ece1-III peptides found by LC-MS/MS.
‡Percentage of SIIGIIMGILGNIPQVIQIIMSIVKAFKGNK or SIIGIIMGILGNIPQVIQIIMSIVKAFKGNKR detected amongst all Ece1p peptides found by LC-MS/MS.
§n/d; not detected.

Extended Data Table 4 | Oligonucleotide primers used in this study

Primer name	Application	Sequence (5′-3′)	Description
ECE1-FG	PCR	atcaaataacccacctatttcaaaattgttttatttttgtttatctctacaaca aacaactttccttttattttactaccaactattttccattcgttaaagaagcttc gtacgctgcaggtc	Construction of *ECE1* deletion construct
ECE1-RG	PCR	cacaaaaaacaacaattaaaaaaatcagttacagcaaaagtgtcacaag acttatggaataaaagattaagcttgtggaaaacaaatttttatctgctgag cattctgatatcatcgatgaattcgag	Construction of *ECE1* deletion construct
ECE1-RecF3k	PCR	gcacgcgtctaaagtggagtaacaac	Construction of *ECE1* complementation plasmid
ECE1-RecR	PCR	ggtcgaccccagacgttggttgc	Construction of *ECE1* complementation plasmid
ECE1-F1	PCR	ggcttctcataaatgaagggctcag	Confirmation of *ECE1* deletion
ECE1-R1	PCR	gccgaatcaatcttgtcgtgccac	Confirmation of *ECE1* deletion
KEX1-FG	PCR	tatctttttttgttttatttacccatccttcatatctttacaacccttgatacctt acctaaacaacacacatctatctttaatcaatcaaacacaaatcaattgaa gcttcgtacgctgcaggtc	Construction of *KEX1* deletion construct
KEX1-RG	PCR	tcacaatctagattattgtaggttgtatagacaaaaaataaaaatcaaact attattcgttatataaatctacaagatctctaatctccactgtaccgaaaaat tctgatatcatcgatgaattcgag	Construction of *KEX1* deletion construct
KEX1-F1	PCR	ggaagcccataagaaattgga	Confirmation of *KEX1* deletion
KEX1-R1	PCR	aggaagctgtggtggtagtg	Confirmation of *KEX1* deletion
HIS-F2	PCR	ggacgaattgaagaaagctggtgcaaccg	Confirmation of *ECE1/KEX1* deletion
HIS-R2	PCR	caacgaaatggcctcccctaccacag	Confirmation of *ECE1/KEX1* deletion
ARG-F2	PCR	ggatatgttggctactgatttag	Confirmation of *ECE1/KEX1* deletion
ARG-R2	PCR	aatggatcagtggcaccggtg	Confirmation of *ECE1/KEX1* deletion
ECE1-FInt1	PCR	ctaacgtttttgatggcgtcctgg	Confirmation of plasmid integration
URAF2	PCR	ggagttggattagatgataaaggtgatgg	Confirmation of plasmid integration
RPF-1	PCR	gagcagtgtacacacacacatcttg	Confirmation of plasmid integration
RPF-2	PCR	cgccaaagagtttcccctattatc	Confirmation of plasmid integration
Pep3-F1	PCR	gaagatatcgattctgttgttgctgg	Excision of Ece1-III$_{62\text{-}93}$ from *ECE1*
Pep3-R1	PCR	cagaatcgatatcttctcttttggtaatagcagtattgaattcttg	Excision of Ece1-III$_{62\text{-}93}$ from *ECE1*
5'ECE1prom-NarI	PCR	gatcggcgcctccagccactattttgtacctgt	Amplification of *ECE1* promoter region for *ECE1* promoter-GFP construct
3'ECE1prom-XhoI	PCR	tcagctcgagtttaacgaatggaaaatagttggtag	Amplification of *ECE1* promoter region for *ECE1* promoter-GFP construct
5'ECE1term-SacII	PCR	gatcccgcggcagcagataaaaatttgttttccacaag	Amplification of *ECE1* terminator region for *ECE1* promoter-GFP construct
5'ECE1term-SacI	PCR	tcaggagctccgttaagaatatgaatgacagttggtc	Amplification of *ECE1* terminator region for *ECE1* promoter-GFP construct
G1-ECE1	PCR	ctcgctgattagagttcaagagt	Confirmation of *ECE1*-GFP plasmid integration (5′ end)
GFP veri rev	PCR	tgatctgggtatctcgcaaagcat	Confirmation of *ECE1*-GFP plasmid integration (5′ end)
G4-ECE1	PCR	tggaagattcacttgagttggaac	Confirmation of *ECE1*-GFP plasmid integration (3′ end)
X3-SAT1	PCR	gtgaagtgtgaagggggag	Confirmation of *ECE1*-GFP plasmid integration (3′ end)
pENO1 FW	PCR	tccttggctggcactgaactcg	Confirmation of pENO1-dTom plasmid integration
dTom REV	PCR	aaggtctaccttcaccttcacc	Confirmation of pENO1-dTom plasmid integration
ACT1-F	qPCR	tcagaccagctgatttaggtttg	Quantification of actin cDNA
ACT1-R	qPCR	gtgaacaatggatggaccag	Quantification of actin cDNA
ECE1-F	qPCR	atcgaaaatgccaagagag	Quantification of *ECE1* cDNA
ECE1-R	qPCR	agcattttcaataccgacag	Quantification of *ECE1* cDNA